Coastline dynamics at Thukela Mouth and the Amatigulu and Umlalazi river estuary areas, KwaZulu-Natal

by

JOZUA ESTERHUIZEN

Submitted in fulfilment of the requirements for the degree

Master of Science (Geoinformatics)

in the

Faculty of Natural and Agricultural Science
Department of Geography, Geoinformatics and Meteorology
University of Pretoria

April 2019

DECLARATION

I, Jozua Esterhuizen, declare that the dissertation entitled **Coastline dynamics at Thukela Mouth and the Amatigulu and Umlalazi river estuary areas, KwaZulu-Natal,** which I hereby submit for the degree **Master of Science (Geoinformatics)** at the University of Pretoria, is my own work and has not previously been submitted by me for a degree at this or any other tertiary institution.

J. Esterhuizen 30 April 2019

SIGNATURE **DATE**

Coastline dynamics at Thukela Mouth and the Amatigulu and Umlalazi river estuary areas, KwaZulu-Natal

Jozua Esterhuizen

Supervisor: Professor P. Sumner (University of Pretoria)

Department: Geography, Geoinformatics and Meteorology

Faculty: Natural and Agricultural Sciences

University: University of Pretoria

Degree: Master of Science (Geoinformatics)

Abstract

The objectives of the study were to observe, record and determine coastal dune changes in northern KwaZulu-Natal. The areas considered in the study were the Thukela River mouth (29° 13’ 29.05” S; 31° 30’ 17.58” E), the Amatigulu-Nyoni estuary (29° 06’ 44.25” S; 31° 36’ 52.23” E) and the Umlalazi estuary (28° 56’ 41.13” S; 31° 48’ 56.63” E). The study focused on survey data and the movement of the relevant dunes adjacent to the coastline to determine whether these dunes were moving in a certain direction and whether there was an increase or decrease in the dune area and/or volume. South Africa’s entire coastline is subject to the force of high-breaking waves on the beaches (littoral), cliffs and shores, tides, wind (aeolian) and runoff from rivers. The estuaries on the KwaZulu-Natal North Coast consist of sandy barriers in the form of wave-built sandy ridges that run parallel to the coastline. The barriers are relatively shallow and water can flow easily between the sea and the estuaries. Some of the dunes studied in this research, such as those in the Amatigulu estuary, have approximately 10% vegetation growth on them and are thus stable, but the remainder of the dunes along this coast are not vegetated at all.

The movement of the dunes was monitored using sophisticated land surveying instruments, such as Global Positioning Systems (GPS) and total stations. Assessments were done with the help of survey instruments and land surveying calculation methods, in combination with the relevant surveying programs and Geographic Information Systems (GIS) to obtain area and

volume results over several years. For example, a baseline was measured at the Umlalazi beach using a total station, and all the surveys that followed were done using GPS instruments, and these surveys were based on and connected to the initial survey. The Umlalazi assessment used three methods. The first was comparing old aerial photographs to how the area appeared at the time of the study. The second was GIS methods to geo-reference aerial and satellite images showing the movement of the dunes at the Umlalazi beach site. The third was establishing a fishnet grid to break down the already surveyed data to yield a more accurate database, containing three times more data than the original database. With the help of aerial photographs, geomorphological changes could be determined for a period of 70 years for the Umlalazi beach site. This comparison was undertaken for practical reasons to check the movement and stability of the dune and to assess the degree of geomorphological change. These methods measured only relative changes or movements over time.

To survey and understand dune movement better, a solid and very reliable survey network was established around the dunes. These networks were established using different surveying methods: GPS, remote sensing, triangulation, traversing, scanning, as well as light detection and ranging (Lidar). A review of the scientific reasons for dune movement provided a better understanding of the amount of movement that takes place, which helps establish prediction methods.

Findings from the assessment of the Thukela River showed, firstly, that the southern and northern beaches at the Thukela River mouth varied only slightly in size and in volume and, secondly, that the southern beach seemed more stable than the northern beach. Both changed in shape, but not much in size or volume. At the Amatigulu estuary, a full survey was done in 2016, and aerial photos from 1953 and Google Earth data up to 2017 were also used. From the survey data, a typical sine graph could be plotted of the changes in size and volume for the calculated areas. At the Umlalazi beach, physical surveys were undertaken during 2016 and 2017. The percentage change in size and volume was positive in 2016, and negative in 2017. It can therefore be assumed that over time, all barriers vary in size, shape and volume, and that whatever is eroded, will build up again to maintain the cycle between beaches, oceans and rivers.

Key words: Amatigulu-Nyoni River estuary, coastline dynamics, dune change, fishnet grid, KwaZulu-Natal, Thukela River, Umlalazi River estuary.

Acknowledgments

This study was carried out with the financial assistance of the Department of Geography, Geoinformatics and Meteorology of the Faculty of Natural and Agricultural Sciences.

This study was also dependent on Ezemvelo KwaZulu-Natal Wildlife and I thank them for their assistance and co-operation throughout the months of the study.

I am also thankful to my supervisor, Professor Paul Sumner, for his enthusiasm and professional guidance and patience throughout the study.

I am grateful to staff members in the Department of Geography, Geoinformatics and Meteorology. In particular, I would like to mention Erika Pretorius for her assistance with ideas, answering questions and explaining the functions of ArcGIS, Ingrid Booysen for her support on ideas and printing plans of the relevant areas, and Victoria Rautenbach.

I would like to thank the South African Weather Bureau, and in particular Lucky Dlamini, for sending long-term rainfall, wind and temperature data so promptly.

I would like to thank Idette Noomé for language editing.

And, last but not least, I would like to thank my wife, Barendina, for her physical and emotional support in a very difficult surveying field and her encouragement during the days and late nights helping me process data on the computer, and her moral support. Thank you very much!

Contents

Declaration i
Abstract ii
Acknowledgments iv

Chapter 1: Introduction 1
1.1 Short-term Detailed Assessment 2
1.1.1 The Agulhas current. 2
1.1.2 Climate change and sea level. 3
1.1.3 Tides. 3
1.1.4 Aeolian processes and wave energy. 3
1.1.5 Land use. 4
1.2 Aims and Objectives 4
1.3 Project Outline 5
Chapter 2: Background Literature 6
2.1 Introduction 6
2.2 The Rivers in the Research Study 6
2.2.1 The mountain and sub-mountain stage (source). 8
2.2.2 The meandering stage. 9
2.2.3 The delta and tidal stage. 10
2.3 The Effect of Aeolian (Wind-related) Processes on Land Forms 14
2.4 Wave Energy and Sea Currents 15
2.5 Prior Case Studies 19
Chapter 3: Study Area 25
3.1 Location 25
3.2 The Coastline Considered in the Study 25
3.3 Climate and Rainfall 26
3.4 Geology and the Geomorphology of the KwaZulu-Natal Coastline 30
3.5 Vegetation and Land Use 32
3.6 The Thukela Shelf 33
3.7 Overview of the Catchment Areas of the Thukela, Amatigulu and Umlalazi Rivers 34
3.7.1 The Thukela catchment area. 34
3.7.2 The Amatigulu-Nyoni catchment area. 37

3.7.3 The Umlalazi catchment area. 38
3.8 The Individual Sites Studied 39
3.8.1 The Thukela River mouth (29° 13’ 29.05” S; 31° 30’ 17.58” E). 39
3.8.2 Amatigulu-Nyoni River estuary (29° 06’ 44.25” S; 31° 36’ 52.23” E). 40
3.8.3 Umlalazi River estuary (28° 56’ 41.13” S; 31° 48’ 56.63” E). 41
3.9 History of Severe Storms on the KwaZulu-Natal North Coast 42
3.9.1 Cyclone Astrid (December 1957- January 1958). 43
3.9.2 Cyclone Claude (December 1965-January 1966). 43
3.9.3 Cyclone Caroline (February 1972). 43
3.9.4 Cyclone Eugenie (21-22 February 1972). 43
3.9.5 Cyclone Danae (27-31 January 1976). 43
3.9.6 Cyclone Emilie (6-8 February 1977). 43
3.9.7 Cyclone Kolia (March 1980) and Cyclone Justine (March 1982). 44
3.9.8 Cyclone Domoina and Cyclone Imboa (29-31 January 1984). 44
3.9.9 Floods of September 1987. 44
3.9.10 Tropical storm of 19-20 March 2007. 45
Chapter 4: Methods 46
4.1 General Approach to the Study 46
4.2 The Physical Survey 47
4.3 The Thukela Survey 49
4.4 The Amatigulu Survey 50
4.5 The Umlalazi Beach Survey 51
4.6 Short-term Detailed Assessment at the Umlalazi Beach 52
4.7 The Interpretation of the Photographic Model 59
4.8 The Orientation of the Photographic Model/the Rubber Sheeting Process 60
4.9 Accuracy Calculation 62
4.10 Creating the New Features 64
Chapter 5: Results 66
5.1 Overview of the Results from the Three Sites 66
5.2 Climate from 1993 to 2018 67
5.3 Dynamics of the Thukela River Mouth over the Years 68
5.3.1 Thukela River mouth results obtained using the aerial photographs. 68
5.3.2 Thukela River mouth results obtained from the physical survey techniques. 72
5.4 Geomorphic Changes of the Amatigulu-Nyoni River Estuaries 75
5.5 Umlalazi Results 79

5.5.1 First method: Comparing the 1957 data with the 2009 satellite image. 79
5.5.2 Second method: Physical survey and assessment of the dunes. 83
5.5.3 Effect of wind on the results. 85
5.5.4 Third method: The Fishnet method. 90
5.5.5 Coastline and bush line dynamics. 98
Chapter 6: Discussion 103
6.1 Introduction 103
6.2 The Dynamics of the Thukela River Mouth over the Years 104
6.3 Geomorphological Changes of the Amatigulu-Nyoni River Estuaries 105
6.4 Discussion of the Umlalazi Results 105
6.4.1 Results of the comparison of the 1957 data with the 2009 satellite image. 105
6.4.2 Results of the physical survey and assessment of the dunes. 106
6.4.3 Effect of wind on sand transportation. 107
6.4.4 Results of the Fishnet method. 108
6.4.5 Coastline and bush line dynamics. 109
6.5 Opportunities for Future Research 110
Chapter 7: Conclusion 111
7.1 Results of the Research 112
7.2 Limitations of the Surveys of the Three Sites 113
7.2.1 Field problems. 113
References 114
Appendices 120
Appendix A: Coordinate Lists 120
Appendix B: All Points Falling in the Fishnet Grid of 10m x 10m on the Umlalazi Beach During the Survey of March 2016, October 2016, April 2017 and July 2017 174
Appendix C: Accumulative Volumes, Volumes per Contour and Percentage Increase or Decrease in Volume 207
Appendix D: Annual average rainfall in Mtunzini area from 1998 to 2018 211
Appendix E: Wind data 212

List of Tables

Table 2.1: Characteristics of the Thukela, Amatigulu and Umlalazi Rivers 10
Table 3.1: Annual average rainfall (1998-2018) 27
Table 5.1: Percentage increase and decrease in area and volume for the north and south beaches of the Thukela River from 1953 to 2017 75
Table 5.2: Areas of the Amatigulu sand barrier in 1953, 1972, 1989, 2007 and 2017 77
Table 5.3: The registration of points at the Umlalazi beach surveying area on the aerial photograph of 1957 80
Table 5.4: Summary of the cumulative volumes and areas at the Umlalazi beach (surveyed March 2016 to July 2017 85
Table 5.5: Average wind direction (degrees from north) and average wind speed data from January 2016 to middle May 2017 at 8h00 87
Table 5.6: Average wind direction (degrees from north) and average wind speed data from January 2016 to middle May 2017 at 20h00 88
Table 5.7: Summary of Tables 5.5 and 5.6, wind behavior measured at the Umlalazi beach at 08h00 in the morning and 20h00 in the evening from January 2016 to May 2017 ... 89
Table 5.8: Accumulative volume and area of the terrain at the Umlalazi beach. 92
Table 5.9: Percentage of contour areas for the total area showing the changes 95
Table 5.10: Square metres of each individual contour interval and the rise or fall from the first to the second, third and then the fourth survey 97
Table 5.11: Percentage area increase or decrease in the contour interval of the sand on the Umlalazi beach 98
Table 5.12: Summary of the encroachment of the bush area towards the beach area at the Umlalazi beach 100
Table 6.1: Areas and volume of the north and south shores of the Thukela River mouth (1953-2017) 104
Table 6.2: Percentage increase/decrease in the area and volume of the north and south shores of the Thukela River mouth (1953-2017) 104
Table 6.3: Accumulative volume in relation to the area of the contours at the Umlalazi beach.106

List of Figures

Figure 2.1: How different sediments are transported in a river 8
Figure 2.2: Origin of the Thukela in the Drakensberg with steep gradients (July 2017) 9
Figure 2.3: The Thukela, Amatigulu and Umlalazi Rivers, which are relevant to the study: the first section shows the initial part of the Thukela River, the middle section shows the Amatigulu River and the third section the Umlalazi River 11
Figure 2.4: Braided patterns in the Thukela River 12
Figure 2.5: Close-up of the braided patterns in the Thukela River 13
Figure 2.6: The Thukela River in flood 13
Figure 2.7: A destructive wave 16
Figure 2.8: A constructive wave 16
Figure 2.9: Wave energy is concentrated at headlands and dissipated in bays 18
Figure 2.10: Beach and sediment drift – the swash enters the coast at an oblique angle under a longshore current; the sea draws back at 90^0 to the beach (the particle path is shown as 1-3) 18
Figure 2.11: Recording dune changes relative to posts at the edge of a transgressive dune's slip face 21
Figure 2.12: Grand Falls Dune Field migration 1953-2010 plotted on an image from 2005 (wind direction shown at lower left) 22
Figure 2.13: Different instruments that surveyors use: (from left to right) a total station, a GPS and an automatic level (instruments photographed courtesy of the University of Pretoria) 23
Figure 2.14: Methods used by Labuz (2009). .....
A: A small embryo dune is beaconed off with surveying rods.
B: Part of an existing dune is fenced off to identify changes.
C: Survey poles mark a 5 m^2 part of the dune to monitor changes (some hourly).
D: Monitoring continued even at night, using torches planted strategically on embryo dunes and foredunes. 24
Figure 3.1: Small scale map of KwaZulu-Natal showing the position of the Thukela, Amatigulu and Umlalazi Rivers running from west to east to the Indian Ocean 26
Figure 3.2: Average rainfall from 1998 to 2002, measured at the Mtunzini weather station 28

Figure 3.3: Average rainfall from 2003 to 2007, measured at the Mtunzini weather station..... 29
Figure 3.4: Average rainfall from 2008 to 2012, measured at the Mtunzini weather station..... 29
Figure 3.5: Average rainfall from 2013 to 2017, measured at Mtunzini weather station..... 30
Figure 3.6: The structuring of a sand dune 31
Figure 3.7: Distribution of eight recognized facies types on the Thukela Shelf.
The -30, -60 and the -100 m contours define the inner, mid- and outer shelf zones... 34
Figure 3.8: Thukela River catchment..... 36
Figure 3.9: Thukela River drainage and Thukela Shelf in the Kwa Zulu-Natal Bight 36
Figure 3.10: Long profile of the Thukela River drawn from a 1:50 000 Topographical map 37
Figure 3.11: Long profile of the Amatigulu River drawn from a 1:50 000 topographical map..... 38
Figure 3.12: Long profile of the Umlalazi River drawn from a 1:50 000 topographical map..... 39
Figure 3.13: **A:** Indication of the size of the sand dune at the Thukela River mouth.
B: The might of the Thukela River forcing its way on to the mouth.
C & **D:** The river and the sea meet – the Thukela was flowing strongly (April 2017) .. 40
Figure 3.14: **A, B, C** & **D:** The Amatigulu River breaking through the sand barrier during heavy rains in April 2017, reaching the mouth early in June 2017.
C: The barrier (far left) and behind it, the ocean. The sand in the foreground shows where the water forms part of the River estuary (April 2017). 41
Figure 3.15: **A:** At the Umlalazi River beach, there is a steep slip face at an angle of the beach.
B: Prominent vegetated areas in relation to the sand areas.
C: Small embryo dune in the developing stage.
D: The bend (bight) where the coast is about 220^{o} and turns to 250^{o} (April 2017).... 42
Figure 4.1: Trigonometrical beacon Aloes II (left) and Red Hill (right) at the Thukela River site... 50
Figure 4.2: Trigonometrical beacon Baton Rouge No 276 on a 6 m concrete block in the northern part of the Amatigulu River mouth..... 51
Figure 4.3: Model Maker program showing the triangles at the Umlalazi beach area that were physically surveyed on the ground (scale approximately 1:7000) 53
Figure 4.4: The triangles covered on the survey terrain of the Umlalazi beach and the contours generated from the triangles (scale approximately 1:7000)..... 54
Figure 4.5: White rectangle showing the common area that satisfied all the surveys over the two years in the research area of the Umlalazi beach (scale approximately 1:7000)..... 55

Figure 4.6: The terrain on the Umlalazi beach area, covered with a grid network of 10 m^2, exactly the size described by the four coordinates (scale is approximately 1:7000) .. 56
Figure 4.7: The 10 m^2 network pulled over the original contour survey at the Umlalazi beach.... 57
Figure 4.8: Embryo due in the middle of a square ignored by the fishnet method..... 58
Figure 4.9: Selected photographs from the Amatigulu 1953 aerial photo model 59
Figure 4.10: Selected photographs from the Amatigulu 1953 aerial photo model..... 59
Figure 4.11: Selected photographs from the Umlalazi 1957 aerial photo model..... 60
Figure 4.12: Selected photographs from the Thukela 1953 aerial photo model..... 60
Figure 4.13: After the text file was read into the ArcGIS program, all points were converted to a projection system and zoomed to the layer to be visible on the active screen .. 61
Figure 4.14: The photograph and ground coordinates on the Umlalazi beach are drawn in on the active screen. The photograph must be compared to the surveyed points to rectify the photograph. 62
Figure 4.15: The total RMS error is 1.62613, using six control points to orient the photograph and determine the survey accuracy in relation to when the photograph was taken. 63
Figure 4.16: The image target with a transparency of 40% is ready to be oriented. The yellow points are the control points. Point 1 on the ground is joined up with Control 11. After another coordinate orientation the photograph will already be provisionally oriented..... 64
Figure 4.17: In this ArcGIS figure the creating and editing of the different layers has been completed, as displayed in the Table of Contents on the left hand side of the screen. A plan of the Umlalazi estuary is created from the target images. 65
Figure 4.18: The end result of editing the photographic models in the ArcGIS program 65
Figure 5.1: Annual average rainfall per annum in mm per month from 1993 to May 2018 measured at the Mtunzini weather station. 67
Figure 5.2: Annual average rainfall per annum from 1993 to May 2018, measured at the Mtunzini weather station 68
Figure 5.3: The Thukela River in 1953, zigzagging through the sandbanks, with a small outlet in the centre between the north and south shores to the sea..... 69
Figure 5.4: The Thukela River in 1983, showing a braided pattern through the sandbanks 70
Figure 5.5: The Thukela River in 2013 (note that the plans' scales differ because the aerial photograph scales are different)..... 70

Figure 5.6: Diagrams of the Thukela mouth in 1953 (**A**) and the mouth in 1972 (**B**) 71
Figure 5.7: **A:** In 1989 the Thukela mouth shifted south (photograph probably taken in the dry season when the Thukela River almost came to a standstill)
B: In 2017 the Thukela mouth is on the northern side with the river flowing strongly 72
Figure 5.8: The North shore beach at the Thukela River (surveyed in March 2016) 73
Figure 5.9: The south shore beach at the Thukela River (surveyed in March 2016) 73
Figure 5.10: The north shore beach at the Thukela River (surveyed in July 2017)..... 74
Figure 5.11: The south shore beach at the Thukela River (surveyed in July 2017) 74
Figure 5.12: Amatigulu-Nyoni estuary, 1953, when the Nyoni River did not meet the Amatigulu River, which was standing still (georeferenced from the 1953 aerial photographs)..... 76
Figure 5.13: **A, B:** The Amatigulu beach (sand barrier) in 1972 and 1989, showing that the Nyoni River did break through to the Amatigulu River..... 76
Figure 5.14: Position of the Amatigulu-Nyoni mouth in 2007, showing the lagoon forming where the Amatigulu River runs very slowly, although the mouth is open to the sea 78
Figure 5.15: The flat Amatigulu dune forming part of the beach area of 1 056 482 m² in 2017 78
Figure 5.16: **A:** 1957 aerial photograph showing the Umlalazi beach (purple line) and edge of the bush (green) line.
B: 2009 satellite image showing the edge of the encroaching bush (green line)..... 79
Figure 5.17: Beach shift at the Umlalazi in a south-easterly direction (survey points on dry ground in 2017 were under water in 1957). The mean sea level can be seen clearly . 81
Figure 5.18: The mouth of the Umlalazi River and the Siyaya River are open to the sea (1957). Left insert: Close-up of survey points (black figure) 82
Figure 5.19: The Umlalazi estuary in 1983..... 82
Figure 5.20: More extended view of changes in and around Mtunzini and the survey points on the Umlalazi beach 83
Figure 5.21: The 2009 satellite photograph shows the dune extension at the Umlalazi beach, with the bush and dune boundary – red areas show sand encroaching northwards .. 84
Figure 5.22: Young trees and plants encroaching on the sand dunes and the beach at the survey area at the Umlalazi beach (April 2017)..... 86

Figure 5.23: Signs of the beginning of an avalanche on a dune slip face (left) at Umlalazi beach as sand accumulates on the dune crest until it slips over on the slip face side (right) and encroaches onto the bush area (April 2017)..... 86
Figure 5.24: Percentage increase/decrease of sand volumes at the Umlalazi beach (March 2016-July 2017) with more changes close to the beach at the 0-5 m contour levels .. 91
Figure 5.25: The areas of the 2-3 m contour intervals at the Umlalazi beach that changed since March 2016 although sand volumes stayed the same or decreased from April 2017 to July 2017 92
Figure 5.26: Changes in the 2D areas of the survey at the Umlalazi beach in the 2-3 m contour intervals from March 2016 to July 2017..... 93
Figure 5.27: Arc Scene 3D view of the changes found in the four surveys at the Umlalazi beach area in March and October 2016, and April and July 2017. 94
Figure 5.28: Sand area distribution over the four survey periods (March and October 2016, April and July 2017) – the green bar is prominent in the March interval, but decreases up to July 2017, with the yellow bar at its highest peak after the July floods..... 96
Figure 5.29: The percentage increase/decrease in sand areas – graphical summary of data in Table 5.10 (note the substantial rise in the 2 m area from March 2016 to July 2017)..... 96
Figure 5.30: The 1957 aerial photograph of the Umlalazi beach – the purple line runs adjacent to where the parking area would be a few years later 99
Figure 5.31: 2009 satellite image of the Umlalazi beach showing the existing parking area with the new green line 100
Figure 5.32: Plan combining three periods from 1957, 2009 and 2017 at the Umlalazi beach 101
Figure 5.33: Aerial view of the northern bush line's crochet/flame pattern resulting from human activities 102

Chapter 1:

Introduction

This study investigates dune movement or migration of dunes in the KwaZulu-Natal coastal zone. The term coastal zone refers to areas where the sea meets the land, which tend to attract human settlement and are popular for coastal recreation (Palmer, Van der Elst, & Parak, 2011). Such human activities call for very complex management, so planning regarding beaches and estuaries and surrounding areas in respect of town and human development close to the coastal zone and the dunes along the beach needs to address many different scenarios (Palmer *et al.*, 2011). Such management requires careful definition of the coast and the coastal features, as well as cognizance of human-made, historical and natural features such as protective vegetation. Dunes with sensitive vegetation serve as a buffer (provide protection) between the estuary and the sea front.

Estuaries are dynamic and sensitive ecosystems in the interface between the land and the ocean (Pillay *et al.*, 2003) and offer a wide range of habitats (Palmer *et al*., 2011). Begg (1978) has defined estuaries and has classified them into three categories. The first category is estuaries where the estuary mouth is always or frequently open to the sea. The second category is lagoons, which have an infrequent opening to the sea, and the third category is river mouths where there is no interchange with the sea at all, and the seawater and freshwater do not mix (Begg, 1978). Later studies have reclassified estuary mouths using three different classes (Pillay *et al*., 2003). The mouths can be open or closed, and the mouth can be river- or tide-dominated (Cooper, 2001).

Most of the catchment areas in KwaZulu-Natal have very high runoff, and therefore, according to Cooper (2001), the estuaries on that province's coast are more river-dominated. The whole coastline and the beaches of South Africa are subject to the force of high-breaking waves on the beaches (littoral), cliffs and shores, tides, wind (aeolian) and water from the rivers (Elkington, 2012; Tinley, 1985). South African estuaries tend to have sandy barriers in the form of wave-built sandy ridges that run parallel to the coast. These barriers are relatively shallow and water is readily exchanged between rivers and the ocean, as water moves from the sea into the estuary and the other way round (Schumann, 2013). Some of these sandy dune barriers are vegetated and are thus stable against the impact of wind. Vegetation can grow on all types of dunes, even in arid areas with an average annual rainfall of less than 10 mm (Tsoar, 1971). Where there is limited vegetation growth on a dune, this is caused mostly by human influences,

increased wind power and aridity in areas where the average annual rainfall is less than 50 mm (Tsoar, 1971). Coastal dunes are integral to the coastal sedimentary system (Jackson, Cooper, & Green, 2014) – in a sedimentary sense they are often very old, reflecting climate change, sea level changes and sediment supply (Jackson *et al.,* 2014).

1.1 Short-term Detailed Assessment

For this study, in March 2016, October 2016 and April 2017, detailed surveys were executed over the short term (covering data for 13 months). First, in March 2016, a Nikon DTM 522 total station was employed, and then, during October 2016 and April 2017, a Carlson Real Time Kinematic (RTK) GPS was also used to determine changes of the dune barriers at the mouths of the Thukela River, the Amatigulu River and the Umlalazi beach. The aim of these detailed assessments was to determine the changes of the sand barriers at the Thukela River and the Amatigulu River, as well as the beach area at the Umlalazi River, such as the increasing of areas and volumes of the sand. Several factors can have an indirect or a direct influence on changes in the sand areas and the sand volumes, including the Agulhas current, tides, the climate and sea level, wind and wave energy, as well as human factors.

1.1.1 The Agulhas current.

The Agulhas current flows at a distance of approximately 50 km away from the coast. It is a fast-flowing current, and it has a great influence on the local rainfall and climate change (Hutchinson, 2018). According to Palmer *et al.* (2011), some ocean currents flow in a westerly direction until they meet a continent and split and flow either in a northerly or a southerly direction. The Agulhas current follows the outer edge of the continental shelf just off the South African coastline (Bosman, Uken, Leuci, Smith, & Sinclair*,* 2007). Palmer *et al*. (2011) and Bosman *et al.* (2007) have measured the water temperature in the Agulhas current, and found that it is about six degrees warmer than the seawater surrounding this current. Hutchinson (2018) notes that the Agulhas current creates ocean circulation that could cause dramatic changes in climate conditions in the vicinity of the KwaZulu-Natal and the Mozambique coastlines. The Agulhas current meanders south and creates swirling and circular movements called eddies where the main current turns in the opposite direction, right at the coastline. The spinning movements of these eddies form currents that move northwards from the "Agulhas leakage" (Hutchinson, 2018). This leakage sometimes creates extreme weather conditions such as storms and strong rainfall along the KwaZulu-Natal coast (Palmer *et al.,* 2011). During these storms and heavy rainfall along the KwaZulu-Natal coast, the enormous waves that are

generated often have a destructive effect on the beaches, which leads to erosion and a loss of sand.

1.1.2 Climate change and sea level.

When a drastic change in the climate occurs, it can lead to a change in the sea level and the water of the oceans. Changes in the sea level occur mainly when ice melts in the sea and on land. The surface of the earth is dynamic and can move vertically as the water warms up (it expands) or cools down (it contracts). When the water and the land temperatures rise, it thus leads to a rise in the sea level. If the water temperature rises, according to Bernard (1993), there will not necessarily be more storms per year, but the storms will increase in severity. That will lead to more floods and coastal erosion at beaches.

1.1.3 Tides.

Tides are the result of the gravitational pull of the sun and the moon on the oceans (Palmer *et al.*, 2011). The tidal range is 12.5 hours per day, which means that there are two high and two low tides per day. When the moon and the sun line up on the same side of the earth, the "pull" is stronger; then the normal and high tide becomes higher, and the low tide becomes lower (spring tide). According to Palmer *et al.* (2011), at the end of March and September, when the days and nights are equally long, the centre of the sun lies in the same plane as the equator, and if the moon is then also on the same side as the sun, tides will be even higher and lower than normal. This is called the *equinox tide* (Palmer *et al.,* 2011). Together with strong winds and high wave energy, tides are very important in shaping the coastline (Palmer *et al*., 2011).

1.1.4 Aeolian processes and wave energy.

The size and the energy of waves are determined by the littoral effect of the wind speed across the surface of the sea. During storms, the waves are higher and longer, and have a shorter frequency, breaking on the coast with more force (Chorley, Schumm, & Sugden, 1984; Davidson-Arnot 2010; Palmer *et al*., 2011). Davidson-Arnot (2010) describes two wave types: constructive and destructive waves. Constructive waves occur during fair weather (Palmer *et al*., 2011); they deposit sand on the beach and help to build the beach, leaving the beach with a net gain in the amount of sand. The opposite occurs when the wind speed across the ocean rises, and waves become more destructive. The higher the wave, the greater the force on the beach, eroding the sand, not just on the beach, but also against the dune structures. In the deep ocean, the sand ends up in the sea currents. When a beach loses sand, erosion has taken place. Thus the sea can deposit sand on the beach, or it can take sand away (Psuty, 1992). If more sand is deposited

than sand is eroded, dune growth can take place. When the sand dunes encroach on the human environment, it is important to know what driving forces cause such changes and what the relation between the human and natural driving forces are.

1.1.5 Land use.

The KwaZulu-Natal coastline has a very high population density and a very high level of tourism in all its coastal towns because of the attractive beaches, scenery and other opportunities (Palmer *et al*., 2011). Human activities have an enormous impact on this unique coastal environment, not just in terms of normal everyday day activities, but also in terms of agriculture. According to Palmer *et al*. (2011), agricultural activities such as growing sugar cane and subtropical fruit contribute to KwaZulu-Natal's coastal zone economy. Throughout the year, the local people have an important impact on the economic side of the development in coastal towns and the surrounding areas, and this impact is even greater during the vacation season, when many tourists flock to the area. Human activity tends to have a degrading impact on the physical beach and dune barriers. During peak seasons, large numbers of people walking and playing on the dunes and working the sand deeper into the vegetated areas cause avalanches on the slip faces of the dunes. When the dunes are degraded in this way by the human factor, the sand becomes loose, making it easy for the wind and waves to erode the dunes and the beach and to transport the sand away from this littoral zone.

1.2 Aim and Objectives

The overarching aim of the research in this study is to evaluate the changes in the coastal dune geomorphology using surveying techniques. This aim is pursued by achieving three objectives, namely:

a) to construct detailed contour maps of the coastal area corresponding to the aerial photographs by means of photogrammetry to determine sand movement over a temporal period ranging from 1957 to 2017;
b) to assess the physical surveying of a certain area at the Umlalazi beach from March 2016 and July 2017; and
c) to assess the changes to the environment and dune formation at the Thukela River mouth, the Amatigulu estuary and the Umlalazi estuary in relation to the relevant driving forces.

1.3 Project Outline

This research report on the project consists of seven chapters.

Chapter 1 (above) provides an introduction to sand and dune dynamics and outlines the driving forces such as climate change, human presence, the Agulhas current, and wind and waves**.**

Chapter 2 explains the study objects and the typical characters of rivers and how they transport material from inland to the sea.

Chapter 3 outlines the study area, providing information on the three rivers relevant to the study. First, a general description is given of the three catchment areas, followed by a more detailed description of each catchment area, and lastly, the estuaries of the three rivers are described. The chapter also discusses how a dune is formed, and the Thukela shelf, and includes a short briefing regarding severe storms in this area.

Chapter 4 gives more background information on what has already been done in dune surveying around the world. The second part of the chapter explains in detail each method used in this research study.

In **Chapter 5**, the results are presented, indicating the interpretation of the results of using the different methods adopted for the three river sites.

Chapter 6 contains a discussion and analysis of the results.

Chapter 7 outlines the conclusions reached in the study and makes suggestions for possible future studies. The chapter also acknowledges the limitations arising from problems that occurred during the study in the office and in the field.

Chapter 2:

Background Literature

2.1 Introduction

The areas considered in the study are the Thukela River mouth (29° 13’ 29.05” S; 31° 30’17.58” E), the Amatigulu-Nyoni estuary (29° 06’ 44.25” S; 31° 36’ 52.23” E), and the Umlalazi estuary (28° 56’ 41.13” S; 31° 48’ 56.63” E), three rivers in the KwaZulu-Natal province of South Africa. In this research, the movement or the migration of dunes at the KwaZulu-Natal north coast is documented. The three sites are situated approximately 15 to 20 km from each other. The Umlalazi river lies furthest north and the Thukela River furthest south. These rivers lie approximately 150 km north of Durban on the KwaZulu-Natal north coast (the Umlalazi River estuary is about 140 km, the Amatigulu 110 km and the Thukela River 84 km from Durban).

All structures, whether they are made by human hands or are natural, undergo change over the years (McKay, 1978). The main natural forces causing changes on coasts are river discharges, wind action and wave energy. Hence, over time, structures such as dunes, beaches and coast lines can undergo major changes in shape, position, size and volume (Mckay, 1978). As indicated in the aims and objectives set out in Section 1.2, the study aimed to determine the changes of the beaches and dunes of the three study areas related to certain natural driving forces (sometimes affected by human actions), such as the three rivers, wave energy and the influence of aeolian (wind-related) processes relating to sand transportation.

2.2 The Rivers in the Research Study

A river is a body of water that flows in an open channel. Leopold (1953) defines a river as a body of water that flows along a natural channel to where it opens out to the sea. Rivers create changes in the landscape by eroding channels, transporting and depositing sediment in ways that cause erosional and depositional land forms (Summerfield, 1991). Therefore the main action of a river is to produce sediment, then drain the sediment and water, and transport it from the highland to the sea, or to a lake, and deposit the sediment wherever the energy of the river allows it to do so, or that energy decreases (Summerfield, 1991). The main purpose of a river is to drain water from a highland to the sea or form a tributary to another river. The river boundaries are the crests or hills of the adjacent catchment area(s). Rivers always start in a highland, or as Leopold (1953) puts it, at the headwaters, and flow to where they drain into a lake or the sea. The flow of rivers, such as the Thukela, Amatigulu and Umlalazi Rivers, can be

divided into three sections: an upper course or source area, a middle course or the meandering area, and a lower course, which is the floodplain or fluvial area.

Two aspects of a river are interesting to different disciplines (Chorley *et al*., 1984): the water and flow of the water is the domain of hydraulic engineering, whereas the geomorphology of the river, its dimensions, erosion or depositions, any changes that can take place and the pattern of the river channel fall into the field of geomorphology (Chorley *et al.,* 1984). When this drainage takes place on coastal dunes, a wide variety of geomorphological forms can occur (Goldsmith, 1978; Pye, 1983; Tinley, 1985; Tsoar, 1971).

Rivers such as the Thukela River, the Amatigulu River and the Umlalazi River experience two types of frictional forces as gravity forces the water down a slope: friction where the water molecules collide with each other in the stream, and the friction of the water against the banks of the river (Chorley *et al*., 1984). Where a river curves, the friction increases and this leads to erosion, because the banks consist of fine sediments, silts and clays (Chorley *et al*., 1984). Particles are transported when materials are moved within the river. The material is transported as a load until the river deposits it in accordance with the energy of the river (Bagnold, 1980). This load does not refer just to objects (rocks, stones, tree trunks, etc.) in the riverbed – when the river is in flood, it collects sediment and material from the banks of the river and riverbed. If the force of the river is too high against the banks, water erodes the banks of the river, and loose materials can be carried away to the sea, or may be deposited before they reach the sea. This is called hydraulic action (Bagnold, 1980). Bagnold (1980) explains there are four ways of transporting particles in the load, depending on the energy flow of the river, namely solution, suspension, saltation and traction. The Thukela River and the Amatigulu River, which both have very steep gradients where the rivers begin, carry objects over long distances. This is called traction (Bagnold, 1980). When a river starts to lose energy, it flows more slowly and it starts to deposit its load on the riverbed, the sandbanks and dune barriers. Rivers can lose energy due to a rise in the loss of precipitation, an increase in evaporation and human use of river water. For example, where the Thukela enters the gentler plain (after 300 km of steep flow), the energy decreases and all the heavy objects are deposited on the riverbed or on the banks and in dams.

Objects are carried forward by means of suspension, saltation, and traction (see Figure 2.1). Suspension refers to smaller particles that are carried by the river above the riverbed. The speed at which the particles are carried by the river depends on the energy (strength) of the river. Very fine articles travel the last kilometres to the ocean by means of suspension, for example, clay, silt and soluble particles dissolved in the water, such as limestone and chalk. With

a process of increasing erosion, a river often loses soils in its upper course, but gathers more soils and other sediments in the lower parts of the river.

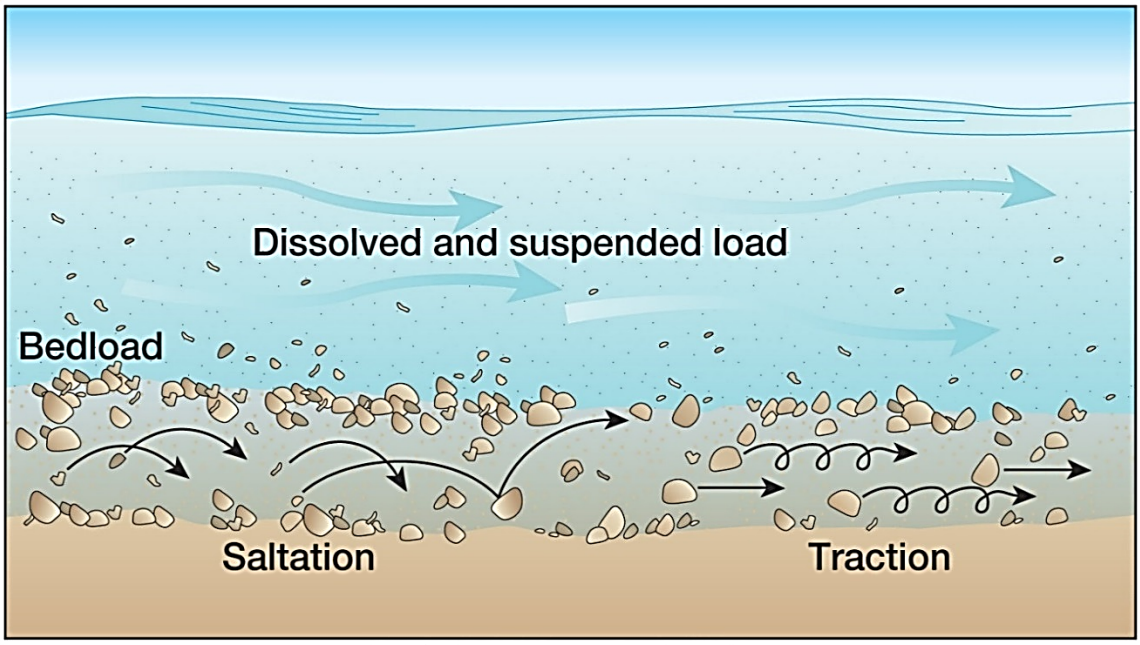

Figure 2.1: How different sediments are transported in a river.

(Source: Glendale Community College, Figure 16-07.jpg)

2.2.1 The mountain and sub-mountain stage (source).

The mountainous areas where rivers start are also known as the source of the river. These areas are characterised by bedrock channels (see Figure 2.2). At the source and in most of its upper course, a river such as the Thukela starts from a very high elevation above sea level, and it is mostly very narrow, flowing through V-shaped valleys with waterfalls (Leopoldt, 1953) (see Figure 2.2). In these areas, the velocity is very high because of a steep gradient of 1:100 to 1:500 or even steeper. At this stage, due to the water's friction with the bedrock, the water cuts into rocks and plants. It gathers sediment that ranges in size from boulders and rocks in the upper area to smaller stones in the middle area, and sand, which is a component of clay, downstream in the plain or lower area close to the river mouth (Anthoni, 2000; Leopold, 1953). In the upper course, there is predominantly erosion because of steep slopes. In this source area of the river, rocks are subject to wear and then break down to smaller pieces (Anthoni, 2000).

Figure 2.2: Origin of the Thukela River in the Drakensberg with steep gradients (July 2017).[1]

Smaller parts with the same properties as the mother pieces lie in the river and are transported further to the sea. When an object has broken down to sand or even clay or loam, it washes out on the riverbanks, or alternatively washes out deep into the sea. The finer sediments are more cohesive and stick together, so they are difficult to erode (Chorley *et al*., 1984). This makes up the clay parts of the sediment and is very fertile soil. River erosion comes in different forms of abrasion when the riverbed is scraped clean of all material, as a solution of chemicals in the water dissolve the sediment that is carried away by the river, and the hydraulic action of the water that is forced into cliffs and open cracks next to the river. Sedimentary ridges and layers can be created over many years, depending on the density of the sediment (Beal & Bryden, 1999).

2.2.2 The meandering stage.

As a river reaches the middle stages, the flow of the water decreases in velocity (Leopold, 1953), and slows down in the downstream direction where the river opens up more and becomes wider before it enters the flood plain. In the case of the Thukela River, when it reaches its middle stages, it has an average height above sea level of 1200 m to 900 m (see Figure 3.2, which shows the Thukela River's long profile). As the rivers flow more slowly, the

[1] Unless stated otherwise, the photographs were taken by the researcher.

larger sediment begins to stay behind and only the smaller deposits are still carried in the flow. When they enter the flood plain and middle stages, rivers tend to meander, following cliffs and slopes that are still steep over some distance, until the rivers reach the fluvial stages.

Table 2.1: Characteristics of the Thukela, Amatigulu and Umlalazi Rivers

River Forms		
Mountain Area	**Meandering stage**	**Delta and Tidal stage**
Very steep slope 1:100*	Slope flattens to 1:1000*	Smooth to equal slope ±1:7000*
Very narrow valley	Wider channel	Flood plains are wide and open
V-shaped	More suspended sediment	Water almost comes to a standstill
Solid and rocky bed	Meandering occurs	Formation of oxbow lakes
Very fast-flowing waters	River energy decreases	Sandbanks in the last 20 km
Large rocky boulders	Start of flood plains	Low river energy

*Slope indications are not to scale according to the real slope changes of the three sections of these rivers.

2.2.3 The delta and tidal stage.

In a river's lower course, the landscape usually has a more graded long profile which reflects the landscape's general slope. To maintain this slope type, a balance is required between erosion, transportation, and deposition (Bagnold, 1980). Erosion and transportation remove sand from or add sand to the beach and deposit it in different places. When the slope starts to flatten out to a gradient of approximately 1:7000, the river deposits clay sediment on the banks of the river (Bagnold, 1980). At this stage, the river meanders widely through the landscape, following a very equal slope over the last 150 km to the sea. This is also known as the alluvial stage, and most sedimentary deposit occurs in this area (Bagnold, 1980) (see Figure 2.3). For instance, when the Thukela enters the more level plain after 300 km of steep flow, the water energy decreases and all the heavy objects are dumped on the riverbed, on the banks and in dams. The sediments are carried forward by means of suspension, saltation, and traction. The fine sediments are in motion for longer, and can continue to flow with the stream for very long distances (Chorley *et al.*, 1984). Rivers deposit the very fine and clay sediments onto the banks of the estuary. Sand tends to wash out on the beaches, while clay settles on the bottom of the river and the seabed (Anthoni, 2000). Clay deposits are very fertile – the resulting very dense vegetation adjacent to the Amatigulu and Umlalazi beaches are very good examples.

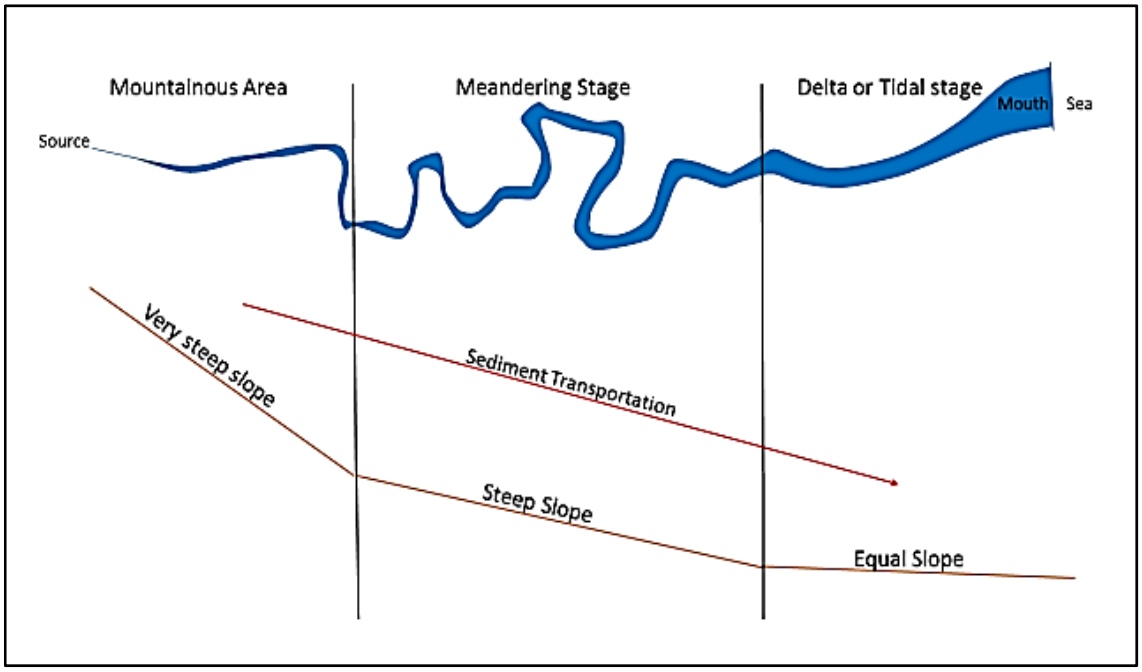

Figure 2.3: The Thukela, Amatigulu and Umlalazi Rivers, which are relevant to the study: the first section shows the initial part of the Thukela River, the middle section shows the Amatigulu River and the third section the Umlalazi River.

Suspension refers to smaller particles that are carried by the river above the riverbed. The speed at which the particles are carried depends on the energy and strength of the river. Very fine particles such as clay, silt and the soluble particles that can dissolved in the water travel the last kilometres to the ocean by means of suspension. With this process of increasing erosion, a river loses soils in its upper course, but gathers more soils and other sediments in the lower parts of the river. When the slope decreases, the river deposits the bigger objects on the riverbed (saltation) but carries the finer sediment to areas where accumulation occurs. In most areas, this happens in the fluvial area where a river flattens out (Chorley *et al*., 1984). A river such as the Thukela River carries suspended particles even beyond the river mouth, and deposits them out to sea (in the Thukela's case, on the Thukela shelf), forming part of the sedimentary layers at the bottom of the sea. With saltation, rocks, pebbles and sand that are too heavy to flow with the suspension along with the river tumble and bounce forward on the riverbed until the river energy slows down and these heavier particles then remain on the riverbed, unless a stronger energy or flood takes them forward again (Bagnold, 1980). Very fine particles travel the last kilometres to the ocean by means of suspension such as clay, silt and the soluble particles.

The sediment is mostly deposited adjacent to the banks of the river during floods. In the lower course of the river, the fluvial area and surrounding plains are low-lying areas, so

during floods, the banks are easily flooded. Sediment is then deposited on the flood plains and riverbanks, especially where rivers such as the Amatigulu and Umlalazi Rivers turn 90^0 to flow into the estuary (Bagnold, 1980). In this stage in a river's flow, the flood plains open up into a wide channel (Leopold, 1953).

Sometimes the slope is so low that rivers such as the Amatigulu and the Umlalazi Rivers come to a standstill, with no forward movement at all. In these cases, the river does not have the velocity to power itself into the sea, and this is when a river mouth is occasionally closed off from the ocean. Estuaries are renewed when rivers overflow their banks and the sediment is deposited on the banks, providing fertile soil for the estuary's ecosystem and benefiting farmers who practise agriculture along the banks. In the case of the Thukela River, in the last 20 km to the sea, braiding patterns occur. The river splits up into smaller streams with islands (sandbanks) in between (eyots) (see Figures 2.4 and 2.5). Braided patterns occur in two ways, either when sediment and sand are actively deposited on the banks of the river or when the riverbanks have a steep slope and the water comes down with enough force to carry the load of material over a wide river area (Chorley *et al.*, 1984). If one stream is not enough, floods make more streams until the load is carried through and this process leaves behind a braided pattern (Chorley *et al.*, 1984). In dry seasons, high discharge is dispatched on the beach and river sandbanks. During floods, sand from the sandbanks is washed into the sea.

Figure 2.4: Braided patterns in the Thukela River.

(Source: Google Earth 14-01-2010). Scale: 1:2150

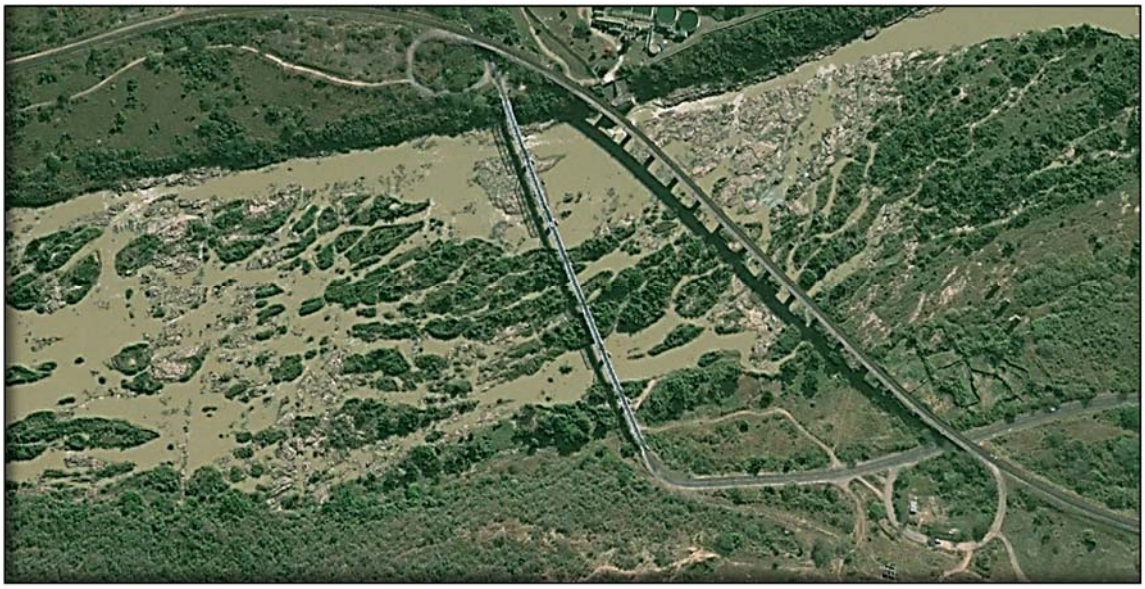

Figure 2.5: Close-up of the braided patterns in the Thukela River.

(Source: Google Earth 13-08-2009). Scale: 1:700

Sediment is pushed out to sea by the Thukela River approximately 20 to 30 km from the beach at a rate of approximately 6.79 x 10 m^3 per year (Bosman *et al.*, 2007). The Google image in Figure 2.6 shows how much sand is pushed about 30 km into the sea by the power of the Thukela River when it floods. Longshore drift takes the sand northward to the coastal bight, where it washes out near the Umlalazi coast. More sand and sediment should reach the coast, but dams starve sedimentation further downstream (Beal & Bryden, 1999).

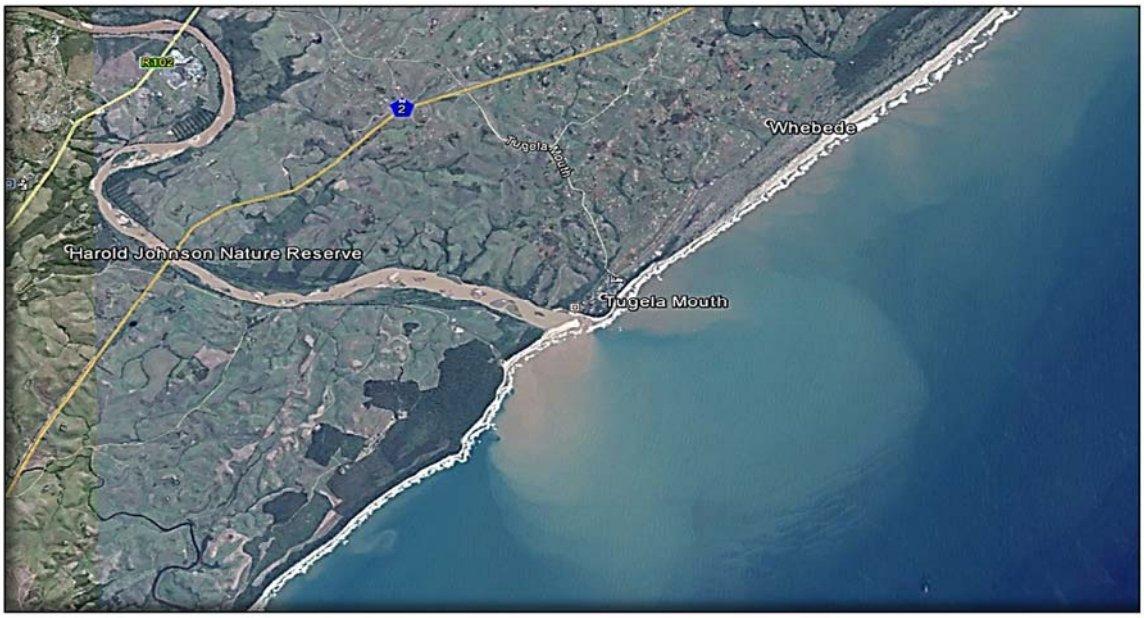

Figure 2.6: The Thukela River in flood.

(Source: Google Earth 19-02-2016); Scale: 1:8500

2.3 The Effect of Aeolian (Wind-related) Processes on Land Forms

Jackson *et al.* (2014) argue that wind can make significant changes to dunes by transporting small sediment to and from the dunes. According to Jackson *et al.* (2014), only a few studies have so far been done on the changes of dune dynamics and the contribution of river water, wind and wave energy and sea currents at the KwaZulu-Natal coast. Aeolian action as a transporter is a very powerful mechanism. Through this mechanism, it is possible for wind to force sand dunes into a specific form (Sparavigna, n.d). The mechanisms used by wind to move sediment is known as saltation (Latin *saltare* – 'to leap') and surface movement, which is called creep or creeping. Materials are moved close to the ground by wind action. Mostly, particles with sizes between 0.1 mm and 1.0 mm (Chorley *et al.*, 1984) are lifted in this way from the surface of the earth and carried by the wind through the air for some distance before landing back on the surface. When these particles land on the ground, they cause a splash movement, causing other particles to scatter and find a new position (Sparavigna, n.d). Bagnold (1941) suggests that the opposite is also true where a patch of sand and/or vegetation occurs, as it acts in such a way that saltation grains stop bouncing any further. Where such a patch grows, over the years, an embryo dune forms, and later a complete dune with proper dune functions develops. Another mechanism involves sand moving on the opposite side of a dune, the slipside (lee side) of the dune. The particles tend to move together in the same direction in which the wind is blowing, but at the crest of the dune the sand gets too heavy from the accumulation of the sand, and it then causes a sand avalanche (Sparavigna, n.d.).

Tidal waves supply large amounts of sand, and together with persistent winds, this makes a sand dune bigger or smaller (Goldsmith, 1978). At low tide, on a sandy beach (such as those on the KwaZulu-Natal coast), a large area of sand is exposed. The sand supply increases if the wind strength is high and the longshore drift washes sand out of the sea or river onto the beaches. According to Goldsmith (1978), persistent winds with moderate velocity are more effective as transporters of large quantities of sand than infrequent storm winds.

Just like water (in the form of rivers and seawater), aeolian processes are important in environments which are overpopulated by people, especially if they keep livestock and there is overgrazing and plants and trees are unnecessarily destroyed. Without any vegetation, the environment changes to semi-desert, where much of the topsoil is blown away (Jackson *et al.,* 2014). With the help of wind and animals exposing and loosening the sand, sand is blown more and more into hollow parts of the landscape where it lands in a dry or current stream which transports these sand particles down to the sea. They can be washed directly into the sea,

although sometimes the sediment comes to rest on a dune, or the dune of an estuary (Jackson *et al.,* 2014). The loss of loose soil that is blown away changes the downstream areas of an estuary.

Thus the key factor for wind to move sediment particles is the shear force exercised by the transporter. On loose sandy soil wind has a lower impact than if it is on rough terrain. Chorley *et al.* (1984) state that when there are grains about 30 mm in diameter or larger, the effective wind velocity drops to zero. When saltation takes place, it mostly does so close to the ground and in areas where it is sandy, and not in areas that are densely vegetated or at sites with rocks and stones.

2.4 Wave Energy and Sea Currents

Over time, people who look only superficially at beaches fail to see changes. According to them, there are no noticeable changes to beaches and dunes (Anthoni, 2000). Changes are usually so slow that people only notice them when a monitoring survey is done and the results are publicised in the media. However, sudden visible changes can take place when there are frequent storms, and the dunes gain or lose a lot of sand. Over the years, the surface waves erode a dune from the base and higher up. Beaches and dunes often change under the influence of the wind, waves and sea currents and changes in the sea level. Definite changes are noticeable when the waves drag more sand from the beaches and dunes during storms. Waves can also wash away sand from the coastal shelf, which is hundreds of metres below the surface of the sea, by means of the transport mechanism of longshore drift.

Davidson-Arnot (2010) describes two types of waves. The first wave type is a destructive wave with high energy that occurs in high energy bays in the form of headlands and very rocky spits. Such waves usually occur during winter and they withdraw the sand from beaches with a strong backwash (see Figure 2.7) and carry the sand deeper into the sea. There the sand flows with the sea currents to be deposited later on the sea shelf.

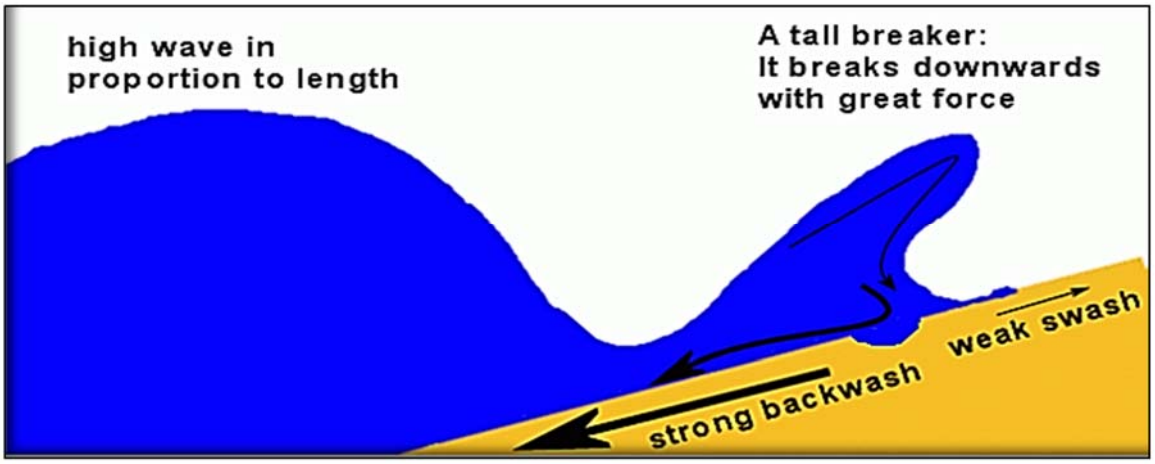

Figure 2.7: A destructive wave.

(Source: Davidson-Arnot, 2010)

A **destructive** wave occurs in a very deep sea where waves rise very high and break with great force onto the sand, then pull backwards immediately and cause a very weak swash and a strong backwash. The second wave type, a **constructive** wave, does the opposite: it has low energy (Davidson-Arnot, 2010) and occurs mostly in the summer months. A constructive wave builds a beach, making it larger by dumping sediment onto the beach or barrier (see Figure 2.8). With a constructive wave, where the direction of the wind is not strong, there is very low oscillation of the waves with a shallow sea, causing a low horizontally breaking wave and swash (the swash moves some distance forward, much further than that of a destructive wave), with low friction in the backwash.

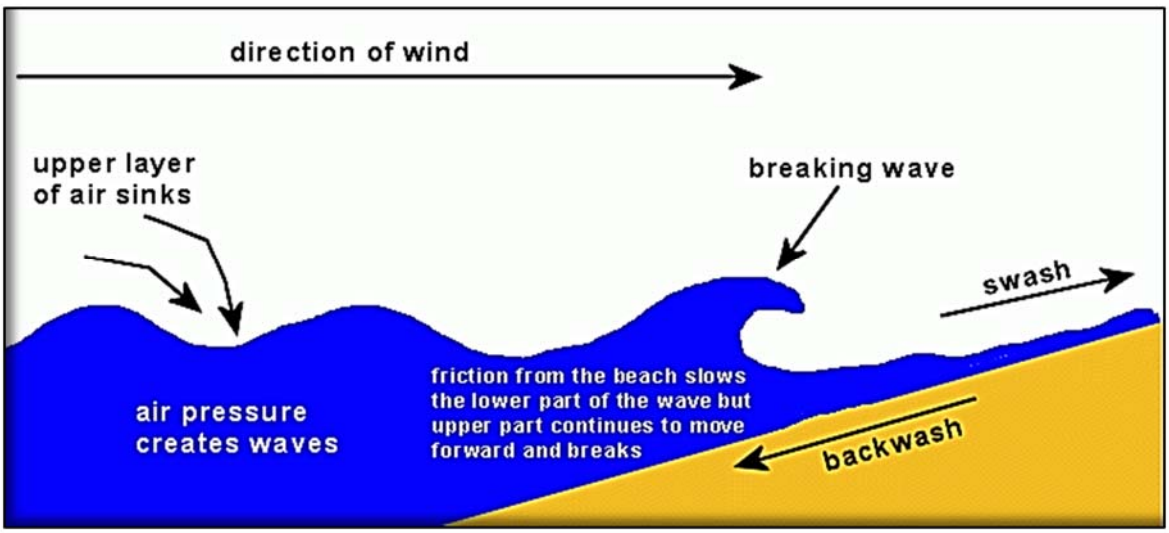

Figure 2.8: A constructive wave.

(Source: Davidson-Arnot, 2010)

As Davidson-Arnot (2010) states, waves are energies that depend on the energy-driven wind force. The more wind energy is generated over the sea surface, the higher the waves and the more friction occurs at the bottom of the sea to stir the sand into a movable condition. About 800 m below the surface, underneath the Agulhas current, there is the counter-flowing Agulhas under-current. This current flows northwards, in the direction of the equator. Some shores, such as those at the Amatigulu and the Thukela River mouths, have a steep downslope of approximately 10 to 20 m, but, according to Anthoni (2000), the shore extends further down into the sea. During heavy storms and spring tides, the sea is much deeper, and the Agulhas under-current stirs up the deposited sand and clay from the shelf (Anthoni, 2000) and washes it out onto the beaches and foredunes of the Umlalazi and Amatigulu beaches. According to Toole and Warren (1993), it can be confidently assumed that most of the sediment on the seabed is collected by the Agulhas under-current. Because it flows parallel to the shoreline, it deposits the sediment between the Umlalazi estuary and the Richards Bay area, as there is a change in the bight in the shoreline that forms a very large bend in the coastline and a change in the direction of the coast. Where the flow is approximately parallel to the coast line and close to the Amatigulu River, it intersects the shoreline at about 30^0 and therefore this sand is washed out on the beaches of the Umlalazi River estuary and further north.

With longshore drift, beaches are created by a process of sediment-dumping because the waves do not break onto the beach at an angle of 90^0 but at an oblique angle, depending on the angle of the beach (Davidson-Arnot, 2010). When the swash breaks, it has a very low energy and it drops the sediment or sand on the beach, and then the backwash draws back 90^0 towards the sea, leaving the sand behind (see Figures 2.9 and 2.10). The next wave does the same, but pushes the sediment a little bit higher up and parallel to the beach. The longshore drift thus causes the beach to move in a certain direction (Chorley *et al*., 1984; Davidson-Arnot, 2010). When the sediment moves away from the beach and in a direction of the breaking wave, barriers are formed and built. When waves push sand outwards to the beach, it does not roll backwards, because on beaches the slope is so shallow that there is no backtracking, only sideways movement because of the longshore drift (see Figure 2.9). When the wave moves back and loses energy, it retreats at a 90^0 angle to the shoreline. On the other hand, when there is a spring tide and/or stormy weather, the backtrack is just as powerful as the breaking wave, so it pulls the sand to deeper waters, where it lands in the Agulhas under-current that flows north and washes out on a beach that has a direction of 250^o, according to the South African coordinate system.

Psuty (1992) has recognized that variations in the spatial and temporal scales of foredune development produce a sequence of distinct developmental forms with characteristic morphologies. The various combinations of dune and beach sediment budgets are implicit to spatial models of foredune sequences. Psuty (1992) notes that coastal foredunes persist and shift inland even in areas where there is continued beach erosion. This would suggest that the foredune morphology may be conceptually separated from the budget of a beach. The optimum condition for foredune growth is a slightly negative beach budget, where sediment is continuously transported from the beach into the foredune.

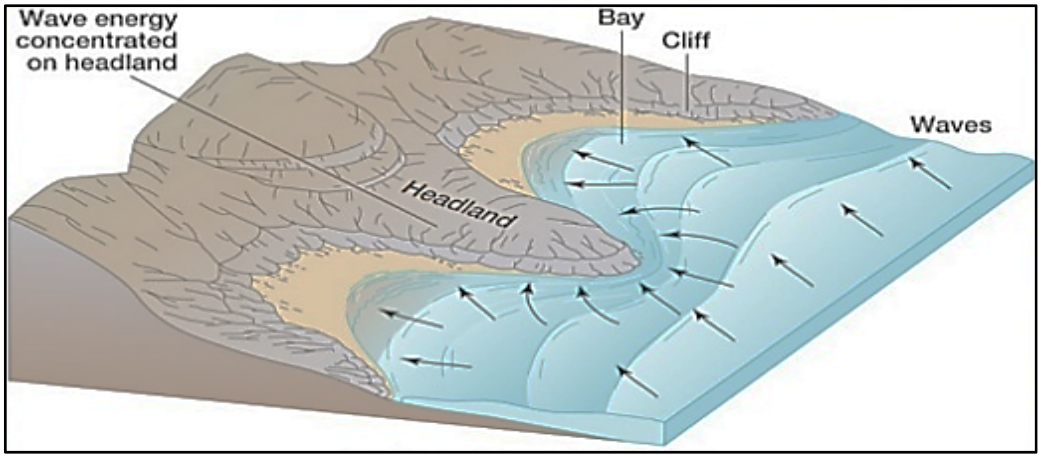

Figure 2.9: Wave energy is concentrated at headlands and dissipated in bays.

(Source: Krishnaprasad, n.d.)

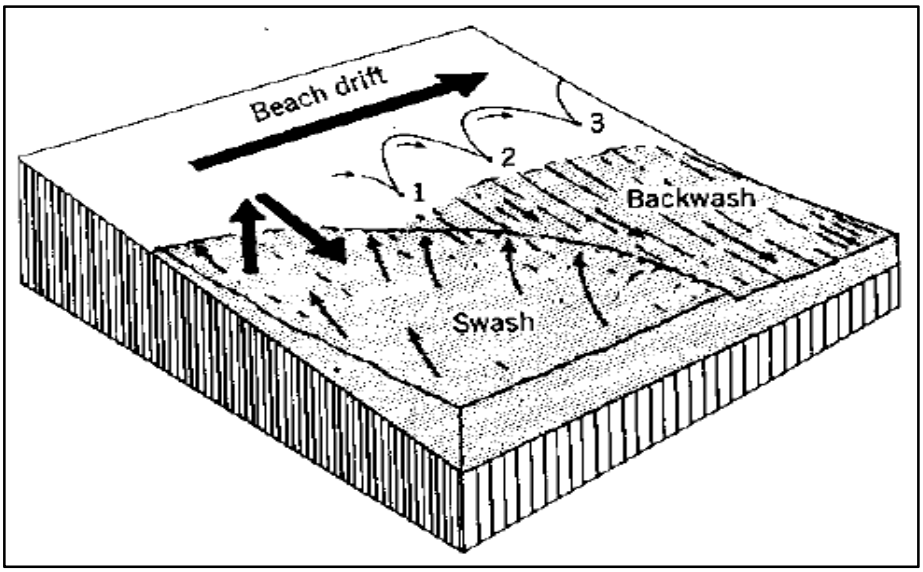

Figure 2.10: Beach and sediment drift – the swash enters the coast at an oblique angle under a longshore current; the sea draws back at 90^0 to the beach (the particle path is shown as 1-3).

(Source: Chorley *et al.*, 1984)

2.5 Prior Case Studies

A number of case studies in the literature have explored changes in dunes, estuaries and beaches. Several of these studies are reviewed below.

a) Marker (2004) found evidence of rapid changes in the Salt River flood plain in the Western Cape (South Africa) and the river's estuary over a period of 60 years. She used aerial photographs taken over that period. She also observed surveys on sedimentary changes that took place during the floods in 1996 (Hodgson & Allanson, 2000). Marker (2004) argues that aerial photographs are appropriate and sufficient for monitoring changes in the environment. She constructed base maps from 1989 using orthophotos with a scale of 1:10 000, and plotted all the changes from 1968 to 1998 and compared these changes with the base map. Marker (2004) overlaid a coordinate grid to help the plotting (in percentages) of the changes in land use for the same period.

b) The only accretion rates, based on aerial photographs, recorded for the Thukela mouth area in 1991 were found on the northern shore of the Thukela mouth (Cooper, 1991b). The aerial photographs indicate a short-term reduction of the sediment supply of the Thukela River (Cooper, 1991b).

   Olivier and Garland (2003) monitored dune changes with regular topographical surveys of embryo dunes and the foredunes at the Thukela mouth. The data that they plotted corresponded with Psuty's (1992) model, and indicate no evidence to confirm that the dunes are retreating backward because of sea erosion. Olivier and Garland (2003) state that their findings could be possibly be attributed to irregular monitoring over a short period. A total station was used to survey the Thukela mouth. Control stations were placed strategically so that these points could be used for further surveying that took place from July 1993 to February 1996. This survey was linked to the South African coordinate system, with survey reference Lo 31^{o}. The beacons used for referencing were Beacon Number 20, Mangete, at a height of 118.8 m above mean sea level, and Beacon Number 140, Redhill, at a height of 88.4 m above mean sea level (Cooper, 1991b). With the total station cross-sections were measured and plotted them using a computer aided design (CAD) program, Stardust, for Microsoft for Windows. Accurate plans were drawn up and volumes were calculated from successive areas or surfaces.

c) In the Taklimakan desert in northern China, Dong, Xunming, and Chen (2000) did a topographical survey from 1991 to 1993 to determine the rate at which the dunes advanced. Dong *et al.* (2000) determined that the mean advance rate of the dunes in 1991 was 7.29 m, and that it was 5.56 m in 1993 in a south-westerly direction, the same as the local wind

direction. The site under survey was located south of Xiaotang and 200 m east of the desert highway. The monitoring site was 100 m x 100 m, at an average height of 940 m above sea level (Dong *et al.*, 2000). The topography of the dune in this 100 m^2 area was surveyed using a theodolite and surveying staff and the plans were plotted against a mapping scale of 1:500. Dong *et al.* (2000) focused on the morphometric parameters of the dunes: their length, width, height and volume. The volumes were calculated by integrating the closed surface of a contour area with the next enclosed contour area. The mean areas of both surfaces were then calculated and multiplied with the vertical distance between the two successive surfaces from the base to the top of the dune. The direction of dune movement was determined by comparing topographic and contour maps surveyed in the preceding years.

d) A study by Jamieson and Van Dijk (2004) in North Beach Park, Ottawa County, Michigan, in the United States, focused on the migration of a parabolic dune that may have a negative impact on the community. The parabolic dune forms part of a popular beach area, playground and parking lot and there is a dune overlook deck (Jamieson & Van Dijk, 2004). The access road, North Shore Road, curves round the landward side of the dune (Jamieson & Van Dijk, 2004). The concern is that according to surveying results, the sand is moving towards the North Shore Road at a rate of 0.7 m per year. Engineers predicted that it will cover the road by about 2022 (Jamieson & Van Dijk, 2004). The results were arrived at by surveying the dune using a Topcon GTS-4 electronic total station. Four posts or poles were also planted in the ground and measurements were taken from points at positions established on the ground to serve as control points to determine the movement of the sand. Fixed points were used as references on the terrain such as markers and flags on trees, corners of walkways and concrete foundations. Figure 2.11, overleaf, contains a diagram showing how dune changes are recorded relative to posts installed at the edge of a transgressive dune's slip face.

   These points were used for and recorded for future surveys and coordinates determined on the surface to cover certain objects such as pathways, grass and sand deposits. Each time the total station was set up, it was oriented with compasses to find north (Jamieson & Van Dijk, 2004). After the total station was oriented, vertical and horizontal angle readings were taken on a prism. The prism reflects a light ray sent by the total station and the total station calculates the time between the two objects for the distance to be displayed between the total station and the prism. The total station displayed a slope distance, a horizontal distance and a vertical distance. With each survey interval, topographical maps were generated, so the migration and the rate of the dune changes could be determined over this period (Jamieson & Van Dijk, 2004). The survey data were entered into a Microsoft Excel

spreadsheet to determine the local coordinates, and thereafter the data were converted to a national grid system using Rock Works software. A critique against this method is the time wasted on the orientation of the total station with the help of compasses to determine north. The total station could simply be oriented using two or three reference markers established during the survey. This survey is relevant to the current research survey at the Umlalazi beach, with the difference that the orientation points were set out using coordinates surveyed and determined by a GPS.

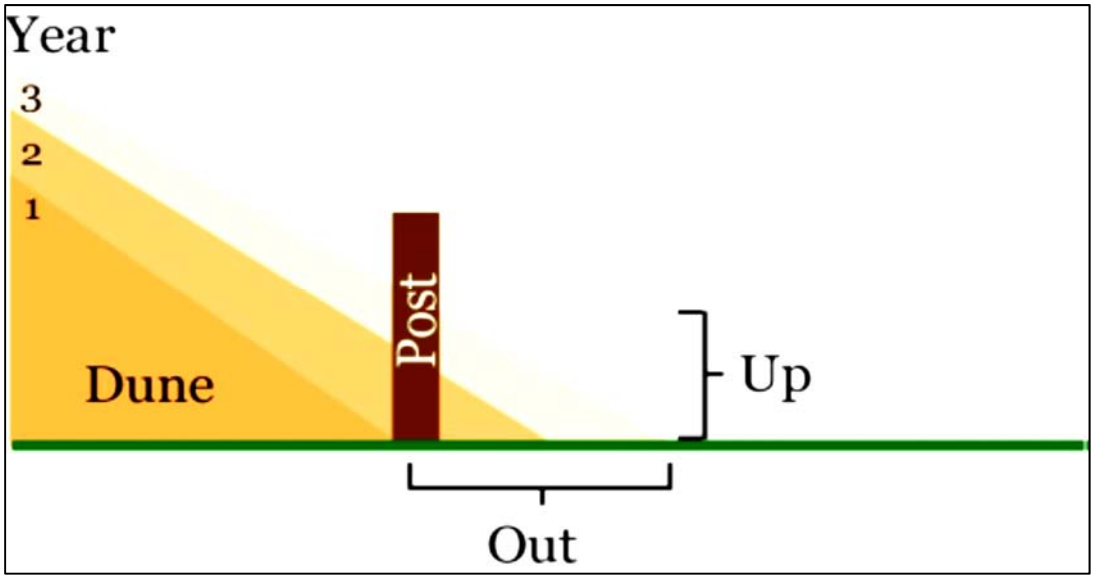

Figure 2.11: Recording dune changes relative to posts at the edge of a transgressive dune's slip face.

(Source: Jamieson & Van Dijk, 2004)

e) In the southern parts of the United States, the Native American Navajo people are challenged by increasing migration of sand volumes that threaten their housing and transport, and pose a health risk for the community. The United States Geological Survey (USGS) did a study on the movement of dunes in this area. This study shows increasing movement of the dunes. Different methods of surveying were used by the USGS. The area was mapped by aerial photography, remote sensing and the use of Global Positioning Systems (GPS). The data were compared to existing older data of the terrain. It was found that the sand moves approximately 35 m per year – Figure 2.12 shows a small part of the Grand Falls dune field indicating recent migration of the dunes (from 2005 to 2010) plotted on a satellite image taken in 2005. These dunes have migrated at a rapid rate of more than 330 feet (100 m) in just five years (Redsteer, Bogle, & Vogel, 2009). The dominant wind direction was from the south-west throughout the period under review.

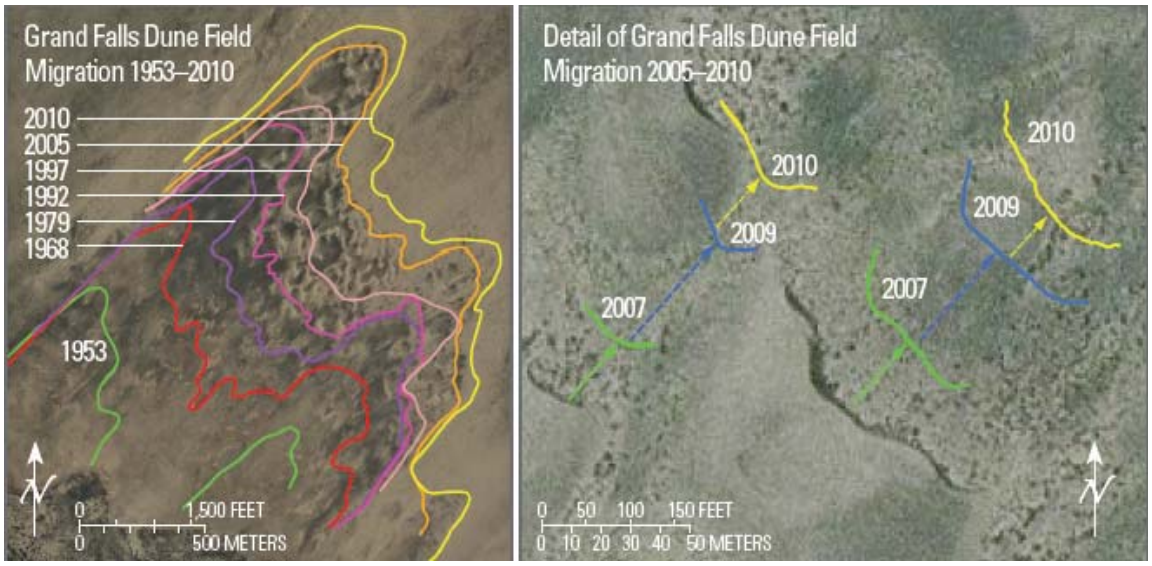

Figure 2.12: Grand Falls Dune Field migration 1953-2010 plotted on an image from 2005 (wind direction shown at lower left).

(Source: Redsteer *et al*., 2009)

f) Labuz (2015) provides a detailed description of the surveying methods and equipment used to survey foredunes on the Polish coastline since 1997. Labuz (2015) explains that 85% of Poland's coastline is covered with different dune types and foredunes. The changing tendencies and variables required research on dune changes and movements which seemed to occur even over a very short period. The morphological changes and the increase in the number of new foredunes was the main reason for his study. Labuz (2015) used levelling, a 3D leveller, Lidar and GPS to determine the position and height of points related to the changes of the beaches and the dunes. The dunes were monitored over a long period, so different instrumentation was used to suit the researcher's purposes, but as time went by, the instrumentation became more technologically advanced (some examples are shown in Figure 2.13). In cases where there were rapid dune changes, like embryo dunes, he placed a rod one metre deep into the sand to monitor the sand volume change and the relief changes over a short period (Labuz, 2009) (see Figure 2.14). In some cases, the relief changed so much and so rapidly that measurements had to be taken at about an hourly rate (Labuz, 2009), especially in stormy conditions with high aeolian velocities. In such situations the Emery method can be used where there are too few human resources: only two rods are planted into the sand at a distance of 10 m from each other and the height readings are taken using the sea horizon as a reference line (Labuz, 2009).

Figure 2.13: Different instruments that surveyors use: (from left to right) a total station, a GPS and an automatic level (instruments photographed courtesy of the University of Pretoria).

At some sites 5 m x 5 m, Labuz (2009) set out squares with rods planted one metre deep into the sand. With this method, it was possible to monitor the height changes and the positional changes of the sand in the square (Labuz, 2009). One of the oldest and most conventional levelling methods is still the use of the popular collimation height method. A level is set up at a position where a great deal of the terrain is visible. A reading on the staff held at a reference benchmark (a point with a known height above a certain reference line, for example, sea level) is taken and then added to the reading to get the height of the level. All readings taken on the surveying site are then subtracted from this instrument height, known as the collimation height. In this method, the staff or survey rod must be visible at all times from a specific levelling setup. Labuz (2015) used the collimation height method for surveying cross-sections on the beach area.

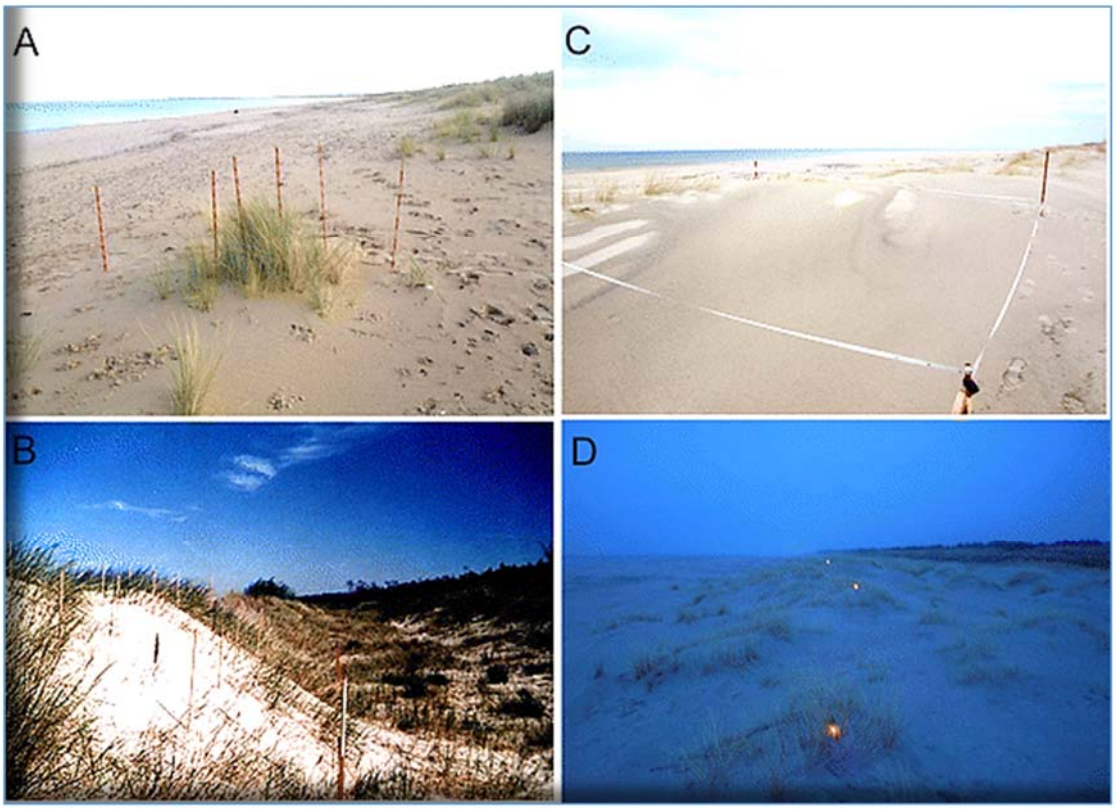

Figure 2.14: Methods used by Labuz (2009).
A: A small embryo dune is beaconed off with surveying rods.
B: Part of an existing dune is fenced off to identify changes.
C: Survey poles mark a 5 m^2 part of the dune to monitor changes (some hourly).
D: Monitoring continued even at night, using torches planted strategically on embryo dunes and foredunes.

The reference height is an established benchmark with a known height above the mean sea level. All the cross-sections taken from that levelling position relate to the benchmark. The disadvantage of taking cross-sections is that the only details measured are those on the section line. If sections of a certain interval are taken, the details between successive cross-sections are lost (Landman, Hunter, & Jackson, 2012). Thus it is always advisable to take cross-sections at the smallest possible intervals. Factors such as the scale, the slope, the contour interval and detail have a significant influence on cross-section distribution, and particularly on the spot level density. In general, it can be assumed that spot levels must not exceed approximately 3 cm x 3 cm in a grid format on any plan. For example, if the scale of the plan is 1:500 and there is a smooth surface or gentle slope, then the cross-section distance could be approximately 15 m on the ground, but the steeper the slope, the more spot levels should be taken, so that not more than one contour goes through between two successive spot levels.

Following on from the background literature, the study area is discussed in more detail in the next chapter.

Chapter 3:

Study Area

3.1 Location

The study area is the coastal zone from the Thukela River mouth northwards to the Amatigulu River estuary and the Umlalazi River estuary on the KwaZulu-Natal north coast. These three sites or areas were identified for the assessment of dune and sand movement. The most southern site, the Thukela River mouth, is situated approximately 84 km from the city of Durban, and the most northern site, the Umlalazi River estuary, is approximately 40 km south of Richards Bay.

A broad outline of the KwaZulu-Natal coastline is given in this chapter, followed by the three catchment areas of the Thukela, Amatigulu and Umlalazi River estuaries. Finally, the relevant study sites chosen for the documentation of the sand barriers are discussed in detail.

3.2 The Coastline Considered in the Study

The Thukela River divides the KwaZulu-Natal coast into a northern and a southern coastline area. KwaZulu-Natal's northern coastline runs approximately from the south-west to the north-east – the coastline runs in approximately a 220^{o} south-easterly direction according to the Gauss conformal coordinate projection system used in South Africa. It has extended sandy beaches all the way past Richards Bay. These beaches are occasionally interrupted by the tidal inlets of rivers and estuaries (Olivier & Garland, 2003). These rivers are fed from many tributaries in their large catchment areas.

The South African coastline is relatively narrow along the remainder of the continent, but at the Natal bight, the coastline is wider, running inland from the coast for about 50 km. However, the beach areas themselves are no more than 80 m wide (Cooper, 1991a). Cooper (1991a) describes this coastline as a prograding beach ridge coast. Most of the dunes have an average height of 5 m and they all run parallel to the coastline (Cooper, 1991b).

In the last decade, the KwaZulu-Natal coastline has been subjected to substantial levels of erosion because of intense storms such as the one on 19 and 20 March 2007, when waves with a height of eight metres hit the KwaZulu-Natal coast and caused extreme damage to the coastline (Breetzke, Parak, Celliers, Mather, & Colenbrander, 2008). The materials at the bottom of the river and on the lower parts of the sandbank are the debris discharged by the Thukela into the sea and estuaries (Begg, 1978). This erosion of the dunes raised the sea shelf. In winter,

this excess sand on the sea shelf is then carried northwards, helped by the sea current (the longshore drift) that runs close to the beach in a north-easterly direction, parallel to the coastline (Breetzke *et al.*, 2008).

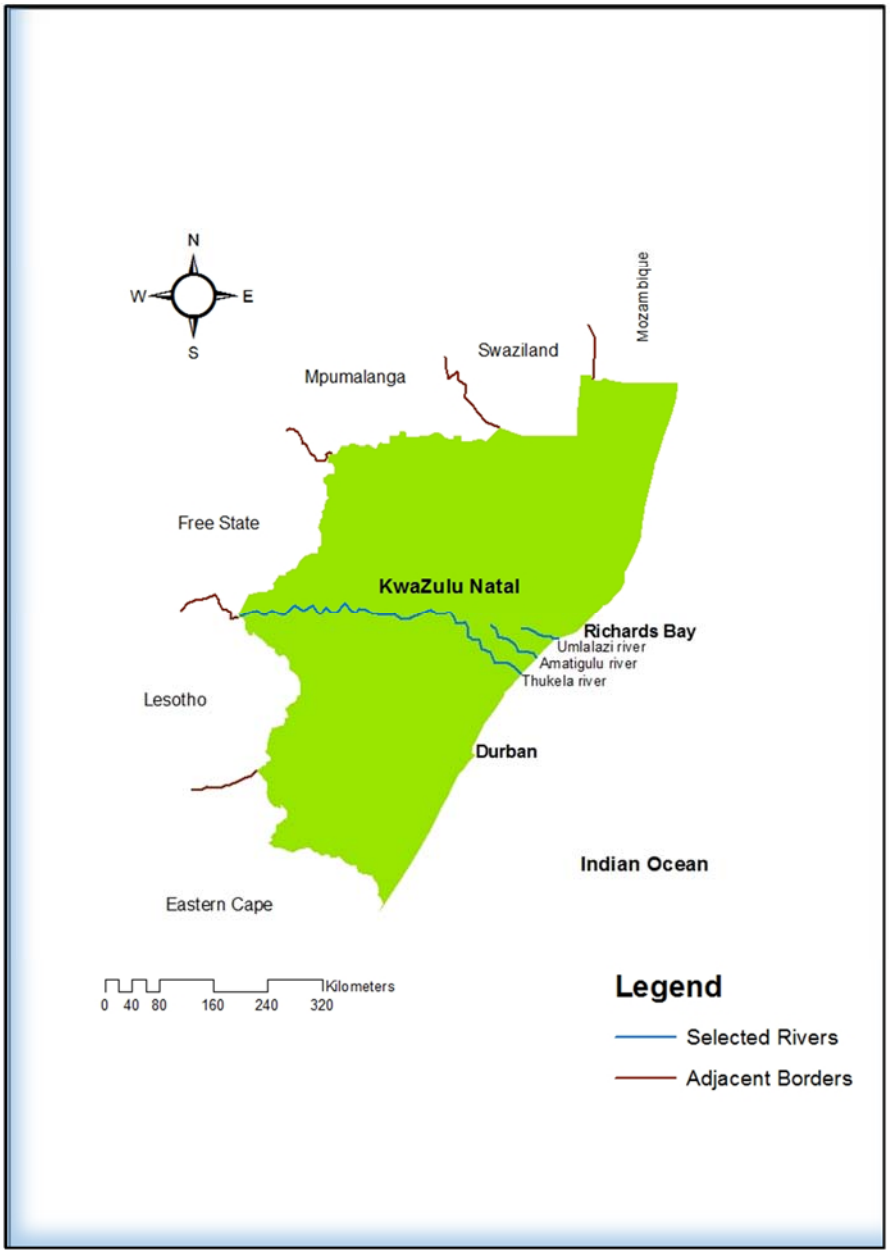

Figure 3.1: Small scale map of KwaZulu-Natal showing the position of the Thukela, Amatigulu and Umlalazi Rivers running from west to east to the Indian Ocean.

3.3 Climate and Rainfall

During most months of the year, temperatures vary from hot to very hot. The minimum temperature during June and July is just over 10°C, and during December and January it is over 25°C to 30°C. Govender (2000) notes that during winter, an average day-time temperature of

27^{o}C is normal, mostly with clear skies and a light breeze. The hot and dry conditions in the winter months makes the vegetation susceptible to veld fires. During the summer months from October to March, the coastal area receives 70% of its rainfall, with an average annual rainfall between 1000 mm and 1200 mm (Pistorius, 1962).

Table 3.1: Annual average rainfall (1998-2018).

Year	JAN	FEB	MAR	APR	MAY	JUN	JUL	AUG	SEP	OCT	NOV	DEC
1998	89.4	136.2	83.4	85.2	17.2	0.0	54.4	14.8	84.0	138.4	60.0	123.8
1999	111.0	311.4	74.6	30.0	88.2	20.2	89.2	96.8	119.6	213.0	64.2	137.0
2000	248.4	89.4	205.2	83.4	126.0	4.8	0.0	0.0	120.4	109.2	426.2	289.6
2001	137.8	158.8	101.6	89.0	24.0	4.0	5.4	8.4	208.8	73.0	117.4	108.0
2002	127.8	84.8	0.4	6.2	2.6	61.4	349.2	21.6	66.0	39.8	127.2	8.8
2003	35.0	43.2	36.0	57.6	9.0	104.0	42.2	18.6	97.0	0.0	136.6	41.6
2004	364.8	218.0	160.6	119.4	26.0	3.4	150.4	51.4	110.2	50.4	168.6	24.2
2005	105.6	133.4	108.4	13.8	50.4	72.6	2.4	25.8	52.8	141.2	174.6	123.2
2006	83.4	139.2	121.8	181.8	133.0	178.2	0.0	185.0	59.4	220.6	249.8	266.4
2007	122.8	14.4	47.2	306.2	4.4	303.0	15.0	64.2	115.6	373.0	253.4	89.8
2008	146.8	142.4	344.2	160.0	20.0	15.2	5.0	54.6	91.0	43.8	85.8	122.8
2009	168.6	82.2	40.6	87.6	33.8	27.0	4.2	122.2	42.8	88.2	115.4	96.0
2010	84.6	99.4	79.4	62.8	23.4	47.0	18.2	40.2	29.2	115.6	120.4	98.4
2011	191.8	80.2	60.4	130.4	22.2	33.2	227.2	83.8	62.8	102.4	238.2	122.0
2012	51.0	96.6	224.6	39.4	4.0	29.2	22.0	9.8	269.8	219.0	86.8	134.4
2013	286.6	142.6	99.8	35.2	39.4	36.2	45.8	25.0	84.6	127.0	144.8	104.6
2014	34.0	93.8	133.4	50.4	41.6	27.6	14.0	12.8	13.2	80.8	25.6	68.0
2015	61.2	118.4	37.6	66.2	6.6	15.8	238.0	5.4	58.8	29.2	76.4	138.2
2016	47.4	14.2	76.8	69.0	206.0	42.8	187.4	50.6	96.4	95.2	96.0	40.0
2017	76.4	244.6	77.4	24.8	59.2	5.8	13.4	14.0	17.4	27.6	16.0	18.4
2018	105.0	133.4	81.4	81.2	230.6	No data available						

Note: The rainfall was measured at the Mtunzini weather station established in 1993, and no data are available from June to December 2018. Mtunzini falls in the study area.

(Source: SA Weather Bureau, 2018)

In the study area, the climate is mild to very warm, with high humidity during the rainy season. In the rainy season, heavy rainfall can occur, but during the dry season, the average monthly rainfall is approximately 45 mm. According to Köppen (1936) and Geiger (1954), this climate is classified as Cfa. This code indicates a humid subtropical climate with hot summers and high rainfall. During the summer months, the ocean surface warms up to create tropical

storms, as described in Chapter 1, with high rainfall peaks. These storms normally occur between the latitudes 25^{o} and 40^{o}, and on the eastern side of a continent, which applies in the case of the KwaZulu-Natal region. The average annual temperature in the study area is 21.2°C (calculated from Appendix D). Rainfall mostly occurs in the months from January to March, with January peaking at 146 mm (see Figure 3.2). As the temperature drops in winter, so does the amount of precipitation.

The precipitation in Mtunzini and the surrounding areas is very high, relatively speaking. There is a definite fixed pattern in the yearly rainfall, with high rainfall from October to March, and a decrease from April to August, during the winter months. In the year 2000, sporadically, high precipitation occurred, and the rainfall in January and March was much higher than usual. Moreover, the precipitation in April and May for that same year was above average, close to 140 mm (see Figure 3.2).

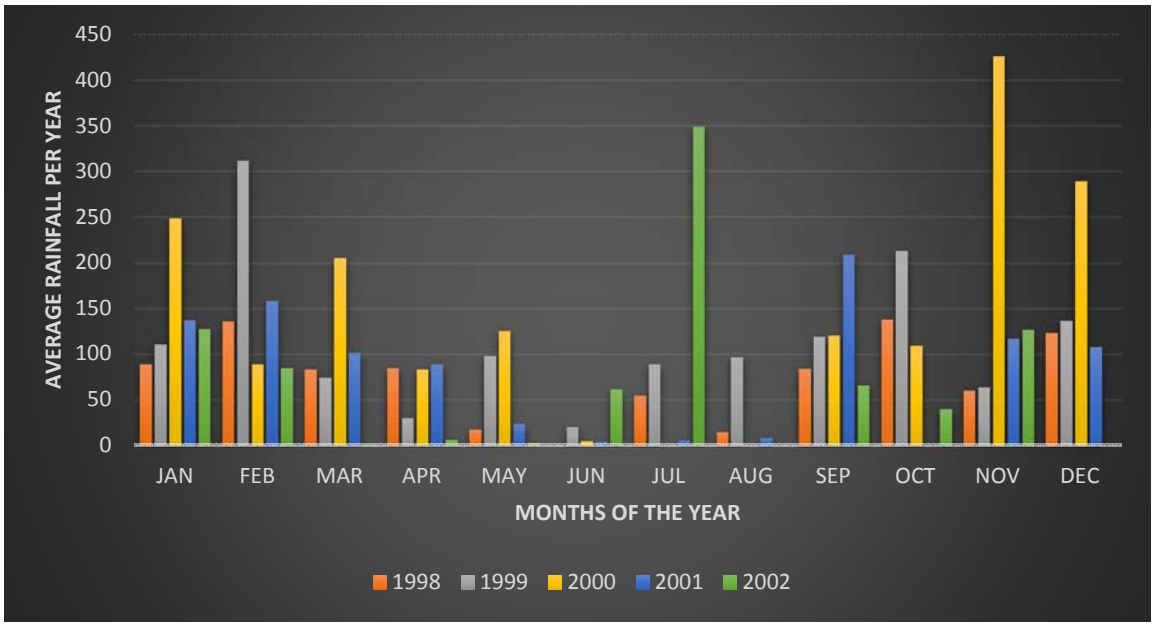

Figure 3.2: Average rainfall from 1998 to 2002, measured at the Mtunzini weather station.

(Source: South African Weather Bureau, 2018)

During the second interval reflected in Table 3.1, from 2003 to 2007, rainfall was fairly even in all the months of the five years, except during June 2004. A steady rise in rainfall and an equal distribution in this rise can be observed for 2006. The same trend can be noted for 2007, with a very high rainfall, averaging about 300 mm every four months, with lower precipitation during the winter months of the year (see Figure 3.3). In the third interval, from 2008 to 2012, a much more normal rainfall pattern can be observed, although there were extreme drops in the pattern in March, September and October 2012 (see Figure 3.4).

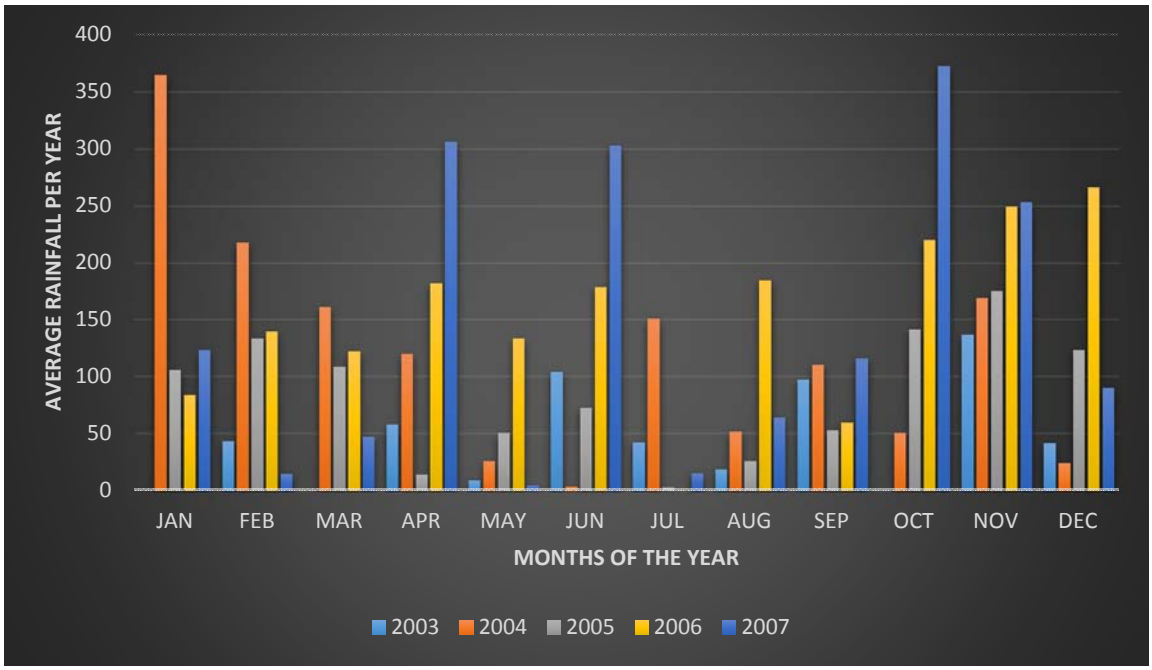

Figure 3.3: Average rainfall from 2003 to 2007, measured at the Mtunzini weather station.

(Source: South African Weather Bureau, 2018)

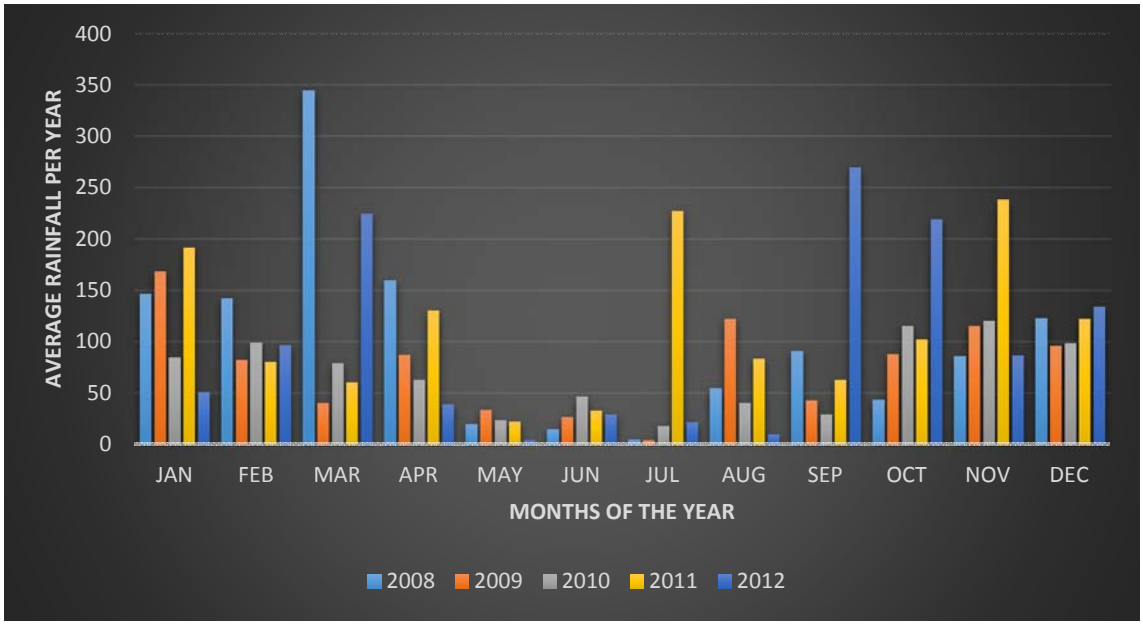

Figure 3.4: Average rainfall from 2008 to 2012, measured at the Mtunzini weather station.

(Source: South African Weather Bureau, 2018)

In the fourth interval (2013 to 2017), January 2013 had an average rainfall of 287 mm. Extreme cases were also recorded in 2016, during May (206 mm), June (46 mm) and July (187 mm), which is not the familiar rainfall pattern for Mtunzini, and there continued to be a high average for most months. In 2014, the more conservative rainfall pattern common to the area was recorded (see Figure 3.5).

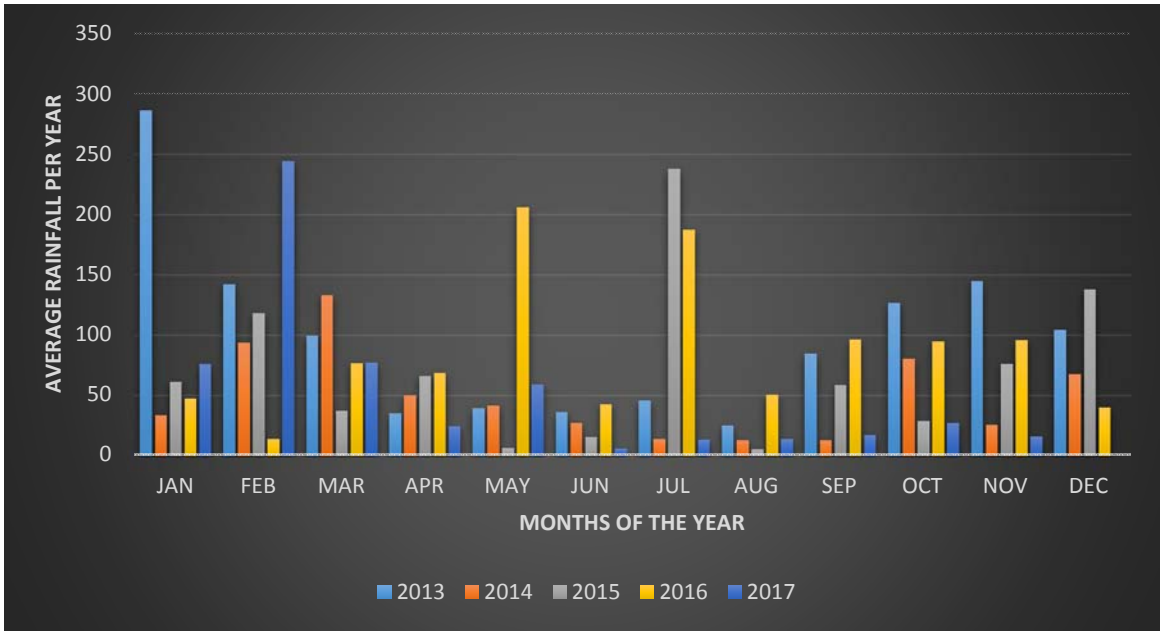

Figure 3.5: Average rainfall from 2013 to 2017, measured at Mtunzini weather station.

(Source: South African Weather Bureau, 2018)

3.4 Geology and the Geomorphology of the KwaZulu-Natal Coastline

The Natal coastline slopes steeply down towards the sea, because it lies on the Natal monocline (Govender, 2000). The landscape slopes down because of the Gondwanaland break-up 150 million years B.P. (Archaeology and Natural Resources of Natal, 1951; Govender, 2000). Govender (2000) notes that the axis of the monocline is about 40 km inland and runs parallel to the coast. East of this axis are the Karoo rocks – the Karoo Super group sediments, which contain extensive coal resources used to generate the bulk of South Africa's electricity. When the Gondwanaland break-up occurred, the movement was so intense that it cut deeply into the surface of the earth, creating a landscape where the rivers run very steep and fast eastwards to the sea. The North coast is underpinned by a granite base, and the seaward side features Natal Group Sandstone, Dwyka Tillite, Lower and Middle Ecca shales and sandstone (Govender, 2000). In the lower courses of the riverbeds, deposits of sediment and sand occur. These sand

concentrations are mostly close to riverbanks, sand dunes and estuaries, and help form the KwaZulu-Natal province's long narrow beaches (Govender, 2000).

The geomorphology of coastal dunes is subjected to sea, atmospheric, fluvial and tectonic processes (Cooper, Smith, & Green, 2013). Dunes constantly move and change shape when the wind is strong, and if it has a high velocity for long times in a certain direction. When very strong winds or storms occur, they drive the sand over the top of the dune where it accumulates. When the sand has accumulated too much, it slips over on the lee side (back), also called the slip face, of the dune. This is known as the avalanching side of the dune. When avalanching takes place, the dune moves forward in the direction in which the wind blows. This is a repeated process, especially when the wind blows for a long time in the same direction. An inter-dune deposit can form (see Figure 3.6).

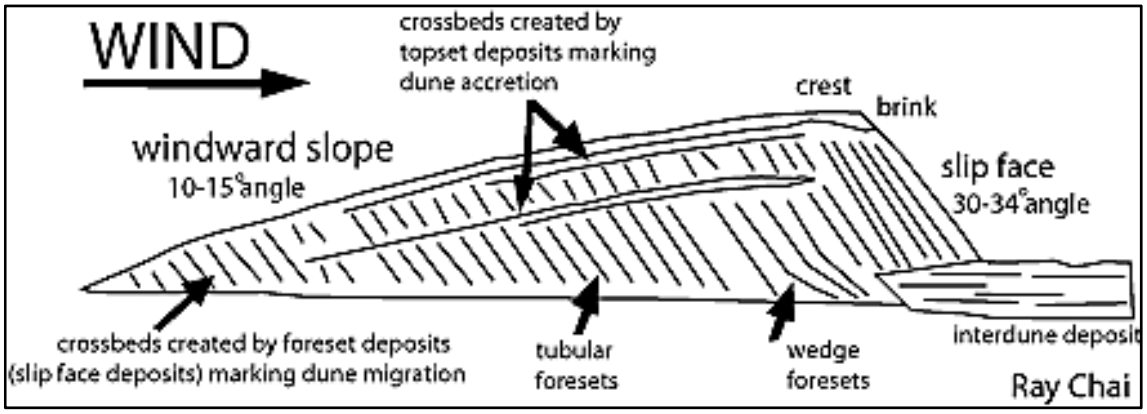

Figure 3.6: The structuring of a sand dune.

(Source: Tresselt, 1960)

With the wind regime and the wave regime, the barriers and the beaches are more dynamic. In KwaZulu-Natal, the wave regime has a direction of 225°, as the coastline is scaled at a direction of 225°, according to the South African coordinate system. There is thus a tendency for the longshore drift to be parallel to the coastline. At the Umlalazi River, the coastline changes from 220° to 250° (a change of 30° to the coastline). Most of the sediments carried with the longshore current are deposited on beaches northwards.

Psuty (1992) indicates that changes to dunes and beaches are frequent but temporary, and that the morphological changes that take place on a dune or beach are cyclical because sand is eroded from the dune and then it is added again, depending on the frequencies to the next storm or sea level change. Psuty (1992) noticed that dunes and beaches have a tendency to

recover themselves over time, with dunes moving further inland if the beach continues to experience constant erosion. Psuty (1992) argues that foredune growth has a more positive sediment budget over beaches, because there is more continuous sediment transport from the beaches to the foredunes over time.

Beaches erode when the sand supply cannot keep up with the loss of sand when storms are more frequent, following rapidly on each other, cutting away the sand into the sea. Beaches and dunes obtain their sand supply from the transportation of rivers coming from inland. However, the transportation of sand through rivers may be reduced when sand is retained by dams in the waterways, especially dams in the Thukela River, such as the Woodstock, Driel and Spioenkop Dams. If these dams were not present in the Thukela, tons more sand would flow down into the sea, where the sea currents distribute the sand onto adjacent and more remote beaches.

The sand or sediment that is washed into an estuary onto a barrier consists of flood deposits originating from the catchment area (Marker, 2004). Changes in the dunes depend on the sediment deposits that are dumped from the river on the banks of the barrier. As the dunes change, there is a complex interaction between wind, sediment supply from the rivers as described above, and the geomorphology of the beach environment (Sloss, Shepard, & Hesp, 2012). Given all these factors, the geomorphology of the Thukela, Amatigulu and Umlalazi Rivers depend on the geology and the erosion that takes place in the various soil formations. The situation is also affected by human occupation, as overpopulation leads to overgrazing, the reduction of water resources through human use leads to less vegetation, less cover and more loose soil. The loose soil is transported easily by wind and heavy rainfall from small rivers to larger rivers (Department of Water Affairs and Forestry, SA, 2004). Heavy rainfall thus contributes to a loss of topsoil and sediment in the catchment areas. With the loss of topsoil, the veld degrades by erosion.

3.5 Vegetation and Land Use

Adcocks (also cited in Govender, 2000) claims that the east coast of KwaZulu-Natal was covered by the indigenous forest until the last 600 years. Since then, these forests have been replaced by false grassland (Adcocks, 1953; Govender, (2000). When there is more grassland, more seasonal veld fires occur, started by humans and by lightning. Many savanna grasslands have the capability to recover after being destroyed by fire, but not all can recover after a veld fire (Govender, 2000). For millennia, vegetation has been eroded by nature itself, but humans have been the main destroyers of all types of land cover, through the introduction of livestock,

the collection of firewood and erection of buildings. Therefore there is always constant change through natural and human processes (Govender, 2000). Therefore, land use involves a percentage of land cover. In this regard, it is worth noting that the north coast, the study area in this research, features the most intensively cultivated and populated sugar cane fields in South Africa (Govender, 2000).

3.6 The Thukela Shelf

A continental shelf, and in particular, the Thukela Shelf, is a plain that extends with a very low gradient into the sea, where it meets the deep ocean (see Figure 3.7). The sedimentary deposits collected from rivers and sandbanks are distributed in different sedimentary levels from the coastline. When the sand from a river is pushed into the sea, it is still in an area called the mouth bar. Over time, the force of the river pushing sand into the sea forms mid-shelf mud, between the -30 m and the -40 m contour lines. The muddy sand and the mud in the outer shelf sink deeper into the sea, and, over the years, it forms what is known as a continental shelf (Bosman *et al.*, 2007). It is relevant to the current study that Bosman *et al.* (2007) note that, in the case of the Thukela Shelf, the KwaZulu-Natal coastal shelf is close to the Thukela drainage system, reaching a width of about 45 km, which is much wider than the remainder of the KwaZulu-Natal coastal shelf.

This shelf is so wide because the power of a very active river such as the Thukela River drives sediment deposits deep into the sea. The sand, with its larger granules, flows deeper into the sea and joins up with the southward-flowing Agulhas current (Bosman *et al.,* 2007). Finer sediments in the form of clay and silt that contain chemical and biological ingredients make possible binding processes and they are deposited on the seabed under enormous pressures, later forming sedimentary rocks. Most of the continental shelf around the coast is approximately 10 to 12 km wide, but the shelf increases in length from Richards Bay to just south of Durban and a width of approximately 45 km from the coastline.

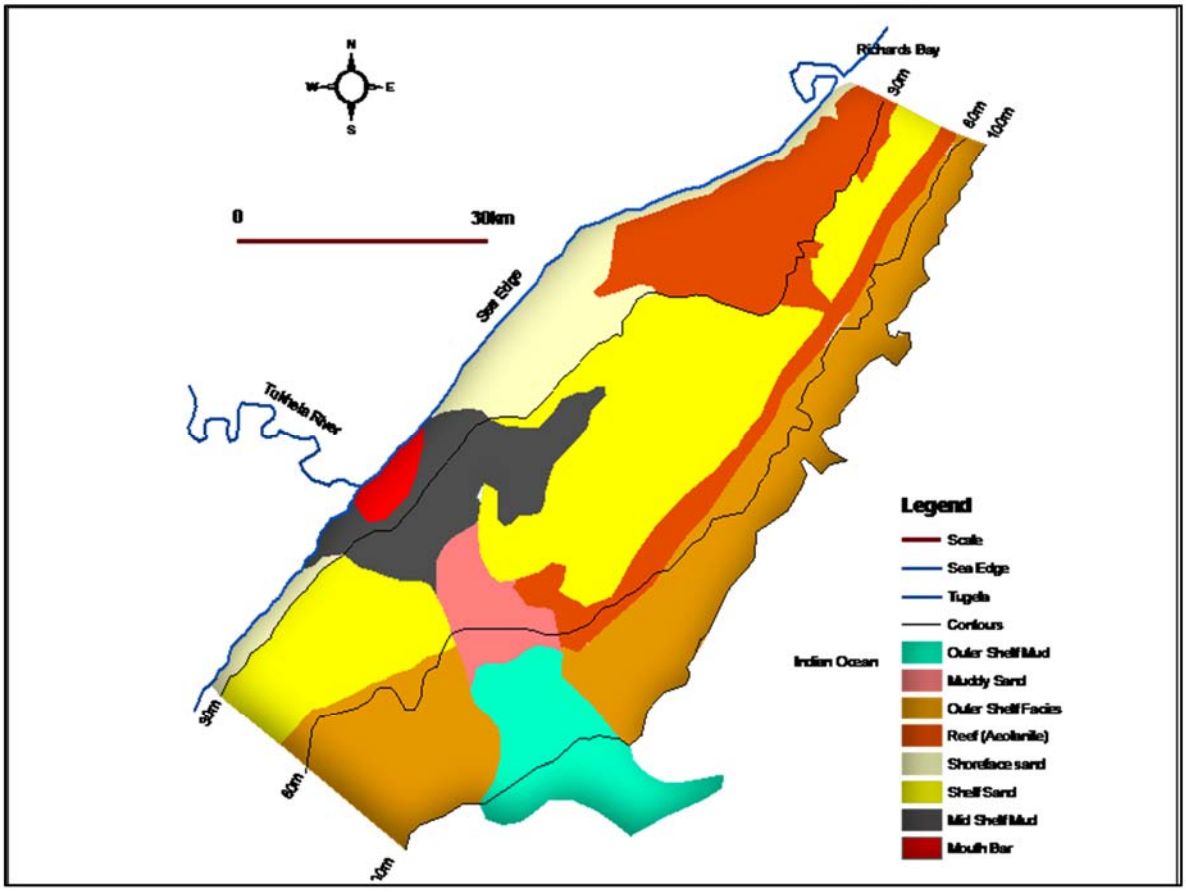

Figure 3.7: Distribution of eight recognized facies types on the Thukela Shelf. The -30, -60 and the -100 m contours define the inner, mid- and outer shelf zones.

(Source: Adapted from Bosman *et al.*, 2007)

3.7 Overview of the Catchment Areas of the Thukela, Amatigulu and Umlalazi Rivers

A catchment area, also called a drainage basin system, collects water from precipitation (Summerfield, 1993), but there is some delay before the water reaches the fluvial system. Two drainage basins adjacent to each other are separated by a watershed, so a catchment area is a very well-defined area.

3.7.1 The Thukela catchment area.

The Thukela has a catchment area of 29 000 square kilometres (see Figures 3.8 and 3.9). The river originates at Mont-Aux-Sources in the Drakensberg on the South Africa/Lesotho border at a height above sea level of approximately 3 280 m (Sumner & Beckendahl, 2017). From there, the river drops 948 m before meandering through the Natal Midlands, where it drops another 1 500 m through sandstone rock over the next 500 km to meet the ocean (see Figure 3.10). The

upper catchment consists mostly of wilderness (administered by various institutions, such as Ezemvelo KwaZulu-Natal Wildlife), private resorts, farmland used for dryland cropping forestry, and recreational areas (Sumner & Beckendahl, 2017). A number of tributaries join the Thukela River (see Figures 3.8 and 3.9). The largest of these tributaries is the Mzinyathi (also called the Buffalo River), which also originates in the Drakenberg, the Little Thukela, the Klipriver, the Mooi River, the Sundays River, the Boesmans River and the Blood River. These tributaries contribute to a flow which reaches an annual average of 184 m^3 per second of water at the mouth of the Thukela River area and into the sea (Brand, 1967).

The Thukela River passes through four geomorphic areas (see Figure 3.10), starting at a height of approximately 3 000 m above sea level in the Drakensberg in the Great Escarpment Group basalt in the north, dropping into the Ladysmith basin, the South Eastern Coastal Hinterland and the South Eastern Coastal Platform, where the river washes out into the sea at zero metres above sea level (Partridge *et al.*, 2010). Precipitation in the catchment area falls mainly in summer, and can exceed 850 mm on the escarpment and increase to 1 300 mm at the coastal areas, with an average temperature of 23^{o}C (Oliver & Garland, 2003).

Quinn (1977) reports areas with weak Beaufort and Ecca sediments, erodible soils and traces of sugar cane farming in the upper and middle course areas of the Thukela. These sediments wash down to the mouth area and are then deposited on the Thukela River's south dune. Longshore drift transports the fine sediment northwards, where it washes out on beaches such as the Amatigulu and Umlalazi beaches (Sumner & Beckendahl, 2017). The Thukela River provides enough sand or sediment to the coastline to keep the beaches in a net progradation state; otherwise the KwaZulu-Natal shoreline would erode faster than it would be built up (Le Vieux, 2010).

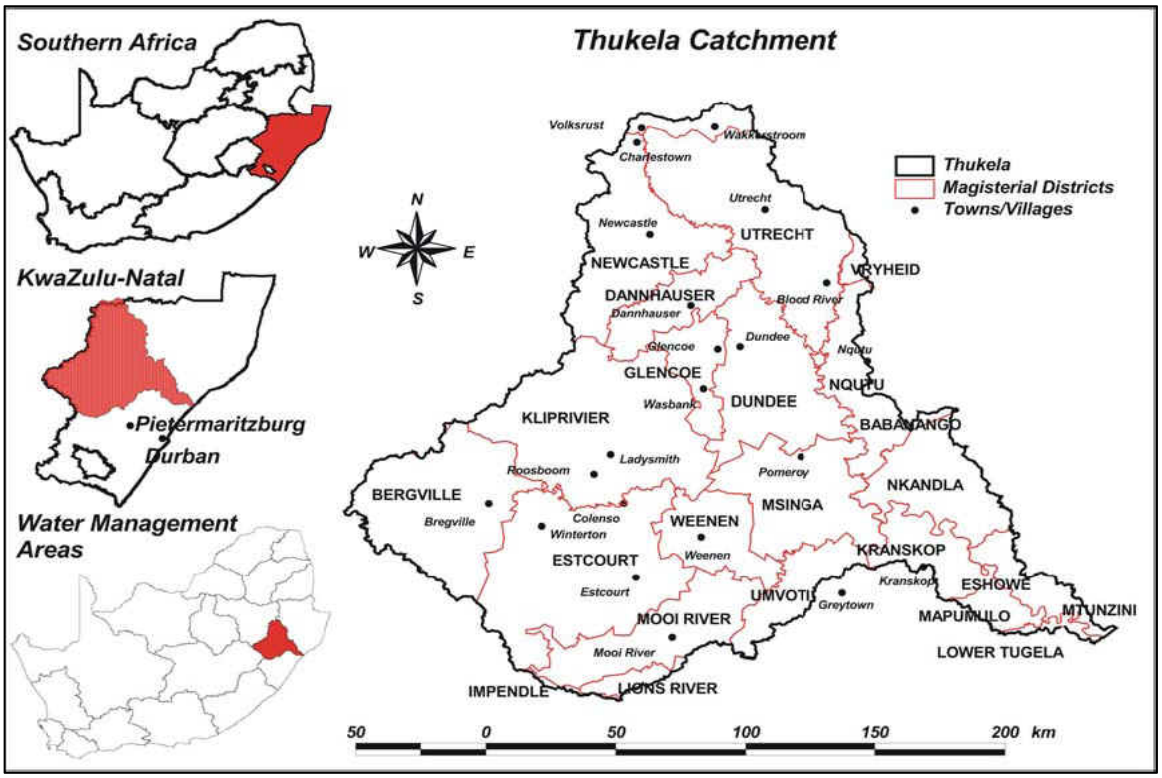

Figure 3.8: Thukela River catchment.

(Source: Schulze *et al.,* 2005)

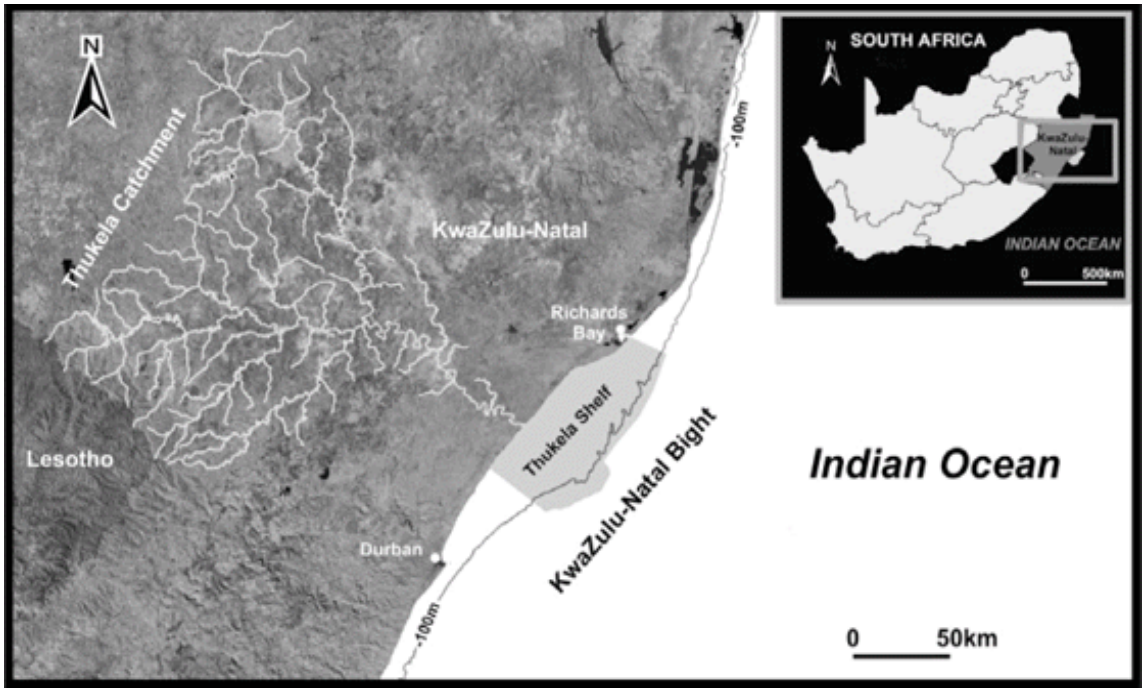

Figure 3.9: Thukela River drainage and Thukela Shelf in the KwaZulu-Natal Bight.

(Source: Bosman *et al.,* 2007)

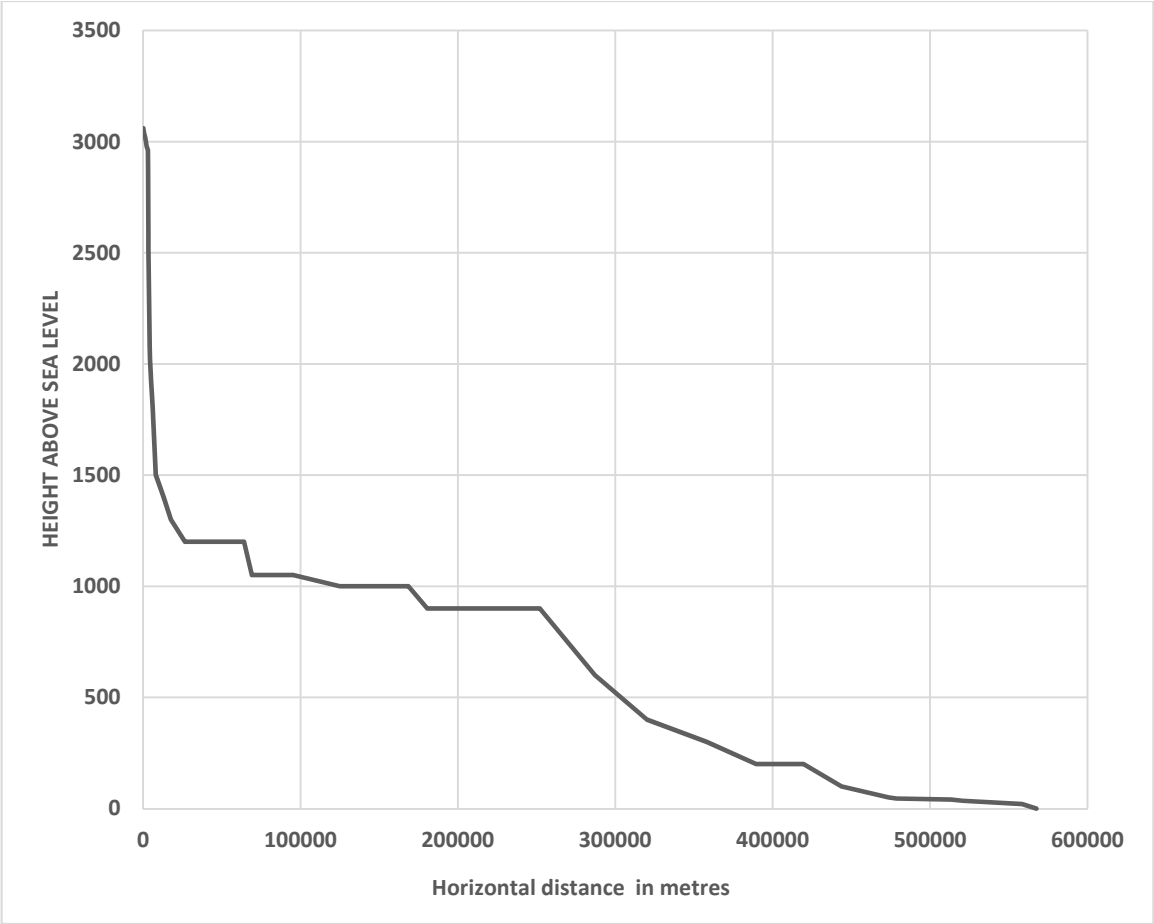

Figure 3.10: Long profile of the Thukela River drawn from a 1:50 000 Topographical map.

3.7.2 The Amatigulu-Nyoni catchment area.

This catchment is situated between the Thukela River and the Umlalazi River estuary, 16 m north of the Thukela River mouth. It is the only South African estuary that is shared by two rivers, namely the Amatigulu and the Nyoni River systems. The Amatigulu River drains an area of more than 900 km^2 of water (Begg, 1978; Uthungulu District Municipality, 2016). In the Amatigulu catchment, there are approximately 33% untouched grassland, bush and forest, 60% commercial agriculture (sugar cane) and forestry, and 1% of the human factor in and around Eshowe. The Amatigulu originates at a height of approximately 600 m above sea level and drops about 380 m over 23 km. The river's gradient then flattens to less than 1%, with a fall of 340 m over 42 800 m. The gradient of the last 29 km of the Amatigulu's flow is 0.1%, as the last section to the sea only has a drop of approximately 30 m (see Figure 3.11). The topography consists of a flat coastal plain, with more hilly areas deeper inland in the catchment area, ranging from sea level to 500 m above sea level. According to the Uthungulu District Municipality (2016), in the north west, the topography is more uneven, with cliffs of 900 to 1400 m (see also Ezemvelo KwaZulu-Natal Wildlife, 2014).

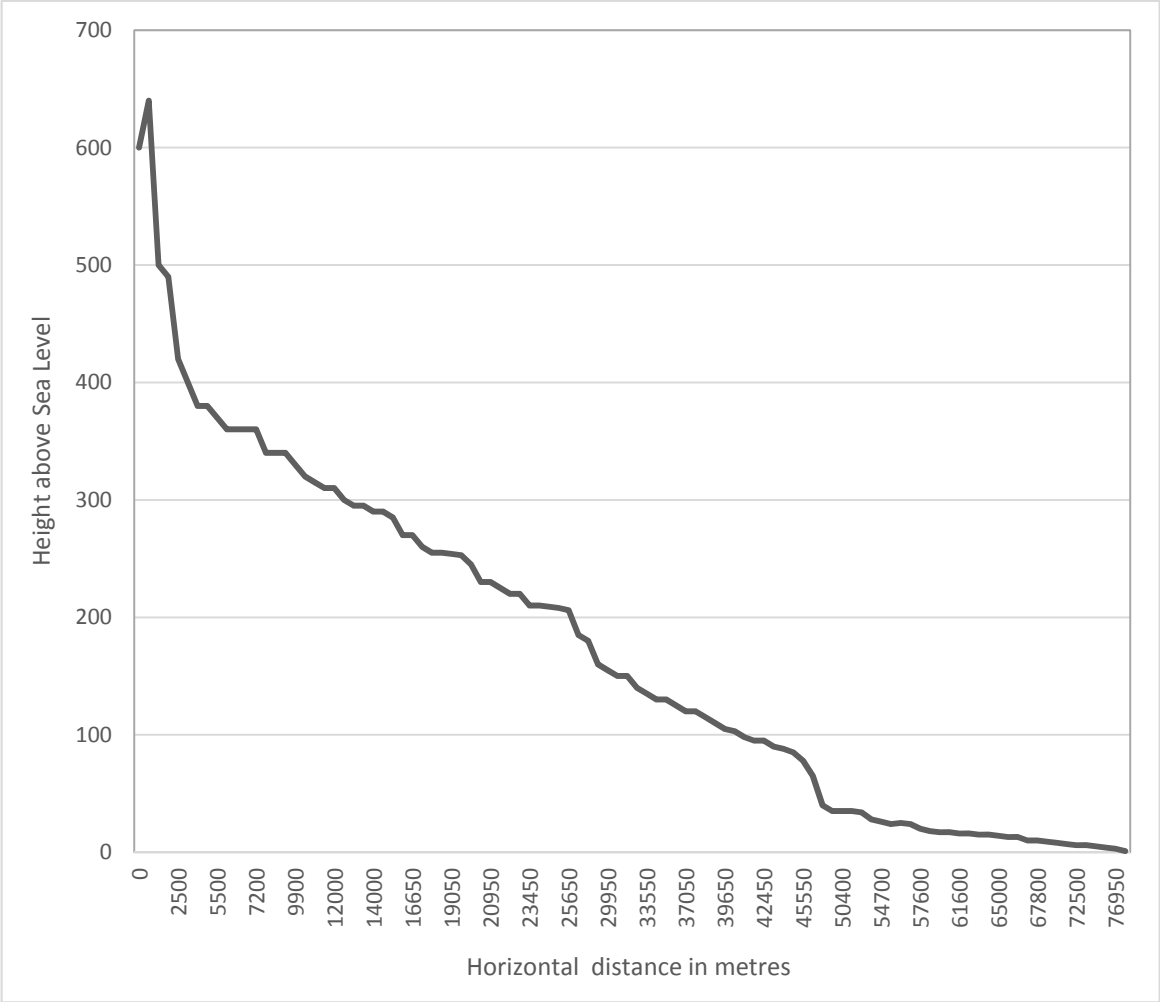

Figure 3.11: Long profile of the Amatigulu River drawn from a 1:50 000 topographical map.

3.7.3 The Umlalazi catchment area.

The Umlalazi catchment area is not nearly as large as that of the Thukela River. It flows approximately 50 km south of Richards Bay. It has a catchment area of 492 km^2, and the Umlalazi River is approximately 55 km long. The river starts 400 m above sea level, and it drops at 1%, with a constant gradient for about 20 km, where after it flattens out in the fluvial area for a distance of 26 km before it reaches the sea (see Figure 3.12). In the Amatigulu and Umlalazi River catchment areas, the climate is very diverse, because of the difference in the topography. These differences can also play a large role in the rainfall, which averages 1 000 mm to 1 200 mm near the coastal region, compared to a mean rainfall of 650 mm deeper inland in the catchment area.

The temperatures at the river mouth for all three rivers are approximately the same, given that these river mouths are all in a radius of 15 km (Uthungulu District Municipality 2016).

The coastal areas around the Umlalazi and Amatigulu Rivers feature extensive wetland systems, such as mangrove forests at the Umlalazi River, salt marshes, swamp forests and very dense trees and bush. Deeper in the catchment areas there is forestry and there are sugar cane farms and industries. According to the Uthungulu District Municipality's (2016) *Integrated Development Plan 2016/2017*, there are still 53% undisturbed forest, grassland and wetlands near the coast and 1% of the land is subject to human activity in Mtunzini and the township of Eshowe.

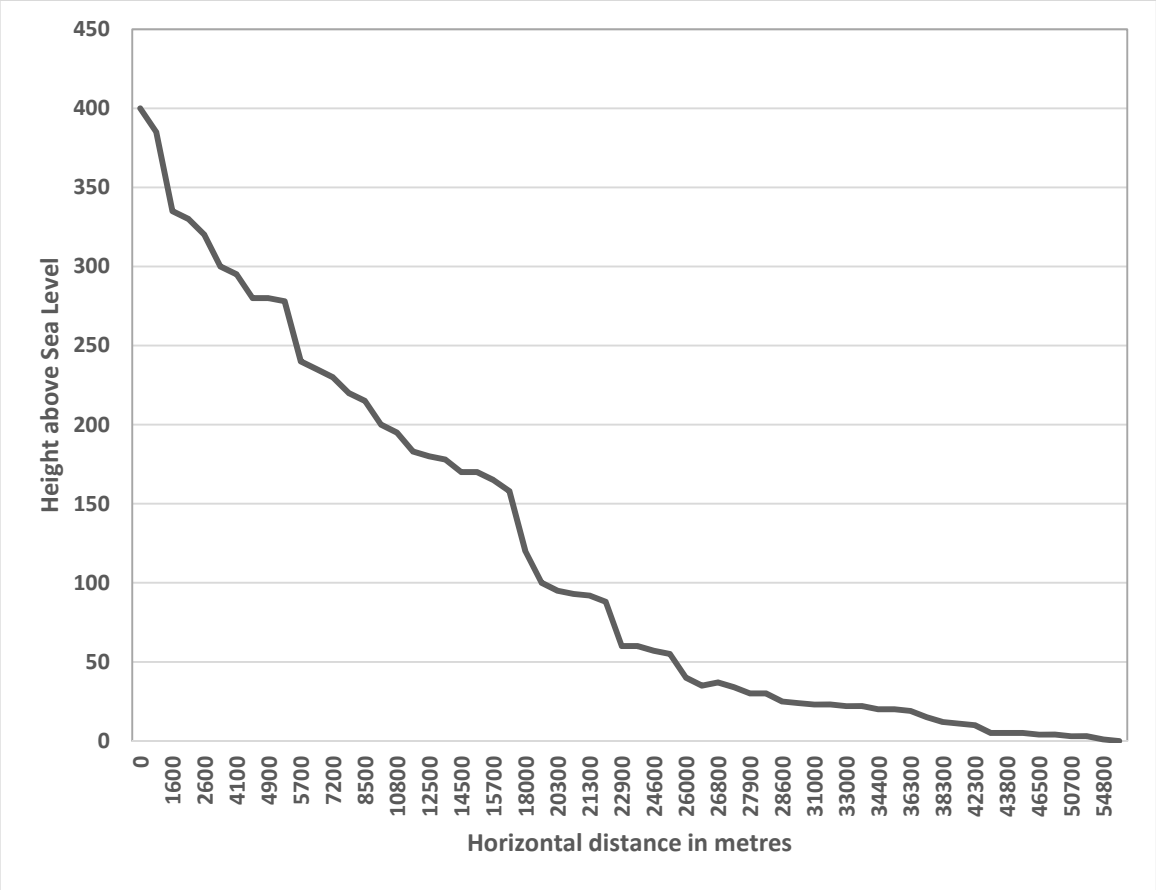

Figure 3.12: Long profile of the Umlalazi River drawn from a 1:50 000 topographical map.

3.8 The Individual Sites Studied

3.8.1 The Thukela River mouth (29° 13' 29.05" S; 31° 30' 17.58" E).

The Thukela River, also known as the Tugela River, enters the sea about 100 km north of Durban on the eastern coast of South Africa (Olivier & Garland, 2003). It is one of the largest rivers in South Africa (Midgley & Pitman, 1969). A relatively unstable sand dune lies across the Thukela River mouth, running in a north-easterly direction for about 700 m. Comparisons of aerial photographs taken over the years and even physical surveys that were conducted only

one year apart reveal that the dune size varies from flood to flood (Begg, 1978) and its form can change even over a very short period (see Figure 3.13).

In dry seasons, in the Thukela mouth and the catchment area, the river follows different streams, especially in the last 20 to 35 km to the sea. In the flood area, numerous large sandbanks occur in the Thukela and Amatigulu rivers. When these rivers are in flood, they carry all this sand to the sea, pushing it out deep onto the shelf. The sediments flooding into the sea are carried along with the wave regime of a current flowing northwards with a longshore drift which carries 1.1 million m^3 of sand flux. This sand washes on the Amatigulu and Umlalazi estuaries and beaches. Orme (1974) estimates that under flood conditions, up to 375 tons per square kilometre per annum of these sediments are delivered in the mouth. It is these sediments that provide material for dune construction and movement (Nicholson, 1983).

Figure 3.13: **A:** Indication of the size of the sand dune at the Thukela River mouth.
B: The might of the Thukela River forcing its way on to the mouth.
C & **D:** The river and the sea meet – the Thukela was flowing strongly (April 2017).

3.8.2 Amatigulu-Nyoni River estuary (29° 06’ 44.25” S; 31° 36’ 52.23” E).

The estuary of the Amatigulu (also pronounced mMatigulu) River is on KwaZulu-Natal’s north coast, in a protected area (EKZNW, 2014), about 20 km north of the Thukela River mouth and near the coastal town of Gingindlovu. It is classified as a subtropical, open-barred medium to large estuary (Whitfield, 2000). The Amatigulu-Nyoni catchment is 84 to 108 km in length.

During floods and rainy seasons, the mouth opens up for the sea to enter where the barrier is weakest and lowest. The Amatigulu River estuary when the mouth is temporarily closed is subject to marine influences such as salt water from the sea, and fresh water from the river and sediment (Leopold, 1953). The estuary has a 6 km sand barrier, extending from the south-east to the north-west. The estuary consists of sand supplied by the Thukela River further south. The southern and middle parts are stabilized with *Casuarina* vegetation. There is considerable movement of the river mouth's position, causing the sand barrier to change size (Begg, 1978). The Amatigulu River also has sand influx on the coast during the flood season (Engelbrecht, 2008). This river-dominated estuary is periodically closed due to low river flow (Green *et al.,* 2012). In the photographs in Figure 3.14, it is clear that the Amatigulu River barrier is more unstable and less vegetated than the Nyoni River barrier. Engelbrecht (2008) argues that the constant migration of the mouth makes the sand more unstable, making it more difficult for vegetation to establish itself on the dune.

Figure 3.14: **A, B, C** & **D:** The Amatigulu River breaking through the sand barrier during heavy rains in April 2017, reaching the mouth early in June 2017.
C: The barrier (far left) and behind it, the ocean. The sand in the foreground shows where the water forms part of the River estuary (April 2017).

3.8.3 Umlalazi River estuary (28° 56' 41.13" S; 31° 48' 56.63" E).

The Umlalazi River has a steep profile, and a length of approximately 40 to 60 km. Floods have occurred in this river where the levels have risen to about 5 m above sea level (Begg, 1978).

The estuary is hidden behind a 3.5 km vegetated sandbar. A shore current runs along the beach at 250° north, transporting materials from the Thukela River onto the sandbar, at the position where the waves break on the sandbar at about at 90°. All three estuaries have a protected sandbar separating the sea from the estuary. These dunes interact with the waves of the sea and aeolian processes on the one side, and river channel runoff and wind on the estuary side (see Figure 3.15).

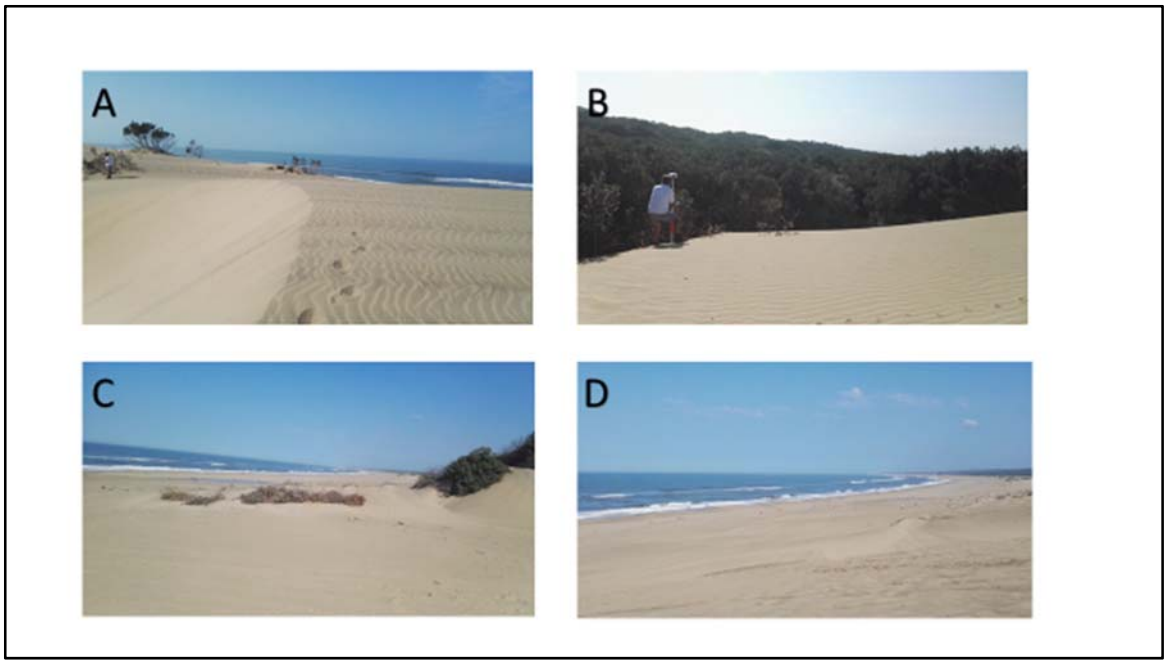

Figure 3.15: **A:** At the Umlalazi River beach, there is a steep slip face at an angle of the beach.
B: Prominent vegetated areas in relation to the sand areas.
C: Small embryo dune in the developing stage.
D: The bend (bight) where the coast is about 220^{o} and turns to 250^{o} (April 2017).

3.9 History of Severe Storms on the KwaZulu-Natal North Coast

The tropical cyclone season, as recorded by the South African Weather Service, is from November to April each year, but the peak storm frequency has been recorded in January and February (SA Weather Service, 2018). The only tropical cyclones that influence South Africa's weather are cyclones moving southwards into the Mozambique Channel (SA Weather Service, 2018). The cyclones that move north of the 25^{o}S latitude and close to the continent are dangerous and very destructive. Mozambique, the northern parts of KwaZulu-Natal and the Limpopo province are the areas where most destruction and flooding take place (SA Weather Service, 2018).

A few of the tropical cyclones that have had some effect on southern Africa are Astrid (December 1957-January 1958), Claude (December 1965-January 1966), Caroline (14 February 1972), Eugenie (21-22 February 1972), Danae (27-31 January 1976), Emilie (6-8 February 1977), Kolia (March 1980), Justine (March 1982), Domoina (29-31 January 1984), Imboa (10 to 20 February 1984) and Eline (8-22 February 2000) (SA Weather Service 2018). These cyclones are discussed in more detail below.

3.9.1 Cyclone Astrid (December 1957- January 1958).

This cyclone developed late in December 1957 and continued into January 1958. It struck Mozambique and produced torrential rain in the northern parts, up to 500 mm.

3.9.2 Cyclone Claude (December 1965-January 1966).

Cyclone Claude ran its destructive course from 24 December 1965 to 10 January 1966.

3.9.3 Cyclone Caroline (February 1972).

Cyclone Caroline wreaked havoc from 3 February to 14 February 1972.

3.9.4 Cyclone Eugenie (21-22 February 1972).

Heavy rain characterised Cyclone Eugenie, falling from Swaziland and south to the Durban area, where approximately 350 mm of rain fell near the coast. The widespread rain also fell in the catchment areas of the Thukela, Amatigulu and Umlalazi Rivers and caused large-scale river flooding.

3.9.5 Cyclone Danae (27-31 January 1976).

This cyclone, also called Terry-Danae, was an intense tropical cyclone that hit the east coast of Mozambique and the South African coast. The storm went over Madagascar. Heavy rains fell and widespread flooding took place. The death toll was 50.

3.9.6 Cyclone Emilie (6-8 February 1977).

In the first week of February 1977, a very intense tropical storm again struck the east coast of Mozambique and the north-eastern parts of South Africa. Flooding occurred in the Limpopo valley, claiming 300 lives.

3.9.7 Cyclone Kolia (March 1980) and Cyclone Justine (March 1982).

Cyclone Kolia lasted 18 days, from 25 February 1980 to 13 March 1980. In 1982, Cyclone Justine developed just north of Madagascar and crossed the island's northern part before moving south-west in the direction of the north-eastern coast of South Africa. Half-way, the storm turned south-east to miss the southern point of the island, and from there it moved in a southerly direction.

3.9.8 Cyclone Domoina and Cyclone Imboa (29-31 January 1984).

Cyclone Domoina was the fourth cyclone to hit the Natal coast in the summer of 1983/1984 (Kovacs *et al*., 1985). The cyclone was first spotted on a satellite image on 17 January to the north-east of Mauritius, and it was moving in a south-westerly direction (Kovacs *et al.*, 1985). It claimed 242 lives. About ten days later, Cyclone Imboa developed in the northern Mozambique Channel and moved south towards the Zululand coast, but on 10 February, Imboa turned back in the direction of the sea (Kovacs *et al*., 1985). As Kovacs *et al.* (1985) noted, only heavy rains fell in a narrow belt on the KwaZulu-Natal coast.

3.9.9 Floods of September 1987.

September 1987 brought one of the greatest flood disasters in KwaZulu-Natal, even more than the tropical cyclone Domoina in 1984. This flood caused disaster in the Umdloti River and the lagoon, and damaged infrastructure. These floods were not the result of a tropical cyclone that developed (as Domoina did) in the Indian Ocean north of Madagascar (Badenhorst *et al.*, 1989). Heavy rains of 800 mm fell in about four days' time, about 73% of the total annual rainfall of 1 100 mm. During the floods at the end of September 1987, surveys on different levels were carried out to determine the effect of the floods' sedimentation, how long it takes for the water to run off, and to what levels the water rose, as well as the extent of the damage caused by the flood (Badenhorst *et al.*, 1989). According to Badenhorst *et al.* (1989), the report concluded the following:

- No development must take place lower than the hundred-year flood area, because these areas are still susceptible to erosion.
- The biggest rivers (for example, the Mgeni, the Mvoti and the Thukela Rivers) could be considered to have a flood drainage time of at least 24 hours.
- The river beds do not necessarily flush away to the sea (getting lower in height), but are getting higher (Badenhorst *et al*., 1989).

3.9.10 Tropical storm of 19-20 March 2007.

The KwaZulu-Natal coastline is very vulnerable to severe storms that lead to significant erosion (Mather & Vella, 2007), due to its exposure of cyclonic storms during summer and extremely high swells during winter. In addition to the storms and cyclones listed above, this coast was hit by three other significant tropical storms: Dora (January-February 2007), Favio (February 2007) and Gamede (February-March 2007). The most severe of these was the storm of March 2007. The storm hit the KwaZulu-Natal coast on 19 and 20 March with the most destructive waves (Mather, 2007), causing significant erosion along the KwaZulu-Natal coast. The coastline moved back overnight by up to 35 m, causing the loss of beaches, the collapse of embankments and severe damage to coastal infrastructure and services. This erosion was driven by a series of large cyclonic wave events (Smith *et al*., 2007). According to Mather (2007), the enormous waves were generated by a low pressure system of 996 kHp off the coast. This took place when two phenomena occurred at the same time: it was spring tide, and the Sun and the Moon exerted maximum gravitational force on the earth. This phenomenon is referred to as the Saros equinox springtide, when the Sun and the Moon were at their 18.6-year peak (Mather, 2011). Mather (2011) points out that the combination of the Saros equinox and the spring tide resulted in abnormally high waves, causing widespread damage to the coasts of KwaZulu-Natal.

Chapter 4:

Methods

4.1 General Approach to the Study

The study emphasises the dune migration or movement of the northern KwaZulu-Natal coastal sand dunes over 72 years (1953-2017) under the driving forces actions described in Chapter 1, such as river runoff, wind and wave energy. For the research, physical survey data were needed, together with aerial and satellite imagery. All these data and information together are relevant to determine whether the dunes are moving in a certain direction, and whether they are getting larger or smaller in area and/or volume. The objectives of the study were to map and represent these changes in the form of contours, graphs or tables to do a forecast assessment of the impact of the dune barriers on the environment and the environment on them, the community and human infrastructure. The study responds to Jackson *et al.*'s (2014) comment that so far, little work has been done on dune dynamics and the changes of dunes, and the contribution of river water, wind and wave energy and sea currents on the dune movements on the KwaZulu-Natal coastline.

The study started from the first aerial photographs taken in 1953 and 1957 and compared them to photographs taken up to 2017. Study of the Thukela River mouth and the Amatigulu estuary began with the 1953 aerial photographs. The first aerial photographs of the Umlalazi estuary were only taken in 1957. These photographs offer visual data for a 70-year time span for the three catchment areas discussed in Chapter 3. For the research on the three chosen sites, the aerial photographs were used in the form of digital copies, provided by the Chief Directorate: Surveys and Mapping. In section 4.7 selected thumbnail photographs are shown that were used to model the Thukela River and the Amatigulu River in 1953, and the Umlalazi River in 1957. After all the fieldwork had been completed, a comparison of the dune and sand movement over the specific time period of the physical survey was analysed of the study period.

McKay (1978) argues there are different reasons why structures, in this case, the dunes, need to be monitored for movement and stability. He points out that there is a practical aspect and a scientific aspect. Practical reasons for monitoring dunes are to check the movements and the stability of dunes and assess the degree of geomorphological changes with the aid of land surveying methods, remote sensing and certain Geo Information System techniques (McKay, 1978). These methods only measure relative changes or movements over time. To survey and understand the movement of dune dynamics, a solid and very reliable survey network has to be

established around the dune. This network could be established with different surveying methods such as GPS, remote sensing, triangulation, traversing, scanning and light detection and ranging (Lidar). According to McKay (1978), researchers can use an absolute surveying network where some of the control points or all the control points are outside the structure or dune, or a relative surveying network where all the network points are located on the dune. Absolute movement must be determined with geodetic measurements (McKay, 1978). Scientifically, three computer programs were used to analyse the research, Model Maker Version 12.03, ArcGIS 10.4.1 and Google Earth as a checking facility to find control points on the ground. Scientific reasons for surveying dunes include gaining a better understanding of the amount of movement and helping to establish certain prediction methods. According to McKay (1978), it can help improve the community's knowledge in planning resorts, shopping malls, roads and railway lines close to beaches and dunes.

Different types of surveys were conducted during the time of the research and the results are compared by overlaying a 10 m^2 grid network on the original field data and plans.

4.2 The Physical Survey

In normal circumstances, a land surveyor determines beforehand what the flight plan for an aerial survey should be, and the placing of the pre-flight ground control points, also called pre-marks. Usually, the three-dimensional determination of the pre-marks takes place before, during and after the aerial photography flight(s). In the case of this research study, the opposite process was followed, due to cost considerations, since existing aerial photographs were used. Once these photographs were received from the Survey and Mapping office, the control points could be selected on the photographs and identified on the ground.

A number of basic rules were applied for the surveying, such as the correct annotation of objects on the photographs in relation to the ground. These control points were identified from the oldest aerial photographs. For the Thukela and the Amatigulu sites, the 1953 photographs were used, and for the Umlalazi site, the 1957 aerial photographs. Landmarks were identified on the photographs that still existed at the time of the research, such as train bridges, roads and street intersections, and other definite spots on the photographs that could be identified on the ground. These points were then determined independently, using three-dimensionality in a Y X Z format to the nearest 0.005 m. In this study, different surveying methods were used to determine the results of the coordinates from the conservative total station and prism method and/or the GPS method. The use of both the total station and GPS has merit. On-site inspection of the terrain at the start of October 2015 indicated that it would

be best to use both methods, but mainly the GPS, and falling back on the total station as an instrument on standby. The reason for this decision is that there are very few trigonometrical beacons in these areas. Several have been destroyed or severely damaged, and/or are unsafe to visit. However, the open dunes could be readily surveyed with the GPS. The base station of a differential GPS was set up or closed on one of the trigonometrical beacons while it collected the satellite information. A hand-held data logger had to be connected by means of Bluetooth with the base station and also with a rover station mounted on a survey telescopic pole. A rover station can move around and visit points, particularly ones to be surveyed for mapping. Each receiver had a built-in radio that linked the receivers together. As long as they were radio-linked to each other, a differential accuracy of 0.005 m to 0.01 m could be achieved. Once the Bluetooth connection was established, the operator was able to survey points in a Y X Z format. Attribute data such as a point's description and point numbering could also be attached to the point data.

One can get the best results from surveys such as this one, where the terrain is partly vegetated, by finding a visible open line between two fixed beacons – this is called a baseline. These beacons are normally permanent in the sense that they consist of a 25 mm galvanized pipe driven up to a half a metre deep into stable ground, with concrete poured around it. Markers with names or numbers were used to identify the control points. In very dense and heavily vegetated areas, established baselines served as orientation lines for the total station and prism. Each terrain (the Thukela River mouth, the Amatigulu-Nyoni estuary and the Umlalazi estuary) had such a baseline on which the survey was based. From this baseline, it was possible to establish a network of control points on the terrain from which future surveys could be done, for example, the identification points on the aerial photographs.

To establish the ground control point network, a method of traversing was followed. With this method, the surveyor measures a horizontal direction forward to the new control point, together with distances – horizontal, slope and vertical distance – that can be read off the display panel of the total station. Using the coordinates of the GPS fixed point, the forward direction and horizontal distance to the unknown control point, it is possible to calculate the new coordinates of this first control point in the survey network. This method must be repeated, so that each time when the total station visits the new determined control point, it can be oriented back to the previous control point, and then the forward reading can be taken to the next point, together with the distance. The main idea behind placing of the control points is that they must serve the purpose of calculating coordinates for the identification points on the aerial photographs. These ID points are then calculated three-dimensionally.

A very important aspect that needs to be considered is the GPS heights. All trigonometrical beacons and benchmarks are related to the mean sea level. From these control beacons, heights can be carried over to the relevant site by means of different surveying types. One method, called levelling, has an accuracy of less than approximately 5 mm. The other method is trigonometrical levelling, which has a lower accuracy of about 0.10 m to 0.15 m. If a GPS is related to any known height, the accuracy is close to 0.01 m, but sometimes these heights could be out by up to 30 m because of the difference in the ellipsoid and the geoid from heights used in the South African coordinate system (see Appendix A). Height measurements are normally taken from the mean sea level (MSL), which is equal to 0 m. Mean sea level is the average reading between low tide and high tide, but determining the mean sea level and deciding where low and high tide fall is a science on its own and falls beyond the scope of this study.

4.3 The Thukela Survey

The Thukela River mouth was divided into the north shore and south shore. The south shore is the prominent volatile sandbank, which changes constantly during strong winds, with high river runoff and wave deposits of sand on or erosion of the sandbank. For the shared area at the Umlalazi and at the Thukela mouth south shore, a fishnet method was used to determine more heights for the areas to determine more triangles and more accurate contours for the volumes (see Appendix A). The Thukela mouth north shore did not fall under the fishnet method, since the terrain does not allow for this method to be effective, because of the size and shape of the terrain, a narrow horseshoe from east to west and north to south.

During the survey of the Thukela beach and sandbank in March 2016, a base station point was set up just outside the Thukela mouth, on the northern side of the Thukela River mouth on one of the highest hills. All the control points were surveyed from Base 1, which included the north shore beach. The Base 1 survey was connected to the trigonometrical beacon Aloes II on the western side of the Thukela River (see Figure 4.1). The western control points, including the south shore, were surveyed from the Aloes II beacon. From the Aloes II beacon, Base 1, including the trigonometrical beacon Red Hill, was surveyed for accuracy checks on the total survey. Both beacons are in a very poor condition and the Chief Directorate: Surveys and Mapping does not maintain these beacons any longer, or consider replacing them. After the calculations had been done and the constants applied to the heights obtained from the raw data,

a total closing error on the terrain was only 0.035 m. During a second survey in July 2017, only Aloes II was used in the survey on the south and north shores of the Thukela River.

Figure 4.1: Trigonometrical beacon Aloes II (left) and Red Hill (right) at the Thukela River site.

4.4 The Amatigulu Survey

The Amatigulu estuary was also surveyed during a visit to the terrain in March 2016. It is a difficult terrain to survey with a GPS, because of the uneven topography, which caused ongoing failures in the radio link between the base station and the rover station. Therefore, a number of base stations were established to reach all the photo control points with the rover station. A base station was established after three days of surveying close to the estuary on the foredune. At that time, it was close to the furthest point of the water end of the Amatigulu estuary. Points were taken on the seaward side of the estuary and the mean sea level of the beach up to where the Amatigulu and the Nyoni join together. Then, the points along the estuary and also on the dune itself were measured up to the end of the Amatigulu River estuary. The survey was closed down at the trigonometrical beacon Baton Rouge No 276 on a 6 m brick and concrete block at the northern part of the Amatigulu terrain. This beacon is situated on the north-eastern part of the Amatigulu estuary site. It is one of the only undisturbed beacons in the area, except for the missing black signal that is normally on top of the white pillar (see Figure 4.2).

Figure 4.2: Trigonometrical beacon Baton Rouge No 276 on a 6 m concrete block in the northern part of the Amatigulu River mouth.

4.5 The Umlalazi Beach Survey

As described previously, the first survey at the Umlalazi beach was conducted mainly with a Nikon total station and a prism. The control points in the area were surveyed using a Fujiyama RTK GPS system. The trigonometrical beacon Ciciwe No 85, with WGS Lo 31^{o} with coordinates of -78659.50; +3199153.59 and a height above mean sea level of 111.90 m was used as a base point to start the survey network. A network of 21 control points, including two points on the beach area, was established to be used later as control points to do the survey of the sand dunes and the beach area. In March 2016, the survey area was divided into an eastern and a western part. The initial survey was done with local coordinates and heights. All the points were then converted by means of a transformation calculation and then re-oriented to the UTM zone 36 system. A height adjustment according to the Ciciwe beacon was also done with a constant of -30.30 m. A baseline was measured between the two control points so that the eastern and the western parts could be linked together.

All the oriented coordinates and the adjusted heights were processed into Model Maker version 12.01 for manipulation of the survey points. Using the points, triangles were generated in the computer for contouring. The triangles were then edited in such a way that the contours displayed the correct topographical image of the terrain as explained above. The results are

shown in Chapter 5. A manhole next to the road and the golf course were named Golf Cont in this survey, with a fixed coordinate and height, and this was used during the March 2016 survey, and has been used as a base station control point since then. During October 2016, a Fujiyama Real time kinematic GPS was used and then a Carlson GPS was used for the next two successive surveys.

4.6 Short-term Detailed Assessment at the Umlalazi Beach

A short-term detailed assessment was done in March 2016, October 2016, April 2017 and July 2017 to determine if there were any significant changes over this short period. During March 2016, the survey was executed using a Nikon DTM 522 total station. With the later surveys to follow, as mentioned above, the survey was done on approximately the same area, first with a Fujiyama differential GPS system, and in April 2017 and July 2017, with a Carlson GPS. The accuracy was the same, and the change of system had no effect on the results. Three systems were used; all the surveys are equal to the accuracy of 0.005 m to 0.010 m. The analysis and assessment of the dune dynamics was conducted using three different methods:

a) Aerial photographs were inspected, comparing the aerial photos of 1957 and very recent aerial and satellite photo images with each other. The 1957 aerial photographs were rectified according to the surveyed ground control points. All the points on the Umlalazi beach were plotted on the rectified photographs to compare the historical situation with the current situation.
b) An analytical and physical survey were combined with ArcGIS 10.4.1 and Model Makes 12.01 to determine the extent of the area of sand moving into the vegetated area.
c) The fishnet method was used for the Umlalazi beach (see Appendix B).

The short-term assessment was important, in the sense that it did not just depend on the physical surveys of the terrains, but also on other methods such as the fishnet method, to determine estimated heights. This method, as McKay (1978) states, has a lower accuracy of up to 0.1m. The accuracy of the fishnet method depends solely on the accuracy of the ground control points and the spot level points on the ground. In the Model Maker survey program, the physical field values were processed in the computer after they were downloaded from the data logger of the GPS in a text file format, so that all raw and coordinate data were stored in the Model Maker database. The total area was then covered with the surveyed points. In the Model Maker menu, navigating to **Tri → Csearh,** triangles are generated, as shown in Figure 4.3, to generate the contours. In the program, the heights and other attribute data can be switched on or off. To edit the triangles, the height data need to be switched on. The legs of each triangle

can be changed if necessary, so that the contours represent the correct pattern of the topography of the terrain in the computer as it is on the ground. All triangles must be edited to reflect the correct contour pattern, as in Figure 4.3.

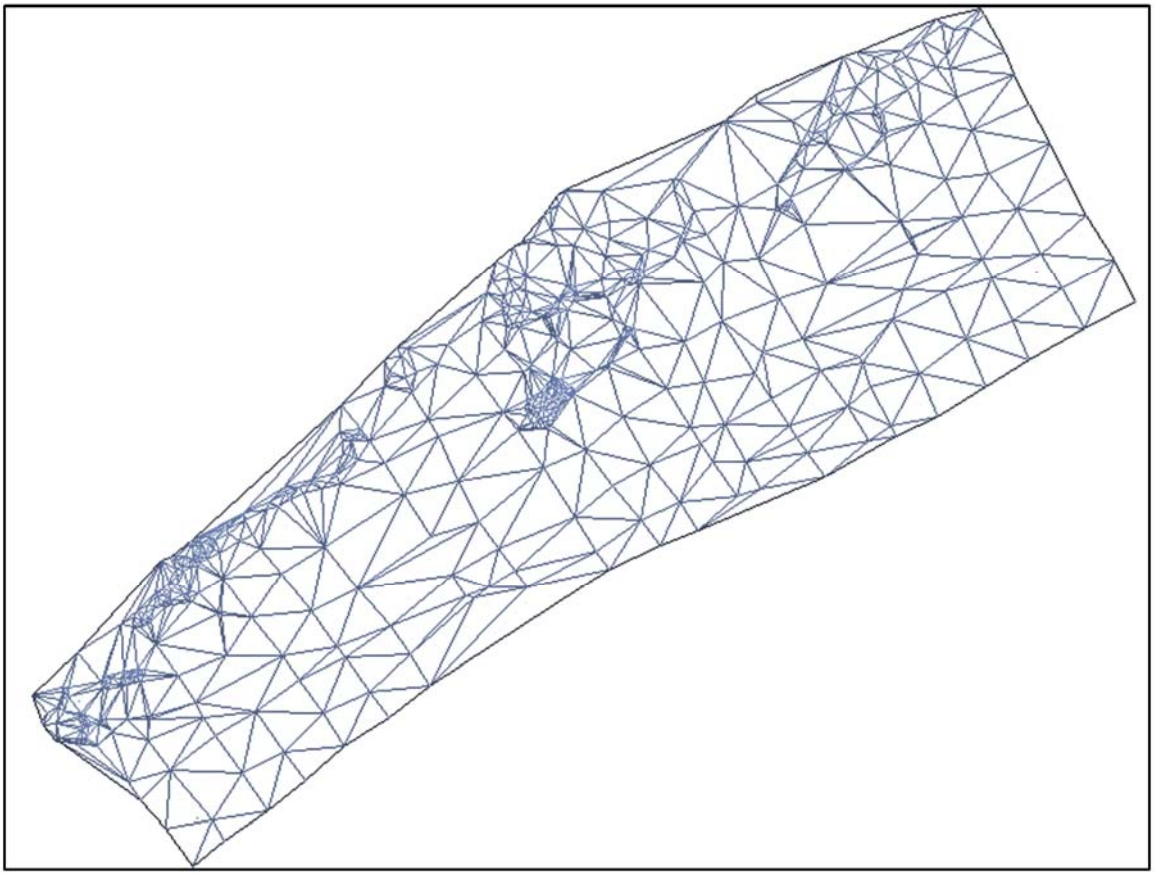

Figure 4.3: Model Maker program showing the triangles at the Umlalazi beach area that were physically surveyed on the ground (scale approximately 1:7000).

For the four surveys at the Umlalazi beach and for the Thukela south shore, similar contour patterns were generated (see Figure 4.4). A problem occurred, in that after six months it was no longer possible to survey exactly the same area perimeter. The reason for this was that the time available for the study was limited, and, although the GPS data logger could navigate to specific points, this became very time-consuming.

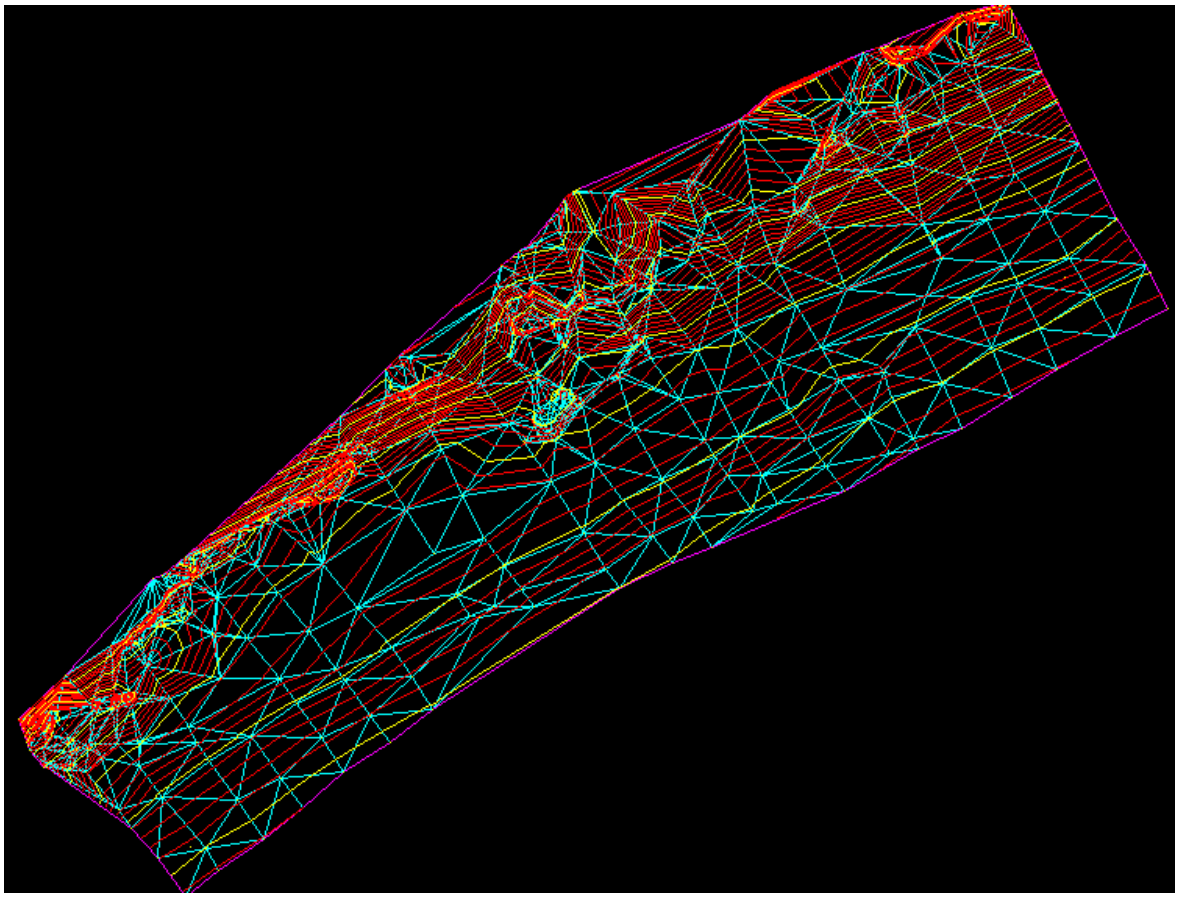

Figure 4.4: The triangles covered on the survey terrain of the Umlalazi beach and the contours generated from the triangles (scale approximately 1:7000).

Each new survey interval started with a radius of approximately 5 to 10 m from the previous survey, but that is not accurate enough for the purposes of volume calculations. To overcome this problem, the four surveyed areas must all be exactly the same size. A common rectangular area was thus established that satisfied all four surveys. Four coordinates were identified to define the common area (see Figure 4.5):

- A +74430.63 +3205696.31
- B +75094.74 +3205190.23
- C +75203.17 +3205348.41
- D +74525.42 +3205790.40

The rectangular figure in white lines in Figure 4.5 represents the area covered by the 10 m^2 fishnet grid whose triangles were used to determine the contours and the dune volumes.

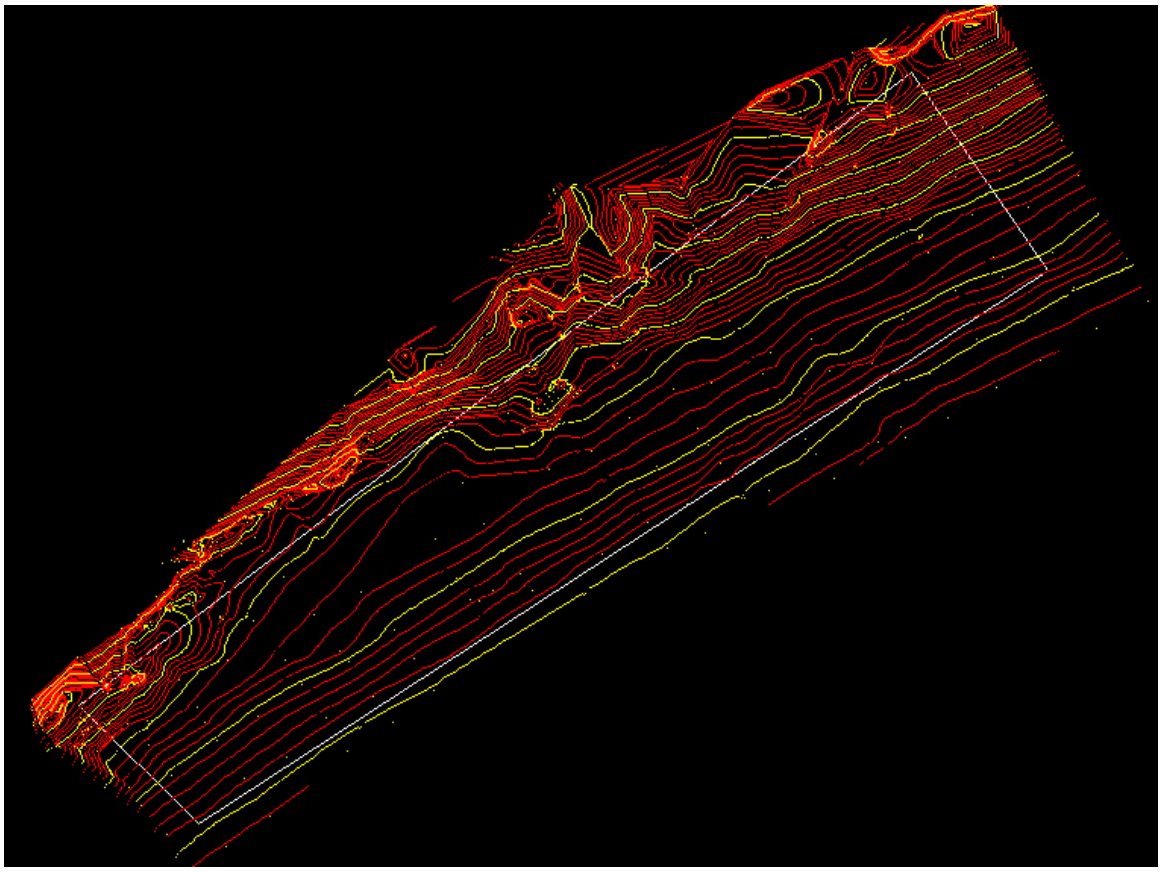

Figure 4.5: White rectangle showing the common area that satisfied all the surveys over the two years in the research area of the Umlalazi beach (scale approximately 1:7000).

In this exercise, the common area stayed the same, defined by the four coordinates above. Only the contours and volumes are the variables in this equation. The grid network is called a fishnet. It can have any dimensions, depending on the accuracy of the original survey and the terrain. In the case of this study, a grid network of 10 m^2 was suitable, because the terrain allowed it, as it is very smooth, especially on the beach side. The Thukela south shore is also a smooth terrain, with heights varying from 0 m to approximately 2 m. This fishnet was pulled over the original surveyed area and each intersection point of the graticule was assigned an estimated height value according to the contours of the original survey (see Figures 4.6 and 4.7). When the 10 m^2 grid was pulled over the original surveyed data, the triangles that the program generates were in the same position as the gridlines, because each grid point had an estimated height value to the nearest 0.1 m. The contours from the grid points were in almost the correct positions, but it was still necessary to edit some triangles.

During each survey, an average of 600 points were taken in the field at each site. With this fishnet method, the boundaried terrain had over 1 500 intersecting horizontal and vertical lines. However, the terrain must have a smooth slope formation for an ideal network to deliver

an accurate contour pattern. An advantage of this method is the number of spot heights generated. A disadvantage or limitation is that some detail can be lost in this process, such as small initial embryo dunes and terrain changes in slope and detail. In the example in Figure 4.7, details have disappeared from the map and cannot be picked up if they do not appear inside a 10 m² area.

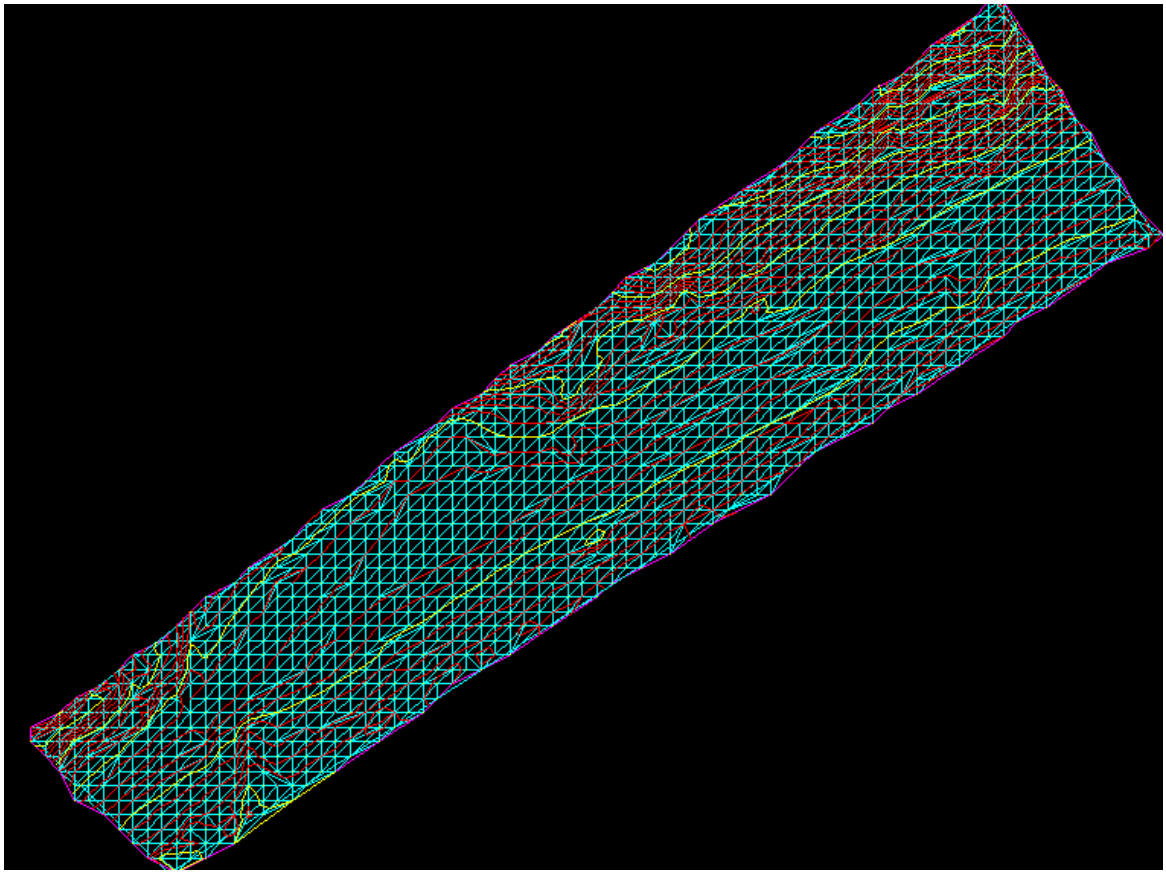

Figure 4.6: The terrain on the Umlalazi beach area, covered with a grid network of 10 m^2, exactly the size described by the four coordinates (scale is approximately 1:7000) (see Appendix B).

As can be seen in Figures 4.7 and 4.8, an embryo dune described by the intersecting vertical lines +74780 and +74790 and horizontal lines +3205470 and +3205480 is hidden in the centre of this 10 m^2 grid network. When a topographical survey is done from normal field data, all important details, made by humans or natural, are surveyed in, even if they fall within a certain grid network. In Figure 4.7, the blue line in the north-west of the figure is a part of the common area's boundary line and no heights were estimated or considered outside these four boundary lines. At the stage when the grid editing was complete and the necessary detail on the map was drawn in by CAD, the figures (such as Figures 4.7 and 4.8) could be exported to

another program, such as an ArcGIS program. A disadvantage of the Model Maker program is that it can only calculate, using different functions in its menus, the total volumes of the terrains. In this study, it was important to determine the volume of each contour interval in the defined area. In the ArcGIS program, it is possible for the computer program to calculate the height and the area above a certain plane height. If the highest point on the terrain is 20 m above sea level and the plane height is 0 m, the program will calculate the areas for each half metre from 0 m to 20 m and every half metre area is multiplied by a contour interval of 0.5 m.

Figure 4.7 shows how a 10 m^2 network was pulled over the original contour survey at the Umlalazi beach – the map's contours were generated from the original survey data with a 40 m^2 grid network and more coordinate points with heights can then be created. Each intersecting line's height was estimated. For example, the +74730; -3205490 has an estimated height of 4.5 m (see Appendix B).

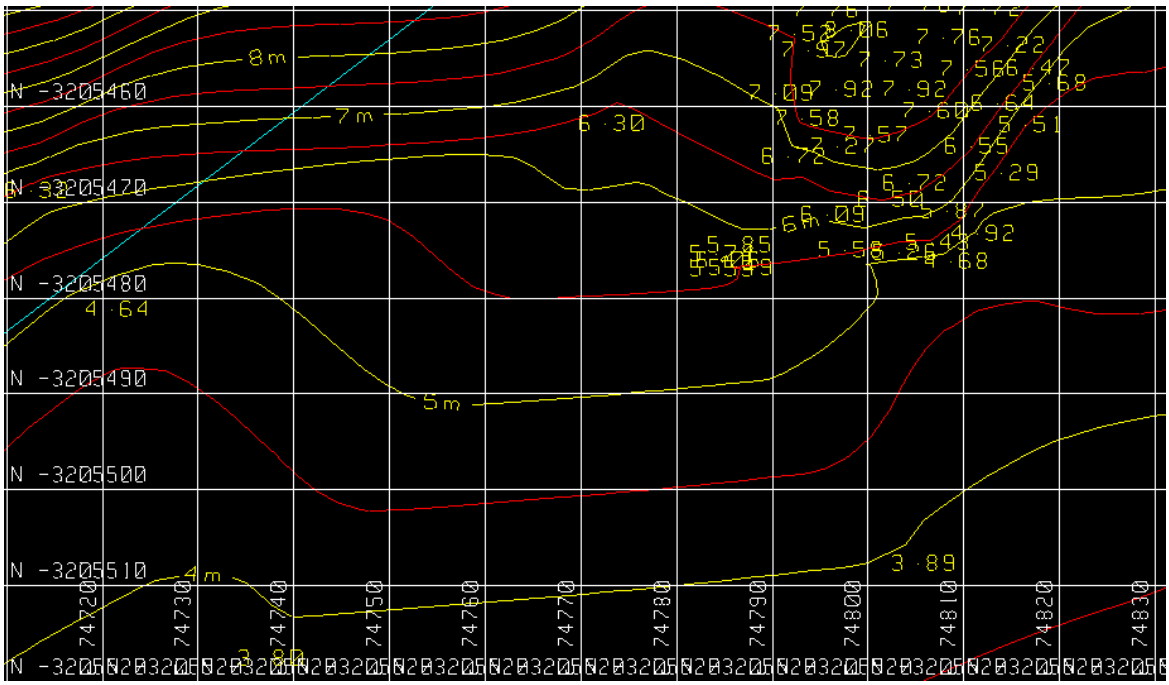

Figure 4.7: The 10 m^2 network pulled over the original contour survey at the Umlalazi beach.

Thus the volume of each contour interval is the mean of the top and the bottom area, times the half metre height. In the methodology, the volume of each plane height was calculated. Where only the volume above the 10 m contour part of the terrain had to be calculated, then the computer solved the volume above the plane height of 10 m. The plane height is important, because volumes above this height are calculated and the end result is an accumulated volume.

Important detail can be lost as a result of this fishnet method, for example, if an embryo dune falls exactly in the middle of a square, the fishnet method generates contours that ignore that detail (see Figure 4.8 and Appendix B).

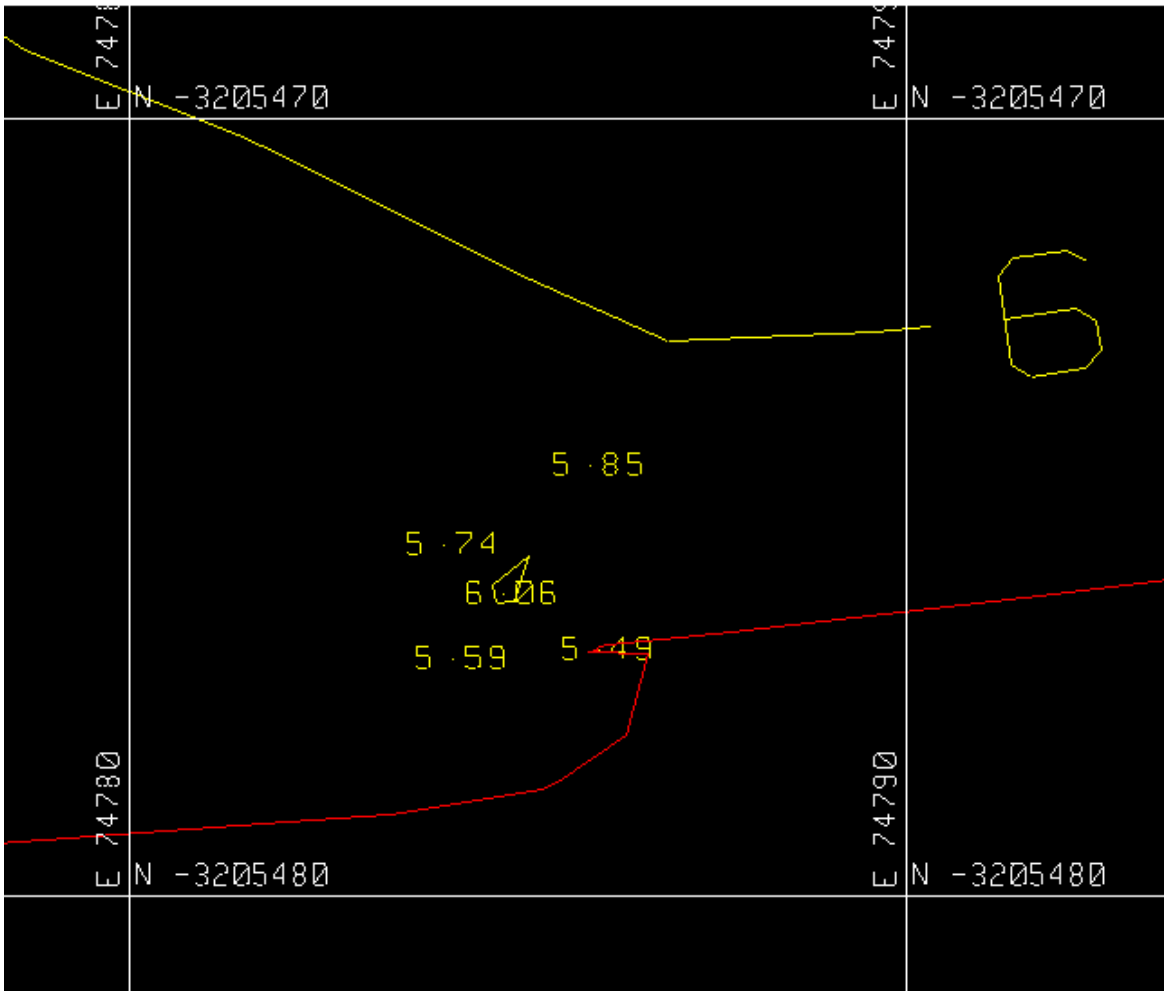

Figure 4.8: Embryo due in the middle of a square ignored by the fishnet method.

All the individual area sizes and volumes were fed into Microsoft Excel. To find each contour interval separately, the successive volumes were subtracted from each other, as shown in the values of the March 2016 survey in Appendix C. In this table, the accumulative volume for contour height 20 is 15.94 m^3, and for the zero contour interval, the accumulative volume is 640799.34 m^3. To determine the individual volumes (the column in blue) for each contour interval, one uses the plane height 19, minus plane height 20, which is 255.00 m^3 and so forth. If all the individual volumes are completely calculated and then added together, the total must equal the total accumulative volume.

4.7 The Interpretation of the Photographic Model

The aerial photographs were obtained from the Chief Director: Survey and Mapping (CD: SM). Strategic points with a good spread all over overlapping photographic pairs and with a good definition were marked on the photographs to be identified later and surveyed three-dimensionally on the ground at all three sites (see Figures 4.9 to 4.12). It meant that the points identified on the ground on the 1957 aerial photographs still had to exist when the land surveying was done in 2015/2016 on the ground. One of the main problems encountered in this study was to find points that have been in existence for over 70 years. At least four or five points are needed on each photograph, where four points must fall in the overlapping photo pair (see Figure 4.13). This is to connect and manipulate the overlapping photographs to form photographic models to each other. The ArcGIS program can handle this function very well by doing rubber sheeting to geo-reference the photographic images. Geo-referencing is a process of associating the chosen prominent point on the photograph with the spatial data measured in the field on the ground.

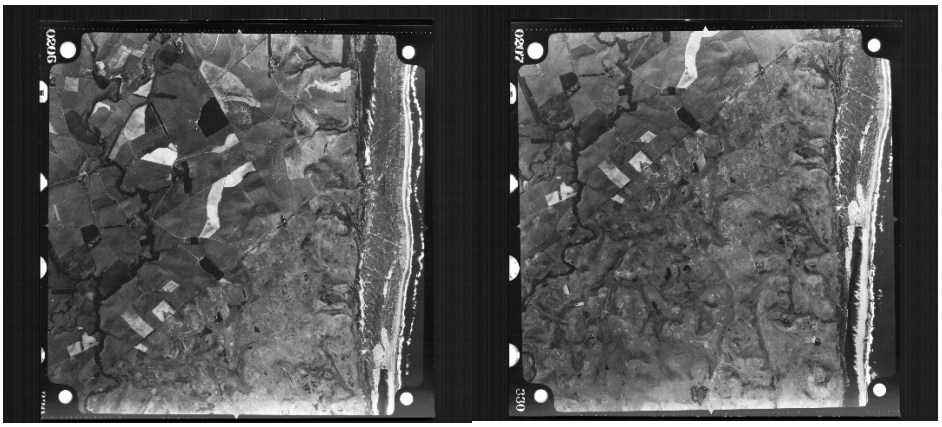

330_0CA_00206330_0CA_00207

Figure 4.9: Selected photographs from the Amatigulu 1953 aerial photo model

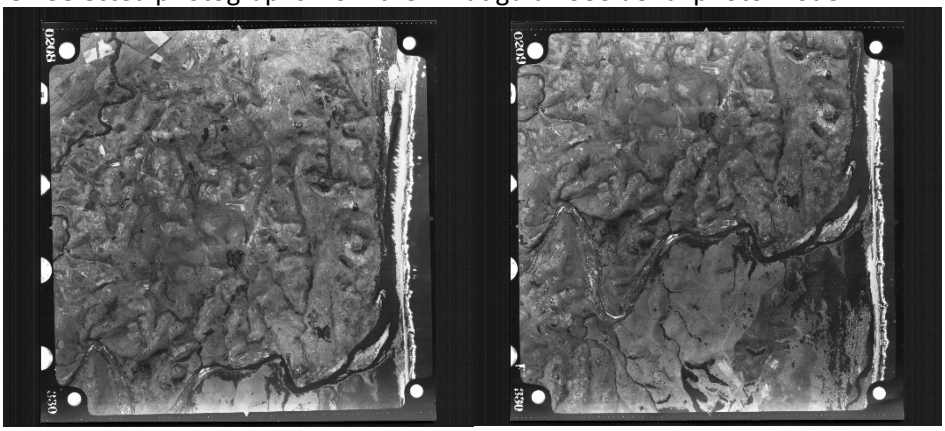

330_0CA_00208330_0CA_00209

Figure 4.10: Selected photographs from the Amatigulu 1953 aerial photo model.

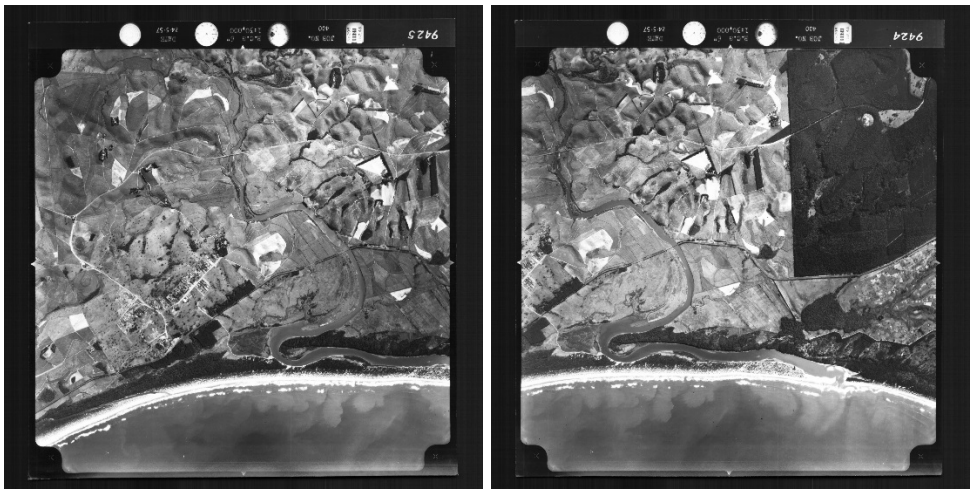

400_015_09424400_015_09425

Figure 4.11: Selected photographs from the Umlalazi 1957 aerial photo model.

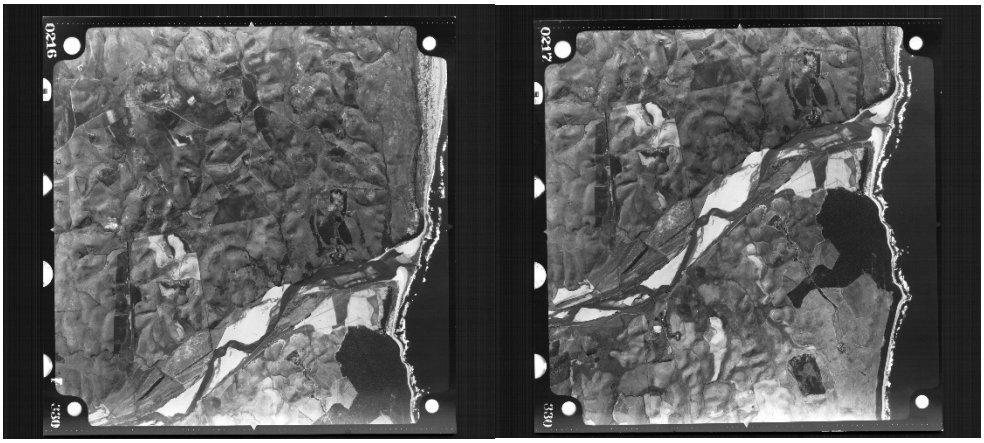

330_0CA_00216330_0CA_00217

Figure 4.12: Selected photographs from the Thukela 1953 aerial photo model.

4.8 The Orientation of the Photographic Model/the Rubber Sheeting Process

This process is also known as image-to-vector conversion. Before the rubber sheeting and geo-referencing can take place, the images need to be projected to the same geographic framework as the ground control points. In this study, all coordinates were projected to WGS_1984_UTM_Zone_36S. This refers to the WGS 1984 ellipsoid of the earth. The projection system is the Universal Transverse Mercator (UTM). All three areas fall in Zone 36 with the 33^{o} longitude as the central meridian. To correct this problem, the aerial photographs had to be orientated or rotated according to the fixed ground control points. All the points on the photograph model are marked in yellow in Figure 4.13. Point 1 on the aerial photographs was measured with the GPS as ground control point 11 in Figures 4.13 and 4.14. The two points were joined together to start with the photographic orientation. At least four points evenly

distributed through the relevant image had to be oriented, but in the study's case, more photo control points were used to ensure better accuracy in the calculation for the rubber sheeting (see Figure 4.15).

To do rubber sheeting successfully from an image to a point on the surface of the earth, enough evenly spaced ground control points must be created and the action of dragging them over each other must be performed as accurately as possible. In Figure 4.13, the ground control points are drawn in on the ArcGIS screen. In Figure 4.16, the first aerial photograph of the photographic model is zoomed to the layer screen with a transparency of 40%. The specific point on the photo is dragged or registered to the correct place on the surface of the earth. This process of rubber sheeting makes the raster layer or photographic image fit on the vector data obtained from the field survey. The image and the ground control points appear on the screen (see Figure 4.16). The difficulty of using such photographs is that there is usually some distortion in the image which occur in the line of flight when photographs are taken at different angles and due to different tilting positions of the aeroplane. To correct this problem, the photographs must be oriented in a stereo plotter where a relative and an absolute orientation can be done.

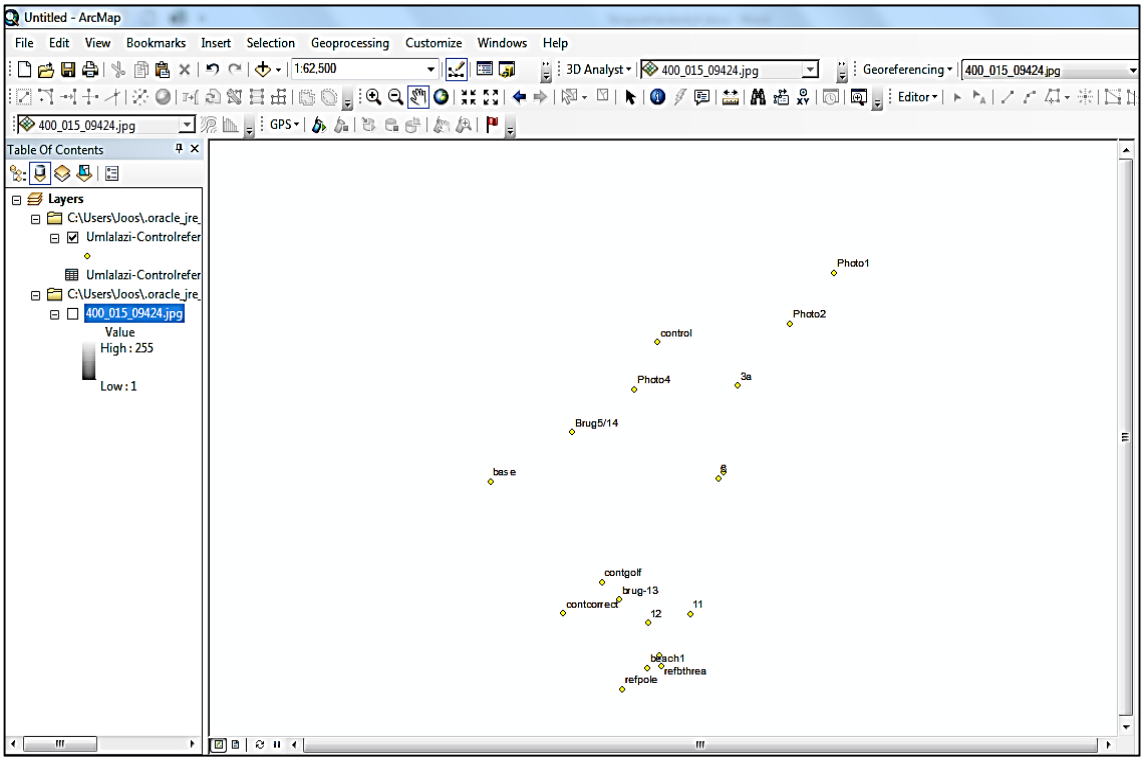

Figure 4.13: After the text file was read into the ArcGIS program, all points were converted to a projection system and zoomed to the same layer to be visible on the active screen.

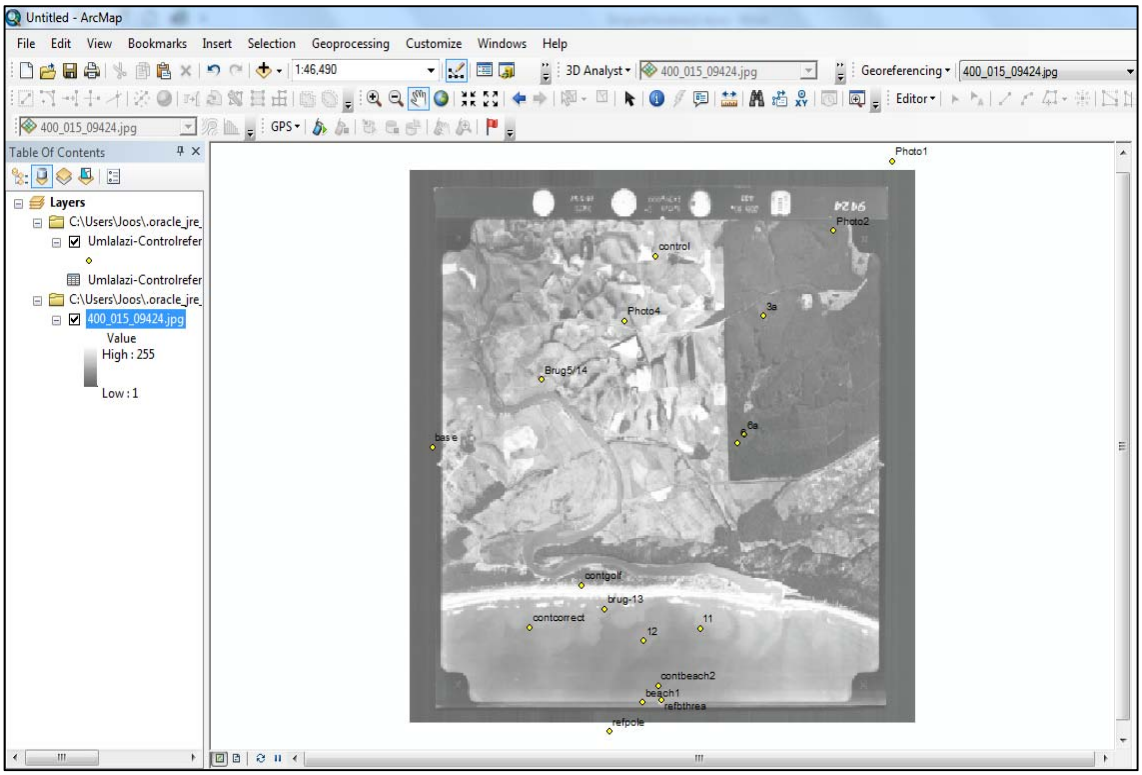

Figure 4.14: The photograph and ground coordinates on the Umlalazi beach are drawn in on the active screen. The photograph must be compared to the surveyed points to rectify the photograph.

4.9 Accuracy Calculation

After the true and data layer coordinates had been recorded, a positional difference was calculated, known as the positional error, the ΔY and ΔX and or the residual value and the residual value y (Bolstad, 2005). The calculation is as follows:

$$e = \sqrt{(Xt - Xd)^2 + (Yt - Yd)^2}$$

Where Xt and Yt are the true ground coordinates, and Xd and Yd are the data layer coordinates for a point.

With all the displacements or residual values in the x and the y of the layer coordinates to the ground control point coordinates, it is possible to calculate the root mean square error (RMSE) (Bolstad, 2005). Once all the RMSE values are known, the National Standard for Spatial Data (NSSDA) can be calculated by multiplying the total RMSE by 1.7308. It means that 95% of the horizontal values must be smaller than the estimated accuracy. In the example in Figure 4.15, the total RMSE is 1.62613 for all the horizontal ground control points, thus 1.62613 x 1.7308 = 2.8145. The residual values in Figure 4.15, in the right-hand column, are all within the limit of 2.8145. After the first target image was georeferenced and it was updated, the other

photographs of the terrain model could be added into the ArcGIS program. The same procedure was followed to geo-reference the photographic model in Figure 4.16. When the photographic model was completely georeferenced, the new feature layers, all referenced to the above relevant projection system, could be created to include features such as roads, railway lines, dunes and beach layers.

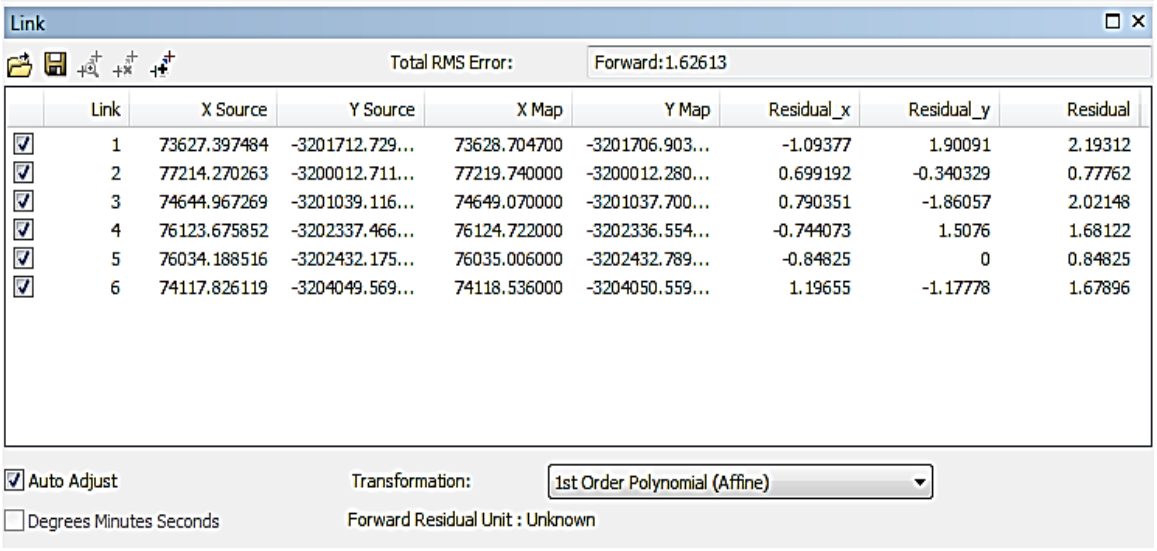

Link	X Source	Y Source	X Map	Y Map	Residual_x	Residual_y	Residual
1	73627.397484	-3201712.729...	73628.704700	-3201706.903...	-1.09377	1.90091	2.19312
2	77214.270263	-3200012.711...	77219.740000	-3200012.280...	0.699192	-0.340329	0.77762
3	74644.967269	-3201039.116...	74649.070000	-3201037.700...	0.790351	-1.86057	2.02148
4	76123.675852	-3202337.466...	76124.722000	-3202336.554...	-0.744073	1.5076	1.68122
5	76034.188516	-3202432.175...	76035.006000	-3202432.789...	-0.84825	0	0.84825
6	74117.826119	-3204049.569...	74118.536000	-3204050.559...	1.19655	-1.17778	1.67896

Figure 4.15: The total RMS error is 1.62613, using six control points to orient the photograph and determine the survey accuracy in relation to when the photograph was taken.

Figure 4.16: The image target with a transparency of 40% is ready to be oriented. The yellow points are the control points. Point 1 on the ground is joined up with Control 11. After another coordinate orientation the photograph will already be provisionally oriented.

4.10 Creating the New Features

In ArcGIS, folders for the Thukela, Amatigulu and Umlalazi River sites were created. Sub-folders for the years were created in each main folder. To create a new feature class such as a road, one right clicks on the specific sub-folder and clicks **New**. The name of the feature class to be created, for example, **Road**, is then typed in, followed by the feature class type, for example, point, polyline, or polygon. The **Road** feature, in this case, is a polyline. The road is now created. On the image, all roads according to their classes of importance can be drawn in by clicking on the **Editor** and then one can **Start Editing** by clicking again on **Editor** and then on **Windows Feature Class**. The cursor becomes a cross for the editing to take place. When one has finished drawing a certain feature class, one clicks on **Editor** and then on **Stop Editing** to save the edits created during the process (see Figure 4.17). In the ArcGIS program different layers can then be switched on and off, for example, all the Umlalazi plans can be compared with each other in relation to the changes in the river or the amount of bush increasing or decreasing over the years. Plans were created for all three sites using three time intervals: for the Thukela and

Amatigulu estuary 1953, 1983 and 2006, and for the Umlalazi estuary 1957, 1983 and 2006 (see Figures 4.17 and 4.18).

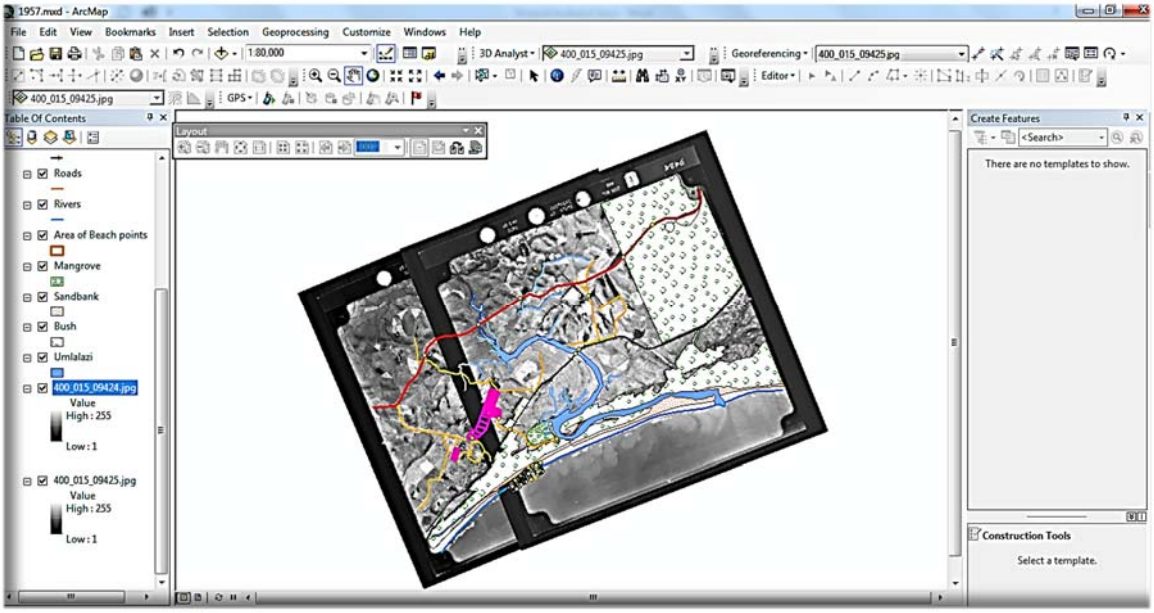

Figure 4.17: In this ArcGIS figure the creating and editing of the different layers has been completed, as displayed in the Table of Contents on the left hand side of the screen. A plan of the Umlalazi estuary is created from the target images.

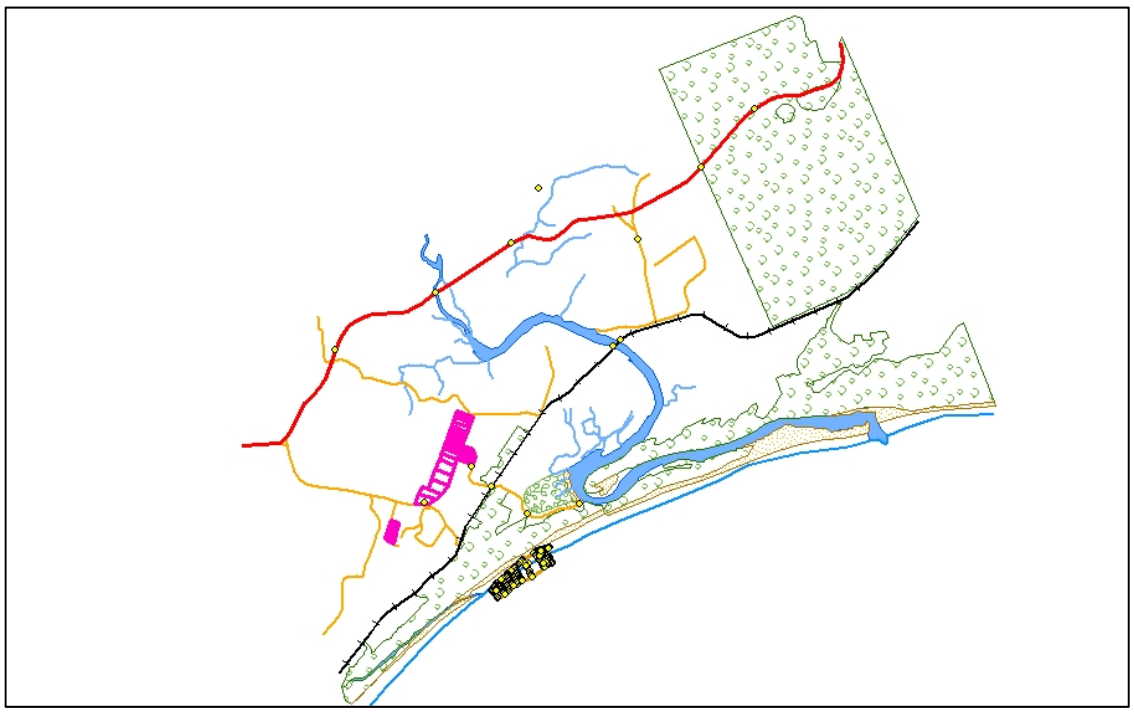

Figure 4.18: The end result of editing the photographic models in the ArcGIS program.

Chapter 5:

Results

5.1 Overview of the Results from the Three Sites

The research focused on three sites: the Thukela River mouth, the Amatigulu-Nyoni River estuary and a section of the coast near the Umlalazi River estuary. The results as discussed in this chapter were derived from surveys and the analysis of aerial photographs.

At the Thukela River mouth, the north and south shores were surveyed twice. Different results were obtained for each survey, not just regarding the surface area, but also regarding the sand volumes of the north and south shores of the Thukela River mouth, because of the dynamics of the Thukela River and the changes in the sand dunes and the beach area. Analysis comparing field data with data from aerial photographs showed the instability of the south shore and also its inconsistency, making it difficult to calculate a sustainable increase or decrease of the south shore. To a lesser degree this also applies to the north shore. The movement of the sand is dependent on changes in the wind direction, rainfall, temperatures and wave energy. The Thukela results such as volumes and areas were calculated with the help of Model Maker and ArcGIS 10.4.1

The Amatigulu River estuary was surveyed once, and the field data were compared with the aerial photographs and satellite images from 1953 to 2017. Again the Amatigulu results such as volumes and areas were calculated with the help of Model Maker and ArcGIS 10.4.1.

At the Umlalazi beach, the emphasis was on a very detailed survey for a short-term assessment (March 2016 and July 2017). The Umlalazi beach was measured four times, with approximately six-month intervals, over two years. Unfortunately, during each visit the survey terrain or cover area differed slightly from that used in the previous survey. Hence, the areas and the volumes could not be calculated using exactly the same figure size. To solve the problem of these irregularities arising from using four different figures, four common coordinates were identified and all four figures are based on these four coordinates for calculation purposes. The areas and volumes were then determined four times from this fixed figure. The preliminary results of the short-term assessment were already an indication of what to expect from the sand and the activity of the sand movement.

5.2 Climate from 1993 to 2018

In respect of climate, data such as the rainfall and temperatures were only available from 1993, because the Mtunzini weather station was established only in 1992. The climate in KwaZulu-Natal is subtropical with mild winters, with temperatures seldom going below 17°C and the sea water maintaining a temperature of 21°C even during the winter months. As temperatures rise, precipitation also increases. The temperatures start to rise from September and reach a peak during January, after which they begin to fall slightly. The warmer months are also the months with the highest rainfall, as illustrated in Figure 5.1 (South African Weather Bureau). During the winter months, the dry season, the rainfall is approximately 60 mm from April to August. In winter, the temperatures average 20°C, so it is still mild and warm, although there is less rain (see Appendix D).

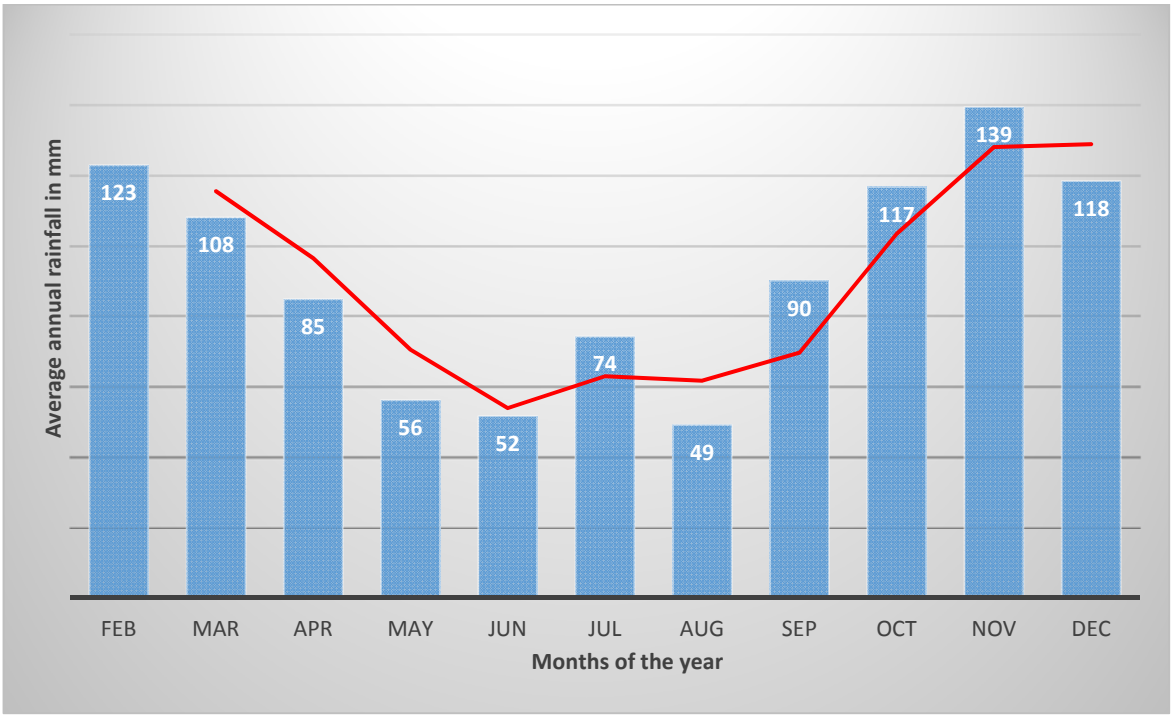

Figure 5.1: Annual average rainfall per annum in mm per month from 1993 to May 2018 measured at the Mtunzini weather station.

(Source: South African Weather Bureau, 2018; also see Appendix D)

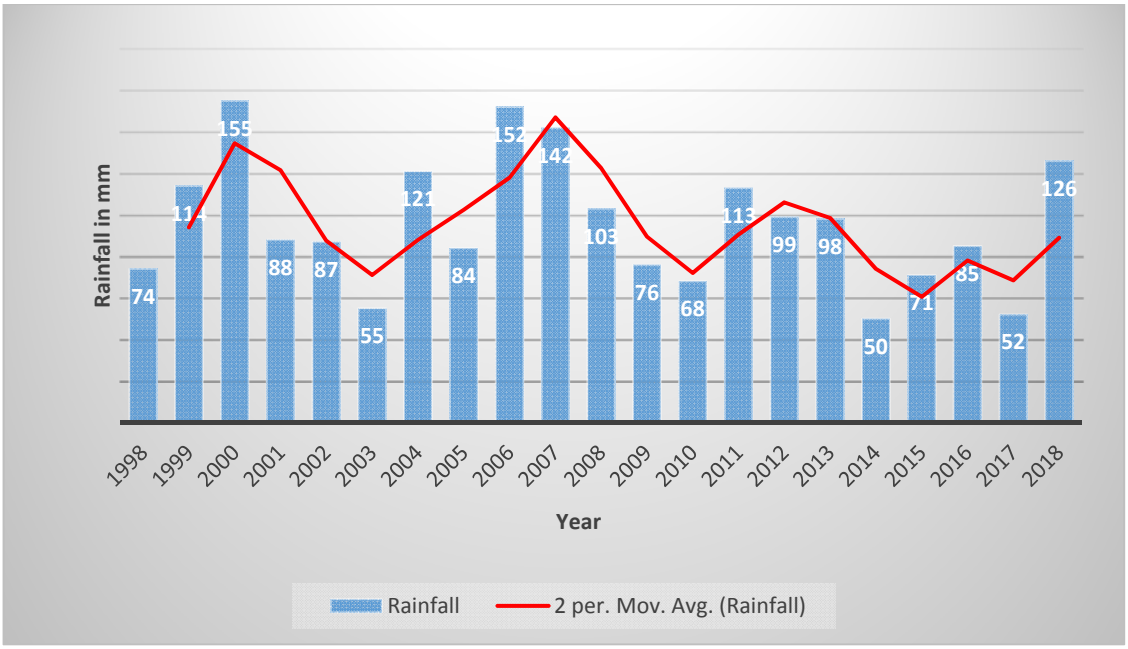

Figure 5.2: Annual average rainfall per annum from 1993 to May 2018, measured at the Mtunzini weather station.

(Source: South African Weather Bureau, 2018; also see Appendix D)

5.3 Dynamics of the Thukela River Mouth over the Years

The Thukela River has changed over the years (see Figure 5.3). Although the plan intervals are 30 years apart, it can be seen that from 1953 to 2017, the river can change from season to season.

5.3.1 Thukela River mouth results obtained using the aerial photographs.

In the 1953 diagram, large sandbanks appear close to the mouth. The ever-present sandbank referred to as the south shore in this study forms a barrier between the river and the sea. The north shore is horseshoe-shaped. The river flows through between the north and south shores. The shores are frequently rearranged, from season to season. Figure 5.3 shows an instance where the estuary has opened up to the sea in the centre of the Thukela River sandbank. By contrast, on the 1953 aerial photograph, more sandbanks are visible upstream and the north shore is much larger. However, for the purposes of the diagram they are not shown. The river was flowing slowly and formed a braided pattern, sandbanks were formed during earlier runoff periods (Blignaut, 2015). The mouth is centred between the two shores with a very small channel entering the ocean.

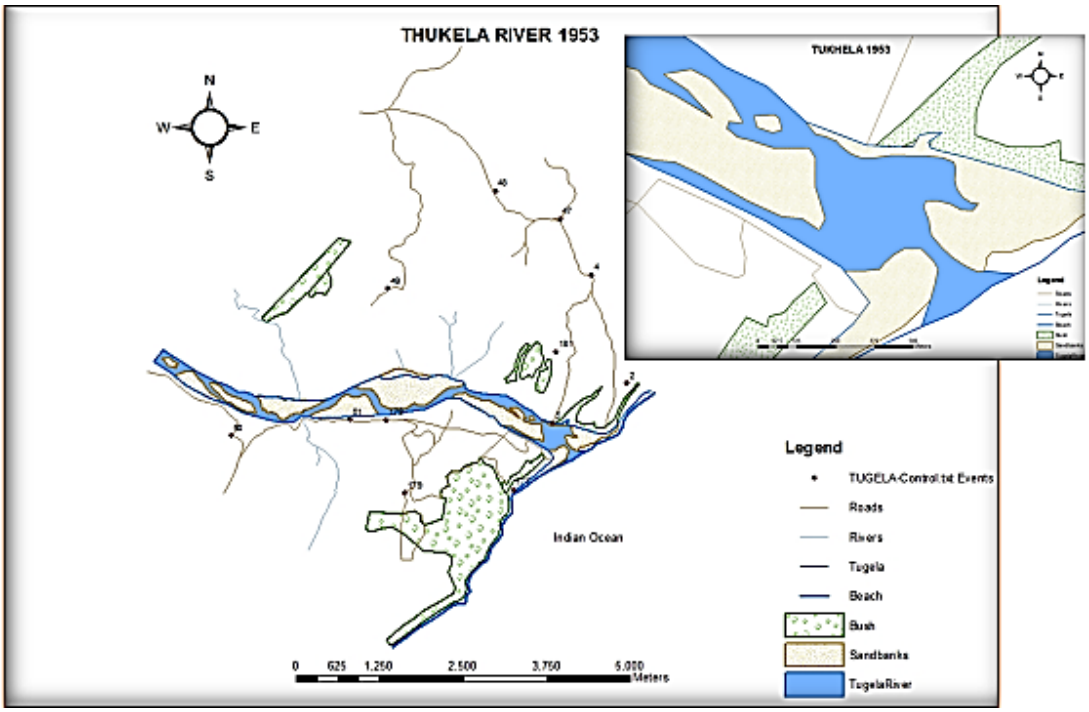

Figure 5.3: The Thukela River in 1953, zigzagging through the sandbanks, with a small outlet in the centre between the north and south shores to the sea.

In the 1983 aerial photograph (used in Figure 5.4), the Thukela River can be seen to have formed a braided pattern close to the mouth, where small, slowly flowing streams flow into the sea. The mouth was open to the sea, but the opening had shifted to the northern side, making the southern sandbank very large. The position of the mouth depends on what time of the year the aerial photograph was taken, because, as stated above, the last 20 km or so to the river mouth has a very equal falling slope. Therefore, it can be assumed that at that stage in 1983, the river was flowing very slowly in this last stage to the sea, forming a small channel entering the sea. The water behind had little forward pushing power, so a lagoon was created backwards from the mouth.

In Figure 5.5, using a photograph taken in 2013, it can be seen that the Thukela Mouth has moved close to the the northern shore. The mouth forms a small channel to the sea with a lagoon about 4 km long. The water in the river can be assumed to have been flowing very slowly, because it is a very even slope and the water is stored in the form of a lagoon before flowing into the sea. The argument is strenghtened by the numerous sandbanks and the braided pattern of the river further upstream.

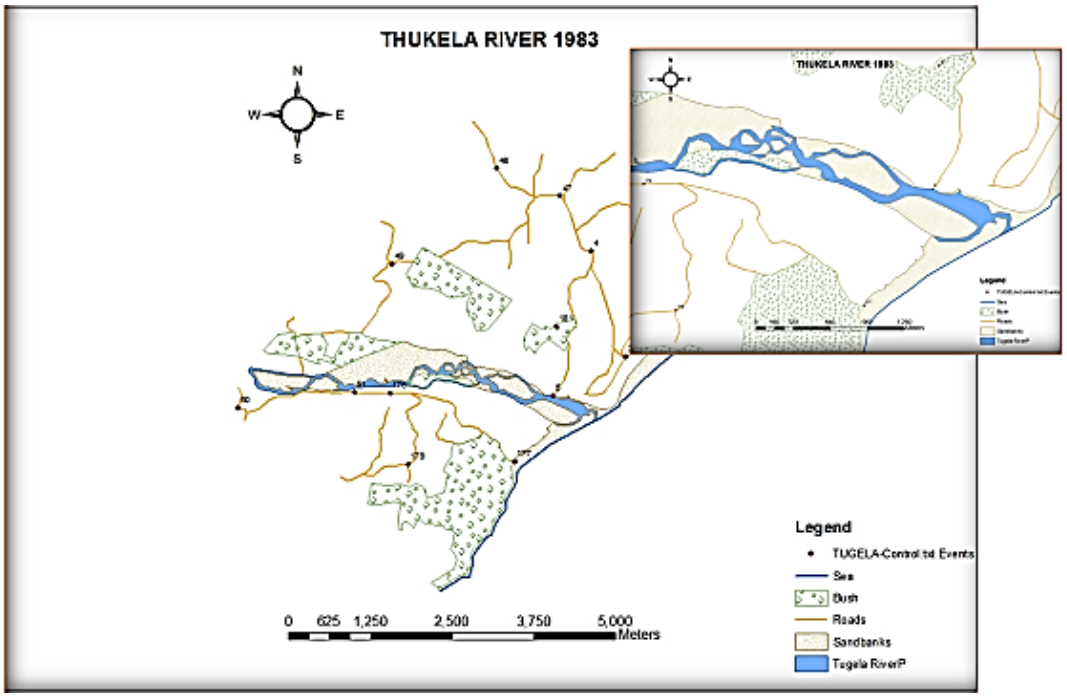

Figure 5.4: The Thukela River in 1983, showing a braided pattern through the sandbanks.

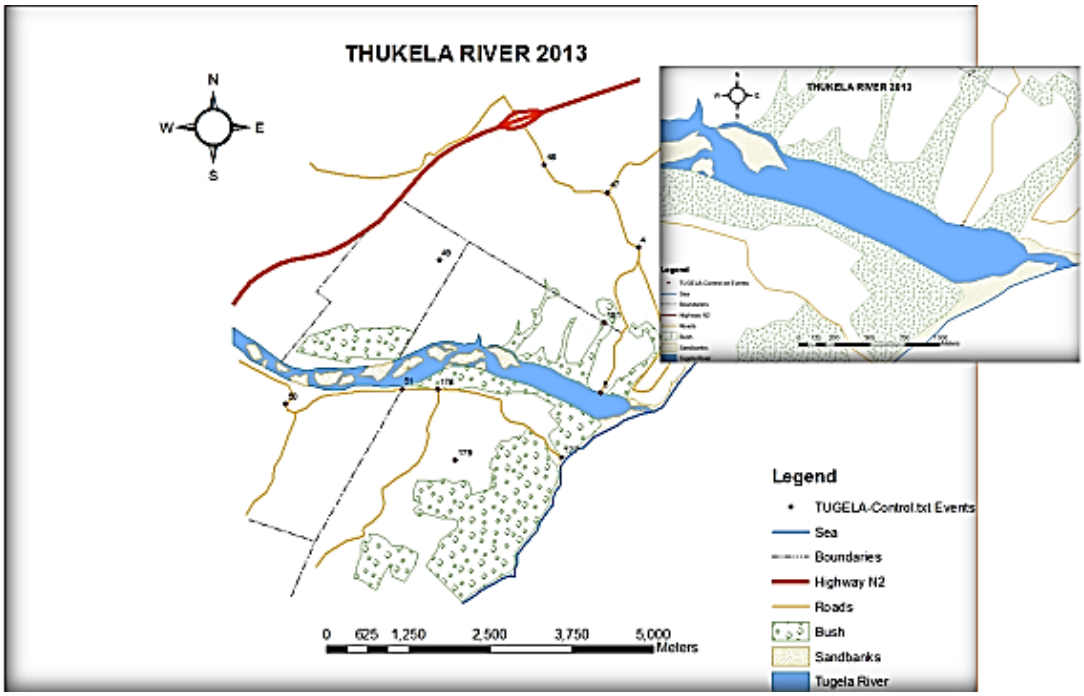

Figure 5.5: The Thukela River in 2013 (note that the plans' scales differ because the aerial photograph scales are different).

Smaller plans for dates between the 30-year intervals were created on ArcGIS, showing just the mouth of the Thukela River with no surrounding details in the area. These smaller inserts

reflect conditions approximately 20 years apart (see Figure 5.6), contrasting the 1953 image (**A**) with the 1972 image (**B**), where the sandbanks have almost disappeared, with significant geomorphological changes. In the aerial photograph of 1972 strong runoff into the sea is visible, suggesting that strong flow has taken sand into the sea. The mouth is almost fully open, with the sandbar mostly confined to the south shore. Strong runoff means floods occurred before the aerial photograph was taken – Blignaut (2015) notes that large flood discharges were recorded at Mandini in 1966. The discharge has removed the sandbanks and the northern beach shore is significantly smaller.

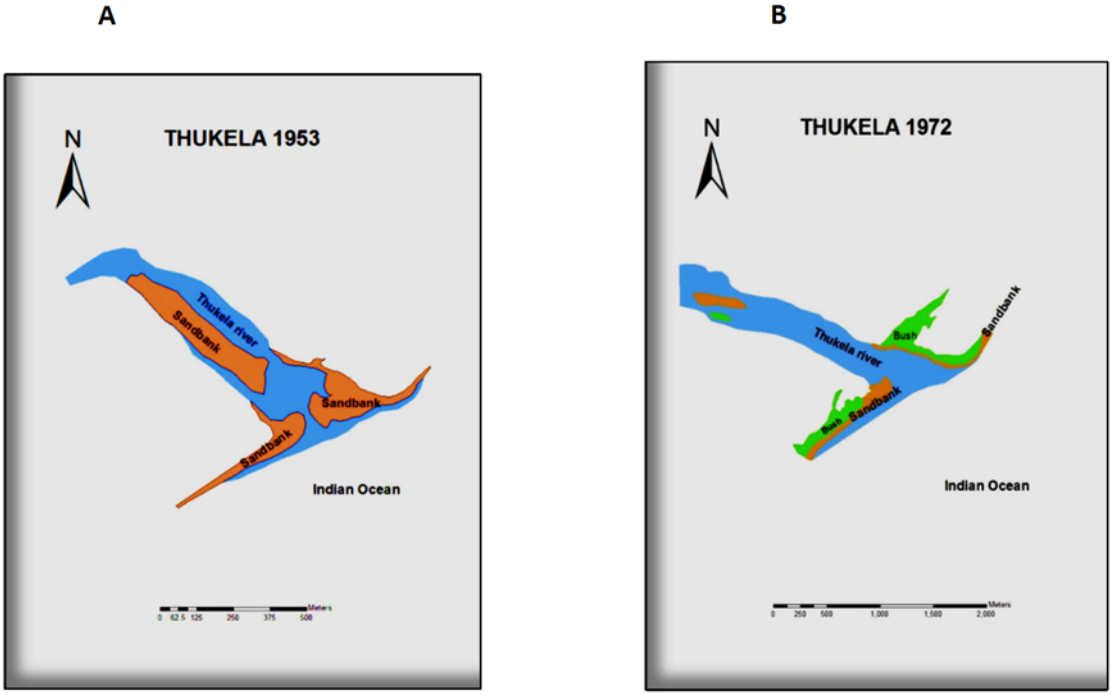

Figure 5.6: Diagrams of the Thukela mouth in 1953 (**A**) and the mouth in 1972 (**B**).

During the period from 1972 to 1989, several geomorphic changes took place. This is clear if one compares the image from 1972 with those from 1989 and 2017. Strong discharge and a low occurrence of sandbanks can be seen for 1989 and 2017. The south shore has increased in size by 2017.

In Figure 5.7, the difference between 1989 (**A**) and 2017 (**B**) is that the narrow opening of the mouth in 1989 has moved further north. In the study, a 2017 satellite photo image was used for the reason that no aerial photos were available at that stage. The 2017 area was also surveyed in March 2016 and the first week of July 2017 (**B**).

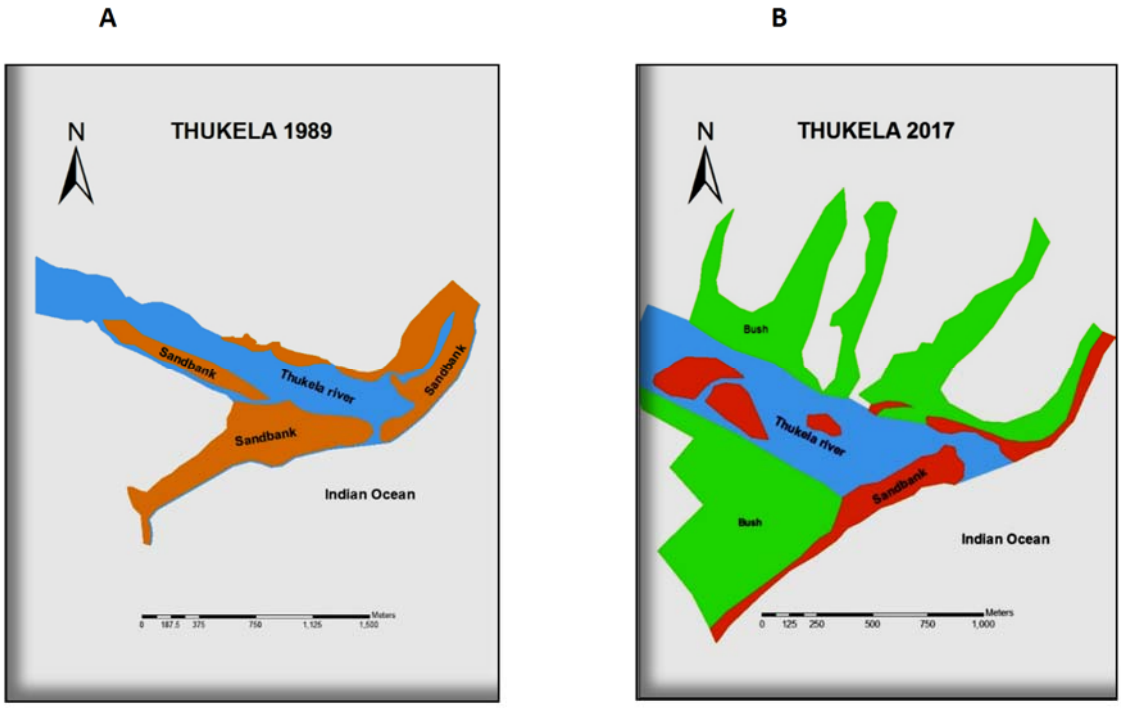

Figure 5.7: **A:** In 1989 the Thukela mouth shifted south (photograph probably taken in the dry season when the Thukela River almost came to a standstill). **B:** In 2017 the Thukela mouth is on the northern side with the river flowing strongly (own observation)

5.3.2 Thukela River mouth results obtained from the physical survey techniques.

At the Thukela River mouth, physical surveys were undertaken to obtain spot levels for the heights and true topographical images of the terrain. As Figure 5.8 shows, the north and south beaches were subject to erosion, most probably during the summer months of 2015 and 2016 when heavy rainfall occurred. The rainfall for January was 125 mm, for February it was 133 mm, and for March it was 146 mm. This caused high, destructive and aggressive waves that eroded the sand deeper into the sea. Figure 5.8 represents the data for the north shore between March 2016 and July 2017.

Heavy rainfall occurred from November 2015 to February 2016, the time preceding March 2016, when the first survey took place (see Figure 5.8). Due to this relatively high rainfall, the Thukela River was flowing strongly and eroded sand from the beach. Both the north and south shores changed in size and volume from the survey in October 2016 to the survey in July 2017. The reason for the change in the shores is that during the winter months, the sea flattens out with fewer windy days and less rainfall. The second survey was conducted in the first week of July 2017. It was found that the north shore had increased in area to 25 171 m^2, an increase of 91%.

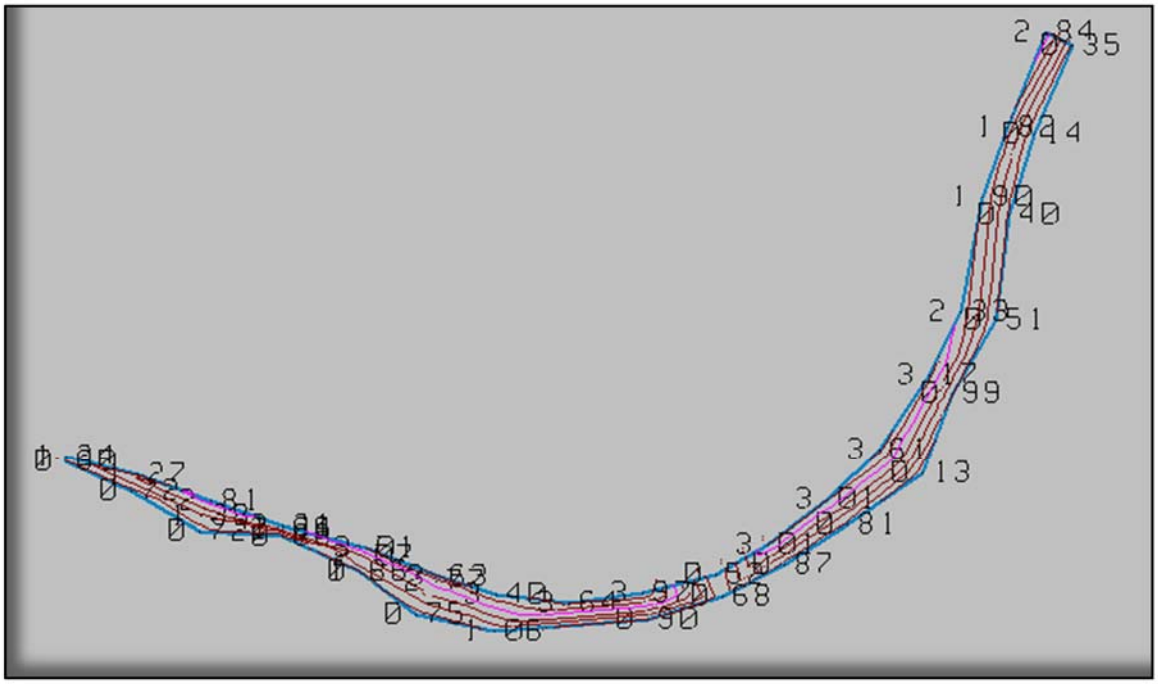

Figure 5.8: The North shore beach at the Thukela River (surveyed in March 2016). Scale: 1: 500

When the sea is calm and the waves have a constructive effect on the beach, it tends to wash more sand out onto the beach to increase its size and volume. In 2016, the Thukela River was also flowing very slowly, with a no transport action. With no rain or little rain in the river and in the catchment area during the winter months, the Thukela's water level dropped and sand accumulated on the north beach. The results can be seen in Figures 5.9 to 5.11 and in Table 5.1.

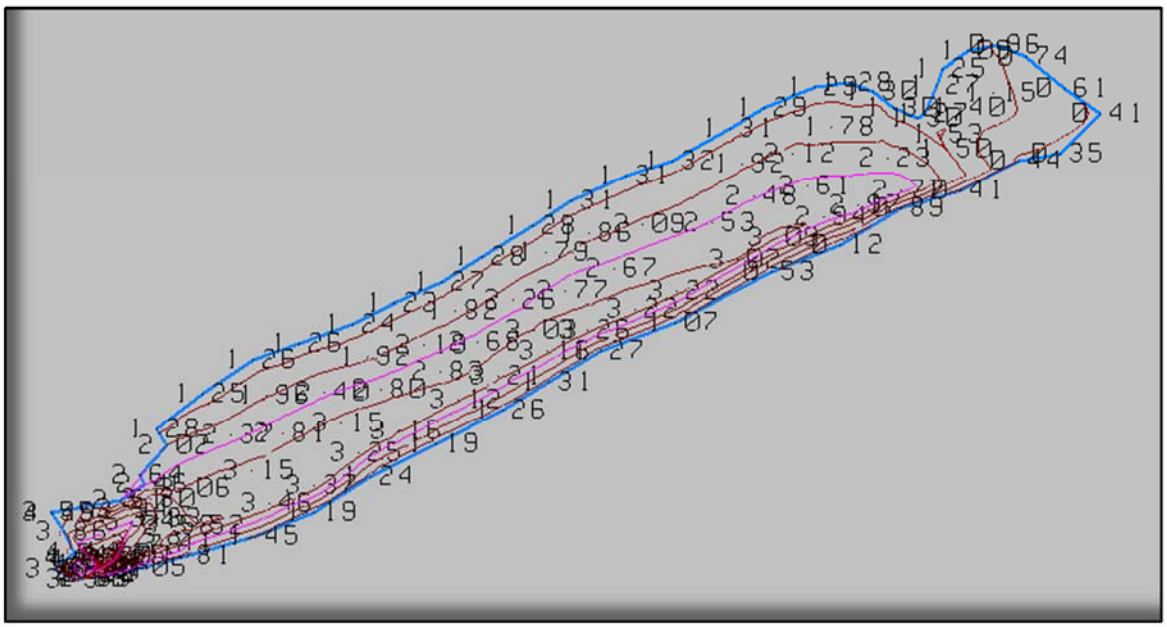

Figure 5.9: The south shore beach at the Thukela River (surveyed in March 2016). Scale: 1: 500

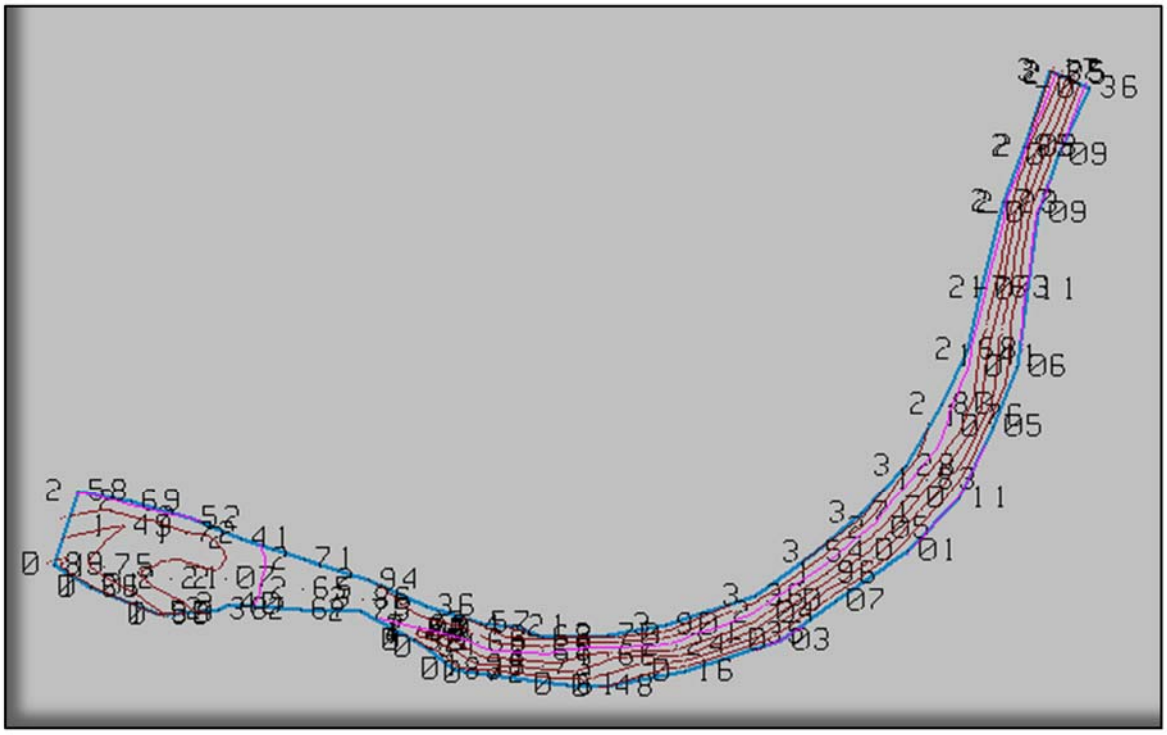

Figure 5.10: The north shore beach at the Thukela River (surveyed in July 2017) Scale: 1: 500.

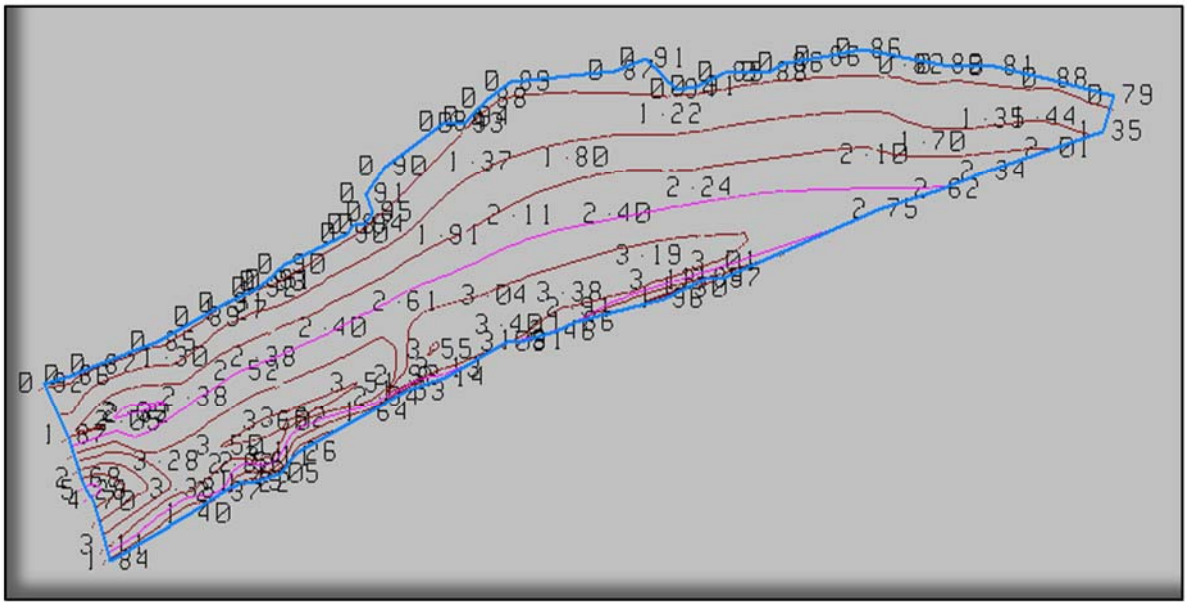

Figure 5.11: The south shore beach at the Thukela River (surveyed in July 2017). Scale: 1: 500

Table 5.1: Percentage increase and decrease in area and volume for the north and south beaches of the Thukela River from 1953 to 2017

North beach				
Year	**Area (m^2)**	**Volume (m^3)**	**% Area**	**% Volume**
1953	163228	94672		
1983	58783	32331	-63.98	-65.85
2013	44483	26690	-24.33	-17.45
2016	13152	21110	-70.43	-20.91
2017	25171	55433	91.39	31.03
South beach				
Year	**Area (m^2)**	**Volume (m^3)**	**% Area**	**% Volume**
1953	52866	111019		
1983	66954	140603	26.65	26.65
2013	85215	179804	27.27	27.88
2016	67125	143162	-21.23	-20.38
2017	87954	185784	31.03	29.77

5.4 Geomorphic Changes of the Amatigulu-Nyoni River Estuaries

The Nyoni River and the Amatigulu River mouths were both closed to the sea in 1953, as Figure 5.12 (overleaf) shows. According to Engelbrecht (2008), there are signs of tidal overwash from the sea into the Amatigulu River. In the aerial photograph 1953, no vegetation is visible on the barrier, but during the time interval to 1972, *Casuarina* vegetation has grown in this area, and since then, this kind of vegetation has established itself on the beach.

In 1972, as can be seen in Figure 5.13 (**A** and **B**) (overleaf), the river is open to the ocean (Engelbrecht, 2008) and enters the sea at two positions. Subsequently, the Nyoni is captured by the Amatigulu River, and 19 years later, the Nyoni River, which has been diverted north-east for 8 km (Orme, 1980) is part of the Amatigulu River. The barrier is much shorter, because the river has come to a standstill. When the river stops flowing, more sandbanks appear in the river and only a narrow stream reaches the estuary.

In 1989, the river was closed again. However, the width of the beach area had increased since 1972 – the beach is also wider than the 2007 observation (see Figure 5.13 **B**).

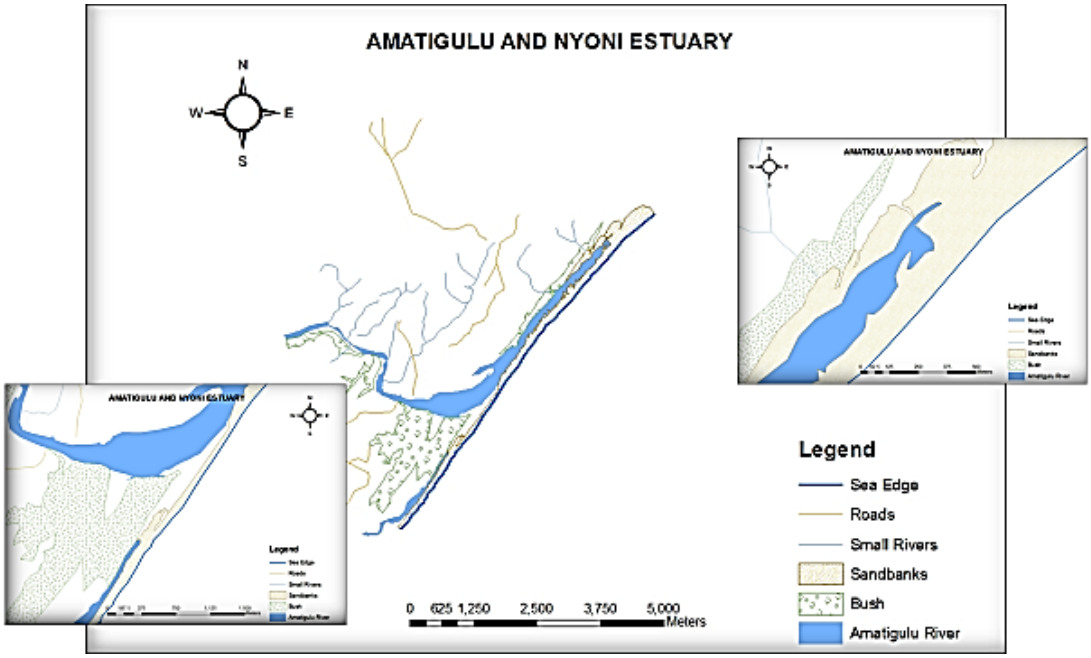

Figure 5.12: Amatigulu-Nyoni estuary, 1953, when the Nyoni River did not meet the Amatigulu River, which was standing still (georeferenced from the 1953 aerial photographs).

Fewer sandbanks are visible in the 1989 observation than for 2007. This suggests that the Amatigulu and the Nyoni Rivers flowed more strongly in 1989 than in 2007, even though the mouth was open to the ocean in 2007. The 2007 aerial photographs, taken during the rainy season, show that the beach (which also forms the sand barrier) had decreased since 1989. The Amatigulu barrier becomes very long, measuring over 4 km from south to north.

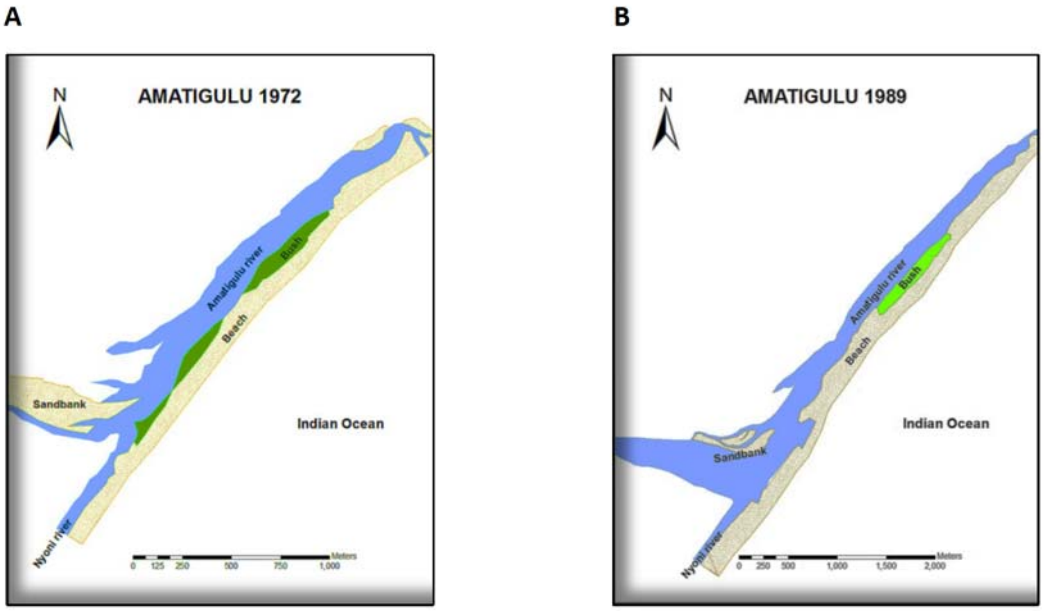

Figure 5.13: **A, B:** The Amatigulu beach (sand barrier) in 1972 and 1989, showing that the Nyoni River did break through to the Amatigulu River.

The area of the sand barrier between the estuary and the sea is directly related to the distance the river pushes northwards, which was in turn related to the runoff of the river in flood when there was rain in the catchment area. According to Table 5.2, the 1953 and the 2017 barriers were by far the largest in square metres. The fluctuations between the intervals for which data are known are not clear. It is assumed that the estuary's barrier experiences geomorphological changes due to variations in the aeolian forces, the wave energy and changes in the rainfall in the catchment, as shown by Begg (1978) and Engelbrecht (2008).

Table 5.2: Areas of the Amatigulu sand barrier in 1953, 1972, 1989, 2007 and 2017.

Year	**Years Interval**	**Area (m²)**
1953	-	1 034 397
1972	19	314 350
1989	17	975 403
2007	18	586 031
2017	10	1 056 482

In March 2016 and July 2017, the Amatigulu estuary was surveyed intensively using GPS methods (see Figure 5.15, overleaf). According to these measurements, the sandbank increased dramatically in the ten-year time span from 2007 to 2017 with 1 056 482 m². The sandbar has migrated further north as the waves washed the sand at an oblique angle to the coastline. The waves strike the coast at an angle, but withdraw at a 90^{o} angle. This effect pushes the sand northwards, making the beach estuary longer and therefore making the sandbar larger. By July 2017, the sandbank had increased to 1 056 482 m².

Figure 5.14 (overleaf) shows the position of the Amatigulu-Nyoni mouth in 2007. The dune furthest to the east is the relevant site under survey (Begg, 1978). The Amatigulu River forms a lagoon where the rivers run very slowly, even though the mouth was open to the sea at the stage when this aerial photograph was taken.

In Figure 5.15 (overleaf), the Amatigulu dune (shown in the figure as the "Beach") can be seen clearly. The dune is flat and forms part of the beach area. The beach/dune was surveyed using the GPS. It had an area of 1 056 482 m² in 2017.

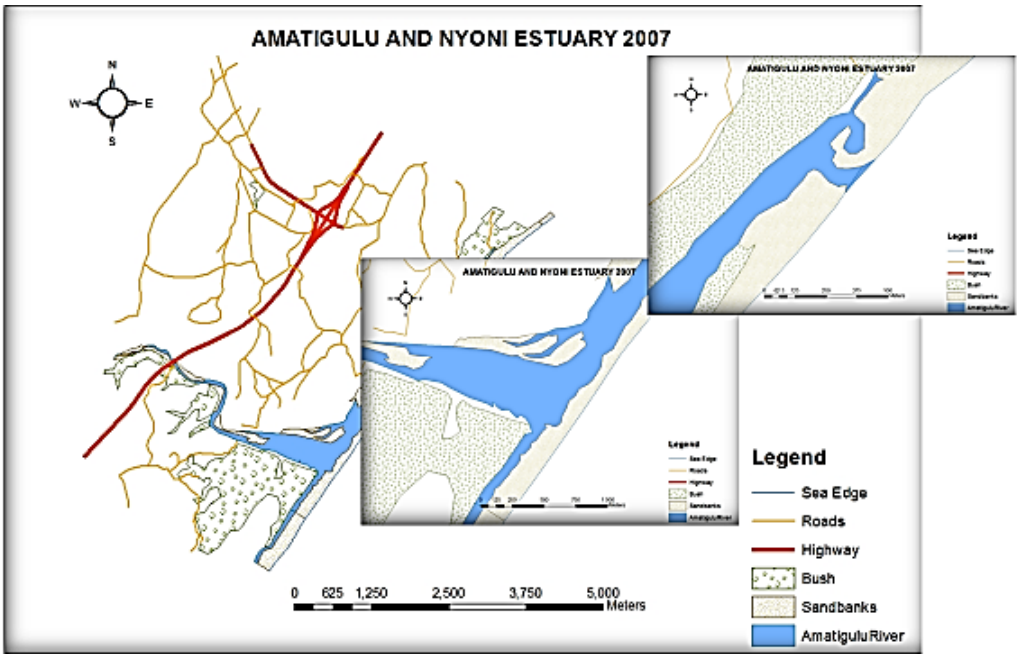

Figure 5.14: Position of the Amatigulu-Nyoni mouth in 2007, showing the lagoon forming where the Amatigulu River runs very slowly, although the mouth is open to the sea.

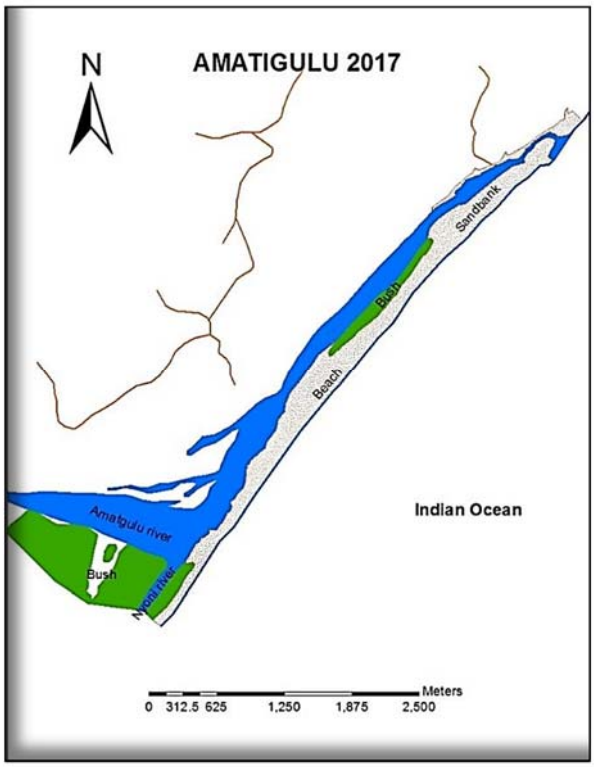

Figure 5.15: The flat Amatigulu dune forming part of the beach area of 1 056 482 m² in 2017.

5.5 Umlalazi Results

5.5.1 First method: Comparing the 1957 data with the 2009 satellite image.

Observations from aerial photographs taken since 1957 were compared with recent satellite images, and the field data. This method involves simple comparison through inspection of the 1957 and the 2009 photographs. The outcome of the comparison leads to the analytical and scientific methods used in the study (see Section 5.5.5). During the geo-referencing of the 1957 aerial photographs, all the control points and the assessment points that were surveyed on the beach were plotted on the aerial photographs of 1957, as seen on Figure 5.16 (**A**).

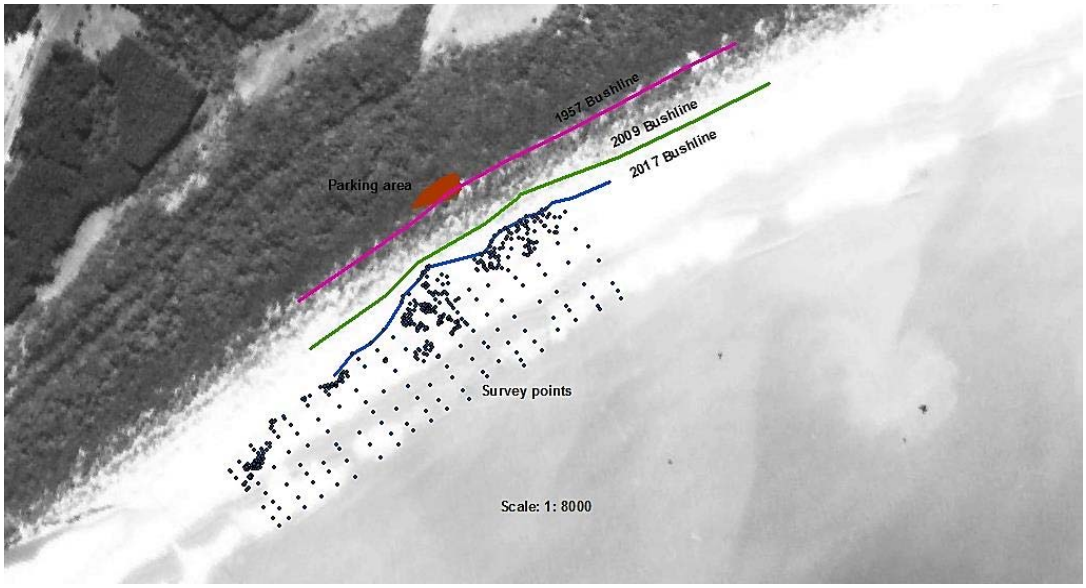

A

B

Figure 5.16: **A:** 1957 aerial photograph showing the Umlalazi beach (purple line) and edge of the bush (green) line.
B: 2009 satellite image showing the edge of the encroaching bush (green line).

For these observations of the aerial photographs and the comparison with the surveys, the aerial photographs **A** and **B** in Figure 5.16 were very accurately registered, as can be seen in Table 5.3, and as described in Chapter 4, with an RMS error of 0.00 m. The points on the Umlalazi beach are all related to the survey ground control points, and it can be assumed that the points on the beach all fall very accurately on the correct part of the surface of the earth. In the 1957 aerial photograph (**A**), the Umlalazi beach is represented by the purple line, which in 1957 indicated the edge of the bush line. The green line is the edge of the vegetation, where small bushes were coming up and going over into the sand dune. In the 2009 satellite image (**B**) the green line that represents the edge of the bush has shifted. It is noticeable how far the bush has encroached onto the sand dune between 1957 and 2009.

Table 5.3: The registration of points at the Umlalazi beach surveying area on the aerial photograph of 1957.

Link

Total RMS Error: Forward:0

	Link	X Source	Y Source	X Map	Y Map	Residual_x	Residual_y	Residual
☑	1	390.085491	-1490.888651	73473.050000	-3204534.050...	0	0	0
☑	2	604.468478	-420.185497	73628.700000	-3201706.900...	0	0	0
☑	3	753.821648	-1451.190335	74391.790000	-3204319.110...	0	0	0
☑	4	663.709404	-1335.948380	74118.100000	-3204049.850...	0	0	0
☑	5	753.821648	-1451.190335	74391.790000	-3204319.110...	0	0	0

From the 2009 satellite image, using the ground control points as orientation, the "Parking Area" was drawn in on the 1957 aerial photograph (it did not yet exist in 1957). On the 1957 aerial photograph, the bush just north of the beach area is separated from the beach by a pink line known as the bush line at the top of the sandbank. It indicates the edge of the bush and the immediate transition from the bush to the top of the sandbank. There seems to be a definite shift from the bush southwards in the direction of the beach, as can be seen in Figure 5.16 (**B**). The green line in the polygon falls under the water, according to the 1957 aerial photograph, whereas that same line was on the dry sand of the beach, according to the 2017 field survey. It is debatable whether it was high water when the 1957 aerial photograph was taken. Admittedly, in the survey in 2017, when it took a day to survey the area, the tides changed from low to high tide in the time it took to do the survey. Therefore, the southern boundary line of the survey points is an average of the low and high tide. However, that does not change the fact that the northern bush boundary has shifted.

On the 1957 aerial photograph, the pink line runs along the edge of where the Parking Area is now (it was drawn in on the 1957 aerial photograph for explanatory purposes). It can be

clearly seen where the Parking Area is, on the edge of the transitional vegetation line, separating the very dense bush from the less dense bush, established plants from plants coming up. Between 1957 and 2009, the small bushes have grown (the edge forming the 2009 bush line is indicated by the green line in Figure 5.16 (**B**)). It seems that the bush has encroached even further on the beach area since then: by 2017, the edge of the bush, represented by the blue line, is approximately 60 m away from the 2009 bush line. This observation shows that the bush has been encroaching onto the beach, while the sea has retreated. This comparison suggests argued that the beach has become smaller in area and in volume over a defined terrain between 1957 and 2009.

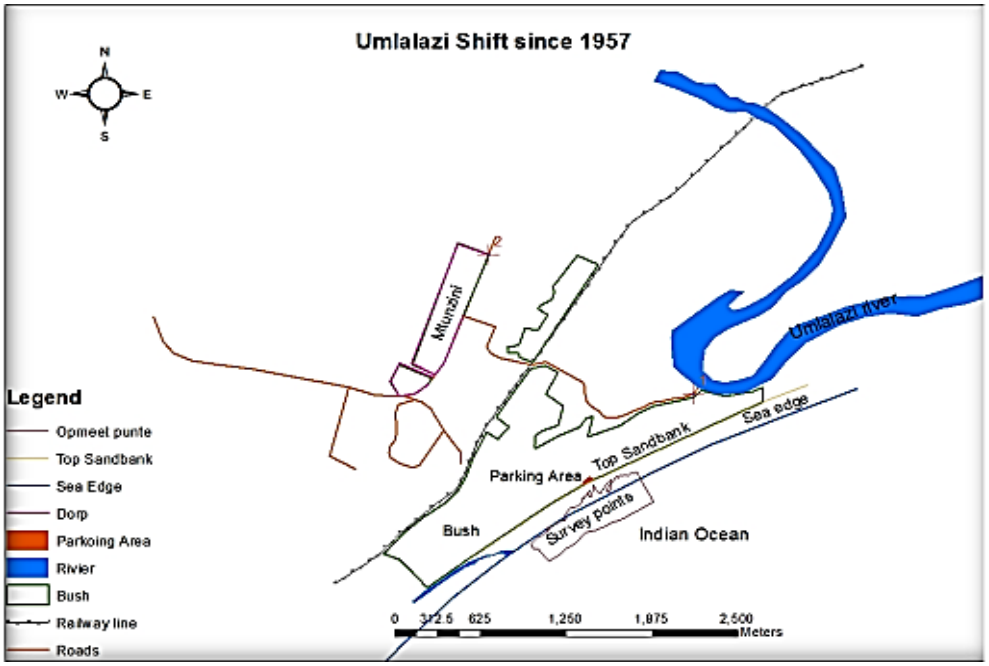

Figure 5.17: Beach shift at the Umlalazi in a south-easterly direction (survey points on dry ground in 2017 were under water in 1957). The mean sea level can be seen clearly.

In Figure 5.18 (overleaf), the mouth of the Umlalazi is wide open to the sea. The black area in the insert on the left in Figure 5.18 and in Figure 5.19 represent the survey points taken during the research surveys in 2016 and 2017. The pink area in the insert on the lower right side of Figure 5.20 is an enlargement of the survey points. At the time of the survey, the Siyaya River also joined up with the ocean. The mouth forms a braided pattern joining the sea. In the lower insert in the figure, the pink area shows the points that were surveyed during the research in this study. The Siyaya River is closed off from the sea.

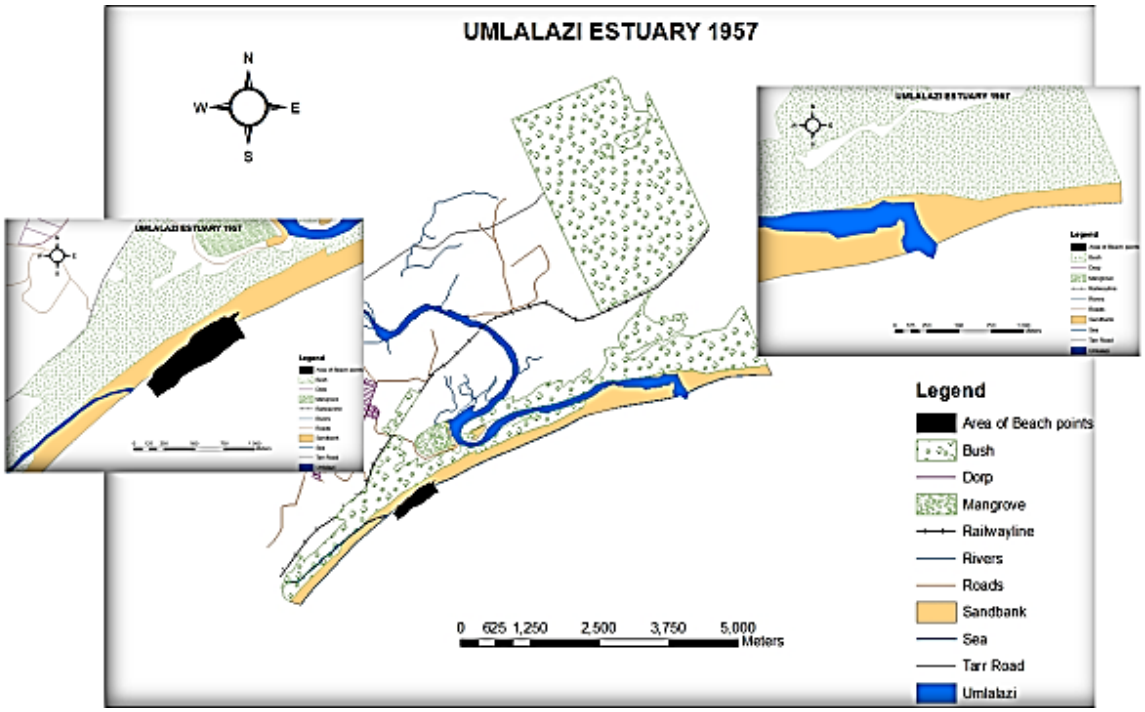

Figure 5.18: The mouth of the Umlalazi River and the Siyaya River are open to the sea (1957). Left insert: Close-up of survey points (black figure).

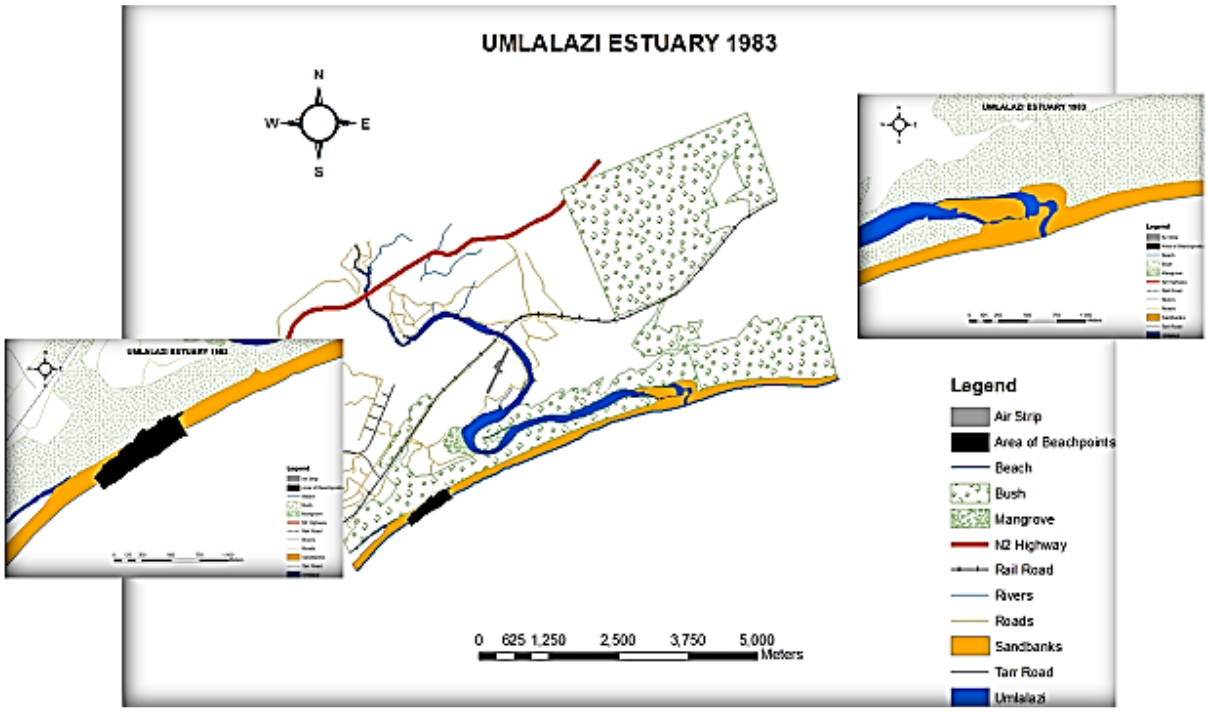

Figure 5.19: The Umlalazi estuary in 1983.

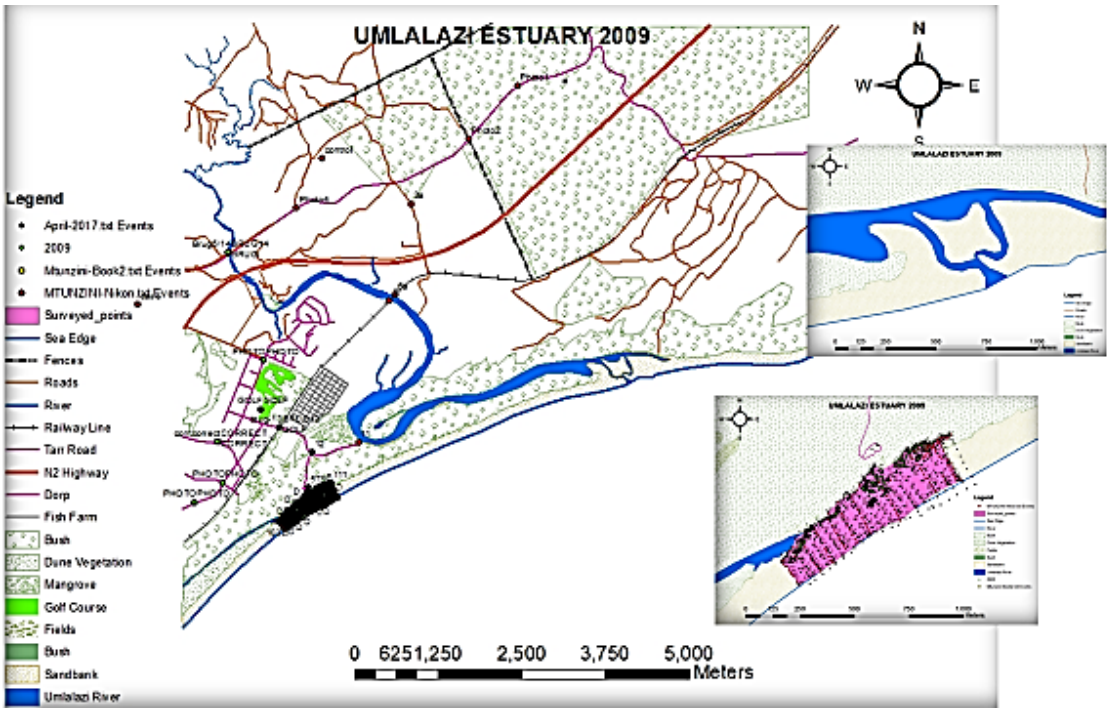

Figure 5.20: More extended view of changes in and around Mtunzini and the survey points on the Umlalazi beach.

5.5.2 Second method: Physical survey and assessment of the dunes.

Various kinds of hardware and software were used to determine changes at the Umlalazi beach in an intensively analytical way to get first, preliminary and, at a later stage, final results at the Umlalazi beach. A combination of physical surveying in the field and different software programs such as Model Maker Version 12.03, ArcGIS 10.4.1 and Microsoft Excel were used to create tabulated and graphical results from the data in the form of areas and volumes. These methods made it possible to determine why sand is also creeping deeper into the forest, and why there is not only bush encroachment onto the sand dunes.

Wind is in one of the most important transportation factors, carrying and depositing sand on dunes. According to the data obtained from the South African Weather Bureau, at Umlalazi beach, in the early mornings wind blows inland for approximately 216 days out of a possible 498 days (43% of the time), and in the direction of the sea for only 126 days. In the evenings, the wind blows inland for approximately 210 days (43%) of a possible 498 days, and it blows seaward only 197 days (39%). This is why the sand forms a slip face on which sand slides downwards into the forest to form an interdune deposit there. Wind blows sand seaward for about 27% of the days in the mornings and 40% in the evenings, which implies a gain of sand transported from the beach onto the dunes at a percentage of 16% in the mornings and 2% in the evenings. When the wind blows seawards over the treetops, it deposits the sand on the

windward side of the dunes. Therefore it can be assumed that this is why the dune slopes are approximately equal. A satellite image taken in 2009 shows that sand has encroached in a northerly direction of the vegetated areas since the 1957 photograph was taken (see Figure 5.21). The red areas indicate the intersection of survey areas and where the sand has encroached on the bush area and is creeping northwards. The bush and dune form a definite boundary between the two entities.

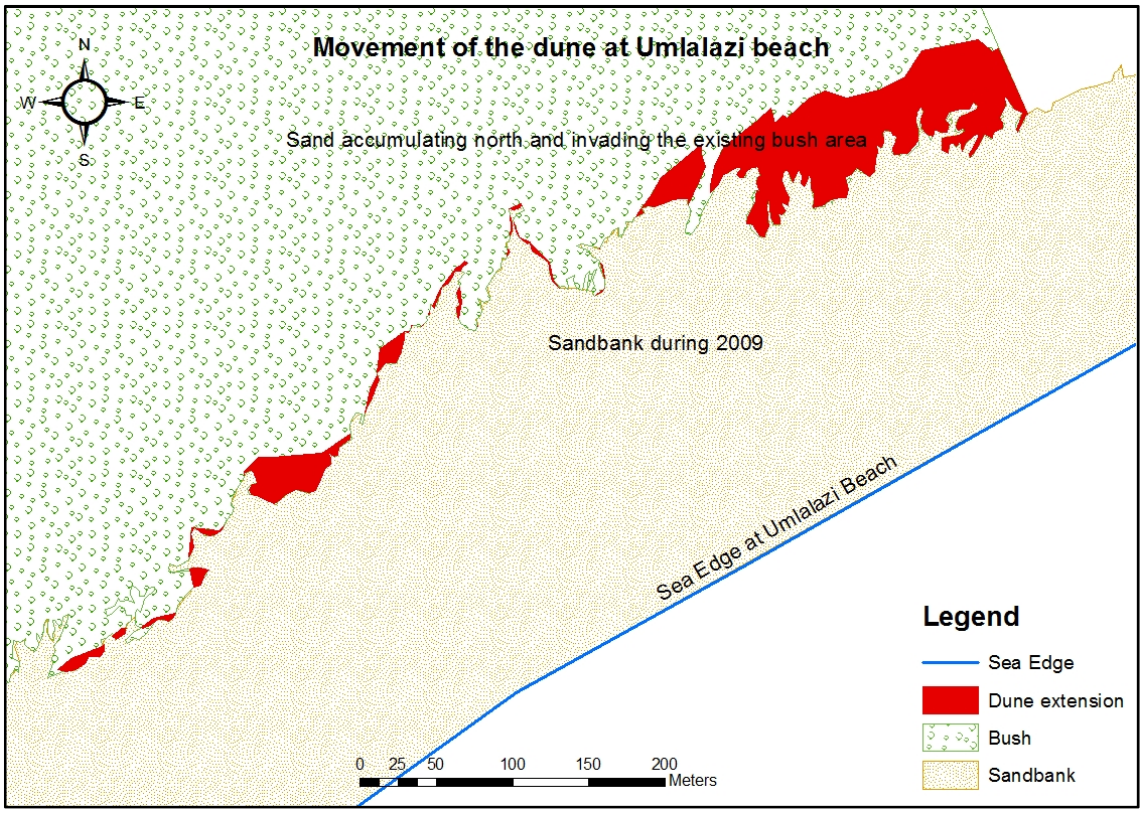

Figure 5.21: The 2009 satellite photograph indicates the dune extension at the Umlalazi beach, with the bush and dune boundary – red areas show sand encroachment northwards.

Table 5.4 (overleaf) shows a comparison of the four survey time intervals. The areas and cumulative volumes are tabulated and added together for each contour to get a cumulative volume for the whole area. A slight decrease in the rise of the volume of 11% was experienced from March 2016. It can be assumed that during this period calmer seas occurred, pushing more sand onto the beaches.

Table 5.4: Summary of the cumulative volumes and areas at the Umlalazi beach (surveyed March 2016 to July 2017

Survey Time	Cumulative Volumes (m^3)	Areas (m^2)	Percentage decrease/ increase
Mar-16	777 247.6715	850 737	
Oct-16	689 364.3146	757 605	-11.30
Apr-17	834 099.2001	903 741	+21.0
Jul-17	813 080.8632	883 693	-2.52

5.5.3 Effect of wind on the results.

One of the key factors of transportation and the depositing of sand is the wind factor. Wind has a significant influence on beach changes when very strong winds blow inland from the sea to deposit sand on the dunes, making the dunes steeper and higher. Sand encroachment occurs when the wind picks up very small grains of sand, collecting them on the coastal areas, or where they have been deposited by river runoff on the beach, to an area of accumulation. This accumulative area is usually dunes or sandbanks. Sand encroachment could be of such significant dimensions that it can damage roads, railway lines, and many more human-made structures, as well as naturally vegetated areas. It is thus possible for sand encroachment to have a serious socioeconomic impact.

Over the last 70 years, parts of the forest have encroached on the dunes, but the dunes have also encroached on some parts of the forest (see Figure 5.22, overleaf). If the wind blows from a south westerly direction (SW), it blows sand further into the forest. A slip face forms as usual on the side of the dune opposite to the wind direction, and sand then slides deeper into the forest (see Figure 5.23, overleaf). At the Umlalazi beach, when the wind turns around, blowing from the north-eastern (NE) to the east-north-eastern (ENE) side, it blows from the forest side, over the top of the trees, and it is then difficult for dunes to form a crest with a slip face in the opposite direction. Figure 5.23 illustrates the fact that, in this case, in the study area, there is only a small difference between the gradient of the windward slope and that of the slip face. However, according to the data of the South African Weather Bureau (see Appendix E), the wind blows from a south-western (SW) to a west-south-western (WSW) direction for approximately 43% of the year.

Figure 5.22: Young trees and plants encroaching on the sand dunes and the beach at the survey area at the Umlalazi beach (April 2017).

Figure 5.23: Signs of the beginning of an avalanche on a dune slip face (left) at Umlalazi beach as sand accumulates on the dune crest until it slips over on the slip face side (right) and encroaches onto the bush area (April 2017).

Table 5.5: Average wind direction (degrees from north) and average wind speed data from January 2016 to middle May 2017 at 8h00.

Year	Month	Days of no wind	Wind days in a month	Wind Direction	Geographical wind direction	Average Wind Speed in m/s
2016	January	3	11	230-270	WSW-W	3
			17	30-70	NE-ENE	
	February	2	14	230-270	WSW-W	3.6
			11	30-70	NE-ENE	
	March	6	14	230-270	WSW-W	2.5
			10	30-70	NE-ENE	
	April	8	11	230-270	WSW-W	2.4
			9	30-70	NE-ENE	
	May	15	10	230-270	WSW-W	1.3
			5	30-70	NE ENE	
	June	14	8	230-270	WSW-W	1.5
			7	30-70	NE-ENE	
	July	11	14	230-270	WSW-W	1.7
			6	30-70	NE-ENE	
	August	11	12	230-270	WSW-W	1.7
			8	30-70	NE-ENE	
	September	8	13	230-270	WSW-W	2.5
			8	30-70	NE-ENE	
			1	350	N	
	October	3	8	230-270	WSW-W	2.6
			6	30-70	NE-ENE	
			5 to 18 October no data were recorded			
	November	6	18	230-270	WSW-W	3.1
			6	30-70	NE-ENE	
	December	6	18	230-270	WSW-W	3
			7	30-70	NE-ENE	
2017	January	6	17	230-270	WSW-W	3.1
			7	30-70	NE-ENE	
	February	6	16	230-270	WSW-W	2.5
			6	30-70	NE-ENE	
	March	4	15	230-270	WSW-W	2.2
			12	30-70	NE-ENE	
	April	13	12	230-270	WSW-W	1.5
			5	30-70	NE-ENE	
	May	6	5	230-270	WSW-W	2.5
			4	30-70	NE-ENE	
			15 to 31 May no data were recorded			

(Source: South African Weather Bureau at the Mtunzini weather station:
[0304357 6] - MTUNZINI -28.9470 31.7070 41 m (Extracted 2017/05/16 14:16))

Table 5.6: Average wind direction (degrees from north) and average wind speed data from January 2016 to middle May 2017 at 20h00.

Year	Month	Days of no wind	Wind days in a month	Wind Direction	Geographical wind direction	Average Wind Speed in m/s
2016	January	2	19	50-100	ENE	2.8
			9	200-250	SSW-WSW	
	February	5	12	230-270	WSW-W	3.6
			12	30-70	NE-ENE	
	March	3	12	200-250	WSW-W	2.6
			15	30-70	NE-ENE	
	April	6	10	200-250	WSW-W	2.3
			14	30-70	NE-ENE	
	May	11	6	200-250	WSW-W	1.7
			16	30-70	NE-ENE	
	June	5	10	200-250	WSW-W	2
			15	30-70	NE-ENE	
	July	4	17	200-270	WSW-W	2
			11	30-70	NE-ENE	
	August	5	10	200-270	WSW-W	2.7
			16	30-70	NE-ENE	
	September	3	17	200-270	WSW-W	2.3
			9	30-70	NE-ENE	
	October		8	200-250	WSW-W	2.5
			7	30-70	NE-ENE	
			3 to 17 October no data were recorded			
	November	4	16	200-270	WSW-W	3.3
			11	30-70	NE-ENE	
	December	2	17	200-270	WSW-W	3.5
			12	30-70	NE-ENE	
2017	January	4	14	200-270	WSW-W	3
			13	30-70	NE-ENE	
	February	3	13	200-270	WSW- W	3
			12	30-70	NE- ENE	
	March	5	14	200-270	WSW- W	2.5
			12	30-70	NE- ENE	
	April	7	14	200-270	WSW- W	2
			9	30-70	NE- ENE	
	May	1	7	200-270	WSW- W	3.7
			7	30-70	NE- ENE	
			15 to 31 May no data were recorded			

(Source: South African Weather Bureau at the Mtunzini weather station:
[0304357 6] - MTUNZINI -28.9470 31.7070 41 m (Extracted 2017/05/16 14:16))

According to the South African Weather Bureau's 08h00 statistics, the wind blew inland from the sea on 216 days out of a possible 498 days, from the WSW to W direction, in other words, 230^{o} to 270^{o}. For 134 days out of 498 days, the wind direction was NE to ENE and the wind blew from the land to the sea, between 30^{o} and 70^{o} (see Table 5.7).

Table 5.7: Summary of Tables 5.5 and 5.6, wind behaviour measured at the Umlalazi beach at 08h00 in the morning and 20h00 in the evening from January 2016 to May 2017.

Wind data from January 2016 to May 2017 @ 8h00 is equal to 498 days in total				
Wind direction	**Days on which the wind blew WSW- W**	**Days on which the wind blew NE- ENE**	**Total number of days**	**Percentage**
Total days wind was blowing 230^{o}-270^{o}	216		498	43.37
Total days wind was blowing 30^{o}-70^{o}		126	498	26.91
Total days wind did not blow	128		498	25.70
Wind data from January 2016 to May 2017 @ 20h00 is equal to 498 days in total				
Wind direction	**Days on which the wind blew WSW- W**	**Days on which the wind blew NE- ENE**	**Total number of days**	**Percentage**
Total days wind was blowing 230^{o}-270^{o}		210	498	42.57
Total days wind was blowing 30^{o}-70^{o}	197		498	39.16
Total days wind did not blow	70		498	13.65

The results regarding the wind's direction show that it was blowing inland from the sea at 08h00 for 216 days out of 498 days, measured according to the calculated data. That is 43.37% of the total measured time. The wind blew from the land to the sea at certain times for 134 days out of 498 days (26.91% of the time). According to the 08h00 data, the "no wind" data was also very significant: this occurred especially during winter, when there was not much of a temperature difference between the land and the sea. Out of 498 days, 128 days had no wind at all (25.70% of the time). Overall, there is more wind blowing towards the land, transporting sand onto the dunes.

The measurements for 20h00 show that 42.17% of the time, wind blew towards the land at an average wind speed of 3m/s, and that 39.56% of the time, the wind blew in the direction of the sea. During the evenings, it is windstill only 14.06% of the time.

During the two periods of the day at which the wind speed was recorded, more aeolian activity takes place to transport sand inland onto the beach and dunes. These processes return in a lesser way towards the sea, preventing the sand from encroaching totally on the vegetated area. It seems that after the rainy season started in October, more sand was eroded again from the beach into the deep sea. The overall increase in sand volume was due to the sand deposited by the rivers on the beach.

5.5.4 Third method: The Fishnet method.

In Chapter 4, the physical surveys were described. The surveys were conducted over a period of just longer than a year, with the first survey in March 2016 and the last survey in July 2017. After the surveys at the Umlalazi beach were completed with a spot level interval accuracy of approximately 50 m apart, a grid with 10 m^2 accuracy, a so-called fishnet, was pulled over the original surveying of the points. At each 10 m grid intersection, a height was then estimated (see Appendix B). The coordinates of each 10 m grid were known from the data of the control points. The results of the areas and volumes are illustrated in the discussion, graphs and tables. Figure 5.24 (overleaf) shows the percentage increase or decrease in change activities on the Umlalazi beach between the two years, from 2016 to mid- 2017. The greatest increase in sand occurred close to the waterline, between the 2 and 3 m water intervals.

The data in Figure 5.24 (overleaf) were derived from the survey measurements, which were taken and then converted to a comparable unit in percentages. Higher up on the beach, the dune had an even slope and there were no significant visible changes to the dune. However, according to the calculations, there was an increase in the sand area that led to an increase in the sand volumes. In the October 2016 survey, there was an increase of just over 18%, compared to the July 2017 and April 2017 volumes. The reason was that from April through the winter to September 2017, the rainfall decreased, and an above-average number of windstill days were experienced during these months. From April to September 2016, there were 34 windstill days, according to the evening measurements, and 67, according to the morning measurements (South African Weather Bureau). Calm seas have a positive influence on dune building and increases in their area and volume; hence the drop from 777 247 m^3 to 689 336.3 m^3. Table 5.8 (p. 92) indicates the rise and fall of the accumulative volume and the increase or decrease in the 2D area, expressed as a percentage.

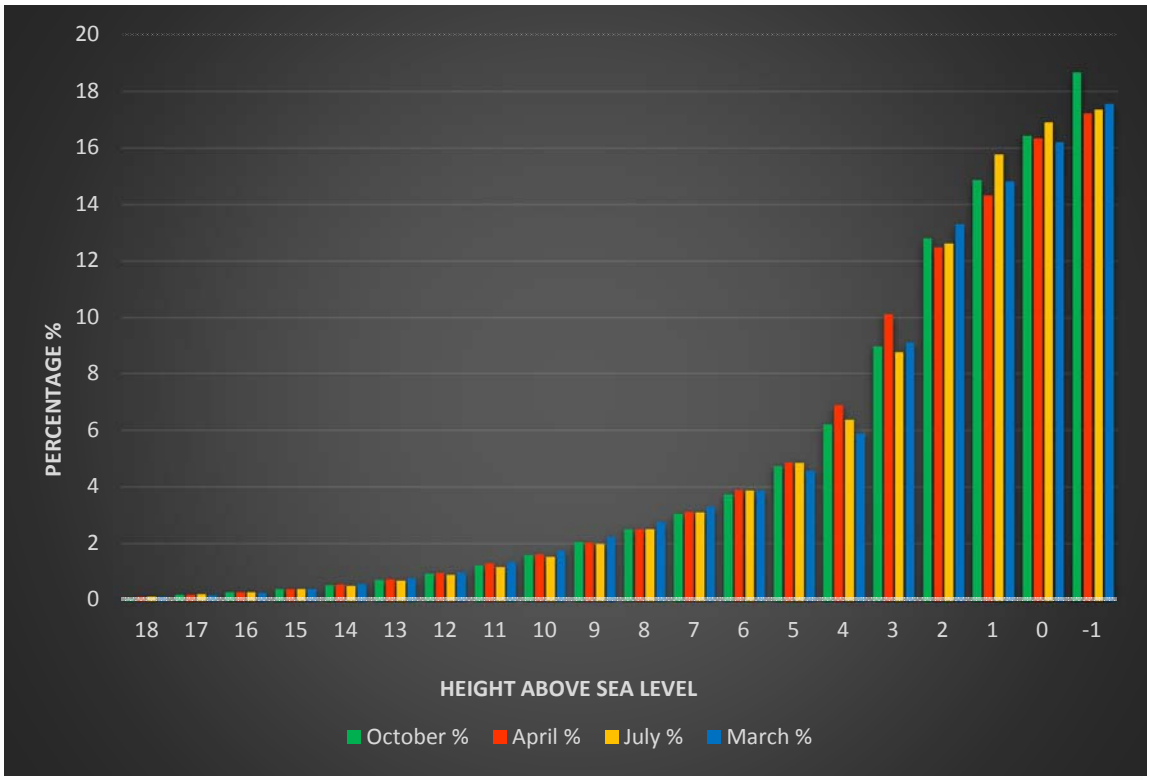

Figure 5.24: Percentage increase/decrease of sand volumes at the Umlalazi beach (March 2016-July 2017) with more changes close to the beach at the 0-5 m contour levels

In March 2016 the 3-4 m contours were very prominent, containing by far the largest area in the beaconed-off terrain. The 2-3 m contours contributed little to the total area; the 2-3 m levels are where the beach is. From March 2016 to October 2016, the sea pushed more sand out, increasing the 2-3 m contour areas. In this case, these contours increased more in relation to the total area than the volume increased per area. In April 2017, the -1 m contour level contained 17.2% of the total defined area (see Figure 4.5). From April to July 2017 (the next survey), the -1 m contour area increased from 17.2% to 17.4%, a gain of 0.2%. In October 2016, the -1 m contour had a volume of 18.7%, but it decreased to 17.2% in April 2017. The decrease was presumably sand eroded during the rainy season from October to March.

Sand volume decreased between October 2016 and April 2017, from 18.7% to 17.2% (see Appendix C). From the 5 m contour level and lower, no significant survey intervals stood out, except at the 4 m and 3 m contour intervals, where volumes in April 2017 (see Figure 5.24) were higher than in other contour intervals. In March and October 2016 and July 2017, the accumulative volumes were respectively 70 678 m^3, 61 690 m^3, and 71 107 m^3, an average of 67 825 m^3, against the April 2017 accumulative volume of 84 404 m^3 (see Appendix C). Table 5.8 (overleaf) summarises the percentage increase/decrease of the changes in the beach geomorphology of the Umlalazi beach.

Table 5.8: Accumulative volume and area of the terrain at the Umlalazi beach.

Month/Year of Survey	Accumulative Volume (m^3)	Sum 2D Area (m^2)	% Increase/Decrease in Volume	% Increase/Decrease in Area
March 2016	777248.67	850736.52		
October 2016	689364.31	757605.16	-11.31	-11.00
April 2017	834099.20	1608540.10	21.00	112.31
July 2017	813080.86	4916073.08	-2.52	205.62

There was a slight decrease of 11.3% in the total volume percentage from March 2016 to October 2016 from 777 247.6 m^3 to 689 364.3 m^3. From October to April 2017, the volume increased by 20%, but it decreased by 2.5% to July 2017 (see Table 5.8), probably due to low rainfall in the catchment areas during the winter months. Low rainfall in the estuaries and catchment areas leads to slow or no river flow, especially in the Umlalazi and Amatigulu Rivers. Slow wind speeds averaging less than 1.7m/s to zero m/s cause the wave energy to be calmer, so for most of the winter season, there is a constructive wave pattern (sand is washed out onto the beach). Although Figure 5.25 reflects a total increase in sand volumes, there were deflections of increasing and decreasing results as can be seen in Figure 5.26 (overleaf). The areas per contour level got larger in relation to the total area, but the sand per contour has just flattened out over some contour areas, especially the 2-3 m contour areas.

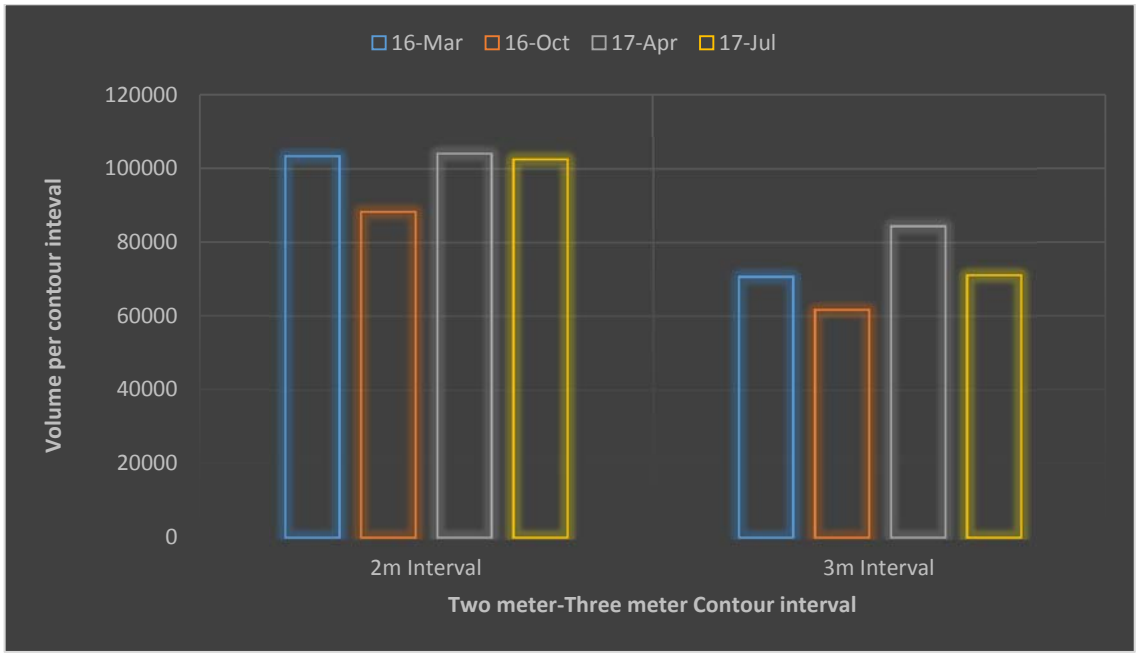

Figure 5.25: The areas of the 2-3 m contour intervals at the Umlalazi beach that changed since March 2016 although sand volumes stayed the same or decreased from April 2017 to July 2017.

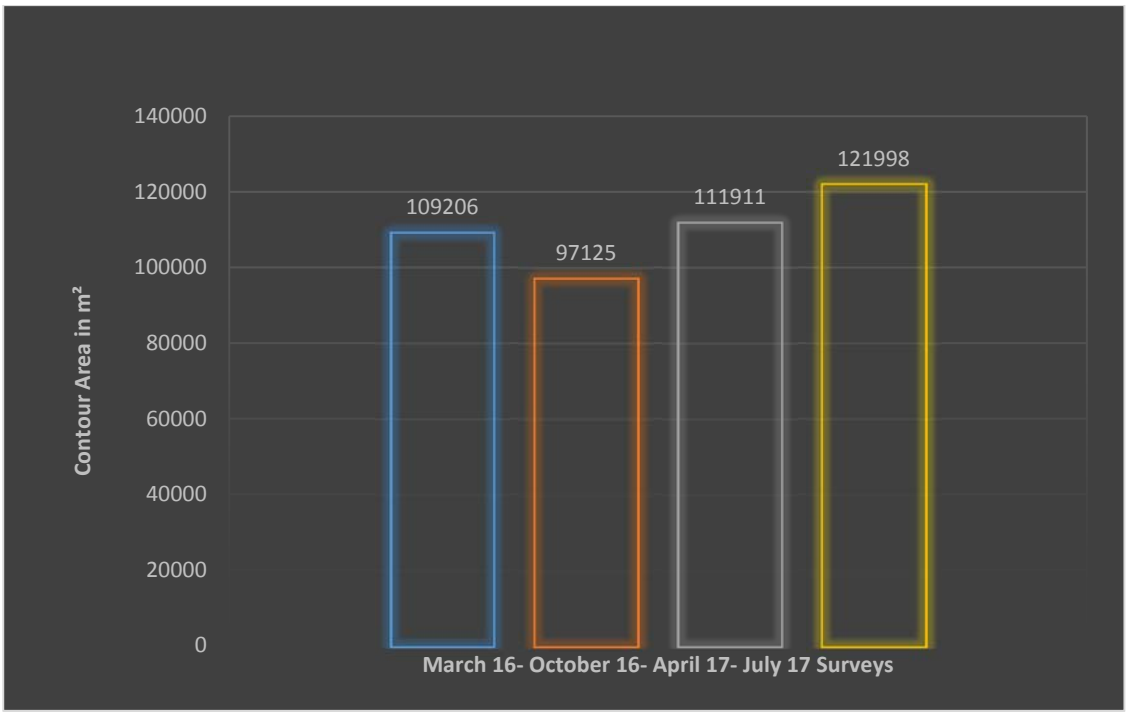

Figure 5.26: Changes in the 2D areas of the survey at the Umlalazi beach in the 2-3 m contour intervals from March 2016 to July 2017.

In the areas between the 2 m and 3 m intervals, more drastic geomorphological changes took place. In March 2016, the 2 m contour interval contained 12.79% of the total area of the terrain of 133 338 m², but at that time, the 3 m level was 28.19 % of the total area. The 2 m contour level increased by the October 2016 survey to 16.7%, most probably because of the start of the summer rainfall season, only to decrease back to 12.19% in April 2017 (compare the March 2016 green area with the yellow area in Figure 5.27, overleaf). In April 2017, heavy rainfall occurred in the catchment areas in the midlands of KwaZulu-Natal. The runoff arrived at the ocean by the end of June and beginning of July 2017. In addition to the Thukela mouth, which is always open to the sea, the Amatigulu and Siyaya estuaries also opened up to the sea. From Table 5.8, it is clear that the 2 m contour interval increased from 12% to approximately 30% of the total area during the July floods.

In Figure 5.27, the four terrains are compared, and the changes are very clear and prominent. The figure shows the surveys done during March 2016, October 2016, April 2017 and July 2017 in the Arc Scene 3D view.

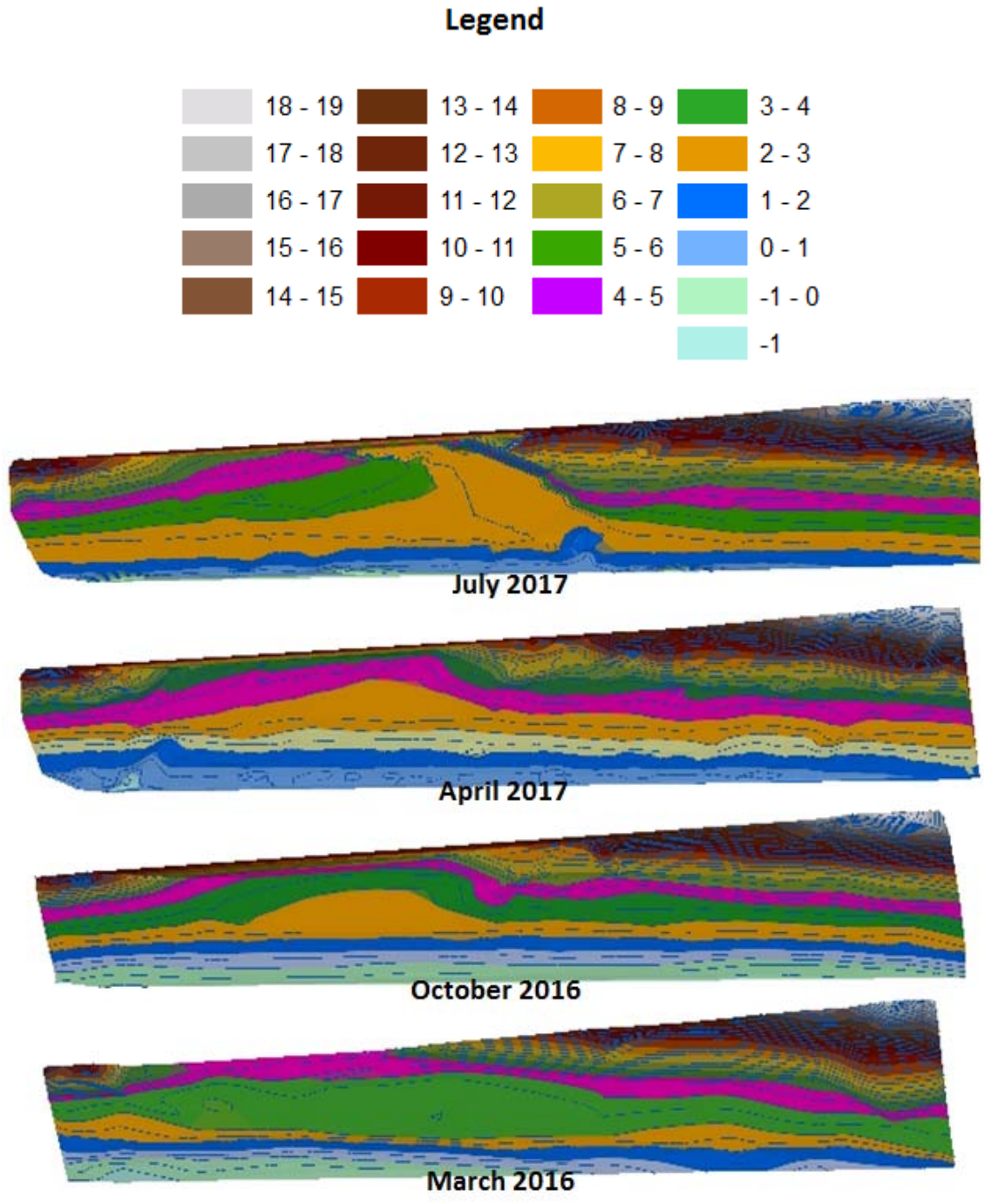

Figure 5.27: Arc Scene 3D view of the changes found in the four surveys at the Umlalazi beach area in March and October 2016, and April and July 2017.

Table 5.9: Percentage of contour areas for the total area showing the changes.

(also see Figure 5.5)

Plane_ Height	% Area			
	March	October	April	July
20	0	0	0	0
19	0.28	0	0.39	0.56
18	0.42	0.72	0.58	0.53
17	0.41	0.57	0.51	0.40
16	0.78	0.49	0.66	0.50
15	0.92	0.53	0.80	0.79
14	1.10	0.88	1.02	0.84
13	1.22	1.09	1.29	1.14
12	1.23	1.28	1.79	1.46
11	2.60	1.70	2.07	1.94
10	2.51	2.19	2.20	2.54
9	3.01	2.28	2.70	2.91
8	3.05	2.58	3.34	3.33
7	3.18	3.05	4.47	4.19
6	3.50	4.11	4.96	5.21
5	4.88	6.04	8.04	7.04
4	12.14	10.09	17.51	11.27
3	28.19	18.59	19.40	17.18
2	12.79	16.66	12.19	29.65
1	8.23	7.86	11.37	8.73
0	7.30	8.91	11.96	4.88
-1	9.21	13.63	0.47	1.31

In Figure 5.28 (overleaf), representing the March 2016 time interval, the 3 m green bar represents 18.18% of the total area, but it decreases gradually as the 2 m contour interval encroaches. On the other hand, the yellow bar representing the 2 m interval increases over time to nearly 30% of the total area.

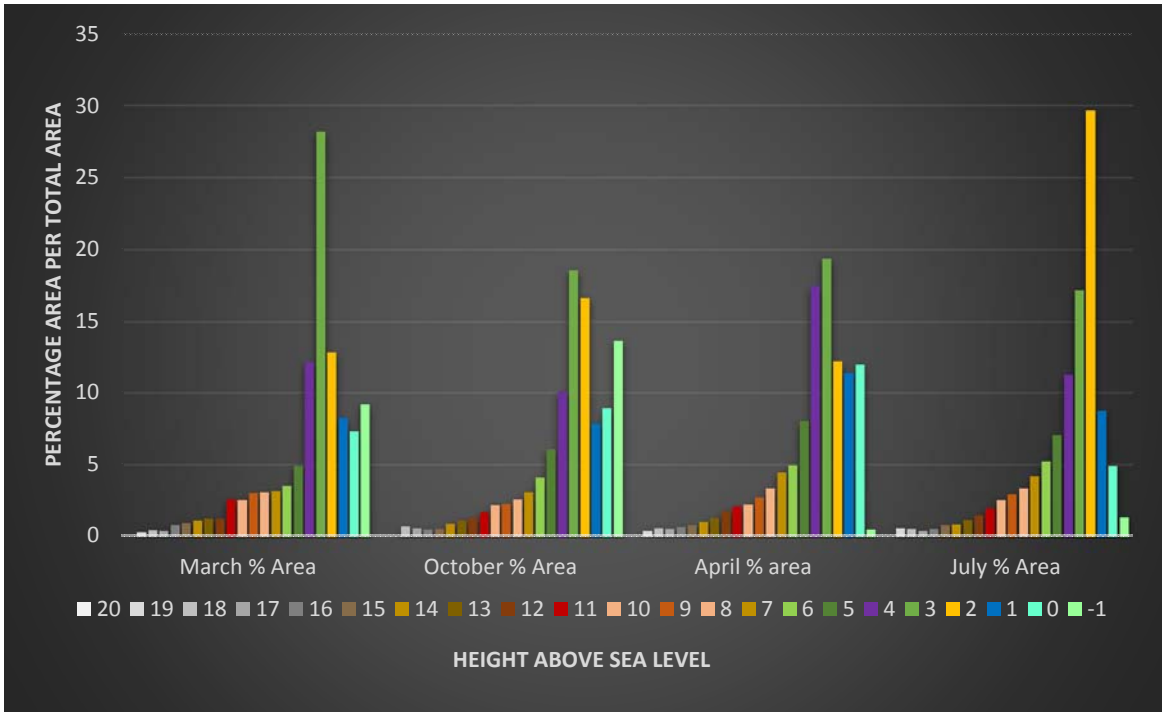

Figure 5.28: Sand area distribution over the four survey periods (March and October 2016, April and July 2017) – the green bar is prominent in the March interval, but decreases up to July 2017, with the yellow bar at its highest peak after the July floods.

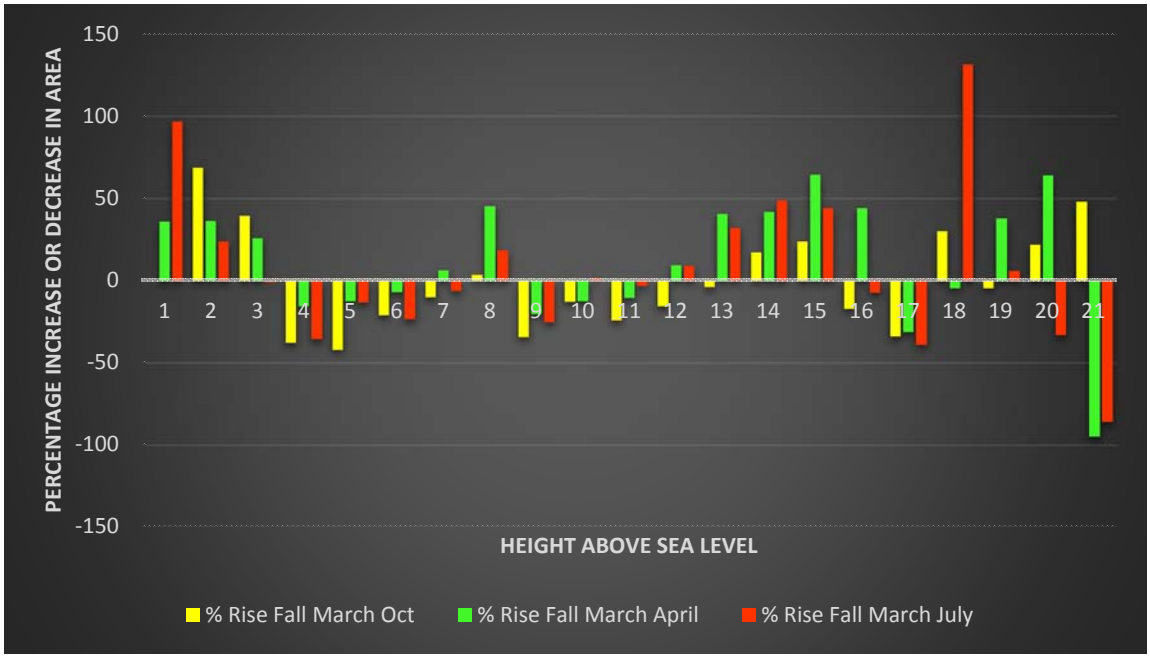

Figure 5.29: The percentage increase/decrease in sand areas – graphical summary of data in Table 5.10 (note the substantial rise in the 2 m area from March 2016 to July 2017).

Table 5.10: Square metres of each individual contour interval and the rise or fall from the first to the second, third and then the fourth survey.

Height in m.	16-Mar m^2	16-Oct m^2	17-Apr m^2	17-Jul m^2
19	381.87	0	519.36	752.02
18	567.01	957.42	774.12	703.00
17	541.49	754.56	681.07	538.50
16	1044.70	648.94	882.09	672.54
15	1222.92	710.35	1070.84	1059.00
14	1462.52	1157.91	1357.96	1118.68
13	1622.84	1456.08	1724.81	1525.44
12	1644.40	1701.04	2390.04	1947.40
11	3464.56	2270.34	2759.14	2589.70
10	3349.77	2926.15	2934.77	3389.13
9	4013.33	3043.74	3599.30	3882.96
8	4072.02	3433.84	4458.28	4437.74
7	4233.63	4066.63	5957.15	5589.79
6	4669.64	5480.79	6618.63	6941.94
5	6511.45	8058.54	10719.71	9386.73
4	16192.74	13447.92	23340.99	15020.70
3	37581.25	24793.21	25862.34	22909.00
2	17055.97	22217.83	16260.87	39533.76
1	10975.93	10475.41	15156.91	11640.88
0	9732.40	11879.08	15951.54	6504.56
-1	12276.04	18168.25	632.13	1743.70

Table 5.11: Percentage area increase or decrease in the contour interval of the sand on the Umlalazi beach.

Height in m.	% Rise Fall March-Oct	% Rise Fall March-April	% Rise Fall March-July
19	0	36	97
18	69	37	24
17	39	26	-1
16	-38	-16	-36
15	-42	-12	-13
14	-21	-7	-24
13	-10	6	-6
12	3	45	18
11	-34	-20	-25
10	-13	-12	1
9	-24	-10	-3
8	-16	9	9
7	-4	41	32
6	17	42	49
5	24	65	44
4	-17	44	-7
3	-34	-31	-39
2	30	-5	132
1	-5	38	6
0	22	64	-33
-1	48	-95	-86
	-4	**+244**	**+139**

5.5.5 Coastline and bush line dynamics.

Three aerial photograph intervals of the Umlalazi River have been scientifically analysed with the help of ArcGIS 10.4.1, namely the 1957, the 2009 and the 2017 photographic series. On the aerial photograph taken in 1957, a defined area is described by the waterline northwards by the surveying points. The eastern and western boundaries are part of the survey points on the beach. The northern bank indicated the edge of the sand dune. The bush line varied from 1957 to 2009 (see Figure 5.30). In Figure 5.31, no definite identifiable bush line could be recognised

from the 1957 aerial photographs. The vague transitional line between the bush and the sandbank was drawn as a straight line. Both the areas of 1957 and 2009 (as stated in this discussion) have one southern boundary, which was determined by the surveying points of the area and is thus not a variable. The calculations were based on the area described based on the 1957 photograph (see Figure 5.30). The calculations determine the amount of sand that has changed up to 2009 and then to 2017. This is the area where the bush has advanced towards the ocean by 27.60% – the northern section on the plan or the green line has moved about 60 m to 70 m south over the last 52 years. If this change in distance is calculated from 1957 to 2009, then per year the green line has moved approximately just over 1 m per year. During the research, it was clear that the bush line has definitely shifted over the years, in a southerly direction.

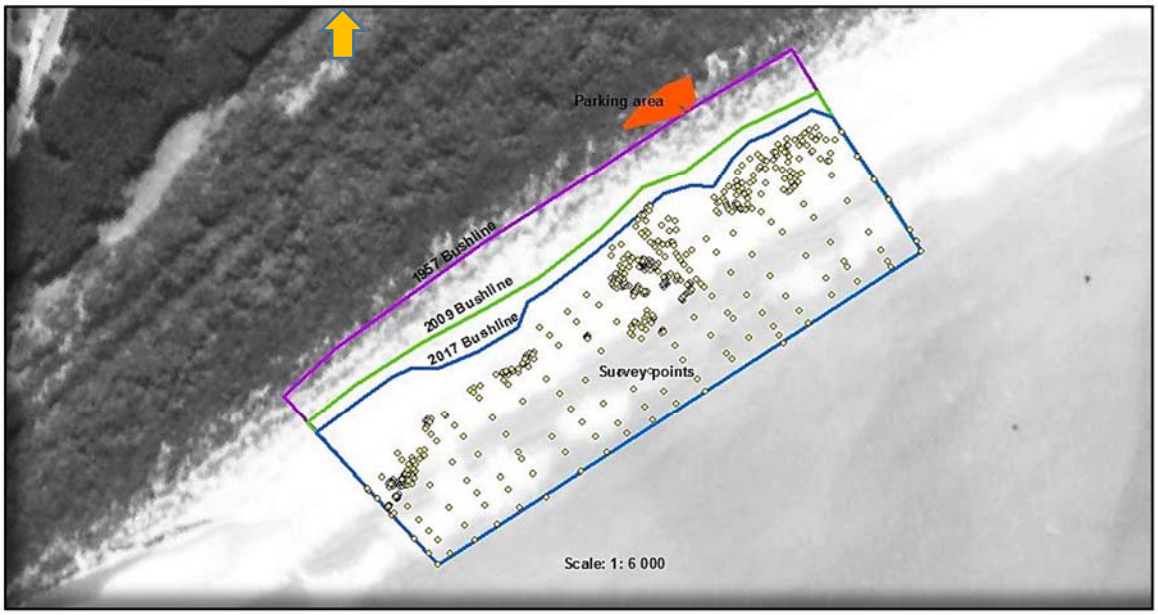

Figure 5.30: The 1957 aerial photograph of the Umlalazi beach – the purple line runs adjacent to where the parking area would be a few years later

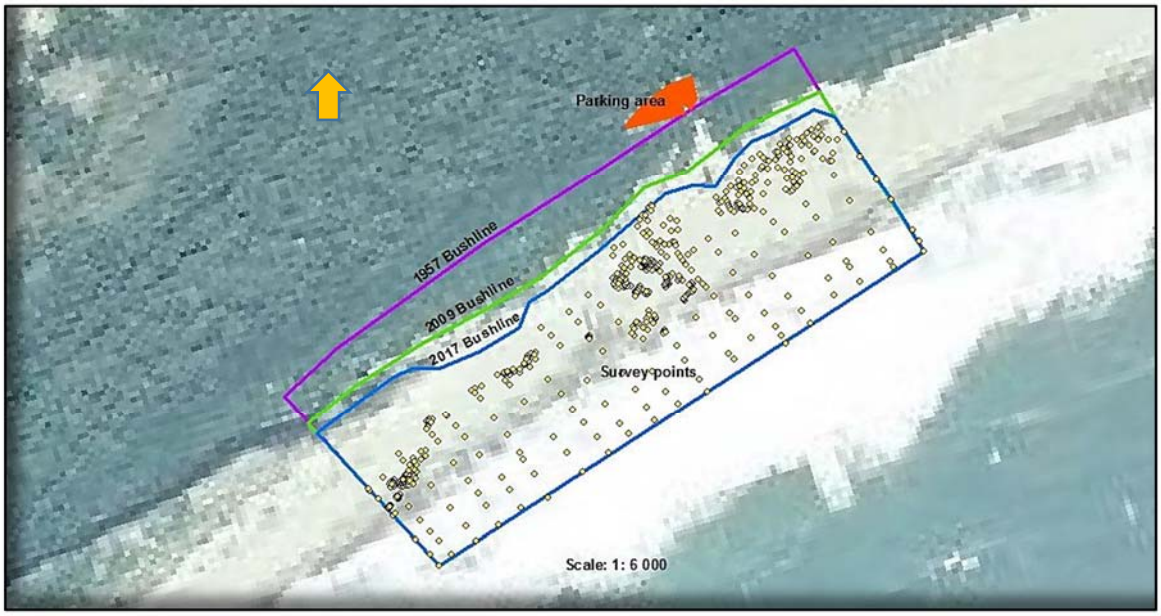

Figure 5.31: 2009 satellite image of the Umlalazi beach showing the existing parking area with the new green line

It can be argued that during the flight time when the aerial photographs were taken, it would sometimes have been high tide and sometimes low tide. The sea lines taken into account in the calculations were therefore treated not as variables, but the basis for the calculations of the areas. All calculations were based on the 1957 northern boundary bush lines. Approximately the same amount of bush has encroached on the sandbank. The sea level has moved increasingly further south (see Figure 5.30, p. 99). In 1957, the Siyaya River opened up into the sea, and its mouth is an indication of where the sea line was at that time. As Table 5.12 shows, the total measured area from the sea to the bush line of the sandbank in 1957 was 290 634 m². The area of the 2009 sandbank is 231 392 m². This is an indication that the bush has increased from 1957 to 2009. Over those 52 years, the sand has diminished by 20.38%. The 2009 bush line has moved an average of 65 m southwards.

Table 5.12: Summary of the encroachment of the bush area towards the beach area at the Umlalazi beach

Year	Total area (m²)	Excluded area from 1957	% Change in relation to the 1957 area	% Change in relation to each interval
1957	290634			
2009	231392	59242	-20.38	20.38
2017	208817	81817	-28.15	27.60

If the 2009 measurement was approximately 65 m and the second measurement of the 2017 satellite image about 100 m from the 1957 baseline, the encroachment by the vegetated area increased by about 1 m per year. In the georeferencing of the 2009 aerial photograph, an uneven sandbank line or bush line was noted. It presumably means that more human traffic occurs, as the uneven bush line that looks like a flame or crochet pattern is characteristic of such human impact.

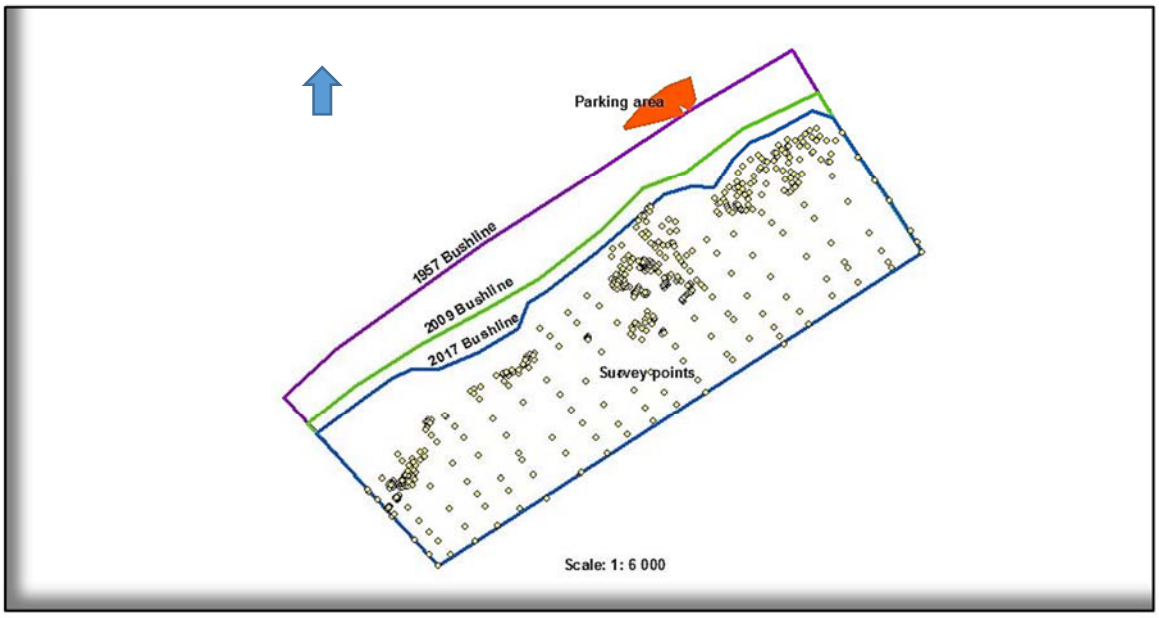

Figure 5.32: Plan combining three periods from 1957, 2009 and 2017 at the Umlalazi beach

The study shows that the northern bush line is increasingly displaying more of a crochet pattern, as can be seen from an aerial view (see Figure 5.33). It can be argued that since the early years (1953 and 1957, which provided the earliest data included in the research), up to 2009 and 2017, the beaches have become more and more commercialised, especially with the development of the township of Mtunzini, which barely existed in the early 1950s. As more people visit holiday resorts on the KwaZulu-Natal coast, there is more human traffic. One of the consequences of the human footprint is that unfortunately footpaths appear in the bush areas, from the lodges to the beach and river areas. This has a trigger effect, allowing the sand to move inland underneath the trees. The flame-like pattern is clearly slanted in the same direction, allowing sand to be carried inland by the wind. The human presence could also be the reason that some dunes have a steeper gradient than others in same vicinity.

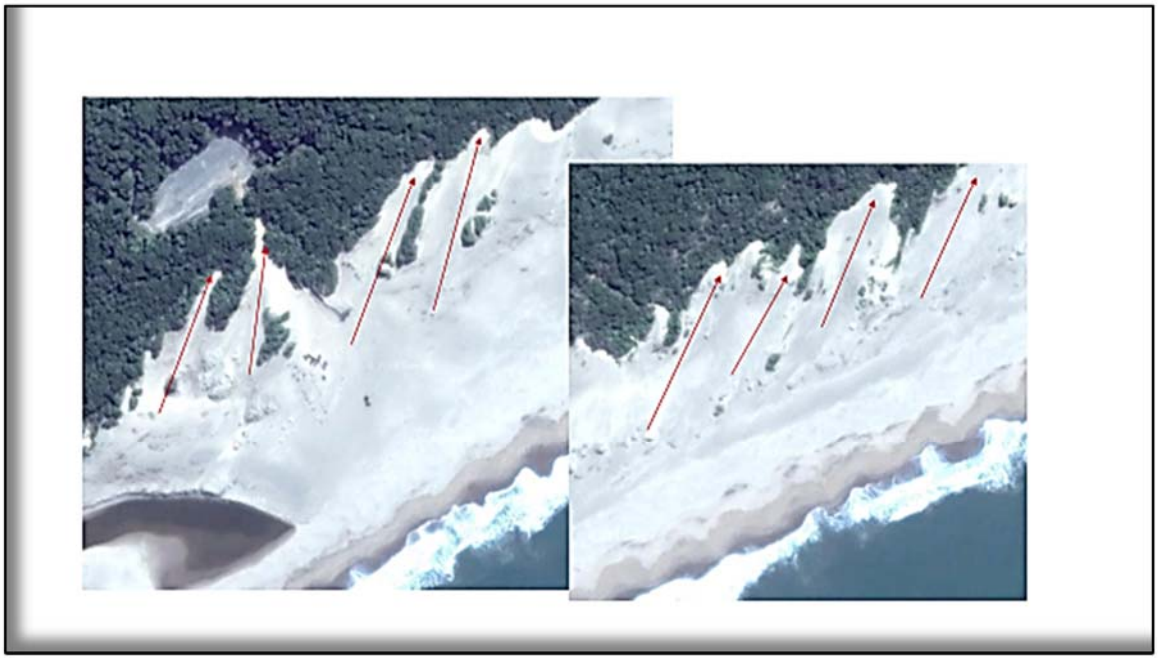

Figure 5.33: Aerial view of the northern bush line's crochet/flame pattern resulting from human activities

The results presented in this chapter are discussed in Chapter 6.

Chapter 6:

Discussion

6.1 Introduction

Dune dynamics (movement or changes in sand areas and volumes) are related to many factors. These factors are predominantly natural and/or human-related. Some dynamics start and happen directly at the beach, for example, elements that come into direct contact with the sand dune itself, such as aeolian processes (wind is a transporting mechanism for sand on the beach and also in various directions). For example, in the study, it was determined that there is a south-south-western (SSW) wind blowing inland, accumulating more sand on the higher parts of the Umlalazi beach. Other direct factors are the waves and the amount of their changing energy. Storms and heavy rains in the vicinity of or directly on the beach can lead to erosion. More indirect change factors are river runoff when heavy rains occur in the catchment areas (some of these river floods reach the coast only four to five weeks after the storms). This runoff water carries sediment to the coast. The runoff water causes high rises in the river's lower parts and the estuaries and open up the mouth from time to time.

The main aim of the research study was to determine the dynamics of the movement of sand barriers at the Thukela River mouth, Amatigulu River estuary and the Umlalazi River estuary. Three objectives were identified in the research. The main objective was to construct detailed contour maps of the coastal littoral zone using aerial photographs to determine sand movement over the period from 1953 to 2017. The dynamics at two of the three estuaries, the Amatigulu and Umlalazi, are more wave-dominated, because their mouths are only occasionally open to the sea, but those at the Thukela mouth are predominantly-river dominated, as the river mouth is open to the sea. The sandbanks' protection from the ocean is highly dominated by the rivers feeding and flowing into them. When the rivers are in flood because of high rainfall in the catchment areas, especially the Thukela River, they push sand deep into the sea, and the sand is then transported by the longshore drift flowing close to the coast in a northerly direction. These sediments are then washed out on the beaches by the wave energy, energized by the wind speed, and transported further inland by the wind. Normally the wind speed is not more than 4m/s and it mostly blows from a SE and ESE direction (41% of the time) and some of the time from a NW to NNW direction (28% of the time). During the winter months from May to August, there is little to no wind and thus limited sand transport.

6.2 The Dynamics of the Thukela River Mouth over the Years

Three objectives were identified during the research. The one main objective of the study is to conduct detailed contour maps of the coastal littoral zone using the aerial photographs to determine the sand movement over a temporal period, from 1953 to 2017. The climate at the KwaZulu-Natal north coast is subtropical, with hot and rainy summers, and it cools down in the winter months to a mild temperature of seldom lower than 17^{o}C, with relatively little rain. In some years, July could be an exception, with higher than usual rainfall of approximately 70 mm. There is definitely a direct relation between a rise in the temperature and a rise in the rainfall. The variation in temperature is not as drastic from interval to interval as the precipitation data. For the purposes of the study, it was unfortunate that the temperature and rainfall data were only available from 1992, when the weather station at Mtunzini was established.

Table 6.1: Areas and volume of the north and south shores of the Thukela River mouth (1953-2017)

Year	Area (m^2)		Volume (m^3)	
	North	South	North	South
1953	34 505	22 904	58 659	48 098
1983	58 783	197 048	82 296	403 948
2013	74 848	149 697	112 272	317 358
2016	13 152	67 125	21 110	143 162
2017	25 171	87 954	55 433	185 784

Table 6.2: Percentage increase/decrease in the area and volume of the north and south shores of the Thukela River mouth (1953-2017)

Years (From… to…)	Area (%)		Volume (%)	
	North	South	North	South
1953- 1983	28.72	88.09	760.32	739.84
1983- 2013	26.70	-27.29	-24.03	-21.44
2013- 2016	-431.84	-121.68	-55.16	162.59
2016- 2017	61.92	22.94	31.03	29.77

The results of the study are based on 30-year time intervals, starting in 1953 and ending in 2013. It was possible to take a few heights stereoscopically to determine the sand volumes

from 1953 to 2013. In 2016 and 2017, the terrain was physically surveyed (twice in each of those years) and covered using spot levels. The results are shown in Table 6.1. No real pattern in the increases or decreases was visible in the chosen time intervals. However, it is significant that the north shore of the Thukela mouth was larger in area and in volume during 1953. Arguably, the 30-year interval could be regarded as a limitation of the study, and shorter intervals could be used, but even with shorter intervals it is unlikely that a definite pattern would emerge. It could be argued that during times when the river mouth was situated further towards the southern side, the north shore tended to become larger and the south shore tended to become smaller. Thus it could be argued that the sizes and volume depend on where the mouth is situated at a certain stage during the season.

6.3 Geomorphological Changes of the Amatigulu-Nyoni River Estuaries

Observations from 1953 and 1964 show that the Nyoni River did not break through to the Amatigulu River in those years. The next aerial photograph, taken in 1972, showed an opening from the Nyoni River to the Amatigulu River (Engelbrecht, 2008). It is unclear exactly when during the period from 1964 to 1972 it broke through, because there is no aerial photograph available for that interval. Orme (1980) claims that the Amatigulu River mouth had opened up to the sea, with two streams entering the sea by/in 1972.

The observation of the aerial photographs of 1989 shows that there was an increase in the width of the beach since 1972. In the years 2000, 2004 and 2006, heavy rains fell on the KwaZulu-Natal north coast. The waves were more destructive, eroding the beach sand and transporting it deeper into the sea. When erosion takes place, the beach width shrinks. This demonstrates that the sea and the beach also interact with each other. It can thus be assumed that this interaction will always be present: the ocean will take more space, but it can also retreat, causing the sand and the beach to increase their space from time to time.

6.4 Discussion of the Umlalazi Results

6.4.1 Results of the comparison of the 1957 data with the 2009 satellite image.

The study set out to understand the three-dimensional movement of dunes, and the changes they have undergone in the past and may undergo in future. Another objective was to assess the surveying of a defined area at the Umlalazi beach from March 2016 to July 2017. This is an extension of the study, defining the first objective more clearly. Table 6.3 contains a summary of the most important results. The square metre per contour area of the defined area decreased from 850 737 m² to 757 605 m² from March 2016 to October 2016. Table 6.3 shows

that there is a very close relation between the volumes that accumulate and the accumulative areas. The decrease and increase of the volumes and areas vary by approximately 2.5%, from 8.4% in April 2017 to 9.9% in October 2016.

Table 6.3: Accumulative volume in relation to the area of the contours at the Umlalazi beach

Month/Year	Accumulative Volumes (m^3)	Sum 2D Area (m^2)	Percentage Vol/Area
March 2016	777 247	850 736	9.5
October 2016	689 364	757 605	9.9
April 2017	834 099	903 740	8.4
July 2017	813 080	883 692	8.7

Some of the results show that one cannot just concentrate on the accumulation and movement of sand in a certain direction – the encroachment of vegetation on the dune area also contributes to the ever-changing beach area. The surveys done in 2016 and 2017 determined coordinates for where the beach area was in 1957, where the parking area next to the Umlalazi beach is now. The bush line has moved over the last half century in the direction of the beach. Sand has also moved in amongst the bush areas and trees, probably due to human factors. The bush has encroached on the sand area, by approximately 60 m.

The third objective of the study was to understand the relation between the driving forces and to assess the changes, and the results obtained from the data, and to make these results acceptable and understandable to the environment and the community. Driving forces include the tourism industry, waves and wind energy, tides, climate change and the rise in the sea level.

6.4.2 Results of the physical survey and assessment of the dunes.

A relative increase in areas did occur during the time when the surveys were done (2016 and 2017). These increases can be ascribed to river runoff, storms at sea and strong winds blowing in from the sea towards the land, creating strong wave energy. With the physical surveys in March 2016, October 2016, April 2017 and July 2017, the contour interval areas in square metres rose and fell, presumably due to the different driving forces influencing the beach structures. In July 2017, the most drastic changes were noted, as the area of the 2 m contour increased dramatically because of floods related to heavy rainfall earlier in April 2017 in the catchment areas in the KwaZulu-Natal midlands and on the Drakensberg. The initial research proposal indicated that, to meet the third objective, the contours would be generated with

stereoscopic plotters, but as a result of limitations that emerged during the actual research, a new approach to the third objective was introduced, as discussed in Section 4.6.

Geomorphological changes were evident from the analysis of the results. The longshore transport of sediment and depositions with the help of the sea currents, wind, tides and waves are the most important influences on beach and dune changes where there is a wave-dominated coastline. The exception is the river-dominated Thukela River mouth, where the river is constantly pushing water into the sea and the river mouth does not close on occasion, as a wave-dominated estuary does (Oliver & Garland, 2003). Beaches and dunes are all dependent on seasonal changes that influence the geomorphological changes. Beaches and dunes along the KwaZulu-Natal north coast tend to build up in a northerly direction, because the waves do not impact on the coastline at 90^{o} to the beach line, but at an oblique angle.

6.4.3 Effect of wind and wave on sand transportation.

The movement of sand deposited on a dune depends on three factors: the wind speed, how long the wind blows from a certain direction, and the size of the granules that are transported. When these factors are all considered, the wind speed, the height of the wind above the surface, granule size and the wind direction determine the intensity and the amount of sand transported. Appendix E contains data provided by the South African Weather Bureau, obtained from the Mtunzini weather station from January 2016 to May 2017, showing data on days with no wind, the number of days the wind blew from a certain direction and the wind speed. In wind data tables, the data show only the number of days on which the wind was blowing in a certain direction in a month, and not on which day of the month it has blowing in a certain direction. The tables indicate the 8h00 and 20h00 measurements from the Mtunzini Weather station.

In the October 2016 survey, a decrease in area was noted from the March 2016 survey from the 0 m mark up to the 20 m mark. This phenomenon might be the result of rising average rainfall and stormy seas during September (69 mm) and October (98 mm), November (121 mm) and December (122 mm). It could be argued that more destructive waves erode the sand, drawing it deeper into the sea. From April 2017 and during the winter months up to September and October 2017, the sand seems to have drastically increased again from the 1 m mark up to the 3 m areas. The areas from the 6 m contour line are more equal, with approximately the same volume and area amount.

Data on wind action were obtained from the Weather Bureau for 498 days starting from January 2016 to May 2017. According to the data, the wind direction was approximately parallel with the coastline, which is 220^{o} in the South African coordinate system, for 216 days out of a possible 498 days. It thus blew inland 43.37% of the time, allowing sand to accumulate on the beach area. For 27% of the time, the wind turns around approximately 180^{o}, blowing from the land towards the sea, prohibiting sand dunes from forming steep slip faces in this area. If the slip faces are less steep, the dune progress into the vegetated areas is also slower. The change of the wind direction occurs when the land is heated up faster than the sea water during the early hours of the day. As the day gets warmer, the sea water also heats up and stays warmer for longer periods during night time, as the land cools down faster than the sea water. This condition causes the wind to flow from warmer conditions to colder conditions. During winter, the temperature differences are not as extreme as during the summer months, so more windstill days are found from April to August.

6.4.4 Results of the Fishnet method.

When the survey was originally done, the spot levels were taken according to the representative plan scale 40 m apart from each other. Accuracy was improved with a second grid pulled over the original survey grid. It can be argued that the accuracy is higher in certain cases, for example, when the terrain is smooth or the topography displays little ground change (McKay, 1978). The reason is that contours are an indication of potential heights on the terrain and the 10 m^2 grids are all estimated from these contours. Where the grid falls on the contour, the height is interpolated between two consecutive contours. The disadvantage of the fishnet method is that in reality the topography of the ground surface is not even. Drastic consecutive height changes, where more than one contour runs between heights, preclude the required accuracy from the fishnet method.

With the fishnet method, it is clear that there were changes around the -1 m contour line. During the survey in March 2016, more activity was found around the 3 m to 4 m contours in the beaconed off area, while the 2 m and 3 m contours had a relatively small area in relation to the defined total area. According to the photographs, the 2 m and 3 m contours were where the sea was in 2017. It seems that the sea pushed more sand onto the beach and a major increase in the areas and volumes occurred. From April 2017 to July 2017, when the next survey was conducted, the -1 m contour area increased from 17.2% to 17.4%, a gain of 0.2%. In October 2016, the -1 m contour had a volume of 18.7%, but it had decreased to 17.2% by April 2017. The

decrease was presumably due to the erosion of the sand during the rainy season from October 2016 to March 2017.

It can be assumed that there was a very slight tendency for sand to accumulate on the beach, especially in the lower parts of the beach, near sea level. At the 6 m contour interval and the higher parts of the dune, there were almost no changes at all. During the July 2017 visit, the Nyoni River and the Amatigulu River broke through their barriers to open up to the sea. As Figure 5.29 shows, changes on the beach took place with the runoffs of the Nyoni and the Amatigulu Rivers. During the month of April 2017, there was heavy rain in the catchment areas and the water took approximately five to six weeks to get to the mouth of the rivers. More contrasting colours were used in Figure 5.27 to illustrate the changes on the Umlalazi beach. In July 2017, runoff from the Siyaya River changed the contours significantly. More orange colouring in July 2017 indicates the 2 m and 3 m contour areas in the survey periods. With the river runoff in July 2017, more sand flux came down into the Siyaya River. All the sand did not flow into the sea – it settled on the bottom of the Siyaya River. After the river had drawn back, the beach returned to its normal position, with the river mouth closed down some distance from the sea, with the sand flux staying behind. As a result, the sand areas increased from 109 206 m^2 to 97 125 m^2 to 121 998 m^2 from March 2016 to October 2016, and from April 2017 to July 2017 they changed from 111 911 m^3 to 121 998 m^3. Although the 2 m and 3 m contour areas increased substantially, by approximately 25 000 m^2, the volumes per contour interval did not increase in relation to the size of the areas.

6.4.5 Coastline and bush line dynamics.

A definite area was beaconed off to determine reference lines. As discussed in Chapter 5, the 1957 bush line was taken as a baseline to determine the movement of the sand and the vegetated areas in relation to each other. In the defined area as described, the total sand area in 1957 was 290 637 m^2, but during the georeferencing of the 2009 satellite image, it was found that the sand had diminished by 20%. From 2009 to 2017 it diminished by a further 8% to 28.15%. During the research period, the bush line definitely moved in a southerly direction towards the sea. Some points that were surveyed during the research fell on dry ground, but it was clear from the 1957 photographs that those areas were in fact sea areas in 1957. It is not clear whether the photographs were taken during high tide or low tide, but it is very doubtful that there could be such a vast difference in visible area, seeing that during the field survey the tides changed from high tide to low tide (a survey of such a large area takes approximately a day).

6.5 Opportunities for Future Research

The short-term assessment used in the physical surveying of the Amatigulu sand barrier and beach area, combined with polynomial aerial photography, was useful in identifying how much the beach area had increased over the years, with the seaward growth of the shoreline (Le Vieux, 2010). A main source of this growth was the Thukela River, which pushes sediment into the sea during flooding episodes; this sand was then transported with the northward longshore drift onto the beach, and through the processes of calm seas the sediment was then washed out onto the beaches to rebuild them (Le Vieux, 2010).

At the start of the research, the Amatigulu River estuary was one of the main objects for the study. The research focus shifted during 2016 and 2017 and the study then concentrated more intensely on the Umlalazi beach area. The Amatigulu estuary was surveyed physically only once in 2016, partly because of the enormous size of the terrain, and partly because of the time constraints. Doing a proper topographical survey of the barrier took approximately two days. This terrain still needs to be surveyed and analysed intensively for geomorphological changes and beach growth that took place through the years, as has been done with the Umlalazi river estuary.

Chapter 7:

Conclusion

The Amatigulu and the Umlalazi rivers are highly wave-dominated, while the Thukela estuary is river-dominated, but they are all affected by factors emanating from the land and the sea (Blignaut, 2015). The Thukela mouth changes with each weather change – it is not closed to the ocean, so it experiences a high percentage of morphological changes, and the mouth shifts from a northern to a southern position over time. By contrast, the Amatigulu estuary is mostly dormant, and has shown a low percentage of morphological changes over the years (Engelbrecht, 2008). However, the estuary is becoming longer and occasionally breaks through the dune barrier to open up into the sea when there is an increase in rainfall and when periodic floods occur (Begg, 1978). During floods, the rivers carry very fine particles of sediment to the river mouth and into the sea. During this process, rivers lose fine sediment in the upper parts, but gather more soil in the lower parts. These sediment deposits are made adjacent to the banks of the river during floods, especially when the river in the lower parts has no velocity. This deposit of sediment results in an accumulation of sand on the dune, in other words, dune growth. From there, aeolian processes serve as a transporter to blow the sand further onto the dune, or sometimes away from the coastal dune in the form of wind erosion.

The coastal dunes form an integral part of the coastal sedimentary system (Jackson *et al.,* 2014). In a sedimentary sense, they are very old, reflecting climate changes, sea level changes and other driving forces, such as the Agulhas current and the longshore drift which provides sedimentary supply to beaches such as the Amatigulu and the Umlalazi beaches (Jackson *et al.,* 2014). The activity of these driving forces and the resulting changes to the beaches and estuaries require complex management and planning of the beaches, estuaries and the surrounding areas, such as towns and other human developments close to the coastal zone.

The warm Agulhas current follows the outer edge of the continental shelf, flowing south off the South African coastline (Bosman *et al.,* 2007) and it influences the local rainfall and climate changes (Hutchinson, 2018). As the Agulhas current meanders and swirls in a southerly direction, it causes circulation in the ocean, and this in turn alters climate conditions in the surrounding areas, for example, resulting in heavy rainfall and storms along the KwaZulu-Natal coast, or in severe droughts in other parts (Palmer *et al.,* 2011). Enormous waves caused by heavy rainfall and strong winds driven towards the coastline have a destructive effect on the beaches, leading to erosion and loss of sand. Bernard (1993) posits that when the water

temperature rises, there will be more storms per year, and they will increase in severity. That will lead to more floods and coastal erosion at beaches and the loss of sand caused by destructive waves pulling and eroding the sand deeper into the sea.

When there is drastic climate change, it can also lead to a change in the ocean level. The rise in sea level is predominantly a function of melting ice in the sea and on land surfaces. These actions cause the seawater to expand when it warms up. When the water and land temperatures rise, it leads to a rise in the sea level. The surface of the earth is dynamic and can move vertically as the water warms up (expands) and cools down (contracts).

The littoral effect is also a key energy driven by waves affected by the wind speed on the surface of the sea. During storms, waves become higher and longer, and they have a shorter frequency, breaking down on the beach destructively with more force (Chorley *et al*., 1984; Davidson-Arnot 2010; Palmer *et al*., 2011). The opposite is true when the sea is calm and there is no wind: the waves are more constructive and wash the sand out onto the beach. Instead of eroding the beach, the waves help to build the beach with sand deposits (Psuty, 1992). Thus if there are more sand deposits to offset the erosion process, beach and dune growth take place. When the sand on the dunes and beaches is relatively dry and the wind blows inland from the sea to the land, dunes could encroach on the human environment (Palmer *et al*., 2011).

Land use in the form of mining, agriculture (for example, in KwaZulu-Natal, sugar cane, and the subtropical fruit industries), and the vacation season exacerbate the degrading of and changes in dune structures and the beaches (Palmer *et al.*, 2011). Of all these factors, the vacation season has the most immediate impact on the dune and beach environment. Farming and mining have a more gradual impact, at a more constant rate, but the impact can be long-lasting.

7.1 Results of the Research

During the time when the physical surveys at the Umlalazi beach were done, there was a small increase in sand volume, but this change was so small that it was not visible to the local people visiting the area every day.

At the Umlalazi estuary, there was a net increase in the cumulative volumes over the two years of the physical survey. The Amatigulu sandbar has increased in area as a result of the estuary's water tending to push further northwards after the rainy season in April 2017 (Le Vieux, 2010). At the Thukela River, with its very dynamic water force, the sandbars shown in the study as the north shore and south shore are never the same size in area, and continually

differ in volume. During the research, a process of contouring the areas with the help of stereo plotters (had they been available) would have been useful to improve the accuracy of the contouring, but for this study, the fishnet method was used instead, with excellent results, especially at the Umlalazi beach area.

7.2 Limitations of the Surveys of the Three Sites

During the visits at the sites over the two years during which the data were gathered, several problems occurred, not just in the field, but also in the office.

7.2.1 Field problems.

In the field, the main problem was the lack of control beacons in the form of trigonometric beacons where the surveys of the site began. Most of the beacons in the vicinity of the sites have been destroyed or disturbed. Where there were beacons available, they were in unsafe areas. Another aspect is that the existing points currently on the ground coincide only with 20th century aerial photographic images, which are about 20 or more years old.

The size of some of the areas, in particular the Amatigulu River, is enormous. There was also not enough time to do full topographical surveys at the Umlalazi beach and to a lesser extent at the Thukela mouth. During some site visits, rain was a problem, and very dangerous slippery dual-track roads damaged the researcher's vehicle. The terrains are very large and due to hilly terrain, only limited radio linkage was possible using the GPS's radios.

Communication problems repeatedly arose because of language differences between the researcher and local communities. Another problem was the continuous threat of and actual crime along to the beaches and in some areas where the survey was done, especially along the Amatigulu estuary and in the surrounding areas.

References

Adcocks, J. P. H. (1953). Veld types of South Africa. *Memoirs of the Botanical Survey of South Africa*, No. 28. Pretoria: Botanical Research Institute South Africa.

Anthoni, J. F. (2000). *Oceanography: Dunes and beaches.* Retrieved September 20, 2018 from www.seafriend.org.nz/oceano/beach.htm.

Archaeology and Natural Resources of Natal. (1951). *Natal regional survey, Vol. 1*. Cape Town: Oxford University Press.

Badenhorst, P., Cooper, J. A. G., Crowther, J., Gonsalves, J., Grobler, N. A., Illenberger, W. K., Laubscher, W. I., Mason, T. R., Moller, J. P., Perry, J. E., Reddering, J. S. V., & Van der Merwe, L. (1989). *Survey of September 1987 Natal floods*. South African National Scientific Programmes Report Number 164, 1989. Pretoria: Council for Scientific and Industrial Research (CSIR).

Bagnold, R. A. (1941). *The physics of blown sand and desert dunes*. London: Methuen.

Bagnold, R. A. (1980). An empirical correlation of bedload transport rates in flumes and natural rivers. *Proceedings of the Royal Society*, 372A.

Beal, L. M., & Bryden, H. L. (1999). The velocity and vorticity structure of the Agulhas current at 32°S. *Journal of Geophysical Research, 104*, 5151-5176.

Begg, G. W. (1978). *The estuaries of Natal*. Natal Town and Regional Planning Report 41. Pietermaritzburg: Natal Town and Regional Planning Commission.

Bernard, W. H. Jr. (1993). *Global warming unchecked: Signs to watch for*. Bloomington, IN: Indiana University Press.

Blignaut, H. (2015). *Geomorphic changes in the Tugela River mouth: A time series analysis*. (Unpublished Honours research project). Department of Geography, Geoinformatics and Meteorology, University of Pretoria, Pretoria.

Bolstad, P. (2005). *GIS fundamentals: A first text on Geographic Information Systems*. 2nd ed. White Bear Lake, MN: Eider Press.

Bosman, C., Uken, R., Leuci, R., Smith, A. M., & Sinclair, D. (2007). Shelf sediments off the Thukela River mouth: Complex interaction between fluvial and oceanographic processes. *South African Journal of Science*, *103* (11-12), November-December, 490-492.

Brand, P. A. J. (1967). *Water quality and abatement of pollution in Natal Rivers, 1. Objectives of river surveys, descriptions of methods used and discussion of water quality criteria.* Report 13. Pietermaritzburg: Natal Town and Regional Planning Commission.

Breetzke, T., Parak, O., Celliers, L., Mather, A., & Colenbrander, D. R. (eds.) (2008). *Living with coastal erosion in KwaZulu-Natal: a short-term, best practice guide*. Pietermaritzburg: KwaZulu-Natal Department of Agriculture and Environmental Affairs, Cedara.

Chorley, R. J., Schumm, S. A., & Sugden, D. E. (1984). *Geomorphology*. London: Methuen.

Cooper, J. A. G. (1991a). *Sedimentary models and geomorphological classification of river-mouths on a subtropical, wave-dominated coast, Natal, South Africa.* (Unpublished PhD Thesis). University of Natal, Durban.

Cooper, J. A. G, (1991b). *Shoreline changes on the Natal coast: Tugela mouth to Cape St Lucia.* Report 76. Pietermaritzburg: Natal Town and Regional Planning Commission.

Cooper, J. A. G. (2001). Geomorphological variability among microtidal estuaries from the wave-dominated South African coast. *Geomorphology*, *40* (1), 99-122.

Cooper, J. A. G. Smith, A. M., & Green, A. N. (2013). Backbeach deflation aprons: Morphology and sedimentology. *Journal of Sedimentary Research*, *83*, 395-405.

Davidson-Arnott, R. (2010). *An introduction to coastal processes and geomorphology.* Cambridge: Cambridge University Press.

Department of Water Affairs and Forestry, South Africa. (2004). *Internal strategic perspective: Thukela Water Management Area*. DWAF Report No. P WMA 07/000/00/0304 prepared by Tlou & Matji (Pty) Ltd, WRP (Pty) Ltd, and DMM cc on behalf of the Directorate: National Water Resource Planning (East).

Dong, Z., Xunming, W., & Chen, G. (2000). *Monitoring sand dune advance in the Taklimakan Desert*. Report. Lanzhou, People's Republic of China: Cold and Arid Regions Environmental and Engineering Research Institute, Chinese Academy of Science.

Elkington, L. (2012). *Morphology, patterns and process in the Oyster Bay Headland Bypass dunefield*. Unpublished Master of Science dissertation, Department of Geography, Rhodes University, Grahamstown, South Africa.

Engelbrecht, H. (2008). *Changes in the Matigulu/Nyoni estuary: A time series analysis.* (Unpublished Honours research project). Department of Geography and Geoinformatics, University of Pretoria.

Ezemvelo KZN Wildlife, Conservation, Partnerships and Ecotourism. *Annual Integrated Report 2014/2015*. KwaZulu-Natal Nature conversation board.

Geiger, R. (1954) "Klassifikation der Klimate nach W. Köppen" Glendale Community College. n.d. Figure 16-07.jpg. Website. Retrieved from web.gccaz.edu.

Goldsmith, V. (1978). Coastal dunes. In: R.A. Davis (Ed.), *Coastal sedimentary environment* (pp. 171-230). New York, NY: Springer.

Govender, I. (2000) A study of vegetation change along the North Coast of KwaZulu-Natal from the Umgeni to the Tugela River. (MSc Degree). Department of Geographical and Environmental Sciences, University of Natal, Durban.

Green, A., Cooper, J. A. G., & Le Vieux, A. (2012). Unusual barrier/inlet behaviour associated with active coastal progradation and river-dominated estuaries. *Journal of Coastal Research*, Special Issue 69: Proceedings, Symposium in Applied Coastal Geomorphology to Honor Miles O. Hayes, 35-45.

Hutchinson, K. (2018). PhD Candidate, South African Environmental Observations Network, and Department of Oceanography UCT, University of Cape Town.

Jackson, D. W. T., Cooper, J. A. G., & Green, A. N. (2014). A preliminary classification of sand dunes of the KwaZulu-Natal Coast. In: A. N. Green & J. A. G. Cooper (Eds.), Proceedings 13th International Coastal Symposium (Durban, South Africa). *Journal of Coastal Research*, Special Issue No. 70, 718-722.

Jamieson, K., & Van Dijk, D. (2004). *A study of the active parabolic dune in North Beach Park, Ottawa County, Michigan*. Report to the Ottawa County Parks and Recreation Commission and Construction Aggregates Corporation, Department of Geology, Geography and Environmental Studies Calvin College.

Köppen, W. (1936) "C". In W. Köppen & R. Geiger (Eds.), *Das geographische System der Klimate* [*The geographic system of climates*]. *Handbuch der Klimatologie*. Berlin: Borntraeger.

Kovacs, Z. P., Du Plessis, D. B., Bracher, P. R., Dunn, P., & Mallory, G. C. L. (1985). *Documentation of the Domoina Floods*. Technical Report TR122, Directorate of Hydrology, Department of Water Affairs.

Krishnaprasad, P. K. (n.d). C*oastal geomorphology landforms of wave erosion and deposition*. (MSc dissertation). Department of Geology, University of Calicut, Kerala, India.

Labuz, T. A. (2009). The increase of the coastal dune area of the Swina Sandbar, West Polish coast. *Zeitschrift der Deutschen Gesellschaft fur Geowissenschaften, 160*, 123-135.

Labuz, T. A. (2015). Coastal dunes: Changes of their perception and environmental management. In: C. H. W. Finkl, O. Cervantes, & C. M. Botero (Eds.), *Beach managements tools-concepts, methodologies and case studies.* Coastal Research Library 24. Cham: Springer.

Landman, K., Hunter, T., & Jackson, J. (2012). *An introduction to engineering surveying*. Cape Town: Juta.

Leopold, L. B. (1953). Downstream change of velocity in rivers. *American Journal of Science, 251* (8), 606-624.

Le Vieux, A. (2010). *Sediment dynamics of the Amatikulu Estuary, Central KwaZulu-Natal Coast, South Africa*. (Unpublished Masters dissertation). School of Geological Sciences Faculty of Science and Agriculture University of KwaZulu-Natal, Westville Campus.

Marker, M. E. (2004). Changes in the Salt River, tributary to the Knysna estuary, South Africa: 1936-1998. *South African Geographical Journal*, *86* (2), 131-140.

Mather, A. A. (2011). Sea level rise and its anticipated impacts along the east coast of South Africa. In: Zietsman, H. L. (Ed.), *Observations on environmental change in South Africa* (pp. 217-221). Stellenbosch: SUN Press.

Mather, A. A., & Vella, G. F. (2007). *Report on the March 2007 coastal erosion event*. Report prepared for the KwaZulu-Natal minister of Agricultural and Environmental Affairs.

McKay, A. J. (1978). *Introduction to measuring techniques in monitoring surveys*. Pretoria: Department of Water Affairs.

Midgley, D. C., & Pitman, M. V. (1969). *Surface water resources of South Africa*. Report 2/69, Hydrological Research Unit, University of the Witwatersrand. Johannesburg: University of the Witwatersrand.

Nicholson, J. (1983). Sedimentary aspects of the Mvumase Project. In: A. McLachlan, & T. Erasmus (Eds.), *Sandy beaches as ecosystems. Proceedings of the 1st International Symposium on Sandy Beaches, Port Elizabeth, South Africa, 17-21 January 1983.* Developments in Hydrobiology series, Vol 19 (pp. 191-197). Dordrecht: Springer. doi: 10.1007/978-94-017-2938-3_13

NRIO (National Research Institute of Oceanography) (1981). *Hydrological Study of Natal Estuaries Data Report 1 Mtamvuna NSI*. NRIO Data Report: Stellenbosch.

Olivier, M. J., & Garland, G. G. (2003). Short-term monitoring of foredune formation on the east coast of South Africa. *Earth Surface, Processes and Landforms*, *28*, 1143-1155.

Orme, A. R. (1980). *Barrier and lagoon systems along the Zululand coast, South Africa, Coastal Geomorphology*. London: Allen & Unwin.

Palmer, B., Van der Elst, R., & Parak, O. (2011). *Understanding our coast: A synopsis of KZN's coastal zone*. Pietermaritzburg: KwaZulu-Natal Department of Agriculture, Environmental Affairs and Rural Development, Cedara.

Partridge, T. C., Dollar, E. S. J., Moolman, J., & Dollar, L. H. (2010). The geomorphic provinces of South Africa, Lesotho and Swaziland: A physiographic subdivision for earth and environmental scientists. *Transactions of the Royal Society of South Africa, 65*, 1- 47.

Pistorius, R. A. (1962). *Natal north coast survey*. Town and Regional Planning Commission, Durban, Natal.

Pye, K. (1983). Coastal dunes. *Progress in Physical Geography: Earth and Environment*, *7* (4), 531-557. doi: 10.1177/030913338300700403

Psuty, N. P. (1992). Spatial variations in coastal foredune development. In: R. W. G. Carter, T. G. F. Curtis, & M. I. Sheehy-Skeffington (Eds.), *Coastal dunes* (pp. 3-13). Rotterdam: Balkema.

Quinn, N. (1977). *Tugela estuarine freshwater requirements: An initial assessment*. Pretoria: Department of Water Affairs and Forestry.

Redsteer, M. H., Bogle, R., & Vogel, J. (2009). *Monitoring and analysis of sand dune movement and growth on the Navajo Nation, Southwestern United States*. Factsheet 3085. US Geographical Survey: Science for a Changing World.

Schulze, R. E., Dlamini, D. J. M., & Horan, M. J. C. (2005). The Thukela catchment: Physical and socio-economic background. In: R. E. Schulze, (Ed.), *Climate change and water resources in Southern Africa: Studies on scenarios, impacts, vulnerabilities and adaptation* (pp. 191-209). WRC Report 1430/1/05. Pretoria: Water Research Commission.

Schumann, E. H. (2013). Sea level variability in South African estuaries. *South African Journal of Science*, *109* (3/4). Article No: 1332.

Sloss, C. R., Shepard, M., & Hesp, P. (2012). Coastal dunes: Geomorphology. *Nature Education Knowledge, 3* (10), 2.

Smith, A. M., Guastella, L. A., Bundy, S. C., & Mather, A. A. (2007). Combined marine storm and South Africa spring high tide erosion events along the KwaZulu-Natal coast in March 2007. *South African Journal of Science*, *103* (7-8), 274–276.

South African Weather Bureau, Wind and Rainfall data Appendix D and E (2018).

Sparavigna, A. C. (n.d.). *Moving sand dunes*. Report. Dipartimento di Fisica Politecnico di Torino Version 2 CE IIT.

Summerfield, M. A. (1991). *Global geomorphology, an introduction to study and learning.* London: Routledge.

Sumner, P. D., & Beckendahl, H. (2017). F*ield Guide for the SAAG Preconference Excursion, July 2017, Drakenberg and KZN north coast on route to Swaziland*. Pretoria: University of Pretoria and University of Swaziland.

Tinley, K. L. (1985). *Coastal dunes of South Africa*. South African National Scientific Programmes Report No. 109. Pretoria: CSIR.

Toole, J. M., & Warren, B. A. (1993). A hydrographic section across the subtropical South Indian Ocean. *Deep-Sea Research*, 1 (40), 1973-2019.

Tresselt, P. (1960). *Recent beach and coastal dune sands at Pismo Beach California*. (Master's thesis). Department of Geology, University of California, Los Angeles.

Tsoar, H. (1971). Types of aeolian sanddunes and their formation. In: N. J. Balmforth & A. Provenzale (Eds.), *The Language of Pattern and Form* (pp. 403-429). Berlin: Springer.

Tsoar, H., & Illenberger, W. (1998). Re-evaluation of sand dunes mobility indices. *Journal of Arid Land Studies*, *75*, 265-268.

Uthungulu District Municipality (2016) *Integrated Development Plan 2016/2017*. Section C Situation Analysis.

Whitfield, A. K. (2000). *Available scientific information on individual South African estuarine systems*. WRC Report No: 577/3/00. Pretoria: Water Research Commission.

Appendices

Appendix A:

Coordinate Lists

Thukela Coordinates

March 2016 North Shore

Point	Y	X	Z
1	49541.369	-3232877.583	64.018
2	49298.659	-3233349.777	13.563
3	50564.838	-3231697.716	16.671
4	48770.843	-3231732.405	65.82
5	48193.221	-3233944.911	2.201
6	49261.009	-3233828.052	2.735
7	49275.131	-3233837.179	0.352
8	49255.908	-3233880.422	0.142
9	49240.648	-3233876.245	1.818
10	49226.888	-3233917.419	1.898
11	49242.026	-3233928.101	0.403
12	49234.564	-3233988.356	0.507
13	49214.111	-3233984.297	2.332
14	49195.381	-3234021.068	3.17
15	49209.048	-3234031.665	0.986
16	49191.433	-3234078.001	0.13
17	49166.793	-3234064.328	3.611
18	49136.751	-3234093.393	3.007
19	49148.022	-3234107.396	0.807
20	49111.194	-3234130.511	0.871
21	49101.76	-3234118.925	3.011
22	49071.349	-3234136.293	0.524
23	49075.453	-3234149.62	0.678
24	49032.554	-3234163.118	0.903
25	49028.849	-3234147.234	3.966
26	48986.999	-3234152.604	3.641
27	48942.957	-3234169.9	1.059
28	48944.651	-3234147.847	3.397
29	48911.089	-3234137.307	3.631
30	48909.722	-3234140.66	2.774
31	48898.084	-3234159.712	0.751
32	48864.539	-3234135.13	0.661
33	48864.796	-3234134.467	1.258

Point	Y	X	Z
34	48867.539	-3234125.544	2.069
35	48868.748	-3234121.499	3.006
36	48820.502	-3234114.215	0.679
37	48820.603	-3234110.65	1.643
38	48820.642	-3234110.07	2.263
39	48820.855	-3234108.094	2.31
40	48779.257	-3234093.616	2.812
41	48773.294	-3234102.738	1.376
42	48771.908	-3234111.748	0.722
43	48732.569	-3234088.248	0.723
44	48736.113	-3234078.515	1.274
45	48694.594	-3234071.303	0.9
46	48695.081	-3234068.282	1.243
47	48299.593	-3230892.599	73.657
48	47335.071	-3230469.334	76.655
49	45730.299	-3231931.872	53.92

March 2016 South Shore

Point	Y	X	Z
52	48217.6057	-3234498.914	2.0515
53	48236.3218	-3234470.65	3.582
54	48247.1431	-3234491.154	1.8082
55	48293.6069	-3234478.493	1.4503
56	48333.4419	-3234461.921	1.1887
57	48371.7038	-3234437.906	1.2359
58	48415.0542	-3234415.977	1.1943
59	48460.3482	-3234393.039	1.2582
60	48491.6418	-3234373.66	1.3096
61	48526.9141	-3234352.37	1.2678
62	48577.2454	-3234333.106	1.069
63	48642.7562	-3234299.413	0.5328
64	48688.7995	-3234280.807	0.1152
65	48730.4214	-3234255.743	0.8927
66	48770.2259	-3234243.986	0.4115
67	48810.0175	-3234223.906	0.44
68	48837.591	-3234218.462	0.3517
69	48864.9152	-3234192.005	0.4147
70	48840.7378	-3234174.132	0.6143
71	48814.8974	-3234152.989	0.7421
72	48795.8337	-3234145.283	0.9587
73	48775.3256	-3234148.945	1.0919

Point	Y	X	Z
74	48758.5596	-3234161.396	1.2517
75	48753.9818	-3234172.839	1.2684
76	48770.6304	-3234187.528	1.3955
77	48792.1822	-3234177.148	1.1501
78	48756.1934	-3234206.131	1.5317
79	48761.2214	-3234216.219	1.5017
80	48730.559	-3234243.484	2.7729
81	48721.114	-3234221.463	2.2307
82	48746.4205	-3234191.386	1.2727
83	48741.8237	-3234194.763	1.3017
84	48725.4495	-3234187.441	1.2975
85	48711.2309	-3234176.048	1.3016
86	48694.7936	-3234170.72	1.2759
87	48672.2252	-3234173.561	1.2885
88	48683.253	-3234201.074	1.7755
89	48701.1783	-3234254.376	2.9727
90	48678.3872	-3234261.889	2.9435
91	48667.3774	-3234240.582	2.6057
92	48656.6097	-3234218.673	2.1179
93	48638.1811	-3234187.981	1.292
94	48614.5082	-3234201.448	1.3113
95	48622.8152	-3234225.898	1.9207
96	48630.9686	-3234248.08	2.4833
97	48645.8809	-3234275.673	3.0877
98	48620.096	-3234291.298	3.0227
99	48602.4677	-3234266.398	2.5324
100	48575.0935	-3234224.151	1.3185
101	48544.1261	-3234234.302	1.3059
102	48555.658	-3234267.289	2.0908
103	48578.8392	-3234312.379	3.2171
104	48550.3409	-3234324.775	3.2174
105	48535.7397	-3234297.665	2.6717
106	48519.3162	-3234273.149	1.8567
107	48506.8836	-3234250.775	1.3059
108	48480.5519	-3234268.122	1.2757
109	48489.4949	-3234286.067	1.7877
110	48502.7266	-3234312.534	2.7747
111	48517.8525	-3234337.934	3.2589
112	48491.1185	-3234352.269	3.1589
113	48482.3255	-3234338.141	3.0346
114	48468.0103	-3234318.005	2.2627
115	48447.0162	-3234289.036	1.2834

Point	Y	X	Z
116	48419.1823	-3234306.619	1.2714
117	48428.3308	-3234325.108	1.8177
118	48443.4133	-3234346.648	2.6817
119	48457.8959	-3234369.522	3.2136
120	48430.1933	-3234385.438	3.1247
121	48418.1376	-3234367.041	2.8347
122	48407.1463	-3234348.6	2.1862
123	48387.6605	-3234320.447	1.2295
124	48359.3476	-3234334.554	1.241
125	48369.7074	-3234356.121	1.92
126	48378.3916	-3234378.787	2.7952
127	48390.1101	-3234406.501	3.1622
128	48362.794	-3234422.355	3.249
129	48351.3753	-3234401.66	3.1489
130	48339.8674	-3234380.507	2.404
131	48323.0166	-3234347.882	1.2612
132	48291.726	-3234358.921	1.2568
133	48300.986	-3234382.553	1.9625
134	48311.7901	-3234409.229	2.8063
135	48332.6256	-3234444.168	3.373
136	48302.6493	-3234455.632	3.4559
137	48290.469	-3234434.204	3.1528
138	48277.0335	-3234410.24	2.365
139	48257.1565	-3234381.705	1.2458
140	48226.2954	-3234405.508	1.2791
141	48233.689	-3234417.338	2.0247
142	48247.6407	-3234445.823	3.0625
143	48257.1303	-3234470.992	3.5216
144	48235.4533	-3234483.601	3.4075
145	48227.4526	-3234466.084	3.8264
146	48222.6269	-3234453.511	3.8044
147	48218.0656	-3234443.102	2.4558
148	48215.6308	-3234437.46	2.6391
149	48202.3997	-3234453.621	2.5143
150	48205.6423	-3234459.834	3.942
151	48210.2484	-3234468.414	5.0425
152	48214.1303	-3234484.689	3.7818
153	48202.9724	-3234490.812	4.1483
154	48198.1124	-3234495.618	3.8702
155	48194.7528	-3234491.966	6.7947
156	48192.3816	-3234489.913	6.5036
157	48189.9109	-3234493.96	6.8235

Point	Y	X	Z
158	48191.4115	-3234495.799	7.1714
159	48186.9081	-3234499.145	6.5123
160	48184.7447	-3234497.234	4.8121
161	48184.8138	-3234497.222	4.7847
162	48184.3603	-3234502.026	4.5974
163	48185.4673	-3234503.475	3.712
164	48182.0124	-3234503.665	3.2842
165	48179.9331	-3234506.741	2.6463
166	48157.0238	-3234500.212	3.8938
167	48170.6431	-3234493.164	4.0884
168	48171.2833	-3234507.4	3.9432
169	48177.0708	-3234506.039	4.3349
170	48178.2319	-3234500.88	5.5851
171	48176.3808	-3234497.787	4.8471
172	48173.4996	-3234494.074	4.8238
173	48171.0917	-3234489.352	4.1361
174	48164.3891	-3234475.036	3.8627
175	48156.512	-3234463.441	4.4949
176	48155.1734	-3234462.161	3.5488

July 2017 North Shore

Point	Y	X	Z
1	49261.5948	-3233821.628	3.1669
2	49264.4092	-3233823.031	2.8533
3	49265.963	-3233823.761	2.2531
4	49284.6889	-3233832.533	-0.3574
5	49266.3937	-3233871.538	0.0868
6	49249.0269	-3233866.075	2.0843
7	49247.022	-3233865.679	2.9537
8	49234.6148	-3233898.448	2.769
9	49237.4943	-3233898.975	2.225
10	49254.6691	-3233905.549	-0.0923
11	49248.7843	-3233949.908	-0.1112
12	49232.8969	-3233949.575	1.6349
13	49221.8066	-3233949.321	2.7739
14	49213.7252	-3233984.921	2.6822
15	49225.8563	-3233989.165	1.4063
16	49242.7024	-3233995.376	0.057
17	49228.1242	-3234030.244	0.0468
18	49217.4587	-3234024.685	1.755
19	49198.3978	-3234017.638	2.803

Point	Y	X	Z
20	49177.0918	-3234053.097	3.2835
21	49189.4412	-3234061.268	1.8348
22	49209.0186	-3234072.715	-0.1107
23	49179.0156	-3234103.701	0.0114
24	49162.2015	-3234089.878	2.053
25	49151.7804	-3234080.878	3.7092
26	49124.1877	-3234103.994	3.5371
27	49131.252	-3234116.277	1.962
28	49136.8437	-3234132.388	0.068
29	49104.732	-3234155.683	-0.0337
30	49095.4061	-3234139.133	2.0363
31	49089.8497	-3234129.381	3.3568
32	49089.4546	-3234150.819	1.3543
33	49048.9426	-3234173.103	0.1606
34	49043.13	-3234158.702	2.2442
35	49037.9159	-3234146.348	3.897
36	49003.4747	-3234151.994	3.6954
37	49003.0419	-3234164.767	1.6638
38	49001.3966	-3234182.807	0.481
39	48979.6882	-3234181.274	0.6135
40	48965.8511	-3234170.276	1.7337
41	48965.5863	-3234161.478	2.6808
42	48965.0911	-3234153.182	3.6822
43	48929.722	-3234145.549	3.571
44	48927.294	-3234156.1	2.6614
45	48926.6579	-3234170.083	1.377
46	48926.8427	-3234173.887	0.7163
47	48913.2984	-3234172.156	0.8276
48	48896.9648	-3234159.218	0.8446
49	48890.6895	-3234154.825	0.898
50	48891.6623	-3234151.239	1.4408
51	48892.1394	-3234150.329	1.8347
52	48892.6497	-3234149.015	2.0008
53	48893.1991	-3234147.465	2.6779
54	48896.9273	-3234134.873	3.3626
55	48864.226	-3234119.898	2.941
56	48860.3952	-3234130.943	2.8587
57	48859.2467	-3234138.359	2.7477
58	48824.799	-3234137.21	2.6704
59	48825.7103	-3234125.031	2.6489
60	48826.4062	-3234107.899	2.7133
61	48789.4153	-3234095.838	2.409

Point	Y	X	Z
62	48780.0527	-3234119.388	2.0699
63	48781.8621	-3234134.1	2.4043
64	48776.6879	-3234137.404	2.3794
65	48742.2207	-3234138.813	1.5005
66	48741.8807	-3234140.708	0.8852
67	48748.4783	-3234119.657	2.2052
68	48757.5242	-3234093.162	1.7156
69	48760.7316	-3234084.476	2.5157
70	48725.2402	-3234074.037	2.689
71	48720.7335	-3234088.855	1.4915
72	48709.619	-3234112.106	1.7536
73	48701.9494	-3234123.761	1.0118
74	48701.5226	-3234124.394	0.8635
75	48675.3185	-3234111.405	0.8897
76	48644.8512	-3234101.935	0.9084
77	48645.0115	-3234091.632	1.9965
78	48650.5883	-3234067.645	2.4733
79	48653.5303	-3234050.33	2.1746
80	48950.915	-3234147.55	4.2064
81	47596.9943	-3234947.787	4.6253
82	48227.3935	-3234501.381	1.8409

Amatigulu Coordinates

Point	X	Y	Z
1	58335.85	-3216897.391	44.832
2	58562.954	-3216631.194	46.611
2A	58256.363	-3216773.453	57.453
3	58692.739	-3217870.208	62.391
4	59680.31	-3217648.209	54.808
5	60372.305	-3218891.715	68.578
7	61063.028	-3219309.194	17.644
8	61365.951	-3218078.896	46.977
9	64860.244	-3212756.285	89.71
10	61866.918	-3213747.594	41.945
11	61236.026	-3213962.47	25.449
11A	61236.379	-3213961.773	23.526
12	62082.807	-3216748.804	64.7
14	61788.813	-3216197.637	57.294
15	60757.878	-3217995.925	104.949
15A	60520.598	-3218106.519	85.919
15B	60758.5	-3217998.523	102.261

Point	X	Y	Z
16A	63151.928	-3215469.544	102.893
16AA	63151.158	-3215469.616	101.02
16B	64363.148	-3213402.902	108.79
17	62609.067	-3216089.011	78.84
17A	62609.898	-3216089.872	76.91
21	59101.097	-3221846.435	4.884
22	59099.972	-3221846.326	4.969
23	59099.95	-3221846.335	4.965
24	59099.698	-3221840.47	4.039
25	58617.054	-3221685.335	4.063
26	58418.975	-3221605.923	5.606
27	58223.571	-3221810.616	24.114
28	58041.669	-3221550.261	44.213
29	57639.924	-3221534.984	30.827
30	62993.356	-3215639.35	114.421
31	58713.366	-3220708.475	15.16
32A	56852.184	-3219539.481	101.282
33	63500.224	-3217804.372	17.788
34A	58220.724	-3218759.992	93.613
38A	60136.709	-3218148.612	74.033
41A	61359.154	-3215173.405	42.982
100	63424.123	-3217969.099	6.075
101	63472.964	-3217940.145	8.105
102	63494.393	-3217903.967	10.222
103	63521.967	-3217927.96	4.841
104	63559.817	-3217964.563	5.538
105	63587.28	-3218000.938	3.65
106	63388.616	-3218217.033	3.812
107	63267.811	-3218329.733	3.957
108	63252.882	-3218314.867	5.324
109	63069.798	-3218493.919	4.302
110	63063.399	-3218486.701	5.406
111	62965.476	-3218597.231	4.452
112	62954.73	-3218587.695	5.497
113	62738.366	-3218801.085	3.677
114	62687.393	-3218771.672	5.57
115	62294.36	-3219276.426	4.413
116	62011.754	-3219594.988	4.468
117	61869.181	-3219747.98	3.704
118	61672.185	-3220031.315	4.445
119	61266.648	-3220529.144	4.124
120	60964.681	-3220891.647	3.945

Point	X	Y	Z
121	60562.996	-3221459.145	4.217
122	60220.356	-3221914.555	4.547
123	59975.886	-3222299.21	4.461
124	59903.039	-3222256.436	9.042
125	59893.822	-3222245.76	4.194
126	59871.277	-3222216.802	4.648
127	59854.754	-3222204.608	9.357
128	59818.65	-3222191.52	3.963
129	59928.634	-3222113.017	3.366
130	59963.679	-3222110.472	3.315
131	60023.892	-3222070.156	3.838
132	60109.806	-3221895.531	3.797
133	60188.442	-3221805.856	3.74
134	60266.212	-3221711.4	3.78
135	60372.92	-3221504.994	3.485
136	60584.502	-3221232.535	3.726
137	60747.179	-3221039.169	3.759
138	60838.879	-3220874.638	4.065
139	60978.033	-3220673.466	3.737
140	61036.243	-3220615.284	4.281
141	61033.802	-3220581.628	4.173
142	61253.057	-3220339.722	3.835
143	61200.414	-3220218.76	4.047
144	61350.373	-3219996.342	3.694
145	61783.271	-3219552.56	4.924
146	62217.368	-3218995.133	3.809
147	62270.134	-3219059.387	3.893
148	62259.391	-3219127.908	4.115
149	62298.805	-3219102.189	4.037
150	62323.404	-3219050.214	3.981
151	62277.88	-3218957.157	4.041
152	62298.722	-3218950.389	3.766
153	62353.396	-3219021.334	3.793
154	62426.318	-3218942.717	3.976
155	62500.734	-3218808.963	3.714
156	62595.732	-3218729.25	3.644
157	62777.207	-3218573.575	3.722
158	62925.495	-3218461.442	3.724
159	62973.198	-3218494.596	3.84
160	63118.883	-3218367.364	3.858
161	63076.637	-3218327.813	3.678
162	63126.898	-3218283.311	3.717

Point	X	Y	Z
163	63225.807	-3218182.108	3.581
164	63310.028	-3218112.612	3.658
165	63328.056	-3218073.21	3.616
166	63357.046	-3218106.764	4.112
167	63360.887	-3218110.69	4.391
168	63314.076	-3218053.978	3.79
169	63261.49	-3218102.628	3.668
170	63215.394	-3218149.111	3.648
171	63105.065	-3218225.459	3.643
172	63030.032	-3218245.438	3.656
173	62926.718	-3218305.206	3.651
201	63474.69	-3214971.08	119.1
202	60527.605	-3219381.743	62.614
276BR	63475.187	-3214970.897	119.1

Umlalazi Coordinates

July 2017

Point	Y	X	Z
12	-74873.7344	3204686.013	2.2382
600	-74862.8965	3205271.499	13.6267
601	-74866.9299	3205295.813	15.2834
602	-74883.619	3205305.785	14.239
603	-74890.0311	3205300.443	13.9115
604	-74886.8346	3205328.381	12.3867
605	-74895.6776	3205344.958	11.1933
606	-74916.4795	3205319.193	14.1311
607	-74922.319	3205315.302	14.0299
608	-74920.75	3205312.359	14.1451
609	-74914.5038	3205315.995	14.155
610	-74907.5339	3205301.751	14.41
611	-74914.9002	3205289.988	15.1238
612	-74911.3578	3205272.695	19.9609
613	-74926.8069	3205264.097	20.4808
614	-74941.4225	3205249.982	20.6908
615	-74951.3601	3205226.644	19.7815
616	-74963.7969	3205214.211	19.4791
617	-74973.9092	3205206.717	19.4815
618	-74979.385	3205210.969	21.514
619	-74986.5119	3205199.271	12.8283
620	-74984.3067	3205194.66	10.9046
621	-74999.9452	3205198.986	19.4872

Point	Y	X	Z
622	-75009.4461	3205192.038	20.1747
623	-75019.8894	3205181.987	19.7768
624	-75033.0944	3205184.122	20.4602
625	-75034.5105	3205187.364	20.3679
626	-75059.1794	3205168.033	17.298
627	-75063.6319	3205170.015	17.6379
628	-75068.5926	3205179.322	20.0637
629	-75079.5096	3205182.578	20.3104
630	-75093.5167	3205175.83	19.0221
631	-75106.5079	3205165.261	19.9974
632	-75130.0507	3205145.3	19.8288
633	-75152.4211	3205147.153	22.5507
634	-75143.0881	3205156.086	22.0814
635	-75162.7881	3205194.854	16.0747
636	-75182.8112	3205229.046	8.5424
637	-75208.7008	3205282.123	3.887
638	-75232.4184	3205323.58	2.2962
639	-75242.579	3205342.664	1.4485
640	-75187.5989	3205366.943	1.2765
641	-75153.3909	3205319.07	3.6434
642	-75098.2289	3205249.372	10.8309
643	-75077.984	3205223.442	17.6683
644	-75073.2597	3205224.894	18.0402
645	-75073.3097	3205219.561	19.3774
646	-75081.4756	3205212.34	18.7054
647	-75052.2824	3205198.903	19.8944
648	-75045.3431	3205194.967	18.6711
649	-75037.376	3205219.116	19.6069
650	-75026.6353	3205226.622	18.8625
651	-75009.6202	3205252.004	16.9386
652	-75014.4555	3205263.383	16.2179
653	-75024.3644	3205258.19	15.2299
654	-75034.2222	3205246.12	16.9368
655	-75028.5829	3205235.749	19.3694
656	-75018.7901	3205244.293	20.7376
657	-75020.3385	3205252.449	18.0028
658	-75058.1592	3205306.273	6.6112
659	-75083.7983	3205348.689	3.992
660	-75103.9538	3205390.172	2.1636
661	-75120.4343	3205414.279	0.7719
662	-75059.902	3205435.458	1.0456
663	-74984.4492	3205318.204	10.3247

Point	Y	X	Z
664	-74988.2156	3205317.262	10.1474
665	-74989.447	3205312.737	10.9339
666	-74985.9291	3205316.625	11.337
667	-74984.8543	3205315.32	10.6257
668	-74957.6113	3205282.831	16.2474
669	-74958.6045	3205271.235	17.224
670	-74963.2124	3205256.106	19.289
671	-74971.751	3205236.781	21.1777
672	-74978.2195	3205220.489	22.2993
673	-74977.5859	3205216.205	22.2449
674	-74958.7876	3205231.385	19.6938
675	-74966.2419	3205239.894	20.9995
676	-74960.0551	3205255.937	19.6119
677	-74954.176	3205267.771	19.7877
678	-74944.9487	3205274.369	17.7073
679	-74937.5061	3205271.217	17.8453
680	-74946.2514	3205287.695	17.4921
681	-74970.6405	3205277.12	16.3056
682	-74979.0121	3205248.562	19.1602
683	-74981.6138	3205227.269	20.6664
684	-74984.6599	3205218.656	20.7751
685	-74997.8261	3205235.239	18.7495
686	-74990.6014	3205257.974	16.2261
687	-74967.2052	3205299.871	13.0313
688	-74939.5865	3205300.049	15.5896
689	-74926.6454	3205297.469	15.2987
690	-74940.7777	3205320.951	13.0549
691	-74924.7571	3205333.334	11.4311
692	-74960.6748	3205377.306	5.4347
693	-74986.3563	3205408.965	4.8707
694	-74986.7439	3205408.99	3.994
695	-75014.7129	3205446.171	2.2804
696	-75023.4967	3205463.164	0.936
697	-74969.9275	3205490.609	1.3347
698	-74904.2507	3205387.529	7.5287
699	-74892.3461	3205371.749	10.2452
700	-74882.3184	3205358.609	12.6402
701	-74886.3129	3205331.863	12.2254
702	-74870.8881	3205344.616	17.3363
703	-74871.0645	3205344.823	16.1715
704	-74875.9003	3205335.978	17.2672
705	-74875.6751	3205332.692	17.1594

Point	Y	X	Z
706	-74850.6978	3205355.223	14.6927
707	-74855.1974	3205337.831	16.9109
708	-74860.3469	3205329.597	18.7491
709	-74856.9652	3205313.909	19.6923
710	-74862.0303	3205312.045	20.935
711	-74866.7794	3205311.232	20.3965
712	-74867.3287	3205313.959	20.5142
713	-74867.2931	3205316.614	20.8081
714	-74859.4392	3205300.534	19.6042
715	-74851.7422	3205278.788	18.9029
716	-74846.1831	3205300.717	18.2009
717	-74850.9582	3205306.438	19.0492
718	-74840.5507	3205299.867	18.46
719	-74819.9811	3205325.41	19.4655
720	-74827.788	3205332.419	17.095
721	-74830.9671	3205335.662	17.4296
722	-74836.4845	3205344.092	15.5114
723	-74834.2121	3205347.894	15.9704
724	-74831.7228	3205346.488	15.4814
725	-74831.2135	3205349.9	15.0561
726	-74834.5653	3205354.527	14.5022
727	-74838.0147	3205354.126	14.2321
728	-74839.0173	3205349.228	14.8039
729	-74836.1599	3205352.143	15.1394
730	-74834.4091	3205348.329	15.878
731	-74828.8298	3205340.047	17.2665
732	-74824.5551	3205350.673	17.5825
733	-74823.4405	3205353.478	16.7577
734	-74820.3054	3205352.361	16.4183
735	-74814.1003	3205358.091	15.5546
736	-74815.8152	3205360.079	15.5071
737	-74818.7493	3205363.233	16.6171
738	-74822.2464	3205363.876	16.0013
739	-74826.847	3205357.334	14.8928
740	-74828.7446	3205359.396	14.7051
741	-74827.2429	3205360.978	15.3737
742	-74824.7401	3205361.697	14.8587
743	-74824.3867	3205369.623	14.2542
744	-74827.7407	3205371.517	13.88
745	-74829.5823	3205369.244	13.3365
746	-74830.936	3205367.527	13.781
747	-74829.9846	3205365.895	14.1755

Point	Y	X	Z
748	-74829.1017	3205364.385	14.101
749	-74828.1963	3205362.537	14.9084
750	-74826.9368	3205361.108	15.4644
751	-74818.1394	3205365.14	16.6628
752	-74814.9582	3205368.109	15.9975
753	-74811.7987	3205371.072	15.4186
754	-74813.1747	3205367.336	15.3185
755	-74812.2316	3205366.366	15.5628
756	-74815.1502	3205362.304	15.8935
757	-74813.5772	3205363.74	15.9345
758	-74813.5801	3205361.598	15.1568
759	-74812.7888	3205360.322	15.484
760	-74810.9626	3205361.903	15.7651
761	-74809.3177	3205362.921	15.8145
762	-74810.4662	3205363.818	15.7276
763	-74811.7574	3205364.606	15.2903
764	-74808.2275	3205365.352	14.7319
765	-74808.4443	3205367.501	14.5647
766	-74805.8045	3205373.08	13.5753
767	-74808.1397	3205374.482	13.3859
768	-74809.482	3205372.533	13.9528
769	-74810.4087	3205369.806	14.7449
770	-74809.6272	3205368.688	15.5851
771	-74810.4702	3205375.08	13.3067
772	-74810.9639	3205377.911	12.8266
773	-74814.0038	3205373.97	13.8263
774	-74812.9592	3205372.707	13.9337
775	-74816.893	3205369.505	15.1975
776	-74815.1667	3205372.751	14.2686
777	-74816.4627	3205373.008	14.8947
778	-74814.5983	3205375.528	14.4897
779	-74812.6364	3205377.331	13.8593
780	-74813.4737	3205378.248	13.9882
781	-74815.6521	3205376.581	14.4058
782	-74816.8814	3205377.834	13.9076
783	-74820.0457	3205377.267	13.9137
784	-74819.431	3205373.978	14.8035
785	-74823.1752	3205372.583	14.5924
786	-74823.6564	3205369.602	14.4354
787	-74827.3878	3205371.753	13.9291
788	-74833.5444	3205368.858	13.3301
789	-74827.9169	3205376.769	11.5174

Point	Y	X	Z
790	-74827.7741	3205376.64	11.3122
791	-74817.1757	3205385.696	11.7861
792	-74817.2571	3205385.63	11.1553
793	-74809.5353	3205381.216	12.3105
794	-74805.0117	3205384.476	11.9288
795	-74806.2666	3205384.725	12.3249
796	-74808.0209	3205385.264	12.3739
797	-74806.8774	3205385.745	11.9429
798	-74804.3126	3205354.447	15.392
799	-74813.5708	3205343.921	17.8443
800	-74819.0522	3205340.424	18.042
801	-74815.666	3205344.726	18.5336
802	-74817.8936	3205346.021	18.285
803	-74817.0666	3205349.774	17.5103
804	-74812.6127	3205354.093	17.4089
805	-74810.7388	3205355.207	17.2603
806	-74810.2511	3205353.755	17.1679
807	-74811.5524	3205352.037	17.5116
808	-74809.7282	3205349.317	17.9226
809	-74812.4192	3205346.65	18.0847
810	-74815.9769	3205326.554	19.7333
811	-74812.9474	3205315.998	20.745
812	-74812.8566	3205313.447	20.594
813	-74811.7216	3205305.006	21.2758
814	-74815.4456	3205305.445	19.6955
815	-74816.8286	3205298.547	19.6737
816	-74818.6711	3205291.96	19.5438
817	-74818.8242	3205291.911	19.4663
818	-74824.2937	3205283.378	16.983
819	-74824.2116	3205283.206	17.0052
820	-74824.7376	3205280.205	15.8227
821	-74819.0823	3205284.002	19.3919
822	-74818.5162	3205285.052	19.9361
823	-74817.8151	3205285.018	19.036
824	-74817.8186	3205285.044	19.0374
825	-74812.5947	3205293.296	21.4957
826	-74806.3395	3205301.614	21.6621
827	-74793.1784	3205324.924	20.5131
828	-74787.0238	3205324.107	20.9667
829	-74781.1229	3205329.631	20.2354
830	-74774.7565	3205346.109	18.4193
831	-74770.9763	3205340.426	18.6984

Point	Y	X	Z
832	-74766.0248	3205339.434	18.8713
833	-74763.9864	3205350.627	19.0203
834	-74761.0873	3205361.653	18.5974
835	-74756.9724	3205365.683	18.2093
836	-74750.6075	3205370.087	17.3032
837	-74747.5215	3205380.077	17.9145
838	-74744.7584	3205386.907	17.5865
839	-74751.7643	3205389.173	16.8306
840	-74758.5746	3205383.542	15.7797
841	-74764.4904	3205368.822	16.2045
842	-74767.6841	3205360.15	16.773
843	-74781.5475	3205350.286	17.2458
844	-74787.591	3205349.472	16.5454
845	-74792.3616	3205350.008	16.8033
846	-74788.7707	3205357.953	16.8089
847	-74786.583	3205361.237	16.7374
848	-74781.0883	3205360.014	14.7889
849	-74774.2616	3205359.431	16.2249
850	-74770.1766	3205370.203	15.3097
851	-74773.0731	3205370.464	14.6611
852	-74774.7424	3205377.095	13.7696
853	-74778.2803	3205384.922	12.7125
854	-74782.1414	3205390.592	12.7416
855	-74788.0619	3205390.865	12.5445
856	-74794.6428	3205387.755	11.9746
857	-74799.2053	3205380.489	11.6016
858	-74793.4736	3205378.961	10.6364
859	-74788.1325	3205384.588	9.785
860	-74788.6241	3205386.423	10.3379
861	-74782.6067	3205383.59	9.9401
862	-74778.3015	3205380.394	11.9557
863	-74776.6306	3205370.988	13.5447
864	-74795.8861	3205357.39	14.9057
865	-74801.9532	3205362.989	14.0397
866	-74790.937	3205370.252	11.8137
867	-74789.2645	3205378.308	10.5277
868	-74811.1426	3205410.721	10.0197
869	-74811.2921	3205411.37	9.9437
870	-74813.6421	3205410.465	9.6007
871	-74815.9615	3205407.532	9.7347
872	-74812.9409	3205406.533	10.4047
873	-74821.5413	3205432.807	7.6267

Point	Y	X	Z
874	-74811.0193	3205437.516	7.3487
875	-74802.9201	3205446.773	7.1307
876	-74798.0014	3205451.691	7.6057
877	-74797.9516	3205451.564	7.6007
878	-74805.2576	3205452.261	7.3787
879	-74814.5515	3205454.411	7.1857
880	-74823.7925	3205458.01	4.8127
881	-74841.6697	3205461.014	4.3157
882	-74873.3669	3205474.415	3.4967
883	-74887.4059	3205477.583	3.4067
884	-74906.8041	3205481.124	2.6227
885	-74912.4083	3205500.037	2.0847
886	-74907.1015	3205510.234	2.0587
887	-74918.1509	3205515.555	1.9567
888	-74892.1571	3205528.039	1.2947
889	-74910.1308	3205512.546	1.7647
890	-74909.6736	3205512.455	1.8327
891	-74906.5273	3205510.755	1.8017
892	-74910.8495	3205489.339	2.1017
893	-74892.4878	3205479.887	2.3967
894	-74868.3865	3205474.065	2.3817
895	-74842.6666	3205463.693	2.3357
896	-74748.6907	3205454.643	7.3893
897	-74717.5229	3205465.028	6.5302
898	-74717.267	3205465.275	5.917
899	-74685.0491	3205475.949	7.5134
900	-74652.7297	3205527.592	2.7435
901	-74616.0936	3205543.056	2.4972
902	-74553.3788	3205566.356	2.7977
903	-74524.5498	3205590.259	5.7302
904	-74516.2374	3205601.247	7.6733
905	-74510.7048	3205601.953	6.7972
906	-74500.3178	3205613.751	7.2959
907	-74502.8915	3205617.01	8.2631
908	-74505.3392	3205614.883	7.5771
909	-74504.5367	3205619.685	7.3715
910	-74499.3969	3205620.191	7.4929
911	-74482.1759	3205629.447	6.969
912	-74481.6287	3205632.713	7.4855
913	-74479.5988	3205633.99	7.0059
914	-74485.0838	3205633.529	7.4603
915	-74492.6083	3205632.831	8.1585

Point	Y	X	Z
916	-74476.1794	3205639.659	9.3457
917	-74462.7333	3205646.897	10.0886
918	-74436.4006	3205668.121	11.3506
919	-74420.9257	3205682.674	12.559
920	-74417.4665	3205684.182	12.1549
921	-74421.421	3205684.688	12.3719
922	-74422.2255	3205687.173	12.4415
923	-74418.115	3205686.893	13.443
924	-74434.0004	3205704.051	10.6947
925	-74430.4066	3205706.948	10.609
926	-74430.544	3205710.448	10.2396
927	-74433.0404	3205708.031	10.3563
928	-74432.0472	3205707.646	11.0249
929	-74440.1183	3205711.272	8.8049
930	-74437.6386	3205713.487	8.8814
931	-74437.808	3205715.5	8.7362
932	-74438.5556	3205714.15	9.0753
933	-74439.9068	3205714.824	8.2899
934	-74447.2548	3205714.289	7.685
935	-74449.2748	3205713.567	7.3331
936	-74450.302	3205710.382	7.722
937	-74447.3725	3205712.507	7.7386
938	-74448.0662	3205712.938	8.3086
939	-74457.4245	3205720.654	6.1156
940	-74457.3626	3205720.75	5.6207
941	-74481.104	3205742.297	4.0036
942	-74505.5664	3205764.649	2.3952
943	-74525.4744	3205783.011	1.8593
944	-74562.4236	3205763.835	1.028
945	-74513.6197	3205711.888	4.0547
946	-74490.644	3205704.634	5.0748
947	-74487.5687	3205708.945	5.5922
948	-74486.0832	3205708.156	5.2261
949	-74486.2107	3205710.72	5.1963
950	-74488.5163	3205710.471	4.9856
951	-74475.1844	3205681.468	8.8751
952	-74474.5299	3205673.531	9.8814
953	-74474.5374	3205673.363	9.8488
954	-74481.5703	3205669.044	9.9572
955	-74483.0982	3205676.267	8.4965
956	-74478.89	3205673.154	11.7326
957	-74478.1424	3205675.006	11.8055

Point	Y	X	Z
958	-74476.462	3205676.557	11.2199
959	-74472.4389	3205669.801	10.4485
960	-74465.4627	3205672.529	10.9027
961	-74463.3631	3205679.054	10.4438
962	-74464.6306	3205683.605	9.9086
963	-74469.2451	3205680.792	9.7658
964	-74465.9561	3205679.13	11.6323
965	-74467.0508	3205676.602	12.2828
966	-74468.166	3205674.017	11.9084
967	-74456.4669	3205674.303	11.1587
968	-74450.2779	3205678.332	11.039
969	-74449.904	3205683.244	10.9757
970	-74453.8361	3205685.179	10.2932
971	-74456.401	3205680.372	10.6144
972	-74453.6215	3205678.194	11.7087
973	-74452.2825	3205680.25	12.6017
974	-74505.3476	3205633.768	8.3394
975	-74506.8673	3205634.964	8.6342
976	-74508.1829	3205636.208	8.2607
977	-74579.6613	3205700.328	2.5839
978	-74598.4618	3205722.272	2.1133
979	-74607.1491	3205732.763	1.0764
980	-74654.0156	3205700.077	0.7534
981	-74623.6911	3205666.888	2.6216
982	-74575.8269	3205629.89	4.2665
983	-74538.7127	3205594.285	6.65
984	-74578.2047	3205567.074	5.6622
985	-74627.2745	3205610.584	3.8561
986	-74668.8949	3205652.367	2.2645
987	-74682.8474	3205667.421	1.9319
988	-74692.9271	3205678.252	0.3643
989	-74737.3943	3205646.978	0.4545
990	-74723.2283	3205630.605	2.1021
991	-74689.5266	3205605.985	2.9912
992	-74701.3643	3205593.625	2.7054
993	-74690.678	3205597.2	3.4186
994	-74659.0664	3205567.702	3.8768
995	-74633.6122	3205541.165	4.9025
996	-74654.6467	3205531.123	4.4349
997	-74691.4209	3205506.914	2.5657
998	-74694.5296	3205511.511	3.9074
999	-74730.9137	3205547.356	3.2851

Point	Y	X	Z
1000	-74774.6982	3205584.68	2.5877
1001	-74794.1766	3205606.16	0.6255
1002	-74833.7424	3205574.005	0.8971
1003	-74837.3561	3205577.541	0.7629
1004	-74816.998	3205553.853	2.7659
1005	-74779.4073	3205516.309	2.5889
1006	-74749.9261	3205489.074	2.5226
1007	-74747.5467	3205484.36	2.2196
1008	-74756.8116	3205485.034	2.215
1009	-74757.9745	3205488.325	2.4741
1010	-74785.8526	3205489.028	2.4752
1011	-74786.7246	3205484.41	2.1732
1012	-74805.8211	3205492.031	2.207
1013	-74802.4064	3205499.343	2.3966
1014	-74814.6053	3205501.92	2.2043
1015	-74809.1902	3205507.366	2.2014
1016	-74809.759	3205508.464	2.1912
1017	-74811.6956	3205511.054	2.2685
1018	-74833.4772	3205506.716	2.3272
1019	-74832.1011	3205501.973	2.164
1020	-74859.4446	3205528.235	2.5824
1021	-74871.7645	3205544.528	1.8338
1022	-74880.3041	3205553.114	0.3407
1023	-74917.2412	3205532.593	0.3581
1024	-74917.1555	3205512.568	2.2831
1025	-74916.042	3205514.292	2.0347
1026	-74911.316	3205511.902	2.2034
1027	-74911.2651	3205512.734	1.8851
1028	-74907.3683	3205510.613	2.0567
1029	-74906.9819	3205510.919	1.8121
1030	-74909.831	3205507.153	2.0957
1031	-74909.1945	3205506.72	1.9753
BRG13	-74391.6436	3204318.769	22.140
PARK	-74829.1521	3205189.343	8.7805

Umlalazi Coordinates

April 2017

Point	Y	X	Z	Tag
1C	74393.855	-3204320.268	52.484	Brug/13
9	74120.674	-3204053.151	75.805	ContGol
9A	74118.89	-3204050.28	44.679	ContGol

Point	Y	X	Z	Tag
13	74456.85	-3205720.51	5.207	RefPole
14	74457.41	-3205720.52	5.291	RefPole
50	74874.714	-3204684.948	2.23	12
51	75161.217	-3205140.818	20.145	D
52	75158.722	-3205136.327	17.315	D
53	75149.066	-3205151.283	22.566	D
54	75137.184	-3205152.313	22.541	D
55	75127.42	-3205149.591	20.447	D
56	75121.666	-3205143.776	15.934	D
57	75110.73	-3205160.854	19.414	D
58	75098.475	-3205174.828	19.911	D
59	75094.195	-3205169.541	15.798	D
60	75085.977	-3205180.806	18.499	D
61	75075.649	-3205185.222	20.378	D
62	75068.039	-3205183.922	20.656	D
63	75058.645	-3205170.498	17.974	D
64	75072.067	-3205174.683	14.305	D
65	75047.769	-3205175.023	18.047	D
66	74976.891	-3205204.999	17.806	D
67	74977.415	-3205212.078	21.723	D
68	75009.111	-3205257.17	16.751	D
69	75013.193	-3205245.514	17.141	D
70	75018.421	-3205235.17	18.353	D
71	75006.394	-3205227.098	19.524	D
72	75031.518	-3205211.173	19.628	D
73	75035.903	-3205212.19	19.295	D
74	75043.488	-3205215.292	19.861	D
75	75038.738	-3205221.812	19.835	D
76	75034.26	-3205233.377	19.189	D
77	75033.941	-3205244.838	17.713	D
78	75014.517	-3205265.88	15.562	D
79	75009.743	-3205260.498	17.055	D
80	75022.824	-3205236.174	19.691	D
81	75029.738	-3205237.779	19.417	D
82	75021.418	-3205242.908	20.823	D
83	75018.403	-3205246.073	20.678	D
84	75178.126	-3205171.544	17.504	D
85	75185.137	-3205188.711	15.058	D
86	75197.587	-3205212.973	9.604	D
87	75214.21	-3205244.445	5.84	D
88	75227.755	-3205272.84	3.858	D
89	75243.016	-3205302.813	2.546	D

Point	Y	X	Z	Tag
90	75266.382	-3205339.369	0.161	D
91	75282.981	-3205372.376	-0.784	D
92	75242.543	-3205394.27	-0.872	D
93	75223.611	-3205362.641	0.051	D
94	75207.252	-3205333.969	2.419	D
95	75188.022	-3205298.202	3.77	D
96	75165.165	-3205268.837	5.802	D
97	75151.063	-3205234.339	10.618	D
98	75138.749	-3205207.361	15.864	D
99	75133.505	-3205184.207	18.893	D
100	75130.397	-3205173.944	20.771	D
101	75122.299	-3205183.096	19.519	D
102	75107.258	-3205194.925	18.934	D
103	75099.164	-3205201.07	18.64	D
104	75109.715	-3205228.298	14.652	D
105	75129.515	-3205274.17	6.643	D
106	75143.02	-3205303.9	4.314	D
107	75159.821	-3205338.258	3.038	D
108	75166.819	-3205353.856	2.222	D
109	75183.693	-3205388.399	-0.016	D
110	75197.689	-3205419.846	-1.033	D
111	75162.384	-3205442.472	-1.16	D
112	75146.837	-3205402.699	0.111	D
113	75129.61	-3205364.593	2.275	D
114	75107.968	-3205333.887	3.94	D
115	75100.239	-3205322.857	4.705	D
116	75100.594	-3205321.027	4.794	D
117	75102.968	-3205320.536	4.759	D
118	75100.992	-3205322.093	4.999	D
119	75084.655	-3205261.214	12.158	D
120	75081.128	-3205240.083	14.484	D
121	75078.883	-3205239.153	15.131	D
122	75079.4	-3205238.745	15.728	D
123	75078.447	-3205237.139	15.302	D
124	75081.739	-3205234.891	15.37	D
125	75077.18	-3205225.534	17.252	D
126	75078.302	-3205217.807	18.77	D
127	75073.393	-3205214.763	19.816	D
128	75070.802	-3205221.144	18.86	D
129	75075.066	-3205221.151	19.692	D
130	75039.055	-3205203.532	18.889	D
131	75048.421	-3205220.755	19.302	D

Point	Y	X	Z	Tag
132	75065.032	-3205255.906	13.436	D
133	75051.133	-3205262.621	13.575	D
134	75048.314	-3205265.046	13.353	D
135	75048.742	-3205266.846	13.037	D
136	75050.568	-3205265.958	13.04	D
137	75049.41	-3205265.416	13.492	D
138	75093.75	-3205307.755	5.345	D
139	75102.792	-3205319.684	4.802	D
140	75100.162	-3205321.341	4.816	D
141	75100.321	-3205322.943	4.771	D
142	75102.12	-3205322.622	4.623	D
143	75087.647	-3205387.803	2.215	D
144	75108.995	-3205430.823	-0.06	D
145	75123.111	-3205466.423	-1.397	D
146	75069.495	-3205442.086	0.078	D
147	75085.524	-3205473.126	-0.786	D
148	75089.357	-3205481.41	-1.245	D
149	75062.79	-3205423.133	1.199	D
150	75060.066	-3205417.672	2.086	D
151	75034.288	-3205358.614	4.475	D
152	75015.269	-3205309.723	8.289	D
153	75005.12	-3205288.785	12.496	D
154	75001.769	-3205295.975	12.549	D
155	74996.895	-3205297.326	12.981	D
156	74994.317	-3205296.915	13.432	D
157	74993.078	-3205298.121	13.001	D
158	74995.992	-3205300.079	12.388	D
159	75002.41	-3205299.077	11.518	D
160	75004.709	-3205294.634	11.847	D
161	74994.394	-3205277.013	15.45	D
162	74962.457	-3205295.462	14.06	D
163	74978.787	-3205337.483	7.849	D
164	74995.413	-3205369.944	4.803	D
165	75014.997	-3205403.12	3.291	D
166	75029.507	-3205428.175	1.897	D
167	75050.393	-3205457.999	0.017	D
168	75068.367	-3205485.571	-0.584	D
169	75032.334	-3205513.98	-0.784	D
170	75005.856	-3205472.803	0.727	D
171	74982.157	-3205414.181	3.881	D
172	74950.132	-3205340.387	9.514	D
173	74937.071	-3205318.105	13.321	D

Point	Y	X	Z	Tag
174	74926.229	-3205299.118	15.131	D
175	74915.952	-3205274.215	18.544	D
176	74910.274	-3205273.378	19.94	D
177	74910.449	-3205282.073	18.878	D
178	74916.346	-3205319.107	14.098	D
179	74922.351	-3205315.229	14.089	D
180	74920.665	-3205312.327	14.167	D
181	74808.318	-3205209.721	8.871	D
183	74916.603	-3205319.065	14.27	BRUG
184	74918.1	-3205323.095	13.136	SL
185	74934.714	-3205356.95	8.796	SL
186	74949.783	-3205388.132	5.399	SL
187	74975.44	-3205430.947	3.411	SL
188	74989.538	-3205452.162	2.647	SL
189	75003.673	-3205473.313	0.495	SL
190	75017.83	-3205495.304	-0.083	SL
191	74981.006	-3205524.157	-0.255	SL
192	74969.022	-3205501.979	0.302	SL
193	74951.625	-3205471.677	2.51	SL
194	74935.166	-3205437.67	3.981	SL
195	74919.181	-3205406.123	4.914	SL
200	74829.587	-3205192.774	9.194	SL
201	74835.74	-3205197.521	9.071	SL
202	74888.335	-3205304.876	13.853	SL
203	74910.066	-3205336.483	11.684	SL
204	74889.808	-3205330.708	12.15	SL
205	74885.636	-3205334.298	12.472	SL
206	74879.339	-3205345.793	12.51	SL
207	74882.72	-3205346.817	12.42	SL
208	74885.811	-3205347.627	11.507	SL
209	74881.867	-3205357.061	12.476	SL
210	74882.651	-3205358.978	12.675	SL
211	74886.176	-3205354.02	12.128	SL
212	74881.49	-3205352.491	13.133	SL
213	74877.996	-3205353.284	13.469	SL
214	74875.204	-3205358.104	12.527	SL
215	74872.422	-3205359.504	12.67	SL
216	74869.711	-3205355.124	13.606	SL
217	74862.83	-3205347.909	16.575	SL
218	74852.535	-3205354.458	15.488	SL
219	74855.361	-3205335.96	17.52	SL
220	74858.767	-3205322.456	19.439	SL

Point	Y	X	Z	Tag
221	74858.583	-3205307.85	19.97	SL
222	74852.306	-3205282.905	18.84	SL
223	74837.875	-3205313.483	17.308	SL
224	74828.916	-3205327.253	17.215	SL
225	74816.087	-3205327.35	19.637	SL
226	74811.957	-3205313.255	20.909	SL
227	74811.696	-3205299.41	21.563	SL
228	74808.584	-3205297.847	21.622	SL
229	74817.579	-3205294.432	19.893	SL
230	74823.729	-3205282.963	17.357	SL
231	74821.96	-3205281.765	17.458	SL
232	74816.135	-3205286.897	19.56	SL
233	74805.717	-3205302.753	21.719	SL
234	74797.168	-3205321.26	20.601	SL
235	74793.124	-3205324.62	20.7	SL
236	74787.036	-3205324.248	21.134	SL
237	74781.636	-3205328.673	20.541	SL
238	74775.782	-3205345.494	18.618	SL
239	74766.499	-3205339.769	18.961	SL
240	74764.004	-3205356.359	18.487	SL
241	74759.614	-3205366.299	18.062	SL
242	74771.839	-3205373.007	14.167	SL
243	74772.958	-3205383.228	13.479	SL
244	74775.616	-3205392.185	12.777	SL
245	74779.177	-3205394.791	12.467	SL
246	74786.408	-3205393.511	11.741	SL
247	74795.438	-3205381.62	11.018	SL
248	74789.314	-3205388.803	10.178	SL
249	74780.73	-3205390.568	9.886	SL
250	74776.188	-3205384.572	11.465	SL
251	74772.826	-3205378.848	13.358	SL
252	74773.558	-3205369.509	14.323	SL
253	74777.689	-3205376.203	13.534	SL
254	74780.884	-3205363.841	15.156	SL
255	74777.973	-3205354.807	17.045	SL
256	74791.152	-3205352.919	16.876	SL
257	74786.747	-3205361.697	16.811	SL
258	74791.362	-3205363.983	14.04	SL
259	74790.066	-3205376.765	11.225	SL
260	74786.664	-3205380.972	10.685	SL
261	74809.135	-3205381.943	12.507	SL
262	74807.637	-3205384.657	12.541	SL

Point	Y	X	Z	Tag
263	74805.349	-3205384.82	12.613	SL
264	74804.775	-3205383.814	12.051	SL
265	74804.204	-3205386.159	11.773	SL
266	74807.675	-3205388.045	11.134	SL
267	74807.353	-3205386.554	11.729	SL
268	74810.094	-3205385.537	11.46	SL
269	74811.002	-3205378.926	13.059	SL
270	74812.324	-3205375.092	13.814	SL
271	74817.211	-3205370.819	15.377	SL
272	74819.198	-3205370.919	14.78	SL
273	74814.085	-3205377.058	14.534	SL
274	74817.227	-3205378.959	13.362	SL
275	74818.847	-3205381.475	12.457	SL
276	74824.872	-3205380.076	11.414	SL
277	74829.701	-3205373.46	12.138	SL
278	74832.563	-3205368.985	12.655	SL
279	74832.591	-3205365.142	13.595	SL
280	74829.577	-3205364.388	14.295	SL
281	74830.402	-3205366.732	14.157	SL
282	74828.41	-3205364.432	14.329	SL
283	74830.705	-3205360.362	14.295	SL
284	74827.306	-3205359.627	15.117	SL
285	74824.887	-3205360.045	15.365	SL
286	74826.36	-3205363.375	14.743	SL
287	74826.239	-3205361.082	15.613	SL
288	74828.077	-3205361.508	15.414	SL
289	74828.105	-3205363.249	14.931	SL
290	74829.913	-3205365.762	14.315	SL
291	74830.701	-3205367.659	13.918	SL
292	74853.316	-3205366.019	13.972	SL
293	74854.578	-3205368.507	13.944	SL
294	74855.664	-3205369.518	13.433	SL
295	74862.731	-3205378.964	12.321	SL
296	74870.955	-3205392.225	8.52	SL
297	74873.624	-3205396.309	7.904	SL
298	74872.67	-3205398.459	7.901	SL
299	74875.126	-3205399.263	7.4	SL
300	74876.527	-3205398.526	7.276	SL
301	74877.609	-3205395.1	7.555	SL
302	74874.35	-3205397.197	8.352	SL
303	74871.452	-3205400.566	7.686	SL
304	74868.201	-3205402.579	7.626	SL

Point	Y	X	Z	Tag
305	74868.561	-3205404.388	7.455	SL
306	74870.166	-3205404.258	7.282	SL
307	74869.496	-3205403.155	7.827	SL
308	74883.094	-3205412.098	5.719	SL
309	74904.971	-3205443.168	4.121	SL
310	74924.316	-3205474.717	3.067	SL
311	74932.742	-3205488.254	2.361	SL
312	74942.375	-3205502.151	0.909	SL
313	74961.861	-3205530.501	-0.108	SL
314	74930.301	-3205558.147	-0.232	SL
315	74915.958	-3205534.923	0.277	SL
316	74891.71	-3205504.89	2.651	SL
317	74869.696	-3205465.868	4.128	SL
318	74847.434	-3205429.044	6.52	SL
319	74856.031	-3205425.254	6.268	SL
320	74857.806	-3205425.64	6.067	SL
321	74859.526	-3205423.133	6.162	SL
322	74856.07	-3205423.808	6.375	SL
323	74856.997	-3205424.482	6.568	SL
324	74826.952	-3205411.163	7.405	SL
325	74816.519	-3205404.536	9.507	SL
326	74816.056	-3205402.601	9.978	SL
327	74816.554	-3205403.293	10.006	SL
328	74816.886	-3205402.35	10.147	SL
329	74817.642	-3205401.64	9.636	SL
330	74814.725	-3205399.202	10.297	SL
331	74813.22	-3205398.836	10.476	SL
332	74813.014	-3205400.458	10.494	SL
333	74814.521	-3205400.743	10.284	SL
334	74813.906	-3205399.642	10.714	SL
335	74755.246	-3205389.139	16.245	SL
336	74773.739	-3205411.256	12.237	SL
337	74789.628	-3205429.927	9.216	SL
338	74792.551	-3205427.487	9.577	SL
339	74793.98	-3205427.435	9.369	SL
340	74795.085	-3205423.728	9.923	SL
341	74792.615	-3205426.01	9.746	SL
342	74793.208	-3205426.528	9.869	SL
343	74802.926	-3205447.066	7.669	SL
344	74804.727	-3205449.496	7.775	SL
345	74807.801	-3205452.934	7.764	SL
346	74810.326	-3205456.201	7.556	SL

Point	Y	X	Z	Tag
347	74813.534	-3205459.781	6.638	SL
348	74816.39	-3205461.986	5.512	SL
349	74818.894	-3205457.679	5.68	SL
350	74817.19	-3205456.057	6.475	SL
351	74814.624	-3205453.688	7.221	SL
352	74812.117	-3205449.813	7.718	SL
353	74809.246	-3205445.662	7.674	SL
354	74806.681	-3205442.383	7.365	SL
355	74809.084	-3205437.987	7.349	SL
356	74811.624	-3205439.407	7.886	SL
357	74813.114	-3205440.205	8.068	SL
358	74814.479	-3205441.019	8.152	SL
359	74816.283	-3205441.762	8.079	SL
360	74817.636	-3205442.766	7.719	SL
361	74820.114	-3205444.265	7.781	SL
362	74821.461	-3205446.412	7.388	SL
363	74823.178	-3205448.015	6.539	SL
364	74825.055	-3205448.839	6.152	SL
365	74826.645	-3205446.392	6.228	SL
366	74824.407	-3205443.517	7.145	SL
367	74822.295	-3205441.469	7.681	SL
368	74819.425	-3205439.569	7.781	SL
369	74816.522	-3205437.318	8.041	SL
370	74814.044	-3205436.426	7.935	SL
371	74812.847	-3205437.121	8.121	SL
372	74812.216	-3205434.951	7.579	SL
373	74819.369	-3205435.988	7.215	SL
374	74826.361	-3205440.137	6.883	SL
375	74830.647	-3205443.953	6.295	SL
376	74827.893	-3205446.858	6.229	SL
377	74828.068	-3205448.93	6.03	SL
378	74829.928	-3205448.451	5.811	SL
379	74829.574	-3205447.612	6.382	SL
380	74813.934	-3205466.979	5.285	SL
381	74810.707	-3205464.207	6.55	SL
382	74806.457	-3205460.493	7.6	SL
383	74804.255	-3205458.25	7.92	SL
384	74801.848	-3205455.317	7.734	SL
385	74798.274	-3205452.107	8.064	SL
386	74795.049	-3205449.963	7.759	SL
387	74792.353	-3205452.541	7.523	SL
388	74793.742	-3205454.199	7.97	SL

Point	Y	X	Z	Tag
389	74796.647	-3205458.255	7.915	SL
390	74800.212	-3205463.065	7.566	SL
391	74804.253	-3205468.071	6.718	SL
392	74808.288	-3205471.02	5.872	SL
393	74811.401	-3205473.339	4.923	SL
394	74808.704	-3205476.303	4.683	SL
395	74806.65	-3205474.273	5.433	SL
396	74801.708	-3205469.83	6.503	SL
397	74796.755	-3205464.228	7.27	SL
398	74793.068	-3205461.379	7.583	SL
399	74790.272	-3205458.704	7.09	SL
400	74791.636	-3205465.328	6.72	SL
401	74795.697	-3205471.322	6.09	SL
402	74797.631	-3205475.058	5.578	SL
403	74803.179	-3205475.313	5.259	SL
404	74839.408	-3205492.231	3.966	SL
405	74860.693	-3205521.637	2.528	SL
406	74883.601	-3205549.676	0.39	SL
407	74899.72	-3205569.979	-0.052	SL
408	74857.937	-3205589.591	-0.003	SL
409	74847.432	-3205574.544	0.4	SL
410	74830.847	-3205546.707	2.322	SL
411	74805.242	-3205507.755	3.887	SL
412	74784.172	-3205476.969	5.593	SL
413	74786.054	-3205476.855	5.492	SL
414	74785.937	-3205474.471	5.847	SL
415	74784.063	-3205475.507	5.737	SL
416	74784.824	-3205476.127	6.063	SL
417	74772.528	-3205461.895	6.298	SL
418	74750.402	-3205431.906	11.508	SL
419	74728.035	-3205408.32	17.931	SL
420	74719.129	-3205424.327	16.753	SL
421	74702.999	-3205429.872	17.659	SL
422	74693.458	-3205434.75	17.903	SL
423	74681.692	-3205433.601	17.677	SL
424	74680.875	-3205429.326	17.613	SL
425	74690.304	-3205416.288	19.173	SL
426	74695.205	-3205410.766	18.219	SL
427	74686.209	-3205410.695	17.961	SL
428	74676.737	-3205420.15	17.884	SL
429	74677.323	-3205441.963	16.649	SL
430	74697.508	-3205443.345	14.367	SL

Point	Y	X	Z	Tag
431	74698.996	-3205447.005	12.6	SL
432	74712.557	-3205468.843	6.316	SL
433	74720.97	-3205481.232	4.638	SL
434	74736.942	-3205517.652	3.802	SL
435	74753.667	-3205550.879	3.696	SL
436	74768.638	-3205573.096	2.45	SL
437	74781.797	-3205590.438	1.421	SL
438	74791.912	-3205603.79	0.686	SL
439	74760.896	-3205604.31	1.586	SL
440	74749.669	-3205612.494	1.412	SL
441	74741.885	-3205610.87	1.691	SL
442	74732.122	-3205594.709	2.534	SL
443	74714.06	-3205562.483	3.623	SL
444	74692.571	-3205528.589	4.008	SL
445	74677.115	-3205503.351	5.625	SL
446	74658.194	-3205475.641	10.972	SL
447	74642.504	-3205456.9	17.375	SL
448	74640.342	-3205478.248	13.907	SL
449	74642.905	-3205485.407	12.013	SL
450	74648.374	-3205483.281	12.221	SL
451	74653.477	-3205480.064	10.754	SL
452	74650.857	-3205485.748	9.981	SL
453	74655.994	-3205481.062	9.319	SL
454	74661.102	-3205483.117	8.647	SL
455	74664.524	-3205485.477	8.295	SL
456	74655.224	-3205500.896	6.304	SL
457	74651.711	-3205499.004	4.789	SL
458	74648.398	-3205497.697	4.761	SL
459	74643.742	-3205496.259	6.874	SL
460	74636.583	-3205512.233	2.808	SL
461	74638.027	-3205513.5	2.88	SL
462	74641.061	-3205520.341	5.712	SL
463	74626.309	-3205524.697	6.37	SL
464	74612.121	-3205527.217	6.851	SL
465	74599.144	-3205531.483	6.681	SL
466	74597.556	-3205528.257	5.87	SL
467	74608.665	-3205523.426	5.14	SL
468	74617.504	-3205520.921	4.108	SL
469	74630.792	-3205518.729	3.339	SL
470	74617.623	-3205516.919	6.104	SL
A	74392.38	-3204318.68	22.224	BRUG
A1	74916.597	-3205319.043	14.275	BRUG

Point	Y	X	Z	Tag
BASE	74828.895	-3205189.402	8.939	Base
CICIWE	78659.5	-3199153.59	111.9	Trig85
471	74596.141	-3205523.025	7.223	SL
472	74596.842	-3205525.588	6.013	SL
473	74597.913	-3205528.419	5.747	SL
474	74584.282	-3205536.84	4.694	SL
474a	74583.585	-3205535.281	4.575	SL
475	74562.688	-3205546.199	4.358	SL
476	74563.052	-3205542.976	6.104	SL
477	74564.684	-3205549.152	4.135	SL
478	74551.799	-3205559.897	3.37	SL
479	74549.262	-3205557.223	3.617	SL
480	74548.123	-3205555.862	4.602	SL
481	74536.252	-3205562.385	4.329	SL
482	74535.252	-3205560.135	5.596	SL
483	74537.239	-3205564.879	4.08	SL
484	74529.402	-3205567.759	4.875	SL
485	74524.591	-3205567.078	5.229	SL
486	74527.439	-3205563.501	5.087	SL
487	74522.528	-3205565.69	5.741	SL
488	74522.477	-3205567.353	5.679	SL
489	74522.773	-3205569.142	5.937	SL
490	74527.825	-3205569.457	5.278	SL
491	74526.427	-3205571.59	5.431	SL
492	74527.874	-3205574.117	5.594	SL
493	74528.093	-3205576.441	5.278	SL
494	74540.959	-3205565.603	3.685	SL
495	74538.042	-3205568.588	3.756	SL
496	74535.932	-3205569.166	3.8	SL
497	74532.789	-3205576.086	3.724	SL
498	74530.075	-3205579.176	3.85	SL
499	74526.959	-3205580.683	3.318	SL
500	74526.027	-3205580.811	3.105	RIVIER
501	74521.746	-3205580.957	3.099	RIVIER
502	74515.949	-3205580.235	3.075	RIVIER
503	74510.414	-3205580.718	3.064	RIVIER
504	74507.026	-3205580.914	3.075	RIVIER
505	74503.998	-3205579.851	3.062	RIVIER
506	74497.188	-3205582.668	3.021	RIVIER
507	74515.722	-3205578.487	3.696	RIVIER
508	74508.606	-3205578.797	3.627	RIVIER
509	74524.671	-3205581.967	3.104	RIVIER

Point	Y	X	Z	Tag
510	74519.165	-3205583.607	2.997	RIVIER
511	74512.808	-3205587.272	3.075	RIVIER
512	74508.885	-3205589.876	3.096	RIVIER
513	74505.967	-3205592.852	3.075	RIVIER
514	74502.829	-3205600.945	3.09	RIVIER
515	74498.578	-3205605.018	3.086	RIVIER
516	74494.182	-3205608.706	3.057	RIVIER
517	74492.588	-3205609.013	3.082	RIVIER
518	74492.751	-3205610.937	3.072	RIVIER
519	74485.721	-3205617.995	3.071	RIVIER
520	74477.786	-3205623.6	3.052	RIVIER
521	74474.16	-3205629.584	3.092	RIVIER
522	74463.839	-3205634.086	3.049	RIVIER
523	74474.008	-3205636.499	6.416	RIVIER
524	74478.106	-3205634.672	6.674	RIVIER
525	74479.579	-3205636.248	6.866	RIVIER
526	74485.466	-3205634.578	7.144	RIVIER
527	74488.86	-3205631.847	7.132	RIVIER
528	74487.042	-3205629.649	7.141	RIVIER
529	74483.795	-3205633.091	7.694	RIVIER
530	74481.876	-3205632.053	7.528	RIVIER
531	74481.419	-3205630.074	6.855	RIVIER
532	74482.966	-3205625.844	6.153	RIVIER
533	74490.468	-3205621.291	6.526	RIVIER
534	74495.762	-3205618.005	7.377	RIVIER
535	74500.33	-3205611.801	7.035	RIVIER
536	74504.402	-3205607.067	6.471	RIVIER
537	74508.186	-3205604.191	6.678	RIVIER
538	74510.012	-3205600.981	6.395	RIVIER
539	74509.648	-3205595.267	5.318	RIVIER
540	74515.208	-3205590.984	5.162	RIVIER
541	74520.717	-3205587.495	5.273	RIVIER
542	74525.429	-3205586.721	5.415	RIVIER
543	74527.965	-3205585.127	5.803	RIVIER
544	74533.125	-3205580.437	5.446	RIVIER
545	74538.951	-3205573.285	5.001	RIVIER
546	74544.135	-3205575.844	5.569	RIVIER
547	74560.122	-3205565.952	5.698	RIVIER
548	74570.613	-3205561.558	5.767	RIVIER
549	74581.67	-3205540.803	5.397	RIVIER
550	74591.688	-3205538.192	6.283	RIVIER
551	74600.507	-3205532.877	6.863	RIVIER

Point	Y	X	Z	Tag
552	74628.723	-3205571.109	4.503	SL
553	74655.257	-3205605.471	3.665	SL
554	74681.353	-3205635.782	2.308	SL
555	74697.919	-3205658.209	0.835	SL
556	74713.37	-3205683.297	-0.1	SL
557	74680.236	-3205709.253	-0.33	SL
558	74665.499	-3205688.088	0.469	SL
559	74645.038	-3205660.449	2.34	SL
560	74638.938	-3205652.027	3.113	SL
561	74617.717	-3205622.818	3.948	SL
562	74594.146	-3205593.658	4.594	SL
563	74577.242	-3205572.217	6.124	SL
564	74546.448	-3205597.23	6.431	SL
565	74569.528	-3205628.037	4.59	SL
566	74594.795	-3205660.047	3.781	SL
567	74608.58	-3205679.43	2.315	SL
568	74627.612	-3205706.184	0.648	SL
569	74644.692	-3205732.218	-0.381	SL
570	74613.455	-3205760.56	-0.503	SL
571	74596.016	-3205736.981	0.368	SL
572	74572.492	-3205703.877	2.121	SL
573	74548.609	-3205659.812	4.523	SL
574	74545.064	-3205626.408	5.753	SL
575	74544.992	-3205624.924	6.041	SL
576	74544.112	-3205625.229	6.106	SL
577	74542.934	-3205624.993	6.026	SL
578	74543.392	-3205626.155	6.015	SL
579	74521.636	-3205616.153	7.007	SL
580	74527.268	-3205608.609	7.115	SL
581	74520.132	-3205607.211	7.746	SL
582	74514.829	-3205610.132	7.609	SL
583	74515.661	-3205614.43	7.586	SL
584	74518.913	-3205612.76	7.995	SL
585	74516.996	-3205610.566	8.016	SL
586	74506.123	-3205618.777	7.427	SL
587	74504.718	-3205614.792	7.568	SL
588	74502.895	-3205613.37	7.532	SL
589	74499.09	-3205616.929	7.449	SL
590	74500.465	-3205620.297	7.533	SL
591	74502.264	-3205617.959	8.219	SL
592	74503.546	-3205616.926	8.318	SL
593	74491.835	-3205649.787	9.209	SL

Point	Y	X	Z	Tag
594	74510.658	-3205674.907	5.34	SL
595	74524.346	-3205697.223	4.257	SL
596	74531.093	-3205709.629	3.598	SL
597	74540.702	-3205724.331	2.27	SL
598	74561.636	-3205753.5	0.599	SL
599	74582.9	-3205784.331	-0.553	SL
600	74538.318	-3205790.967	-0.025	SL
601	74547.727	-3205808.358	-0.567	SL
602	74504.151	-3205751.126	2.241	SL
603	74485.69	-3205727.507	4.243	SL
604	74487.678	-3205710.901	4.8	SL
605	74488.69	-3205708.49	5.025	SL
606	74485.299	-3205708.62	5.116	SL
607	74485.896	-3205710.736	5.066	SL
608	74486.743	-3205710.121	5.287	SL
609	74468.965	-3205710.21	5.616	SL
610	74449.487	-3205684.964	10.919	SL
611	74448.514	-3205680.497	11.134	SL
612	74451.299	-3205677.024	11.277	SL
613	74455.987	-3205677.079	11.242	SL
614	74455.607	-3205682.603	10.729	SL
615	74453.706	-3205685.768	10.407	SL
616	74451.964	-3205680.532	12.748	SL
617	74464.085	-3205682.49	10.312	SL
618	74464.06	-3205677.554	10.691	SL
619	74466.617	-3205672.077	11.126	SL
620	74470.674	-3205672.566	10.834	SL
621	74472.655	-3205673.281	9.918	SL
622	74472.548	-3205676.889	10.058	SL
623	74468.942	-3205683.114	9.4	SL
624	74465.328	-3205684.062	9.794	SL
625	74466.106	-3205679.081	11.838	SL
626	74467.187	-3205676.549	12.32	SL
627	74468.318	-3205673.743	11.946	SL
628	74474.181	-3205680.022	9.547	SL
629	74480.113	-3205679.782	8.356	SL
630	74483.943	-3205675.126	8.653	SL
631	74483.913	-3205669.942	9.391	SL
632	74477.547	-3205669.954	10.057	SL
633	74479.915	-3205672.316	11.211	SL
634	74479.148	-3205673.592	11.771	SL
635	74477.533	-3205672.903	11.887	SL

Point	Y	X	Z	Tag
636	74478.065	-3205675.684	11.57	SL
637	74476.037	-3205676.243	11.609	SL
638	74412.324	-3205714.16	12.083	SL
639	74401.519	-3205714.922	13.359	SL
640	74399.662	-3205711.576	13.276	SL
641	74404.927	-3205705.495	14.311	SL
642	74412.116	-3205701.059	14.872	SL
643	74415.964	-3205694.217	14.526	SL
644	74417.317	-3205694.74	15.017	SL
645	74414.625	-3205700.243	15.113	SL
646	74416.777	-3205688.425	13.454	SL
647	74417.272	-3205684.623	12.257	SL
648	74421.836	-3205685.504	12.581	SL
649	74421.451	-3205687.897	12.756	SL
650	74418.9	-3205688.87	13.085	SL
651	74421.715	-3205692.823	12.625	SL
652	74418.674	-3205704.657	12.109	SL
653	74392.96	-3205691.188	3.096	SL
654	74412.019	-3205725.489	10.523	SL
655	74411.877	-3205728.165	10.131	SL
656	74414.049	-3205728.541	9.656	SL
657	74414.758	-3205726.29	10.005	SL
658	74412.813	-3205726.72	10.586	SL
659	74426.117	-3205728.139	8.345	SL
660	74426.909	-3205730.131	7.963	SL
661	74429.391	-3205729.507	7.802	SL
662	74433.086	-3205729.772	7.284	SL
663	74435.999	-3205728.696	7.041	SL
664	74436.615	-3205725.013	7.533	SL
665	74433.192	-3205725.706	8.044	SL
666	74429.19	-3205725.995	8.546	SL
667	74433.488	-3205727.132	8.036	SL
668	74430.311	-3205726.839	8.45	SL
669	74427.719	-3205727.652	8.598	SL
670	74434.007	-3205718.914	8.688	SL
671	74435.025	-3205714.83	9.138	SL
672	74432.392	-3205717.047	9.257	SL
673	74432.227	-3205719.067	8.958	SL
674	74432.868	-3205718.287	9.257	SL
675	74430.456	-3205710.898	10.108	SL
676	74430.087	-3205707.571	10.614	SL
677	74431.875	-3205705.95	10.752	SL

Point	Y	X	Z	Tag
678	74434.035	-3205706.735	10.235	SL
679	74432.753	-3205708.922	10.114	SL
680	74431.078	-3205708.985	10.707	SL
681	74432.148	-3205707.301	10.877	SL
682	74437.335	-3205715.497	8.741	SL
683	74439.162	-3205715.611	8.383	SL
684	74439.935	-3205712.381	8.671	SL
685	74437.632	-3205713.531	8.889	SL
686	74438.135	-3205714.467	8.967	SL
687	74446.323	-3205714.553	7.796	SL
688	74448.798	-3205714.429	7.482	SL
689	74450.278	-3205713.39	7.462	SL
690	74450.58	-3205710.051	7.923	SL
691	74447.347	-3205711.884	7.837	SL
692	74447.703	-3205712.806	8.44	SL
693	74457.329	-3205720.745	5.56	SL
694	74445.085	-3205732.787	5.562	SL
695	74470.417	-3205760.649	3.634	SL
696	74480.125	-3205775.284	2.047	SL
697	74500.913	-3205798.879	0.529	SL
698	74522.049	-3205828.524	-0.608	SL

Umlalazi Coordinates

October 2016

Point	Y	X	Z	Tag
1	74863.6012	-3205362.926	39.2963	
2	74855.7758	-3205352.844	41.2219	D
3	74860.0885	-3205358.485	39.853	D
4	74867.896	-3205368.211	38.8564	D
5	74875.3502	-3205377.491	36.1241	D
6	74885.3316	-3205389.898	33.3096	D
7	74891.4717	-3205395.826	32.4305	D
8	74895.9158	-3205399.93	31.578	D
9	74908.0722	-3205412.559	30.2393	D
10	74929.6921	-3205436.401	29.6864	D
11	74937.7601	-3205445.16	29.2313	D
12	74959.3385	-3205472.568	26.8159	D
13	74935.8674	-3205502.329	26.1484	D
14	74927.6524	-3205493.813	26.7156	D
15	74905.0238	-3205468.624	28.9316	D
16	74882.7174	-3205443.658	30.0303	D

Point	Y	X	Z	Tag
17	74866.1286	-3205419.253	31.331	D
18	74864.6187	-3205417.96	32.000	D
19	74863.862	-3205416.63	31.876	D
20	74867.0885	-3205412.742	32.4047	D
21	74870.8031	-3205409.555	32.2653	D
22	74872.9249	-3205408.049	32.7712	D
23	74874.8003	-3205407.174	32.1409	D
24	74877.0522	-3205406.581	32.5503	D
25	74879.4004	-3205403.847	32.2041	D
26	74875.3973	-3205398.88	32.7581	D
27	74877.0218	-3205395.103	33.1074	D
28	74875.6467	-3205394.864	33.5814	D
29	74873.7182	-3205397.125	33.9607	D
30	74872.8202	-3205396.844	33.5077	D
31	74862.7157	-3205391.482	34.5746	D
32	74857.0065	-3205390.738	36.2214	D
33	74858.0014	-3205388.149	36.7632	D
34	74858.6933	-3205384.626	37.4905	D
35	74848.8488	-3205382.177	37.5845	D
36	74844.5516	-3205385.228	37.3998	D
37	74845.5702	-3205386.177	37.6272	D
38	74841.9787	-3205393.988	36.2425	D
39	74843.8811	-3205395.264	36.3085	D
40	74841.8337	-3205396.843	35.7486	D
41	74838.7642	-3205400.451	34.1674	D
42	74837.4319	-3205397.182	34.3744	D
43	74840.2025	-3205396.115	35.0657	D
44	74838.9068	-3205395.598	35.4915	D
45	74840.2402	-3205392.202	35.6238	D
46	74841.2186	-3205389.366	36.7617	D
47	74841.4277	-3205386.642	36.8155	D
48	74839.7257	-3205386.173	36.1503	D
49	74831.1935	-3205377.841	36.1363	D
50	74840.3959	-3205358.379	39.3299	D
51	74832.509	-3205351.536	40.1791	D
52	74826.5751	-3205342.948	42.6058	D
53	74822.5396	-3205339.396	42.3058	D
54	74819.3312	-3205336.41	43.4577	D
55	74812.5938	-3205329.229	44.7711	D
56	74806.8469	-3205324.572	44.8235	D
57	74798.7807	-3205314.72	46.7878	D
58	74803.2256	-3205305.823	46.7292	D

Point	Y	X	Z	Tag
59	74806.3755	-3205298.865	46.3584	D
60	74810.0802	-3205298.97	46.5885	D
61	74815.3835	-3205288.414	45.4757	D
62	74818.3287	-3205285.382	44.5212	D
63	74819.777	-3205286.697	44.4147	D
64	74817.8254	-3205292.775	45.3304	D
65	74814.3539	-3205307.07	44.7209	D
66	74813.1556	-3205320.664	45.3425	D
67	74817.1623	-3205324.393	45.1793	D
68	74835.8904	-3205312.779	43.1725	D
69	74844.91	-3205303.469	43.3899	D
70	74854.6219	-3205307.256	43.1721	D
71	74856.7285	-3205319.565	45.1929	D
72	74847.0216	-3205321.607	45.0247	D
73	74848.6629	-3205336.995	43.8251	D
74	74851.2949	-3205337.454	42.9093	D
75	74854.1098	-3205341.473	42.0946	D
76	74843.3267	-3205340.732	41.8964	D
77	74837.5027	-3205340.534	40.9674	D
78	74831.1739	-3205336.032	42.4765	D
79	74830.6158	-3205367.6	39.2613	D
80	74827.5423	-3205371.017	39.3149	D
81	74824.694	-3205373.287	39.4366	D
82	74822.4125	-3205375.438	39.2709	D
83	74819.3908	-3205376.076	39.7285	D
84	74812.8417	-3205377.47	39.7938	D
85	74815.5137	-3205373.11	40.3653	D
86	74819.0629	-3205369.598	40.0056	D
87	74822.022	-3205364.755	40.7382	D
88	74817.9466	-3205363.049	41.856	D
89	74814.9831	-3205367.9	41.5929	D
90	74811.3203	-3205371.342	41.1012	D
91	74810.7781	-3205369.986	40.7086	D
92	74810.0822	-3205369.009	40.7078	D
93	74813.8559	-3205363.464	41.2316	D
94	74815.5754	-3205363.839	41.3107	D
95	74813.8097	-3205362.182	41.3882	D
96	74812.7339	-3205363.799	41.6746	D
97	74810.9249	-3205366.526	41.2402	D
98	74808.6126	-3205368.62	41.3471	D
99	74806.171	-3205372.555	40.6274	D
100	74804.7247	-3205371.551	39.8644	D

Point	Y	X	Z	Tag
101	74807.0521	-3205367.271	40.2596	D
102	74807.0594	-3205366.235	40.3707	D
103	74806.7111	-3205363.302	40.6512	D
104	74809.5506	-3205360.739	41.0927	D
105	74810.9121	-3205361.177	41.3231	D
106	74808.6378	-3205363.445	41.5775	D
107	74802.4202	-3205362.55	40.5617	D
108	74794.1677	-3205359.909	40.5377	D
109	74788.6766	-3205354.928	42.641	D
110	74778.7116	-3205340.59	44.575	D
111	74765.5091	-3205345.34	44.7198	D
112	74763.8057	-3205355.639	43.9374	D
113	74781.4726	-3205361.126	41.6263	D
114	74777.3517	-3205369.83	40.5507	D
115	74778.2431	-3205378.352	38.8479	D
116	74780.875	-3205373.892	41.8504	D
117	74783.2308	-3205380.978	37.2658	D
118	74789.1057	-3205372.492	38.7027	D
119	74791.3989	-3205363.997	39.8768	D
120	74801.8613	-3205398.864	36.155	D
121	74806.3932	-3205403.24	35.1709	D
122	74811.6286	-3205408.342	35.408	D
123	74810.8024	-3205410.896	34.4511	D
124	74814.1863	-3205409.81	33.9585	D
125	74814.8655	-3205407.333	34.2132	D
126	74812.1171	-3205406.406	35.0424	D
127	74800.8394	-3205406.925	35.2499	D
128	74801.0727	-3205402.476	35.6851	D
129	74797.9262	-3205404.739	35.6079	D
130	74798.9843	-3205405.759	36.1042	D
131	74795.6404	-3205407.611	35.58	D
132	74795.9687	-3205408.944	35.6632	D
133	74798.3177	-3205409.323	35.5297	D
134	74797.2681	-3205407.86	36.0214	D
135	74790.351	-3205399.542	35.1285	D
136	74780.2987	-3205401.075	35.6632	D
137	74773.0172	-3205401.583	37.1927	D
138	74768.1455	-3205399.564	38.0911	D
139	74765.5566	-3205395.266	38.5676	D
140	74765.0048	-3205388.163	38.6223	D
141	74770.0763	-3205381.736	38.353	D
142	74769.4141	-3205389.021	36.933	D

Point	Y	X	Z	Tag
143	74769.3355	-3205393.217	36.1681	D
144	74772.0429	-3205396.557	35.2177	D
145	74777.4046	-3205398.714	34.5466	D
146	74781.58	-3205399.109	34.5473	D
147	74785.563	-3205399.283	34.824	D
148	74781.6189	-3205397.07	34.5843	D
149	74783.1445	-3205393.482	34.8699	D
150	74781.856	-3205390.009	35.3223	D
151	74777.3418	-3205388.439	35.9147	D
152	74773.4559	-3205390.946	35.8379	D
153	74771.6726	-3205395.283	35.387	D
154	74795.9866	-3205413.002	35.5626	D
155	74814.8197	-3205434.156	32.6904	D
156	74821.9623	-3205441.63	32.6395	D
157	74825.2883	-3205445.399	31.693	D
158	74838.101	-3205461.035	30.6224	D
159	74837.2334	-3205463.493	30.7481	D
160	74835.9857	-3205463.592	30.4475	D
161	74836.581	-3205465.034	30.3521	D
162	74838.5575	-3205464.19	30.2504	D
163	74854.2393	-3205483.517	29.4159	D
164	74865.7084	-3205503.262	28.3433	D
165	74886.9597	-3205530.121	26.2517	D
166	74898.535	-3205547.509	25.5414	D
167	74855.7713	-3205565.861	25.6447	D
168	74838.9004	-3205547.91	26.661	D
169	74820.5742	-3205519.05	29.0629	D
170	74795.4303	-3205469.123	31.5295	D
171	74808.0398	-3205473.33	30.4214	D
172	74814.2881	-3205460.59	31.2243	D
173	74821.2067	-3205450.687	31.6093	D
174	74825.199	-3205443.899	31.8628	D
175	74822.9061	-3205439.508	32.5731	D
176	74815.5471	-3205440.372	32.8072	D
177	74811.4874	-3205445.069	32.6704	D
178	74812.8732	-3205449.734	32.6952	D
179	74807.7342	-3205457.348	32.5965	D
180	74800.5108	-3205450.851	33.2515	D
181	74797.776	-3205449.076	32.9929	D
182	74792.3168	-3205455.437	32.5952	D
183	74794.1696	-3205459.74	32.7951	D
184	74791.9534	-3205464.994	31.9357	D

Point	Y	X	Z	Tag
185	74772.4629	-3205449.18	33.3761	D
186	74746.9931	-3205426.344	37.8667	D
187	74728.9762	-3205411.589	42.6803	D
188	74703.2857	-3205435.717	40.9015	D
189	74715.2825	-3205450.316	36.4455	D
190	74731.8257	-3205469.11	32.3214	D
191	74729.9006	-3205471.096	32.0269	D
192	74729.8801	-3205472.679	31.9223	D
193	74730.4932	-3205472.202	32.3753	D
194	74731.6036	-3205472.856	31.5818	D
195	74750.9066	-3205491.435	29.5691	D
196	74777.5869	-3205522.075	29.3937	D
197	74795.536	-3205544.742	28.7199	D
198	74812.2496	-3205570.146	26.383	D
199	74823.9653	-3205588.956	25.508	D
200	74786.9649	-3205608.983	25.5432	D
201	74773.632	-3205594.255	26.3407	D
202	74753.1498	-3205565.227	28.9299	D
203	74728.7608	-3205531.867	29.0437	D
204	74689.1969	-3205482.566	30.9121	D
205	74676.607	-3205468.811	36.4593	D
206	74663.6036	-3205457.157	41.2637	D
207	74654.7719	-3205492.764	31.7658	D
208	74648.3384	-3205494.578	31.9615	D
209	74643.9646	-3205497.377	31.682	D
210	74655.6999	-3205501.73	31.2212	D
211	74646.4001	-3205513.177	30.6458	D
212	74633.3708	-3205521.784	30.2258	D
213	74618.3244	-3205524.357	30.4709	D
214	74601.2712	-3205524.246	31.0324	D
215	74610.1322	-3205523.101	30.2096	D
216	74610.1114	-3205521.505	31.0097	D
217	74615.6703	-3205521.612	29.5493	D
218	74615.8939	-3205519.497	30.5947	D
219	74624.5942	-3205520.089	28.5163	D
220	74623.983	-3205517.136	30.0386	D
221	74632.4882	-3205517.22	27.9476	D
222	74631.9584	-3205515.715	29.1771	D
223	74639.0387	-3205510.284	27.8309	D
224	74638.3348	-3205508.013	29.1251	D
225	74645.2766	-3205504.904	28.6086	D
226	74643.9571	-3205499.923	30.6016	D

Point	Y	X	Z	Tag
227	74652.7538	-3205495.936	30.9424	D
228	74641.4883	-3205501.912	30.5882	D
229	74673.1952	-3205530.299	29.828	D
230	74691.6905	-3205552.195	29.0334	D
231	74706.9969	-3205572.84	28.996	D
232	74722.9746	-3205593.138	28.4701	D
233	74742.2365	-3205614.091	26.4004	D
234	74758.311	-3205635.07	25.4016	D
235	74721.7422	-3205661.821	25.5059	D
236	74699.6665	-3205636.113	26.811	D
237	74680.1316	-3205612.62	28.8417	D
238	74639.2974	-3205562.021	29.7777	D
239	74618.4729	-3205538.797	31.6064	D
240	74612.4305	-3205532.452	31.0398	D
241	74578.7656	-3205539.688	29.672	D
242	74569.5108	-3205544.059	29.6651	D
243	74564.7451	-3205546.154	29.7375	D
244	74569.6321	-3205549.553	30.1833	D
245	74576.4203	-3205558.32	31.3133	D
246	74596.5641	-3205586.133	30.2305	D
247	74614.7437	-3205610.877	29.4295	D
248	74632.6669	-3205635.876	29.1337	D
249	74638.1576	-3205644.405	28.7497	D
250	74653.2164	-3205666.176	26.8204	D
251	74671.678	-3205699.339	25.4379	D
252	74633.9113	-3205713.381	25.5206	D
253	74617.8667	-3205687.939	26.872	D
254	74606.7461	-3205671.18	28.3739	D
255	74575.512	-3205638.129	29.9599	D
256	74555.2805	-3205613.666	30.7469	D
257	74541.6912	-3205598.105	31.8779	D
258	74529.7201	-3205583.903	30.9167	D
259	74527.1653	-3205580.93	28.8296	RIVER
260	74509.366	-3205588.148	28.2294	RIVER
261	74503.6909	-3205588.711	28.2386	RIVER
262	74501.2534	-3205591.136	28.2542	RIVER
263	74503.8333	-3205593.119	28.2506	RIVER
264	74504.63	-3205590.624	28.9706	RIVER
265	74506.8018	-3205592.041	28.6526	RIVER
266	74503.2634	-3205598.653	28.2182	RIVER
267	74501.1916	-3205602.755	28.2599	RIVER
268	74508.8316	-3205610.913	32.6704	D

Point	Y	X	Z	Tag
269	74517.3152	-3205620.127	32.9524	D
270	74538.3103	-3205649.412	30.7414	D
271	74559.8718	-3205675.448	29.5189	D
272	74573.7368	-3205693.464	28.4559	D
273	74585.773	-3205710.2	26.6668	D
274	74602.1925	-3205736.77	25.2998	D
275	74570.1084	-3205759.09	25.162	D
276	74555.7922	-3205739.314	26.1245	D
277	74534.2291	-3205713.377	28.9861	D
278	74507.1412	-3205680.92	30.8849	D
279	74486.0118	-3205661.907	35.3303	D
280	74483.5828	-3205659.656	34.7385	D
281	74479.1673	-3205656.215	35.5041	D
282	74486.4142	-3205653.39	33.9647	D
283	74493.0731	-3205645.623	33.1973	D
284	74498.6774	-3205639.938	33.1675	D
285	74500.0249	-3205632.42	32.939	D
286	74492.7312	-3205633.288	32.8573	D
287	74482.3533	-3205643.578	33.5139	D
288	74483.8729	-3205648.188	33.448	D
289	74476.5394	-3205653.156	35.3803	D
290	74467.587	-3205646.35	34.3513	D
291	74461.0687	-3205637.415	28.1458	D
292	74438.2744	-3205670.019	37.2844	D
293	74448.5028	-3205680.43	37.0527	D
294	74450.4857	-3205684.806	36.7549	D
295	74454.6407	-3205683.109	36.4763	D
296	74455.5704	-3205679.329	36.8096	D
297	74455.6181	-3205672.852	37.1923	D
298	74450.8574	-3205677.018	37.2524	D
299	74453.3066	-3205676.836	37.6847	D
300	74452.6636	-3205678.337	37.7413	D
301	74451.7494	-3205680.232	38.4026	D
302	74463.1317	-3205678.842	36.4376	D
303	74464.4093	-3205682.725	35.9716	D
304	74467.9629	-3205682.892	35.4015	D
305	74472.6589	-3205681.388	35.0133	D
306	74472.9614	-3205679.098	35.6478	D
307	74472.914	-3205674.251	35.8706	D
308	74474.7924	-3205667.781	36.0407	D
309	74477.4706	-3205663.045	35.8113	D
310	74475.3511	-3205661.562	36.2985	D

Point	Y	X	Z	Tag
311	74470.5957	-3205666.524	36.744	D
312	74471.6168	-3205667.79	36.9029	D
313	74469.6757	-3205671.77	37.2684	D
314	74467.01	-3205671.391	36.9472	D
315	74464.113	-3205675.939	36.7376	D
316	74466.5664	-3205678.431	37.6451	D
317	74467.0228	-3205676.087	37.844	D
318	74468.7042	-3205676.239	37.9078	D
319	74469.2752	-3205674.43	37.8939	D
320	74467.9401	-3205673.734	37.8116	D
321	74477.1311	-3205668.709	36.1994	D
322	74482.8572	-3205668.749	35.7661	D
323	74485.2169	-3205671.871	34.6234	D
324	74481.2129	-3205679.377	33.8486	D
325	74475.2292	-3205682.332	34.344	D
326	74474.8924	-3205676.901	37.404	D
327	74476.2771	-3205673.45	37.7745	D
328	74478.8808	-3205673.445	37.3918	D
329	74477.8022	-3205675.494	37.2699	D
330	74476.689	-3205675.703	37.3	D
331	74461.7987	-3205695.217	34.1634	D
332	74458.397	-3205697.847	34.2863	D
333	74457.9572	-3205699.706	34.1923	D
334	74460.0318	-3205700.94	33.7723	D
335	74462.0213	-3205700.392	33.3216	D
336	74463.1425	-3205695.871	33.7427	D
337	74462.2959	-3205694.519	34.1126	D
338	74460.868	-3205697.598	34.389	D
339	74460.673	-3205699.448	34.2744	D
340	74459.2614	-3205699.232	34.404	D
341	74458.6271	-3205698.572	34.5191	D
342	74459.6745	-3205698.083	34.3845	D
343	74476.0925	-3205712.019	30.7396	D
344	74491.0506	-3205730.354	29.6588	D
345	74505.9376	-3205747.453	28.2585	D
346	74518.1953	-3205760.125	26.7049	D
347	74536.516	-3205778.986	25.3469	D
348	74518.3726	-3205793.684	25.4686	D
349	74506.4535	-3205778.627	26.3133	D
350	74485.5919	-3205758.415	28.7443	D
351	74453.3622	-3205723.826	31.3585	D
352	74456.95	-3205720.764	31.2913	POLE

Point	Y	X	Z	Tag
353	74446.2602	-3205714.688	33.4558	D
354	74448.7314	-3205713.865	33.1986	D
355	74449.8716	-3205709.818	33.645	D
356	74447.833	-3205710.885	33.7133	D
357	74446.0678	-3205713.003	33.5925	D
358	74447.2362	-3205713.289	33.9681	D
359	74448.3873	-3205711.918	33.8098	D
360	74431.9692	-3205700.874	36.5338	D
361	74420.6987	-3205688.935	38.23	D
362	74418.0327	-3205687.028	38.6702	D
363	74871.0816	-3205354.38	38.9046	D
364	74878.6177	-3205348.812	37.0687	D
365	74900.0421	-3205332.587	37.7653	D
366	74913.7268	-3205351.634	35.7899	D
367	74934.3455	-3205380.493	31.6922	D
368	74957.1608	-3205411.665	29.6572	D
369	74978.237	-3205437.157	28.4482	D
370	74994.1765	-3205455.655	26.3394	D
371	75003.2625	-3205469.359	25.4657	D
372	75009.1961	-3205480.247	25.0049	D
373	75044.656	-3205450.748	24.9941	D
374	75031.124	-3205434.329	25.9674	D
375	75011.8152	-3205413.277	28.478	D
376	74990.0339	-3205385.497	29.8574	D
377	74964.3087	-3205354.027	32.3366	D
378	74937.3612	-3205324.202	37.8633	D
379	74917.056	-3205295.235	40.3473	D
380	74913.9663	-3205293.005	40.3511	D
381	74915.9817	-3205280.809	42.3823	D
382	74919.2317	-3205280.501	42.3944	D
383	74910.3713	-3205273.954	45.3661	D
384	74924.5765	-3205265.834	45.6654	D
385	74923.0996	-3205275.459	44.3226	D
386	74925.9806	-3205279.382	43.679	D
387	74928.678	-3205284.7	43.0931	D
388	74929.9925	-3205287.47	42.627	D
389	74931.6103	-3205290.6	42.2377	D
390	74935.2771	-3205294.101	41.9047	D
391	74941.2942	-3205281.385	43.2405	D
392	74941.2767	-3205284.498	42.7806	D
393	74942.6048	-3205287.745	42.5124	D
394	74947.8668	-3205290.788	41.7482	D

Point	Y	X	Z	Tag
395	74954.8955	-3205290.644	40.2247	D
396	74948.9859	-3205290.017	41.163	D
397	74945.3861	-3205287.737	41.589	D
398	74943.5837	-3205285.239	41.8238	D
399	74943.6831	-3205282.533	42.4484	D
400	74957.8586	-3205283.812	40.2046	D
401	74958.0502	-3205275.461	42.2118	D
402	74959.0925	-3205266.1	43.721	D
403	74966.2018	-3205250.237	45.6235	D
404	74973.5003	-3205232.42	47.3385	D
405	74975.9819	-3205229.292	47.4539	D
406	74979.7304	-3205219.862	47.457	D
407	74977.9643	-3205216.275	47.4183	D
408	74972.3591	-3205211.699	45.7803	D
409	74960.9539	-3205218.454	45.8763	D
410	74950.8833	-3205227.174	45.3254	D
411	74944.4964	-3205237.649	45.5023	D
412	74941.8787	-3205249.008	46.1877	D
413	74930.7213	-3205257.873	46.4361	D
414	74938.9648	-3205260.069	45.4048	D
415	74943.9859	-3205257.89	45.4532	D
416	74949.7904	-3205253.37	44.8745	D
417	74966.4199	-3205241.288	46.8333	D
418	74961.0419	-3205252.481	45.6291	D
419	74953.35	-3205269.019	45.709	D
420	74949.8111	-3205261.11	43.4951	D
421	74945.6979	-3205265.184	42.688	D
422	74941.8	-3205270.255	42.3696	D
423	74964.028	-3205289.654	38.8824	D
424	74977.8072	-3205269.077	40.7684	D
425	74983.3475	-3205253.136	42.9525	D
426	74983.7703	-3205253.101	42.9664	D
427	74983.2394	-3205232.289	44.9916	D
428	74984.7291	-3205221.877	45.5318	D
429	74994.6152	-3205207.756	45.0705	D
430	75000.2347	-3205198.038	44.2081	D
431	75014.0821	-3205189.478	44.2942	D
432	75025.6276	-3205191.244	44.4167	D
433	75014.406	-3205198.64	44.0947	D
434	75012.9537	-3205207.852	45.0897	D
435	75017.5022	-3205214.888	45.0522	D
436	75014.7774	-3205222.24	45.0529	D

Point	Y	X	Z	Tag
437	75007.9029	-3205234.326	44.4188	D
438	74998.5882	-3205230.471	44.6157	D
439	74995.0963	-3205219.282	44.9469	D
440	74999.7574	-3205213.915	45.0879	D
441	75011.0949	-3205207.733	45.0724	D
442	74997.6079	-3205208	44.7361	D
443	75005.7554	-3205203.461	44.5078	D
444	75014.8617	-3205199.126	44.0801	D
445	75030.9161	-3205198.809	43.6782	D
446	75031.0182	-3205217.598	43.9857	D
447	75018.4199	-3205235.085	43.9533	D
448	75011.14	-3205247.188	42.7113	D
449	75009.1508	-3205262.524	42.2677	D
450	75015.3742	-3205265.452	41.1603	D
451	75018.9191	-3205264.197	40.5953	D
452	75021.2304	-3205259.512	40.6673	D
453	75021.0482	-3205254.092	42.3898	D
454	75020.6176	-3205251.032	43.8096	D
455	75020.4636	-3205241.857	45.719	D
456	75018.5552	-3205244.731	46.1114	D
457	75023.5396	-3205238.678	45.0535	D
458	75028.2641	-3205241.913	45.522	D
459	75034.7149	-3205239.393	43.708	D
460	75030.2661	-3205251.608	42.0017	D
461	75024.6162	-3205257.736	41.328	D
462	75038.2137	-3205283.591	36.6613	D
463	75052.4349	-3205302.888	32.4086	D
464	75075.0391	-3205336.339	30.0558	D
465	75095.0248	-3205364.224	28.687	BATH
466	75099.8419	-3205372.675	27.6575	D
467	75113.4006	-3205391.894	25.7271	D
468	75077.4318	-3205411.123	25.6915	D
469	75068.5637	-3205387.645	27.8561	D
470	75040.7216	-3205356.221	29.9394	D
471	75006.8587	-3205323.395	33.0363	D
472	74991.6905	-3205309.281	36.8761	D
473	74977.7243	-3205293.775	38.5995	D
474	75049.2307	-3205207.951	45.3246	D
475	75060.9562	-3205218.307	45.2346	D
476	75070.389	-3205220.994	44.7556	D
477	75074.043	-3205221.403	45.6702	D
478	75074.8818	-3205210.267	45.6151	D

Point	Y	X	Z	Tag
479	75081.2096	-3205190.525	45.5582	D
480	75069.9627	-3205190.35	46.1672	D
481	75059.4993	-3205184.108	45.6117	D
482	75054.5939	-3205173.527	43.1661	D
483	75044.7787	-3205176.985	43.7535	D
484	75039.0317	-3205181.959	44.302	D
485	75033.1748	-3205188.252	44.9252	D
486	75036.4776	-3205192.452	43.846	D
487	75042.6304	-3205198.626	44.2829	D
488	75048.4747	-3205186.605	44.3023	D
489	75055.1124	-3205191.598	45.8186	D
490	75050.8633	-3205207.025	45.4156	D
491	75077.5366	-3205241.305	40.2116	D
492	75099.2497	-3205279.046	32.9515	D
493	75129.9557	-3205323.074	29.3138	D
494	75146.3594	-3205348.213	27.86	D
495	75156.6964	-3205364.096	26.0286	D
496	75160.9442	-3205371.86	25.4954	D
497	75204.2389	-3205350.184	25.6648	D
498	75198.248	-3205335.69	26.726	D
499	75188.1262	-3205320.058	28.7204	D
500	75158.6981	-3205276.189	31.1441	D
501	75137.9214	-3205248.123	34.655	D
502	75113.8954	-3205215.132	41.3869	D
503	75092.1316	-3205180.192	43.7263	D

Umlalazi Coordinates

March 2016

Point	Y	X	Z
1	-74893.537	3205352.013	11.397
2	-74959.633	3205218.739	20.816
3	-74963.867	3205217.971	21.457
4	-74968.768	3205217.238	21.988
5	-74975.067	3205217.303	21.782
6	-74978.741	3205217.947	21.221
7	-74979.074	3205221.891	21.464
8	-74978.782	3205225.015	21.764
9	-74967.344	3205224.07	22.786
10	-74966.667	3205209.936	17.341
11	-74971.698	3205209.438	17.346
12	-74985.191	3205219.146	20.146
13	-74988.893	3205214.136	19.997

Point	Y	X	Z
14	-74995.79	3205206.058	19.436
15	-74998.073	3205213.359	19.832
16	-75000.852	3205198.578	18.843
17	-75006.245	3205205.301	19.404
18	-75007.823	3205196.405	18.865
19	-74998.228	3205197.744	17.405
20	-74992.027	3205206.104	17.692
21	-75009.775	3205190.492	18.467
22	-75017.457	3205197.414	18.844
23	-75029.974	3205185.467	19.486
24	-75029.343	3205184.467	18.814
25	-75038.421	3205182.811	19.101
26	-75038.897	3205179.267	17.094
27	-75042.563	3205180.561	18.939
28	-75047.626	3205179.409	18.859
29	-75047.636	3205175.7	16.797
30	-75054.327	3205174.824	15.178
31	-75057.972	3205177.946	15.385
32	-75059.873	3205184.671	17.119
33	-75066.093	3205189.122	17.723
34	-75072.256	3205192.527	18.364
35	-75077.665	3205193.593	18.463
36	-75072.617	3205195.538	19.993
37	-75066.952	3205195.699	21.173
38	-75061.231	3205193.858	21.355
39	-75066.262	3205201.575	21.435
40	-75059.654	3205207.592	21.285
41	-75050.496	3205214.364	20.328
42	-75045.347	3205208.62	20.331
43	-75040.938	3205221.501	19.48
44	-75055.842	3205222.319	19.86
45	-75068.229	3205214.869	20.552
46	-75073.488	3205210.918	20.427
47	-75078.016	3205211.236	18.981
48	-75080.692	3205203.11	18.646
49	-75057.196	3205189.46	20.319
50	-75054.695	3205183.275	18.909
51	-75050.573	3205180.065	18.923
52	-75045.903	3205189.007	19.596
53	-75033.046	3205199.762	18.412
54	-75020.372	3205209.047	18.671
55	-75003.766	3205220.76	18.918

Point	Y	X	Z
56	-74983.058	3205235.642	19.704
57	-74978.091	3205229.501	20.468
58	-74975.189	3205225.485	21.681
59	-74971.686	3205219.813	22.533
60	-74967.726	3205217.558	22.07
61	-74964.83	3205216.349	20.681
62	-74987.706	3205246.808	18.42
63	-74995.821	3205257.278	17.77
64	-75013.428	3205280.202	13.464
65	-75027.363	3205299.159	9.866
66	-75036.414	3205311.539	7.58
67	-75046.014	3205325.597	5.506
68	-75058.559	3205343.944	4.527
69	-75071.796	3205363.314	3.755
70	-75081.192	3205376.964	3.142
71	-75088.501	3205386.77	2.366
72	-75097.377	3205400.762	0.996
73	-75101.367	3205408.515	0.52
74	-75095.198	3205363.911	3.292
75	-75215.098	3205353.59	0.911
76	-75210.463	3205347.34	1.549
77	-75200.257	3205334.157	3.59
78	-75191.423	3205320.006	3.443
79	-75178.845	3205297.328	4.165
80	-75166.786	3205276.922	5.777
81	-75158.495	3205260.29	6.731
82	-75146.418	3205239.402	10.844
83	-75135.095	3205217.363	15.984
84	-75124.722	3205198.005	19.694
85	-75117.446	3205180.574	22.359
86	-75116.189	3205165.507	21.984
87	-75114.19	3205161.708	19.141
88	-75110.891	3205169.05	21.438
89	-75106.536	3205173.176	20.613
90	-75111.909	3205184.696	21.838
91	-75101.186	3205179.549	20.082
92	-75099.424	3205176.671	18.325
93	-75088.96	3205186.026	17.977
94	-75086.01	3205182.461	15.098
95	-75091.764	3205196.977	18.711
96	-75097.14	3205207.965	17.398
97	-75122.976	3205161.327	20.466

Point	Y	X	Z
98	-75131.019	3205158.769	20.717
99	-75134.508	3205164.967	20.882
100	-75137.675	3205170.42	20.261
101	-75127.427	3205173.86	20.398
102	-75126.547	3205155.552	17.76
103	-75145.093	3205154.231	20.559
104	-75147.286	3205158.781	20.664
105	-75150.588	3205163.687	20.008
106	-75162.196	3205154.674	20.038
107	-75160.294	3205146.446	20.265
108	-75167.329	3205143.42	19.766
109	-75165.236	3205151.968	19.97
110	-75155.918	3205147.107	19.636
111	-75155.692	3205148.589	20.469
112	-75092.023	3205205.027	17.664
113	-75098.065	3205218.371	15.835
114	-75104.62	3205232.249	14.188
115	-75115.97	3205244.821	12.078
116	-75128.114	3205252.838	9.902
117	-75153.91	3205270.545	5.884
118	-75158.244	3205285.362	5.161
119	-75168.092	3205305.495	3.726
120	-75179.918	3205324.867	3.17
121	-75186.982	3205338.351	3.171
122	-75192.865	3205349.258	1.703
123	-75197.66	3205356.233	0.923
124	-75154.969	3205370.861	1.338
125	-75151.531	3205365.103	1.859
126	-75145.753	3205352.874	3.025
127	-75132.517	3205333.505	3.561
128	-75069.88	3205242.124	15.617
129	-75066.543	3205230.424	18.245
130	-75063.148	3205219.048	20.274
131	-75052.609	3205223.579	19.548
132	-75050.882	3205237.49	16.831
133	-75049.938	3205246.166	14.907
134	-75041.763	3205253.828	14.416
135	-75047.514	3205265.402	13.287
136	-75058.04	3205198.27	21.5
137	-74803.275	3205310.705	21.219
138	-74810.38	3205320.574	19.455
139	-74815.397	3205328.514	19.093

Point	Y	X	Z
140	-74823.446	3205339.834	16.564
141	-74827.349	3205346.014	16.293
142	-74836.121	3205359.305	13.236
143	-74840.551	3205366.306	13.75
144	-74854.838	3205386.747	10.97
145	-74856.928	3205391.196	10.296
146	-74862.694	3205401.075	7.419
147	-74868.231	3205411.865	6.598
148	-74877.98	3205427.936	4.394
149	-74888.9	3205446.677	3.984
150	-74899.599	3205465.631	3.51
151	-74910.398	3205487.134	3.024
152	-74918.936	3205504.077	1.383
153	-74926.92	3205519.13	0.309
154	-74935.821	3205536.331	-0.403
155	-74937.23	3205539.945	-0.586
156	-74766.663	3205345.304	18.996
157	-74754.242	3205369.08	17.608
158	-74749.434	3205378.446	17.819
159	-74737.903	3205400.514	16.613
160	-74725.973	3205413.848	16.361
161	-74704.326	3205416.695	19.762
162	-74706.056	3205421.1	19.208
163	-74711.845	3205432.124	15.477
164	-74721.884	3205451.058	10.711
165	-74732.534	3205469.63	7.165
166	-74740.599	3205487.605	4.691
167	-74753.209	3205508.228	3.248
168	-74763.991	3205528.318	3.407
169	-74773.717	3205547.381	3.541
170	-74778.207	3205555.85	3.129
171	-74784.364	3205567.637	3.314
172	-74792.498	3205583.286	0.921
173	-74798.045	3205595.149	-0.034
174	-74800.377	3205600.667	-0.409
175	-74738.291	3205638.516	-0.552
176	-74729.795	3205624.415	0.315
177	-74719.085	3205605.977	3.095
178	-74707.346	3205581.592	3.245
179	-74694.547	3205558.071	3.192
180	-74682.125	3205535.149	3.936
181	-74674.683	3205521.104	4.366

Point	Y	X	Z
182	-74668.456	3205509.812	3.789
183	-74662.576	3205496.882	5.766
184	-74657.575	3205483.443	9.761
185	-74652.911	3205473.33	12.384
186	-74649.774	3205456.643	18.424
187	-74608.664	3205498.543	16.701
188	-74607.632	3205497.616	16.968
189	-74609.383	3205507.708	14.202
190	-74606.942	3205529.182	4.238
191	-74607.548	3205532.129	5.386
192	-74613.537	3205542.442	5.388
193	-74624.556	3205562.118	4.414
194	-74636.772	3205583.404	3.836
195	-74645.452	3205597.457	3.489
196	-74656.909	3205617.164	3.412
197	-74659.228	3205621.182	3.323
198	-74666.189	3205630.925	3.01
199	-74670.249	3205637.803	3.119
200	-74671.072	3205638.767	2.297
201	-74675.795	3205646.609	0.99
202	-74681.774	3205656.478	-0.003
203	-74686.293	3205667.354	-0.627
204	-74628.35	3205732.127	-0.974
205	-74620.88	3205722.666	-0.717
206	-74609.585	3205705.022	0.09
207	-74597.9	3205681.279	2.82
208	-74593.108	3205668.259	3.264
209	-74582.336	3205643.813	2.881
210	-74572.447	3205626.046	3.359
211	-74560.229	3205606.337	4.682
212	-74553.434	3205593.899	4.944
213	-74546.056	3205581.529	4.182
214	-74539.564	3205571.167	2.863
215	-74537.467	3205567.825	2.885
216	-74535.699	3205562.991	3.422
217	-74522.419	3205569.843	4.587
218	-74528.252	3205574.315	4.573
219	-74456.165	3205620.737	0.904
220	-74478.819	3205634.694	5.372
221	-74484.168	3205640.985	6.799
222	-74491.512	3205652.028	6.797
223	-74461.2	3205661.382	9.67

Point	Y	X	Z
224	-74468.988	3205675.094	11.298
225	-74469.017	3205675.069	11.298
226	-74501.678	3205660.963	5.833
227	-74512.171	3205678.416	3.98
228	-74523.673	3205697.344	2.907
229	-74530.09	3205716.656	2.369
230	-74539.744	3205726.914	1.905
231	-74546.86	3205736.326	0.584
232	-74557.536	3205749.191	-0.962
233	-74563.367	3205758.25	-1.363
234	-74571.956	3205771.152	-1.772
235	-74474.073	3205833.318	-1.994
236	-74464.974	3205817.51	-1.325
237	-74448.393	3205795.072	1.429
238	-74439.201	3205785.13	1.889
239	-74433.298	3205775.078	2.545
240	-74426.906	3205763.628	2.898
241	-74413.088	3205748.928	5.079
242	-74400.362	3205736.321	9.62
243	-74390.217	3205728.703	13.876
244	-74393.503	3205719.182	12.378
245	-74401.957	3205719.061	10.437
246	-74411.212	3205705.462	13.652
247	-74415.491	3205699.575	13.613
248	-74417.376	3205694.272	13.587
249	-74427.773	3205676.93	9.038
250	-74437.219	3205673.186	10.763
251	-74442.914	3205660.509	7.626
252	-74444.039	3205685.005	10.165
253	-74451.158	3205701.685	8.059
254	-74458.745	3205714.109	4.715
255	-74457.358	3205720.56	4.054
256	-74860.79	3205387.47	11.037

Appendix B:

All Points falling in the Fishnet Grid of 10m x 10m on the Umlalazi Beach during the survey of March 2016, October 2016, April 2017 and July 2017

Grid Heights

Point	Y	X	16-Mar	16-Oct	17-Apr	17-Jul
1	74430	3205690	12	10.7	12.1	11.6
2	74430	3205700	9	10.7	10.3	11.2
3	74440	3205690	10.5	10	11.4	11.1
4	74440	3205700	9.8	9	10.3	10.4
5	74440	3205710	8.5	8	9	9
6	74450	3205680	10.5	10.7	12.6	11.3
7	74450	3205690	9.5	10	10.3	11.3
8	74450	3205700	8.4	8.5	9	9
9	74450	3205710	7	6.4	7.9	7.7
10	74450	3205720	5.2	6	6.5	7.5
11	74460	3205670	10.5	11.5	12	10.8
12	74460	3205680	10.6	10.3	10.7	10.5
13	74460	3205690	9.5	9.7	9.5	9.5
14	74460	3205700	7.5	7.7	7.2	8.3
15	74460	3205710	6.5	6.1	6.7	7
16	74460	3205720	5.5	5.2	5.5	5.6
17	74460	3205730	4	4.5	5.2	5.1
18	74460	3205740	3.6	3.7	4.7	4.5
19	74470	3205670	10.5	10.8	10.3	10.6
20	74470	3205680	10.2	10	10	9.8
21	74470	3205690	8	7.6	8.3	8.6
22	74470	3205700	6	6.5	6.9	7.5
23	74470	3205710	4.2	5.3	5.6	6.3
24	74470	3205720	3.7	4.5	5.3	4.3
25	74470	3205730	3.4	4.3	4.7	4.7
26	74470	3205740	2.6	4.7	4.4	4.4
27	74480	3205660	8.8	8.6	8.3	9.7
28	74480	3205670	9.5	9.8	10	10
29	74480	3205680	8.7	7.9	8.5	8.5
30	74480	3205690	6.6	6.5	7.4	7.5
31	74480	3205700	4.5	5.5	6.3	6.6
32	74480	3205710	3.7	4.4	5.3	5.5
33	74480	3205720	3.5	4.2	4.7	5
34	74480	3205730	3.3	3.7	4.4	4.6

Point	Y	X	16-Mar	16-Oct	17-Apr	17-Jul
35	74480	3205740	2.6	2.8	4	4.1
36	74480	3205750	2	3	3.5	3.7
37	74490	3205650	6.7	7.3	9.2	9.4
38	74490	3205660	7.5	7.5	9	9.1
39	74490	3205670	6.7	8.1	8.5	8
40	74490	3205680	7.2	6.5	7.3	7.3
41	74490	3205690	5.1	5.5	6.5	6.4
42	74490	3205700	3.8	4.5	5.5	5.5
43	74490	3205710	3.4	4.4	4.9	4.9
44	74490	3205720	3.3	3.7	4.3	4.6
45	74490	3205730	3	3.4	4	4.3
46	74490	3205740	2.4	3.1	3.5	3.7
47	74490	3205750	1.8	2.6	3	3.4
48	74490	3205760	1.3	2.2	2.5	3
49	74500	3205640	5.9	6.9	8.5	8.6
50	74500	3205650	5.9	6.4	8.6	8.4
51	74500	3205660	6	6.1	7.5	7.5
52	74500	3205670	6	5.7	7.1	6.7
53	74500	3205680	5.5	5.5	6.1	6.3
54	74500	3205690	3.8	4.5	6.3	5.6
55	74500	3205700	3.5	4.3	4.9	5.1
56	74500	3205710	3.3	3.7	4.5	4.6
57	74500	3205720	3.1	4.5	4.2	4.3
58	74500	3205730	2.7	3.3	3.6	3.7
59	74500	3205740	2.2	2.6	3	3.5
60	74500	3205750	1.6	2.3	2.5	3.2
61	74500	3205760	1.2	1.6	2	2.7
62	74500	3205770	0.6	1	1.6	2.4
63	74510	3205640	5.4	5.4	7.7	8
64	74510	3205650	5.7	5.8	8.2	7.5
65	74510	3205660	5.3	5.4	7.7	6.9
66	74510	3205670	4.6	4.6	7	6.4
67	74510	3205680	4	4.25	5.9	5.7
68	74510	3205690	3.6	3.8	4.8	5.4
69	74510	3205700	3.3	3.6	4.6	4.7
70	74510	3205710	3	3.3	4.3	4.3
71	74510	3205720	2.7	2.7	3.7	3.8
72	74510	3205730	2.4	2.7	3.3	3.5
73	74510	3205740	1.9	2.25	2.6	3.2
74	74510	3205750	1.4	1.6	2.2	2.7
75	74510	3205760	0.8	1	1.7	2.4
76	74510	3205770	0.4	0.4	1.4	2.3
77	74510	3205780	-0.7	-0.7	1	2.1
78	74520	3205630	5.3	6.3	7.3	7.6

Point	Y	X	16-Mar	16-Oct	17-Apr	17-Jul
79	74520	3205640	5.3	5.7	7.4	7.3
80	74520	3205650	5.3	5.4	7	6.7
81	74520	3205660	4.6	4.9	6.3	6.3
82	74520	3205670	4	4.5	5.3	5.7
83	74520	3205680	3.7	4.3	4.8	5.3
84	74520	3205690	3.4	3.8	4.6	4.7
85	74520	3205700	2.7	3.6	4.3	4.3
86	74520	3205710	2.5	3.3	3.8	3.8
87	74520	3205720	2.3	2.8	3.4	3.6
88	74520	3205730	2	2.4	2.8	3.3
89	74520	3205740	1.7	1.7	2.3	2.7
90	74520	3205750	1.2	1	1.7	2.5
91	74520	3205760	0.5	-0.4	1.5	2.3
92	74520	3205770	-0.8	-1	1.3	2.2
93	74520	3205780	-0.5	-0.6	-0.3	1.9
94	74530	3205620	5	5.9	6.6	7.1
95	74530	3205630	5.2	5.6	6.7	7
96	74530	3205640	5.1	5.3	6.6	6.6
97	74530	3205650	4.6	4.8	6.3	6.3
98	74530	3205660	4	4.5	5.6	5.6
99	74530	3205670	3.7	4.25	4.7	5.2
100	74530	3205680	3.6	4	4.6	4.6
101	74530	3205690	3.2	3.6	4.3	4.3
102	74530	3205700	2.6	3.3	3.9	3.7
103	74530	3205710	2.5	3	3.6	3.6
104	74530	3205720	2.3	2.5	3	3.3
105	74530	3205730	2	1.7	2.4	2.9
106	74530	3205740	1.4	1.2	1.9	2.6
107	74530	3205750	0.6	0.5	1.6	2.3
108	74530	3205760	0	-0.1	1.3	2.2
109	74530	3205770	-0.5	-0.4	0.8	2.1
110	74530	3205780	-0.8	-0.7	-0.4	1.7
111	74530	3205790	-1.3	-0.9	0	1.3
112	74540	3205610	4.7	5.5	5.4	6.5
113	74540	3205620	4.9	5.7	5.3	6.4
114	74540	3205630	4.9	5	5.1	6.4
115	74540	3205640	4.6	4.6	4.7	6
116	74540	3205650	4	4.4	4.5	5.5
117	74540	3205660	3.6	3.3	4	5
118	74540	3205670	3.6	3.9	4.5	4.5
119	74540	3205680	3.5	3.6	4.3	4.2
120	74540	3205690	3	3.4	4.1	3.7
121	74540	3205700	2.7	3	3.6	3.6
122	74540	3205710	2.5	2.6	3.2	3.3

Point	Y	X	16-Mar	16-Oct	17-Apr	17-Jul
123	74540	3205720	2.2	2	2.6	3
124	74540	3205730	1.5	1.3	2.1	2.6
125	74540	3205740	0.7	0.6	1.7	2.4
126	74540	3205750	0	0.1	1.3	2.3
127	74540	3205760	-0.4	-0.3	0	2.2
128	74540	3205770	-0.3	-0.7	0.6	1.7
129	74540	3205780	-0.8	-1.2	-0.4	1
130	74550	3205600	4.7	4.6	6.4	6
131	74550	3205610	4.5	4.8	6	5.9
132	74550	3205620	4.3	4.6	5.7	5.7
133	74550	3205630	3.8	4.4	5.4	5.6
134	74550	3205640	3.4	4.3	5.1	5.4
135	74550	3205650	2.5	4.2	4.7	4.8
136	74550	3205660	2.4	3.8	4.5	4.4
137	74550	3205670	2.6	3.7	4.3	4.1
138	74550	3205680	2.4	3.4	4.2	3.7
139	74550	3205690	2.8	3.1	4.3	3.6
140	74550	3205700	2.6	2.6	3.6	3.4
141	74550	3205710	2.3	2.3	3.1	3.1
142	74550	3205720	2	1.5	2.3	2.7
143	74550	3205730	1	0.7	1.7	2.4
144	74550	3205740	0.2	0.1	1.4	2.3
145	74550	3205750	-0.5	-0.3	1	2.2
146	74550	3205760	-1	-0.6	0.3	2
147	74550	3205770	-1.3	-1	0.4	1.3
148	74550	3205780	-1.5	-1.3	0.1	0.4
149	74560	3205600	4.8	4.8	5.7	5.6
150	74560	3205610	4.5	4.5	5.5	5.4
151	74560	3205620	4.3	4.3	5.3	5.3
152	74560	3205630	3.8	4.3	5	5.3
153	74560	3205640	3.4	4.2	4.6	4.7
154	74560	3205650	3.4	3.8	4.4	4
155	74560	3205660	3.3	3.6	4.3	4
156	74560	3205670	3.5	3.4	4.2	3.7
157	74560	3205680	3.3	3.2	4	3.5
158	74560	3205690	2.7	2.7	3.4	3.4
159	74560	3205700	2.6	2.4	2.7	3.1
160	74560	3205710	2.2	1.7	2.3	2.6
161	74560	3205720	1.5	1	1.8	2.5
162	74560	3205730	0.5	0.3	1.5	2.3
163	74560	3205740	-0.4	-0.3	1.2	2.3
164	74560	3205750	-1	-0.6	0.7	2.1
165	74560	3205760	-1.3	-0.7	0.4	1.5
166	74560	3205770	-1.4	-1.4	0.3	0.5

Point	Y	X	16-Mar	16-Oct	17-Apr	17-Jul
167	74570	3205590	4.7	4.7	5.6	5.4
168	74570	3205600	4.6	4.5	5.4	5.3
169	74570	3205610	4.3	4.3	5.1	5
170	74570	3205620	3.7	4.2	4.7	4.7
171	74570	3205630	3.4	3.8	4.6	4.6
172	74570	3205640	3.3	3.8	4.4	4.3
173	74570	3205650	3.2	3.6	4.3	4
174	74570	3205660	3.3	3.4	4.2	3.7
175	74570	3205670	3.4	3.3	4	3.5
176	74570	3205680	3.1	2.7	3.5	3.3
177	74570	3205690	2.7	2.4	3	3.1
178	74570	3205700	2.5	2	2.4	2.7
179	74570	3205710	2.7	1.3	2	2.6
180	74570	3205720	0.9	0.5	1.6	2.4
181	74570	3205730	0	0	1.3	2.3
182	74570	3205740	-0.3	-0.4	0.4	2.1
183	74570	3205750	-0.8	-0.7	0.5	1.6
184	74570	3205760	-1	-1.3	0.75	1
185	74570	3205770	-1.3	-1.2	0	-1
186	74580	3205580	4.8	4.6	5.7	5.4
187	74580	3205590	4.8	4.5	5.3	5.1
188	74580	3205600	4.4	4.3	5	4.8
189	74580	3205610	4	4	4.7	4.6
190	74580	3205620	3.5	3.7	4.5	4.4
191	74580	3205630	3.2	3.6	4.4	4.3
192	74580	3205640	3	3.5	4.3	4.3
193	74580	3205650	3	3.4	4.2	4
194	74580	3205660	3.3	3.3	4	3.6
195	74580	3205670	3.3	2.9	3.6	3.5
196	74580	3205680	3	2.5	3.2	3.3
197	74580	3205690	2.7	2.2	1.6	2.8
198	74580	3205700	2.1	1.4	1.2	2.6
199	74580	3205710	1.3	0.7	0.7	2.4
200	74580	3205720	0.3	0.3	0.4	2.4
201	74580	3205730	-0.5	-0.3	0	2.2
202	74580	3205740	-0.7	-0.6	-0.4	2
203	74580	3205750	-1.3	-1	-0.6	1
204	74590	3205580	4.7	4.3	5.4	5.1
205	74590	3205590	4.5	4.2	4.9	4.7
206	74590	3205600	4.3	3.8	4.7	4.6
207	74590	3205610	3.6	3.7	4.5	4.4
208	74590	3205620	3.4	3.6	4.4	4.2
209	74590	3205630	3.3	3.5	4.3	4
210	74590	3205640	3	3.4	4.2	3.8

Point	Y	X	16-Mar	16-Oct	17-Apr	17-Jul
211	74590	3205650	2.9	3.3	4	3.6
212	74590	3205660	3.2	3.1	3.7	3.4
213	74590	3205670	3.3	2.6	3.4	3.2
214	74590	3205680	2.9	2.25	2.8	2.8
215	74590	3205690	2.5	2.2	1.8	2.7
216	74590	3205700	1.5	1.5	1.5	2.5
217	74590	3205710	0.6	0.7	1.2	2.3
218	74590	3205720	0.2	0.3	0.3	2.2
219	74590	3205730	-0.6	-0.3	0.4	2
220	74590	3205740	-1	-0.6	0.2	1.4
221	74590	3205750	-1.3	-1.3	-0.2	-1.1
222	74600	3205570	4.7	4.5	5.6	5.1
223	74600	3205580	4.5	4.1	4.6	4.7
224	74600	3205590	4.3	3.8	4.4	4.6
225	74600	3205600	4	3.6	4.4	4.4
226	74600	3205610	3.5	3.5	4.3	4.3
227	74600	3205620	3.4	3.4	4.3	4.1
228	74600	3205630	3.2	3.3	4.2	3.8
229	74600	3205640	3	3.3	4	3.6
230	74600	3205650	3.2	3.2	3.7	3.4
231	74600	3205660	3.3	2.7	3.6	3.2
232	74600	3205670	3.1	2.4	3	2.9
233	74600	3205680	2.7	1.8	2.5	2.7
234	74600	3205690	2	1.3	2	2.5
235	74600	3205700	1	0.5	1.6	2.4
236	74600	3205710	0.1	0.3	1.3	2.3
237	74600	3205720	-0.4	-0.3	0.7	2.1
238	74600	3205730	-0.7	-0.7	0.5	1.5
239	74600	3205740	-1.1	-1	0.3	1
240	74610	3205560	4.7	4.6	5.3	5.1
241	74610	3205570	4.5	4.3	5.1	4.7
242	74610	3205580	4.3	3.8	4.7	4.6
243	74610	3205590	4.1	3.6	4.5	4.4
244	74610	3205600	3.7	3.5	4.3	4.3
245	74610	3205610	3.4	3.4	4.3	4.1
246	74610	3205620	3.3	3.3	4.1	3.8
247	74610	3205630	3.2	3.3	3.9	3.7
248	74610	3205640	3.2	3.2	3.7	3.5
249	74610	3205650	3.3	3	3.6	3.3
250	74610	3205660	3.2	2.5	3.4	3
251	74610	3205670	2.8	2	2.7	2.7
252	74610	3205680	2.2	1.5	2.3	2.6
253	74610	3205690	1.4	0.7	1.7	2.4
254	74610	3205700	0.5	0.3	1.4	2.3

Point	Y	X	16-Mar	16-Oct	17-Apr	17-Jul
255	74610	3205710	-0.2	-0.9	1	2.1
256	74610	3205720	-0.5	-0.5	0.6	1.7
257	74610	3205730	-0.7	-0.8	0.3	1
258	74610	3205740	-0.1	-1.2	0	0.2
259	74620	3205550	4.9	4.7	5.5	5
260	74620	3205560	4.6	4.3	5.1	4.7
261	74620	3205570	4.3	3.9	4.7	4.6
262	74620	3205580	4.2	3.6	4.5	4.4
263	74620	3205590	4	3.4	4.4	4.3
264	74620	3205600	3.6	3.3	4.3	4.1
265	74620	3205610	3.4	3.2	4.2	3.8
266	74620	3205620	3.4	3.1	3.9	3.5
267	74620	3205630	3.3	3.1	3.7	3.3
268	74620	3205640	3.2	2.8	3.6	3.1
269	74620	3205650	3.1	2.6	3.5	2.7
270	74620	3205660	3	2.3	3.1	2.6
271	74620	3205670	2.5	1.6	2.5	2.5
272	74620	3205680	1.5	1	2	2.5
273	74620	3205690	0.8	0.5	1.5	2.3
274	74620	3205700	0	0.2	1.2	2.3
275	74620	3205710	-0.3	-0.3	0.7	2
276	74620	3205720	-0.6	-0.6	0.4	1.3
277	74620	3205730	-0.6	-1	0.1	0.5
278	74630	3205540	5	4.3	5.5	5
279	74630	3205550	4.6	4.4	5.2	4.8
280	74630	3205560	4.4	4	4.8	4.6
281	74630	3205570	4.3	3.6	4.5	4.4
282	74630	3205580	4	3.4	4.3	4.3
283	74630	3205590	3.7	3.4	4.2	4
284	74630	3205600	3.5	3.3	4.1	3.8
285	74630	3205610	3.4	3.1	3.9	3.4
286	74630	3205620	3.3	3	3.7	3.6
287	74630	3205630	3.3	2.9	3.6	3.3
288	74630	3205640	3.2	2.7	3.4	3.2
289	74630	3205650	3.1	2.5	3.3	2.9
290	74630	3205660	2.6	1.9	2.9	2.7
291	74630	3205670	1.8	1.3	2.2	2.5
292	74630	3205680	1	0.8	1.7	2.3
293	74630	3205690	0.1	0.3	1.7	2.3
294	74630	3205700	-0.3	-0.2	0.8	2.1
295	74630	3205710	-0.6	-0.5	0.5	1.4
296	74630	3205720	-0.7	-0.8	0.3	0.7
297	74640	3205540	4.7	4.4	5.2	4.7
298	74640	3205550	4.4	4.4	4.7	4.6

Point	Y	X	16-Mar	16-Oct	17-Apr	17-Jul
299	74640	3205560	4.3	4	4.5	4.4
300	74640	3205570	4	3.6	4.4	4.3
301	74640	3205580	3.8	3.4	4.3	4
302	74640	3205590	3.7	3.4	4.1	3.8
303	74640	3205600	3.5	3.3	3.9	3.7
304	74640	3205610	3.4	2.9	3.7	3.6
305	74640	3205620	3.3	2.8	3.7	3.4
306	74640	3205630	3.3	2.8	3.5	3.2
307	74640	3205640	3.2	2.6	3.3	3
308	74640	3205650	2.8	2	3.1	2.7
309	74640	3205660	2.1	1.5	2.5	2.5
310	74640	3205670	1.3	0.9	2	2.4
311	74640	3205680	0.5	0.4	1.5	2.3
312	74640	3205690	-0.3	0	1	2.1
313	74640	3205700	-0.5	-0.4	0.6	1.5
314	74640	3205710	-0.7	-0.7	0.4	0.8
315	74640	3205720	-0.8	-0.8	0	0
316	74650	3205530	4.7	4	5.3	5.6
317	74650	3205540	4.5	3.7	4.7	4.5
318	74650	3205550	4.3	3.6	4.5	4.4
319	74650	3205560	4	3.3	4.4	4.3
320	74650	3205570	3.8	3.3	4.3	4
321	74650	3205580	3.7	3.1	4.1	3.9
322	74650	3205590	3.5	2.9	3.9	3.7
323	74650	3205600	3.4	2.8	3.7	3.6
324	74650	3205610	3.4	2.8	3.6	3.5
325	74650	3205620	3.4	2.7	3.5	3.3
326	74650	3205630	3.2	2.6	3.25	3.1
327	74650	3205640	3	2.3	3.1	2.8
328	74650	3205650	2.5	1.6	2.6	2.6
329	74650	3205660	1.5	1	2.3	2.4
330	74650	3205670	0.6	0.5	1.7	2.3
331	74650	3205680	0	0.3	1.7	2.2
332	74650	3205690	-0.3	-0.3	0.8	2
333	74650	3205700	-0.7	-0.5	0.4	1
334	74650	3205710	-0.8	-0.8	0.2	0.7
335	74660	3205520	3.7	4	5.3	5.7
336	74660	3205530	4.5	3.8	4.8	4.4
337	74660	3205540	4.3	3.6	4.6	4.3
338	74660	3205550	4.1	3.4	4.4	4.1
339	74660	3205560	4	3.3	4.3	3.9
340	74660	3205570	3.7	3	4	3.8
341	74660	3205580	3.5	2.9	3.9	3.7
342	74660	3205590	3.4	2.8	3.8	3.7

Point	Y	X	16-Mar	16-Oct	17-Apr	17-Jul
343	74660	3205600	3.4	2.7	3.6	3.6
344	74660	3205610	3.4	2.7	3.5	3.4
345	74660	3205620	3.3	2.6	3.2	3.3
346	74660	3205630	3.1	2.5	3	2.9
347	74660	3205640	2.6	1.8	2.7	2.5
348	74660	3205650	1.7	1.3	2.4	2.5
349	74660	3205660	0.9	0.2	1.9	2.3
350	74660	3205670	0.1	-0.2	1.5	2.2
351	74660	3205680	-0.4	-0.5	1	2
352	74660	3205690	-0.7	-0.4	0.5	1.4
353	74660	3205700	-1	-0.8	0.3	0.5
354	74670	3205510	4	4.3	5.5	2.2
355	74670	3205520	4.3	3.8	5.3	3.2
356	74670	3205530	4.3	3.6	4.6	4.3
357	74670	3205540	4.1	3.4	4.3	4.1
358	74670	3205550	4	3.3	4.2	3.9
359	74670	3205560	3.7	3	4	3.7
360	74670	3205570	3.5	2.9	3.8	3.7
361	74670	3205580	3.4	2.8	3.7	3.7
362	74670	3205590	3.3	2.7	3.7	3.7
363	74670	3205600	3.3	2.7	3.6	3.6
364	74670	3205610	3.3	2.6	3.3	3.3
365	74670	3205620	3.3	2.6	3	3
366	74670	3205630	3	2	2.7	2.7
367	74670	3205640	2.3	1.5	2.5	2.5
368	74670	3205650	1.1	0.9	2	2.5
369	74670	3205660	0.4	0.4	1.6	2.3
370	74670	3205670	-0.3	0.2	1.2	2.2
371	74670	3205680	-0.6	-0.7	0.3	2.1
372	74670	3205690	-0.5	-0.5	0.6	1.5
373	74670	3205700	-0.6	-0.8	0.1	0.5
374	74680	3205500	4.6	4.3	5.3	2.2
375	74680	3205510	4.5	3.8	4.7	2.2
376	74680	3205520	4.4	3.5	4.5	4.1
377	74680	3205530	4.8	3.3	4.4	3.9
378	74680	3205540	4	3.1	4.1	3.6
379	74680	3205550	4	2.8	3.9	3.7
380	74680	3205560	3.5	2.8	3.8	3.7
381	74680	3205570	3.4	2.7	3.7	3.7
382	74680	3205580	3.4	2.7	3.7	3.6
383	74680	3205590	3.4	2.7	3.6	3.6
384	74680	3205600	3.4	2.7	3.4	3.5
385	74680	3205610	2.6	2.6	3	3.1
386	74680	3205620	3.2	2.3	2.6	2.7

Point	Y	X	16-Mar	16-Oct	17-Apr	17-Jul
387	74680	3205630	2.6	1.5	2.4	2.6
388	74680	3205640	1.5	1	2	2.4
389	74680	3205650	0.5	0.5	1.5	2.3
390	74680	3205660	-0.8	-0.3	1.3	2.1
391	74680	3205670	-0.5	-0.8	0.8	1.7
392	74680	3205680	-0.8	-0.6	0.5	1
393	74680	3205690	-1	-0.8	0.3	0.2
394	74690	3205500	5	4.3	5.3	2.2
395	74690	3205510	4.8	3.7	4.8	3
396	74690	3205520	4.3	3.6	4.5	3.9
397	74690	3205530	3.8	3.3	4	3.7
398	74690	3205540	4	3.2	3.9	3.7
399	74690	3205550	3.6	2.9	3.7	3.6
400	74690	3205560	3.4	2.8	3.7	3.6
401	74690	3205570	3.4	2.7	3.7	3.6
402	74690	3205580	3.3	2.7	3.6	3.5
403	74690	3205590	3.3	2.7	3.5	3.4
404	74690	3205600	3.2	2.6	3.2	3.3
405	74690	3205610	3.1	2.5	2.8	2.8
406	74690	3205620	3	1.8	2.6	2.7
407	74690	3205630	2	1.3	2.3	2.5
408	74690	3205640	1	0.7	1.8	2.3
409	74690	3205650	0.2	0.3	1.5	2.2
410	74690	3205660	-0.6	0	1	1.8
411	74690	3205670	-0.7	-0.3	0.6	1.3
412	74690	3205680	-0.8	-0.6	0.7	0.5
413	74700	3205490	5.5	4.3	5.3	2.2
414	74700	3205500	5.5	4	4.7	2.2
415	74700	3205510	4.4	3.6	4.5	3.8
416	74700	3205520	4.3	3.4	4.2	3.7
417	74700	3205530	4.1	3.3	3.9	3.7
418	74700	3205540	3.7	3	3.8	3.6
419	74700	3205550	3.4	2.8	3.7	3.6
420	74700	3205560	3.2	2.7	3.7	3.5
421	74700	3205570	3.2	2.7	3.7	3.4
422	74700	3205580	3.3	2.7	3.6	3.3
423	74700	3205590	3.3	2.6	3.3	3
424	74700	3205600	3.3	2.5	3	2.7
425	74700	3205610	3.2	2	2.7	2.7
426	74700	3205620	2.6	1.5	2.4	2.6
427	74700	3205630	1.5	1	2	2.4
428	74700	3205640	0.5	0.5	1.6	2.3
429	74700	3205650	-0.2	0.1	1.2	2
430	74700	3205660	-0.6	-0.3	0.7	1.4

Point	Y	X	16-Mar	16-Oct	17-Apr	17-Jul
431	74700	3205670	-0.7	-0.5	0.5	0.6
432	74700	3205680	-1.3	-0.9	0.7	0.2
433	74710	3205480	6	4.5	5.5	2.2
434	74710	3205490	5	4.1	4.7	2.2
435	74710	3205500	4.4	3.7	4.4	2.5
436	74710	3205510	4.2	3.5	4.3	3.6
437	74710	3205520	3.8	3.3	4	3.6
438	74710	3205530	3.5	3.2	3.8	3.6
439	74710	3205540	3.2	2.9	3.7	3.6
440	74710	3205550	3.2	2.8	3.7	3.5
441	74710	3205560	3.2	2.7	3.7	3.3
442	74710	3205570	3.2	2.7	3.6	3.2
443	74710	3205580	3.2	2.6	3.5	3
444	74710	3205590	3.1	2.4	3.2	2.8
445	74710	3205600	3.1	2.3	2.7	2.7
446	74710	3205610	3	1.7	2.5	2.6
447	74710	3205620	2	1.1	2.2	2.5
448	74710	3205630	1	0.5	1.6	2.3
449	74710	3205640	0.1	0.3	1.3	2.3
450	74710	3205650	-0.6	-0.2	0.9	2
451	74710	3205660	-0.7	-0.4	0.4	1.4
452	74710	3205670	-0.8	-0.75	0.3	0.5
453	74720	3205470	6.5	6.4	6	2.2
454	74720	3205480	6	4.8	4.7	2.2
455	74720	3205490	5.5	3.9	4.5	3.2
456	74720	3205500	4.5	3.6	4.3	3.4
457	74720	3205510	4.5	3.4	4.2	3.5
458	74720	3205520	4	3.2	3.9	3.5
459	74720	3205530	3.5	2.9	3.8	3.4
460	74720	3205540	3.4	2.8	3.7	3.3
461	74720	3205550	3.3	2.8	3.7	3.1
462	74720	3205560	3.3	2.7	3.6	3.1
463	74720	3205570	3.3	2.6	3.6	3
464	74720	3205580	3.3	2.5	3.3	2.8
465	74720	3205590	3.2	2.3	3	2.7
466	74720	3205600	3.2	2	2.6	2.6
467	74720	3205610	2.5	2.6	2.3	2.6
468	74720	3205620	1.5	0.6	1.8	2.3
469	74720	3205630	0.4	0.3	1.5	2.1
470	74720	3205640	-0.2	0.1	1	2.1
471	74720	3205650	-0.6	-0.4	0.3	1.5
472	74720	3205660	-0.7	-0.7	0.5	0.7
473	74730	3205470	7	5	6	2.2
474	74730	3205480	6	4.8	4.8	2.2

Point	Y	X	16-Mar	16-Oct	17-Apr	17-Jul
475	74730	3205490	5	3.8	4.5	2.2
476	74730	3205500	4.5	3.4	4.3	3.1
477	74730	3205510	4	3.3	4	3.3
478	74730	3205520	3.5	3	3.8	3.3
479	74730	3205530	3.4	2.8	3.7	3.3
480	74730	3205540	3.4	2.8	3.7	3.3
481	74730	3205550	3.4	2.7	3.6	3.1
482	74730	3205560	3.3	2.7	3.6	2.9
483	74730	3205570	3.3	2.7	3.5	2.8
484	74730	3205580	3.3	2.5	3.1	2.7
485	74730	3205590	3.2	2.1	2.7	2.7
486	74730	3205600	3	1.5	2.4	2.6
487	74730	3205610	2	0.9	2	2.5
488	74730	3205620	0.6	0.4	1.6	2.3
489	74730	3205630	0	0	1.3	1.8
490	74730	3205640	-0.5	-0.3	0.8	1.3
491	74730	3205650	-0.7	-0.6	0.6	0.5
492	74740	3205460	8.5	7	7.3	5.4
493	74740	3205470	7	5.7	5.7	2.2
494	74740	3205480	5.7	4.7	5.1	2.2
495	74740	3205490	4.6	3.6	4.7	2.5
496	74740	3205500	4.2	3.3	4.4	2.8
497	74740	3205510	3.6	3.3	4.1	3.1
498	74740	3205520	3.4	3.1	3.8	3.2
499	74740	3205530	3.4	2.8	3.7	3.2
500	74740	3205540	3.3	2.8	3.7	3.1
501	74740	3205550	3.3	2.7	3.7	2.9
502	74740	3205560	3.3	2.7	3.6	2.8
503	74740	3205570	3.2	2.6	3.3	2.7
504	74740	3205580	3.1	2.4	2.9	2.6
505	74740	3205590	3	1.6	2.5	2.6
506	74740	3205600	1.7	1	2.2	2.6
507	74740	3205610	0.5	0.5	1.7	2.4
508	74740	3205620	0	0	1.4	2
509	74740	3205630	-0.5	-0.3	1	1.4
510	74740	3205640	-0.6	-0.5	0.3	0.7
511	74740	3205650	-0.8	-0.8	0.6	-1
512	74750	3205450	9	8	8.6	8
513	74750	3205460	7.5	6.5	7	3.5
514	74750	3205470	6.4	5.5	5.7	2.2
515	74750	3205480	5	4.5	5.3	2.2
516	74750	3205490	4.4	3.5	4.9	2.6
517	74750	3205500	3.7	3.2	4.6	2.7
518	74750	3205510	3.2	3.1	4.1	2.9

Point	Y	X	16-Mar	16-Oct	17-Apr	17-Jul
519	74750	3205520	3.2	3.1	3.8	3.1
520	74750	3205530	3.3	2.9	3.8	3
521	74750	3205540	3.2	2.7	3.8	2.9
522	74750	3205550	3.4	2.7	3.7	2.8
523	74750	3205560	3.2	2.5	3.5	2.7
524	74750	3205570	3.3	2	3	2.7
525	74750	3205580	3.3	1.7	2.6	2.6
526	74750	3205590	3	0.6	2.3	2.6
527	74750	3205600	1.7	0.1	2	2
528	74750	3205610	0.6	-0.3	1.5	2.1
529	74750	3205620	0	-0.5	1.2	1.5
530	74750	3205630	-0.5	-0.6	0.7	0.9
531	74750	3205640	-0.7	-0.8	0.5	0.4
532	74760	3205440	9.5	9	9.9	6.5
533	74760	3205450	8.3	7.5	8.5	7.3
534	74760	3205460	7	6.5	6.9	2.2
535	74760	3205470	5.7	5.3	5.8	2.2
536	74760	3205480	4.6	4	5.5	2.2
537	74760	3205490	4	3.9	5	2.4
538	74760	3205500	3.5	3.3	4.5	2.6
539	74760	3205510	3.4	3.2	4	2.8
540	74760	3205520	3.3	3.1	3.8	2.8
541	74760	3205530	3.4	3	3.8	2.8
542	74760	3205540	3.4	2.8	3.7	2.8
543	74760	3205550	3.4	2.8	3.5	2.7
544	74760	3205560	3.2	2.6	3.2	2.7
545	74760	3205570	3.2	2.1	2.7	2.7
546	74760	3205580	3.1	1.5	2.4	2.6
547	74760	3205590	2.4	1	2.1	2.6
548	74760	3205600	1	0.4	1.7	2.3
549	74760	3205610	0.3	-0.4	1.4	1.7
550	74760	3205620	-0.3	-0.4	0.8	1.3
551	74760	3205630	-0.6	-0.7	0.6	0.5
552	74760	3205640	-0.8	-1	0.7	-1
553	74770	3205440	9	8	9.3	6
554	74770	3205450	7.5	7	8	6.6
555	74770	3205460	6.5	6.1	6.6	2.2
556	74770	3205470	5.1	5.2	5.9	2.2
557	74770	3205480	4.4	4.4	5.5	2.3
558	74770	3205490	3.8	3.9	5	2.3
559	74770	3205500	3.4	3.6	4.5	2.5
560	74770	3205510	3.4	3.4	4	2.6
561	74770	3205520	3.3	3.2	3.8	2.7
562	74770	3205530	3.3	3.1	3.7	2.7

Point	Y	X	16-Mar	16-Oct	17-Apr	17-Jul
563	74770	3205540	3.4	2.9	3.7	2.6
564	74770	3205550	3.5	2.7	3.3	2.6
565	74770	3205560	3.1	2.5	2.9	2.6
566	74770	3205570	3	1.7	2.5	2.6
567	74770	3205580	2	1.1	2.2	2.6
568	74770	3205590	1	0.5	1.7	2.5
569	74770	3205600	0.3	0	1.5	1.8
570	74770	3205610	-0.4	-0.7	1	1.3
571	74770	3205620	-0.6	-0.8	0.4	0.7
572	74780	3205430	9.5	8.5	9.8	4.3
573	74780	3205440	8.4	7.6	8.5	5.8
574	74780	3205450	7	7	7.5	8
575	74780	3205460	5.8	6.1	6.6	2.2
576	74780	3205470	4.6	5.3	6	2.2
577	74780	3205480	4	4.5	5.5	2.2
578	74780	3205490	3.5	4.3	5	2.3
579	74780	3205500	3.4	3.8	4.5	2.4
580	74780	3205510	3.4	3.5	3.9	2.5
581	74780	3205520	3.3	3.1	3.7	2.6
582	74780	3205530	3.3	3	3.6	2.6
583	74780	3205540	3.3	2.7	3.4	2.6
584	74780	3205550	3.2	2.6	3	2.6
585	74780	3205560	3.1	2	2.6	2.6
586	74780	3205570	2.7	1.5	2.4	2.6
587	74780	3205580	1.5	0.7	1.9	2.5
588	74780	3205590	0.5	0.1	1.5	2.1
589	74780	3205600	0	-0.3	1.2	1.5
590	74780	3205610	-0.5	-0.6	0.7	1
591	74780	3205620	-0.8	-0.8	0.5	0.4
592	74790	3205420	10	9	10.5	11
593	74790	3205430	9	8.3	9.2	10.2
594	74790	3205440	7.8	7.5	8.5	9.3
595	74790	3205450	6.5	6.7	7.3	7.6
596	74790	3205460	5.4	6	7	2.2
597	74790	3205470	4.4	5.3	6.3	2.2
598	74790	3205480	3.8	4.7	5.4	2.2
599	74790	3205490	3.5	4.4	4.8	2.4
600	74790	3205500	3.4	3.7	4.4	2.4
601	74790	3205510	3.4	3.4	3.9	2.4
602	74790	3205520	3.4	3.2	3.7	2.5
603	74790	3205530	3.4	2.8	3.5	2.6
604	74790	3205540	3.4	2.6	3.2	2.6
605	74790	3205550	3.2	2.3	2.7	2.7
606	74790	3205560	3.1	1.6	2.5	2.7

Point	Y	X	16-Mar	16-Oct	17-Apr	17-Jul
607	74790	3205570	2.8	1	2.3	2.6
608	74790	3205580	1.5	0.4	1.6	2.3
609	74790	3205590	0.5	0	1.3	1.7
610	74790	3205600	0	-0.5	0.8	1.2
611	74790	3205610	-0.5	-0.7	0.5	0.5
612	74790	3205620	-0.9	-1	0.4	0
613	74800	3205420	9.2	8.5	9.7	10.2
614	74800	3205430	8	8	8.7	9.3
615	74800	3205440	7.2	7.2	8.3	8.5
616	74800	3205450	5.9	7	7.7	7.5
617	74800	3205460	4.7	6.5	8	2.2
618	74800	3205470	4.1	5	6.5	2.2
619	74800	3205480	3.7	4.3	4.8	2.2
620	74800	3205490	3.5	3.8	4.6	2.2
621	74800	3205500	3.4	3.5	4.7	2.3
622	74800	3205510	3.3	3.3	3.8	2.3
623	74800	3205520	3.3	3	3.6	2.5
624	74800	3205530	3.2	2.7	3.3	2.5
625	74800	3205540	3.2	2.5	3	2.6
626	74800	3205550	3.1	2	2.6	2.6
627	74800	3205560	3.1	1.4	2.3	2.5
628	74800	3205570	2	0.6	2	2.5
629	74800	3205580	0.9	0	1.5	1.9
630	74800	3205590	0.3	-0.3	1	1.3
631	74800	3205600	-0.4	-0.7	0.7	0.7
632	74800	3205610	-0.9	-0.8	0.4	0.2
633	74810	3205410	10.4	8.4	8.7	10.3
634	74810	3205420	9	7.7	8.9	9.3
635	74810	3205430	7.8	7	8.1	8.2
636	74810	3205440	6.5	6.5	7.5	7.3
637	74810	3205450	5.4	6.5	7.7	7
638	74810	3205460	4.4	5.5	7.1	2.2
639	74810	3205470	3.8	4.5	5.8	2.2
640	74810	3205480	3.6	4	4.6	2.2
641	74810	3205490	3.4	3.7	4.3	2.2
642	74810	3205500	3.4	3.4	4.1	2.2
643	74810	3205510	3.4	3.3	3.7	2.2
644	74810	3205520	3.3	2.8	3.4	2.3
645	74810	3205530	3.3	2.6	3.2	2.5
646	74810	3205540	3.2	2.1	2.8	2.5
647	74810	3205550	3.1	1.5	2.5	2.6
648	74810	3205560	2.5	1	2.3	2.6
649	74810	3205570	1.5	0.2	1.6	2.1
650	74810	3205580	0.5	-0.3	1.3	1.5

Point	Y	X	16-Mar	16-Oct	17-Apr	17-Jul
651	74810	3205590	0.1	-0.5	0.7	0.9
652	74810	3205600	-0.5	-0.8	0.5	0.5
653	74820	3205400	10	8.5	9.5	10.2
654	74820	3205410	8.7	7.7	8.5	9.4
655	74820	3205420	7.5	7.3	7.6	8.6
656	74820	3205430	5.1	6.3	7.4	7.9
657	74820	3205440	5	6.4	7.8	7
658	74820	3205450	4.9	4.5	7	6.5
659	74820	3205460	4.1	4.9	5.5	2.2
660	74820	3205470	3.7	4.3	5	2.2
661	74820	3205480	3.6	3.7	4.6	2.2
662	74820	3205490	3.4	3.5	4.3	2.2
663	74820	3205500	3.4	3.3	3.9	2.2
664	74820	3205510	3.2	3	3.6	2.3
665	74820	3205520	3.2	2.8	3.3	2.3
666	74820	3205530	3.1	2.3	3	2.5
667	74820	3205540	3.1	1.6	2.7	2.7
668	74820	3205550	2.9	1	2.3	2.7
669	74820	3205560	2	0.5	2.9	2.3
670	74820	3205570	0.9	0	1	1.7
671	74820	3205580	0.2	-0.4	9	1.3
672	74820	3205590	-0.3	-0.7	0.5	0.5
673	74820	3205600	-0.5	-0.8	0.7	0.2
674	74830	3205390	12	9	10	10.4
675	74830	3205400	10.5	8.2	8.9	9.1
676	74830	3205410	9	7.6	7.7	9
677	74830	3205420	8.1	7.2	7.3	8.3
678	74830	3205430	6.5	6.5	7	7.5
679	74830	3205440	5.5	5.7	6.6	6.9
680	74830	3205450	4.5	5.3	5.8	5.7
681	74830	3205460	3.9	4.6	5.4	3.5
682	74830	3205470	3.7	4	4.9	2.2
683	74830	3205480	3.5	3.7	4.5	2.2
684	74830	3205490	3.4	3.4	4.3	2.2
685	74830	3205500	3.4	3.2	3.7	2.3
686	74830	3205510	3.3	2.7	3.5	2.3
687	74830	3205520	3.3	2.5	3.2	2.5
688	74830	3205530	3.1	1.7	2.8	2.5
689	74830	3205540	3	1.3	2.6	2.7
690	74830	3205550	2.5	0.6	2.2	2.6
691	74830	3205560	1.5	0.3	1.6	1.8
692	74830	3205570	0.5	-0.3	1.2	1.3
693	74830	3205580	0.1	-0.6	0.6	0.7
694	74830	3205590	-0.5	-0.8	0.3	0.7

Point	Y	X	16-Mar	16-Oct	17-Apr	17-Jul
695	74840	3205380	12	10.6	11.6	11.5
696	74840	3205390	11.5	9.5	10.4	10
697	74840	3205400	10	8	9	9.3
698	74840	3205410	8.5	7.7	7.5	8.5
699	74840	3205420	7.3	6.6	7	7.7
700	74840	3205430	5.5	6.1	6.6	7.3
701	74840	3205440	4.5	5.3	6	6.7
702	74840	3205450	4.1	4.7	5.8	6
703	74840	3205460	3.7	4.4	5.3	4.5
704	74840	3205470	3.7	3.7	4.7	2.2
705	74840	3205480	3.4	3.5	4.4	2.2
706	74840	3205490	3.4	3.3	4	2.2
707	74840	3205500	3.3	3	3.6	2.2
708	74840	3205510	3.3	2.6	3.4	2.2
709	74840	3205520	3.2	2	3	2.4
710	74840	3205530	3.2	1.5	2.7	2.5
711	74840	3205540	2.6	0.8	2.3	2.5
712	74840	3205550	2	0.3	1.8	2.5
713	74840	3205560	0.8	-0.1	1.4	2.3
714	74840	3205570	0.3	-0.4	0.8	1.5
715	74840	3205580	-0.5	-0.7	0.3	0.9
716	74850	3205380	12	11.6	11.7	10.7
717	74850	3205390	10.8	10.5	10.5	9.5
718	74850	3205400	9.4	9	8.9	8.8
719	74850	3205410	8	6.6	7.4	8.2
720	74850	3205420	6.5	6.3	6.8	7.5
721	74850	3205430	5.5	5.4	6.3	6.9
722	74850	3205440	4.5	4.7	5.7	6.4
723	74850	3205450	4	4.4	5.3	5.7
724	74850	3205460	3.6	3.8	4.8	4.6
725	74850	3205470	3.5	3.6	4.5	2.2
726	74850	3205480	3.4	3.4	4.2	2.2
727	74850	3205490	3.3	3	3.7	2.2
728	74850	3205500	3.2	2.6	3.5	2.2
729	74850	3205510	3.1	2.3	3.2	2.2
730	74850	3205520	3.1	2.6	2.7	2
731	74850	3205530	3	2.1	2.5	2.6
732	74850	3205540	2.3	0.5	2	2.5
733	74850	3205550	1.5	0.1	1.5	2
734	74850	3205560	0.4	-0.3	1	1.3
735	74850	3205570	-0.1	-0.6	0.5	0.5
736	74850	3205580	-0.5	-0.9	0.3	0.1
737	74860	3205370	12.3	12.5	13	13
738	74860	3205380	11.5	11.6	12	10.4

Point	Y	X	16-Mar	16-Oct	17-Apr	17-Jul
739	74860	3205390	10.5	9.4	10.5	9.3
740	74860	3205400	9	8.5	8.5	8.5
741	74860	3205410	7.5	7	6.3	7.7
742	74860	3205420	6	5.6	6.5	7.3
743	74860	3205430	5	4.8	5.7	6.6
744	74860	3205440	4.3	4.5	5.4	6.2
745	74860	3205450	4	4.2	5	5.6
746	74860	3205460	3.7	3.7	4.6	4.9
747	74860	3205470	3.5	3.4	4.3	3
748	74860	3205480	3.4	3.3	3.9	2.2
749	74860	3205490	3.3	2.7	3.6	2.2
750	74860	3205500	3.2	2.4	3.3	2.2
751	74860	3205510	3.1	1.9	2.9	2.2
752	74860	3205520	3	1.4	2.6	2.2
753	74860	3205530	2.4	0.7	2.2	2.5
754	74860	3205540	1.7	0.3	1.7	2.3
755	74860	3205550	0.8	0.8	1.3	1.5
756	74860	3205560	0.1	-0.5	0.6	0.7
757	74860	3205570	-0.4	-0.8	0.3	0.3
758	74870	3205360	12.4	12.5	12.8	13.3
759	74870	3205370	11.6	12	12.4	12.5
760	74870	3205380	10.5	10	11	10
761	74870	3205390	8.5	8.3	9	8.7
762	74870	3205400	7.5	7	7.7	7.4
763	74870	3205410	6.6	6	6.7	7.4
764	74870	3205420	5.5	5.1	6.8	6.8
765	74870	3205430	4.5	4.6	5.6	6.3
766	74870	3205440	4.3	4.3	5.3	5.7
767	74870	3205450	4.1	3.8	4.7	5.3
768	74870	3205460	3.7	3.6	4.4	4.7
769	74870	3205470	3.5	3.3	4	3.7
770	74870	3205480	3.4	3	3.7	2.2
771	74870	3205490	3.3	2.5	3.4	2.2
772	74870	3205500	3.2	2.1	3.2	2.2
773	74870	3205510	3.21	1.6	2.7	2.2
774	74870	3205520	2.5	1	2.4	2.2
775	74870	3205530	2	0.5	1.7	2.4
776	74870	3205540	1.5	0	1.3	2
777	74870	3205550	0.6	-0.3	0.7	1.3
778	74870	3205560	-0.9	-0.7	0.3	0.4
779	74870	3205570	-0.5	-0.9	0.3	0
780	74880	3205350	12	10.7	13	13
781	74880	3205360	11.6	10.4	12.7	11
782	74880	3205370	10.5	10	11.3	9.5

Point	Y	X	16-Mar	16-Oct	17-Apr	17-Jul
783	74880	3205380	9.1	9	9.7	8.3
784	74880	3205390	8.1	7.5	7.3	7.6
785	74880	3205400	7.1	6.3	7	7.1
786	74880	3205410	6.1	5.9	6.2	6.6
787	74880	3205420	5	5.4	5.6	6.1
788	74880	3205430	4.4	4.6	5.3	6.1
789	74880	3205440	4.3	4	4.9	5.5
790	74880	3205450	3.8	3.6	4.5	5
791	74880	3205460	3.6	3.4	4.2	4.5
792	74880	3205470	3.5	3.2	3.8	3.7
793	74880	3205480	3.4	2.7	3.6	2.2
794	74880	3205490	3.3	2.3	3.4	2.2
795	74880	3205500	3.1	1.8	3	2.2
796	74880	3205510	3	1.7	2.6	2
797	74880	3205520	2	0.7	2.1	2.2
798	74880	3205530	1.5	0.3	1.6	2.7
799	74880	3205540	0.5	-0.3	1	1.6
800	74880	3205550	0	-0.5	0.5	0.6
801	74890	3205340	12	11.4	11.7	12
802	74890	3205350	11.6	10.4	12	11.3
803	74890	3205360	10.7	10	12	10.6
804	74890	3205370	9.7	9.5	11	9.2
805	74890	3205380	8.7	8	9.5	8.1
806	74890	3205390	7.6	6.8	8	7.9
807	74890	3205400	6.5	5.7	6.6	7.3
808	74890	3205410	5.5	5.3	5.6	6.7
809	74890	3205420	4.5	4.7	5.3	6.3
810	74890	3205430	4.3	4.1	5	5.7
811	74890	3205440	4.3	3.7	4.6	5.3
812	74890	3205450	3.8	3.6	4.3	4.7
813	74890	3205460	3.7	3.3	3.9	4.3
814	74890	3205470	3.5	3	3.7	3.6
815	74890	3205480	3.4	2.5	3.4	2.2
816	74890	3205490	3.3	2	3.1	2.2
817	74890	3205500	3	1.4	2.7	1
818	74890	3205510	2.5	0.9	2.4	0.9
819	74890	3205520	1.6	0.4	1.8	1
820	74890	3205530	1.1	-0.1	1.3	1.3
821	74890	3205540	0.4	-0.4	0.3	1.3
822	74890	3205550	-0.8	-0.7	0.6	0.2
823	74900	3205340	12	11	11.7	11.5
824	74900	3205350	11.3	10.1	11.5	11
825	74900	3205360	10.2	9.6	11.3	10.6
826	74900	3205370	9.2	8.4	10.3	9.7

Point	Y	X	16-Mar	16-Oct	17-Apr	17-Jul
827	74900	3205380	8.2	7.4	9.2	8.6
828	74900	3205390	7	6.4	7.7	7.5
829	74900	3205400	6	5.2	6.3	7
830	74900	3205410	5	4.6	5.4	6.5
831	74900	3205420	4.4	4	5	6
832	74900	3205430	4.2	3.8	4.7	4.5
833	74900	3205440	4	3.6	4.4	4.9
834	74900	3205450	3.7	3.4	4.1	4.4
835	74900	3205460	3.6	3.1	3.7	3.9
836	74900	3205470	3.4	2.7	3.6	3.4
837	74900	3205480	3.3	2.3	3.3	2.6
838	74900	3205490	3.1	1.6	3	2.2
839	74900	3205500	2.6	1.1	2.6	1.7
840	74900	3205510	2.1	0.6	2.2	1.4
841	74900	3205520	1.4	0.1	1.5	1.3
842	74900	3205530	0.6	0	1	1
843	74900	3205540	0.2	-0.4	0.5	0.5
844	74900	3205550	-0.4	-0.7	0.7	0
845	74910	3205330	12.5	11.5	12.5	12
846	74910	3205340	11.7	10.6	11.5	11.3
847	74910	3205350	10.5	9.7	10.7	10.7
848	74910	3205360	9.5	8.9	10.5	10
849	74910	3205370	8.5	7.9	9.4	8.8
850	74910	3205380	7.5	6.8	8.4	7.9
851	74910	3205390	6.5	5.7	7.3	7.2
852	74910	3205400	5.4	4.8	6	6.6
853	74910	3205410	4.5	4.2	5.1	6.2
854	74910	3205420	4.3	3.8	4.7	5.6
855	74910	3205430	4.1	3.7	4.4	5.1
856	74910	3205440	3.8	3.6	4.2	4.6
857	74910	3205450	3.6	3.3	3.8	4.1
858	74910	3205460	3.5	2.8	3.6	3.6
859	74910	3205470	3.3	2.5	3.4	3
860	74910	3205480	3.2	1.8	3.1	2.6
861	74910	3205490	2.7	1.3	2.7	2.1
862	74910	3205500	2.2	0.7	2.4	2
863	74910	3205510	1.4	0.3	1.8	2.2
864	74910	3205520	0.8	-0.2	1.3	0.4
865	74910	3205530	0.3	-0.4	0.7	0.3
866	74910	3205540	-0.8	-0.7	0.3	0.3
867	74920	3205320	12.8	12	13.5	13.6
868	74920	3205330	11.4	11.4	12.3	12
869	74920	3205340	11	10.5	11	11.1
870	74920	3205350	10	9.4	10.3	10.2

Point	Y	X	16-Mar	16-Oct	17-Apr	17-Jul
871	74920	3205360	9	8.3	9.6	9.3
872	74920	3205370	7.9	7.4	8.5	8.3
873	74920	3205380	6.8	6.3	7.5	7.4
874	74920	3205390	5.7	5.7	6.5	6.7
875	74920	3205400	4.7	4.8	5.5	6.3
876	74920	3205410	4.4	4.1	4.8	5.7
877	74920	3205420	4.2	2.8	4.6	5.3
878	74920	3205430	3.9	2.7	4.3	4.7
879	74920	3205440	3.7	2.4	4.1	4.2
880	74920	3205450	3.5	2.1	3.7	3.5
881	74920	3205460	3.4	2.6	3.5	3.3
882	74920	3205470	3.2	2.2	3.3	2.8
883	74920	3205480	3	1.5	3	2.6
884	74920	3205490	2.4	1	2.6	2.4
885	74920	3205500	1.6	0.4	2.1	2.2
886	74920	3205510	1	0	1.5	2.3
887	74920	3205520	0.5	-0.3	1	1.5
888	74920	3205530	0	-0.7	0.4	0.4
889	74930	3205320	12.8	12	13.3	13.3
890	74930	3205330	11.5	11.3	11.7	11.7
891	74930	3205340	10.4	10	10.7	10.5
892	74930	3205350	9.4	8.7	9.6	9.6
893	74930	3205360	8.3	7.6	8.8	8.7
894	74930	3205370	7.4	6.7	8.7	7.7
895	74930	3205380	6.3	5.6	6.8	6.8
896	74930	3205390	5.3	5	6	6.3
897	74930	3205400	4.4	4.4	4.3	5.7
898	74930	3205410	4.2	3.9	4.7	5.3
899	74930	3205420	4	3.7	4.5	4.7
900	74930	3205430	3.7	3.5	4.3	4.2
901	74930	3205440	3.6	3.3	4	3.7
902	74930	3205450	3.4	2.9	3.6	3.4
903	74930	3205460	3.2	2.4	3.4	3
904	74930	3205470	3	1.7	3.1	2.7
905	74930	3205480	2.6	1.3	2.7	2.5
906	74930	3205490	2	0.6	2	2.2
907	74930	3205500	1.3	0.2	17	2.4
908	74930	3205510	0.6	-0.3	1.1	1.7
909	74930	3205520	0.3	-0.6	0.5	1.1
910	74930	3205530	-0.8	-0.8	0.3	0.4
911	74940	3205310	14	13.5	13.7	14.4
912	74940	3205320	13.8	12	12.8	13.3
913	74940	3205330	13.6	10.6	11.5	11.1
914	74940	3205340	12.1	9.5	10.2	10.1

Point	Y	X	16-Mar	16-Oct	17-Apr	17-Jul
915	74940	3205350	10.7	8.1	9.3	8.7
916	74940	3205360	9.7	7	8.3	8.2
917	74940	3205370	8.6	6	7.5	7.3
918	74940	3205380	5.6	5.4	6.5	6.3
919	74940	3205390	4.5	4.8	56	5.7
920	74940	3205400	4.3	4.3	5.2	5.3
921	74940	3205410	4.1	3.7	4.7	4.6
922	74940	3205420	3.8	3.5	4.3	4.3
923	74940	3205430	3.6	3.3	4.1	3.8
924	74940	3205440	3.4	3.1	3.7	3.6
925	74940	3205450	3.2	2.6	3.5	3.3
926	74940	3205460	3	2	3.2	2.8
927	74940	3205470	2.7	1.5	2.7	2.6
928	74940	3205480	2.3	0.4	2.5	2.4
929	74940	3205490	1.5	0.3	1.8	2.2
930	74940	3205500	1	-0.3	1.3	2
931	74940	3205510	0.7	-0.8	0.7	1.4
932	74940	3205520	0.3	-0.5	0.4	1
933	74940	3205530	0	-0.7	0.2	0.2
934	74950	3205300	14.4	13.5	14.3	13.7
935	74950	3205310	12.8	12.5	13.3	12.6
936	74950	3205320	11.4	11.5	12	11.7
937	74950	3205330	10.1	10.1	10.7	10.3
938	74950	3205340	9.2	8.8	9.5	9.3
939	74950	3205350	8.1	7.5	8.7	8.3
940	74950	3205360	7.1	6.5	7.7	7.6
941	74950	3205370	6.1	5.6	7	6.6
942	74950	3205380	5	5	6.5	5.7
943	74950	3205390	4.7	4.6	5.4	5.3
944	74950	3205400	4.2	4.1	5.2	4.7
945	74950	3205410	3.8	3.6	4.7	4.5
946	74950	3205420	3.6	3.3	4.3	4.3
947	74950	3205430	3.7	3.2	4.2	3.7
948	74950	3205440	3.4	2.6	3.6	3.4
949	74950	3205450	3	2.3	3.3	3.2
950	74950	3205460	2.7	1.6	2.9	2.7
951	74950	3205470	2.6	1	2.6	2.4
952	74950	3205480	1.7	0.5	2	2.3
953	74950	3205490	1.3	0	1.5	2.2
954	74950	3205500	0.7	-0.4	0.8	1.6
955	74950	3205510	0.3	-0.7	0.6	1
956	74960	3205290	15.2	13.5	14.5	15
957	74960	3205300	13.7	13.1	13.6	13.7
958	74960	3205310	12.1	12	12.5	12.6

Point	Y	X	16-Mar	16-Oct	17-Apr	17-Jul
959	74960	3205320	10.5	11	11.3	11.7
960	74960	3205330	9.5	9.5	10	10.3
961	74960	3205340	8.5	8.2	8.9	9.3
962	74960	3205350	7.4	6.9	8.3	8.3
963	74960	3205360	6.5	5.8	7.4	7.3
964	74960	3205370	5.5	5.4	6.5	6.3
965	74960	3205380	4.5	4.7	5.6	5.3
966	74960	3205390	4.3	4.3	5.2	5
967	74960	3205400	3.9	3.8	4.7	4.7
968	74960	3205410	3.7	3.4	4.4	4.3
969	74960	3205420	3.4	3.3	4.1	4
970	74960	3205430	3.3	2.8	3.9	3.6
971	74960	3205440	2.9	2.5	3.6	3.3
972	74960	3205450	2.7	2	3.3	2.9
973	74960	3205460	2.6	1.4	2.9	2.6
974	74960	3205470	2.1	0.6	2.6	2.4
975	74960	3205480	1.5	0.2	2	2.3
976	74960	3205490	1.2	-0.3	1.5	1.9
977	74960	3205500	0.6	-0.6	0.8	1.1
978	74960	3205510	0.3	-1	0.4	0
979	74970	3205280	16	13.5	15.2	16
980	74970	3205290	14.5	12.6	14.5	14.5
981	74970	3205300	13	12.5	13.3	13
982	74970	3205310	11.5	11.5	11.9	12
983	74970	3205320	10	10.5	10.5	11
984	74970	3205330	9	9	9.4	9.7
985	74970	3205340	7.8	7.6	8.3	8.7
986	74970	3205350	6.9	6.3	7.6	7.7
987	74970	3205360	5.9	5.6	6.8	6.7
988	74970	3205370	4.9	5	6	5.6
989	74970	3205380	4.3	4.5	5.3	5.3
990	74970	3205390	4	4	4.7	4.8
991	74970	3205400	3.8	3.5	4.6	4.5
992	74970	3205410	3.5	3.25	4.3	4.3
993	74970	3205420	3.3	3	3.9	3.8
994	74970	3205430	3.1	2.6	3.6	3.5
995	74970	3205440	2.8	2.3	3.3	3.3
996	74970	3205450	2.7	1.6	2.8	2.7
997	74970	3205460	2.5	1	2.6	2.5
998	74970	3205470	1.7	0.7	2	2.3
999	74970	3205480	1.3	-0.3	1.4	2
1000	74970	3205490	0.7	-0.6	0.8	1.5
1001	74970	3205500	0.5	-1	0.3	1
1002	74980	3205280	15.5	15.4	15.3	15.5

Point	Y	X	16-Mar	16-Oct	17-Apr	17-Jul
1003	74980	3205290	13.9	13.6	14.3	14.1
1004	74980	3205300	12.4	12.7	13	12.7
1005	74980	3205310	11	11.8	11.6	11.5
1006	74980	3205320	9.5	11	10.3	10.4
1007	74980	3205330	8.4	9.8	8.9	9.4
1008	74980	3205340	7.3	8.5	7.6	8.3
1009	74980	3205350	6.3	6.4	7	7.2
1010	74980	3205360	5.4	5.6	6.4	6
1011	74980	3205370	4.4	5	5.5	5.4
1012	74980	3205380	4.2	4.5	4.8	5
1013	74980	3205390	3.8	4	4.6	4.7
1014	74980	3205400	4.6	3.5	4.3	4.4
1015	74980	3205410	3.4	3.3	4.1	4.1
1016	74980	3205420	3.2	3	3.7	3.7
1017	74980	3205430	2.8	2.6	3.4	3.4
1018	74980	3205440	2.7	1.9	3.1	3
1019	74980	3205450	2.6	1.3	2.7	2.6
1020	74980	3205460	2	0.5	2.4	2.4
1021	74980	3205470	1.4	0	1.6	2.2
1022	74980	3205480	1.1	-0.5	1	1.7
1023	74980	3205490	0.7	-0.8	0.5	1
1024	74990	3205270	16.3	14.5	15.8	15.1
1025	74990	3205280	14.7	14	15.2	15
1026	74990	3205290	13.8	13.1	14	13.6
1027	74990	3205300	11.9	11.6	12.8	12.5
1028	74990	3205310	10.5	10.5	11.4	11.3
1029	74990	3205320	9	9	9.5	9.7
1030	74990	3205330	7.9	7.5	7.9	8.6
1031	74990	3205340	6.9	6.3	7.3	7.5
1032	74990	3205350	5.9	5.6	6.5	6.5
1033	74990	3205360	4.9	5.1	5.7	5.6
1034	74990	3205370	4.3	4.5	5	5.3
1035	74990	3205380	4	4	4.7	4.7
1036	74990	3205390	3.7	3.5	4.3	4.5
1037	74990	3205400	3.5	3.3	4.1	3.8
1038	74990	3205410	3.3	2.7	3.7	3.6
1039	74990	3205420	3	2.5	3.5	3.6
1040	74990	3205430	2.7	2.1	3.3	3.3
1041	74990	3205440	2.6	1.5	3.2	2.8
1042	74990	3205450	2.3	0.7	2.7	2.5
1043	74990	3205460	1.7	0	2.4	2.3
1044	74990	3205470	1.3	-0.4	1.3	1.9
1045	74990	3205480	0.9	-0.7	0.6	1.3
1046	74990	3205490	0.6	-1.1	0.3	-0.8

Point	Y	X	16-Mar	16-Oct	17-Apr	17-Jul
1047	75000	3205260	17.1	16	16.4	16.3
1048	75000	3205270	15.7	15.1	16	16
1049	75000	3205280	14.3	14	14.5	14.6
1050	75000	3205290	12.7	12.7	13.2	13.4
1051	75000	3205300	11.3	11.3	11.8	12
1052	75000	3205310	10.8	9.7	10.1	10.5
1053	75000	3205320	9.5	8	8.4	9
1054	75000	3205330	7.5	6.6	7.5	8
1055	75000	3205340	6.5	6	6.9	6.8
1056	75000	3205350	5.4	5.4	6.3	5.9
1057	75000	3205360	4.6	4.7	5.5	5.4
1058	75000	3205370	4.3	4.3	4.7	4.9
1059	75000	3205380	3.8	3.7	4.4	4.6
1060	75000	3205390	3.6	3.3	4.1	4.3
1061	75000	3205400	3.4	2.8	3.7	4
1062	75000	3205410	3.2	2.6	3.5	3.6
1063	75000	3205420	2.7	1.3	3.2	3.4
1064	75000	3205430	2.6	1.6	2.8	3.1
1065	75000	3205440	2.4	0.9	2.6	2.7
1066	75000	3205450	2	0.3	2.2	2.4
1067	75000	3205460	1.5	-0.3	1.5	2
1068	75000	3205470	1.3	-0.8	1	1.5
1069	75000	3205480	0.7	-1	0.4	1
1070	75010	3205250	17	16.4	17	17
1071	75010	3205260	16.4	16.2	17	16.6
1072	75010	3205270	15.1	14.8	15.4	15.5
1073	75010	3205280	13.7	13.4	13.5	14.2
1074	75010	3205290	12.3	11.9	12	12.6
1075	75010	3205300	10.7	10.5	10.3	11.3
1076	75010	3205310	9.3	8.7	8.9	9.7
1077	75010	3205320	8	7	7.7	8.3
1078	75010	3205330	7	6.3	7.3	7.3
1079	75010	3205340	5.8	5.6	6.5	6.3
1080	75010	3205350	4.8	5.1	6.9	5.6
1081	75010	3205360	4.5	4.5	5.2	5.2
1082	75010	3205370	4.2	3.8	4.5	4.7
1083	75010	3205380	3.8	3.4	4.3	4.4
1084	75010	3205390	3.6	3.1	3.8	4.3
1085	75010	3205400	3.3	2.7	3.5	3.7
1086	75010	3205410	3	2.3	3.3	3.5
1087	75010	3205420	2.6	1.8	2.7	3.3
1088	75010	3205430	2.4	0.8	2.5	2.8
1089	75010	3205440	2.2	0.5	2.3	2.6
1090	75010	3205450	1.6	-0.3	1.6	2.3

Point	Y	X	16-Mar	16-Oct	17-Apr	17-Jul
1091	75010	3205460	1.4	-0.6	1	1.6
1092	75010	3205470	1.2	-0.8	0.5	1
1093	75010	3205480	0.7	-1.3	0.3	0
1094	75020	3205250	16.3	18	18	18.7
1095	75020	3205260	15.5	15	15.3	16
1096	75020	3205270	14.3	14	13.5	14.7
1097	75020	3205280	13	12.5	11.8	13.4
1098	75020	3205290	12.6	11	10.3	11.9
1099	75020	3205300	10.3	9.5	9.5	10.5
1100	75020	3205310	9.7	8.2	8.1	9
1101	75020	3205320	7.5	5.5	7.5	7.6
1102	75020	3205330	6.5	5.9	7.3	6.6
1103	75020	3205340	5.4	5.4	6.5	5.8
1104	75020	3205350	4.7	4.7	5.9	5.4
1105	75020	3205360	4.4	4.2	4.7	4.9
1106	75020	3205370	4.2	3.6	4.4	4.5
1107	75020	3205380	3.7	3.3	4	4.3
1108	75020	3205390	3.5	2.8	3.6	3.9
1109	75020	3205400	3.3	2.5	3.3	3.6
1110	75020	3205410	2.8	2.1	2.8	3.3
1111	75020	3205420	2.6	1.4	2.5	3
1112	75020	3205430	2.3	0.6	2.3	2.6
1113	75020	3205440	2	-0.1	1.7	2.3
1114	75020	3205450	1.6	-0.5	1.3	1.8
1115	75020	3205460	1.3	-0.8	0.7	1.3
1116	75020	3205470	1	-1.4	0.4	0.7
1117	75030	3205240	16.2	18.7	19.2	20.2
1118	75030	3205250	15.5	16.3	17.2	16.6
1119	75030	3205260	14.7	14.5	15.5	14.6
1120	75030	3205270	13.5	13	13.8	13.5
1121	75030	3205280	12.4	11.6	12.3	12.6
1122	75030	3205290	11	10.1	10.5	11.2
1123	75030	3205300	9.6	8.5	9.1	9.7
1124	75030	3205310	8.2	7	7.7	8.2
1125	75030	3205320	7	6.1	7.1	7
1126	75030	3205330	6.8	5.5	6.4	6.3
1127	75030	3205340	5.2	5	5.7	5.6
1128	75030	3205350	4.6	4.4	5.3	5.3
1129	75030	3205360	4.3	3.7	4.5	4.7
1130	75030	3205370	4	3.4	4.3	4.4
1131	75030	3205380	3.6	3.1	3.7	4.1
1132	75030	3205390	3.4	2.6	3.5	3.7
1133	75030	3205400	3.2	2.3	3.1	3.4
1134	75030	3205410	2.7	1.6	2.7	3.2

Point	Y	X	16-Mar	16-Oct	17-Apr	17-Jul
1135	75030	3205420	2.5	0.9	2.3	2.7
1136	75030	3205430	2.1	0.1	1.8	2.2
1137	75030	3205440	1.8	-0.5	1.4	2
1138	75030	3205450	1.5	-0.7	0.8	1.5
1139	75030	3205460	1.3	-1.3	0.5	0.8
1140	75040	3205230	18.2	18	19	19.3
1141	75040	3205240	16.5	17	17.7	18.2
1142	75040	3205250	15	15.4	16.4	15.5
1143	75040	3205260	14	14.8	14.7	13.8
1144	75040	3205270	13.1	12.3	13.2	12.5
1145	75040	3205280	11.7	11.5	11.5	11.3
1146	75040	3205290	10.3	10.1	10.1	10.4
1147	75040	3205300	9	8.5	8.6	8.9
1148	75040	3205310	7.6	7	7.4	7.4
1149	75040	3205320	6.5	6.1	6.6	6.4
1150	75040	3205330	5.4	5.5	6.1	5.8
1151	75040	3205340	4.9	5	5.4	5.4
1152	75040	3205350	4.5	4	4.7	4.9
1153	75040	3205360	4.3	3.6	4.3	4.5
1154	75040	3205370	3.8	3.3	4.1	4.3
1155	75040	3205380	3.6	2.8	3.7	3.8
1156	75040	3205390	3.3	2.5	3.4	3.6
1157	75040	3205400	3	2	2.8	3.3
1158	75040	3205410	2.7	1.3	2.6	2.8
1159	75040	3205420	2.3	0.4	2.3	2.6
1160	75040	3205430	1.8	-0.3	1.5	2.3
1161	75040	3205440	1.6	-0.6	1.1	1.6
1162	75040	3205450	1.3	-1.1	3	1
1163	75040	3205460	1.1	-1.6	0.7	0.5
1164	75050	3205220	19.6	18.7	19.3	19.5
1165	75050	3205230	18.3	18	18	19.6
1166	75050	3205240	16.5	16.5	16.7	16.8
1167	75050	3205250	14.6	14.5	14.5	14.7
1168	75050	3205260	13.7	13	1	13.1
1169	75050	3205270	12.6	11.5	12.5	11.7
1170	75050	3205280	11.4	10	11.1	10.5
1171	75050	3205290	10.1	8.5	9.6	9.3
1172	75050	3205300	8.7	6.8	8.3	8.2
1173	75050	3205310	7.5	5.7	6.8	6.7
1174	75050	3205320	6.2	5.3	6.3	6.3
1175	75050	3205330	5.3	4.7	5.6	5.7
1176	75050	3205340	4.7	4.3	5	5.3
1177	75050	3205350	4.4	3.7	4.5	4.7
1178	75050	3205360	4.2	3.4	4.3	4.3

Point	Y	X	16-Mar	16-Oct	17-Apr	17-Jul
1179	75050	3205370	3.6	3.1	3.8	4
1180	75050	3205380	3.5	2.7	3.6	3.7
1181	75050	3205390	3.3	2.2	3.1	3.4
1182	75050	3205400	2.8	1.5	2.7	3
1183	75050	3205410	2.5	0.6	2.4	2.7
1184	75050	3205420	1.8	0	2.1	2.3
1185	75050	3205430	1.5	-0.6	1.8	1.8
1186	75050	3205440	1.3	-1	0.7	1.7
1187	75050	3205450	1.1	-1.2	0.4	0.7
1188	75060	3205220	20.2	18.7	19.3	19.5
1189	75060	3205230	18.4	18	17.4	18.3
1190	75060	3205240	16.1	15.5	16	15.8
1191	75060	3205250	14.7	13.9	14.6	13.9
1192	75060	3205260	13.5	12.4	13.3	12.4
1193	75060	3205270	12.3	10.9	12	11.1
1194	75060	3205280	11.3	9.4	10.7	9.7
1195	75060	3205290	10	7.7	9.3	8.5
1196	75060	3205300	8.6	6.3	7.8	7.3
1197	75060	3205310	7.5	5.6	6.5	6.4
1198	75060	3205320	5.1	5.1	5.8	5.8
1199	75060	3205330	5.2	4.5	5.3	5.4
1200	75060	3205340	4.7	4	4.7	4.9
1201	75060	3205350	4.3	3.6	4.4	4.5
1202	75060	3205360	4	3.3	4.1	4.2
1203	75060	3205370	3.7	2.8	3.7	3.7
1204	75060	3205380	3.4	2.5	3.4	3.5
1205	75060	3205390	3.1	1.9	2.8	3.2
1206	75060	3205400	2.6	1	2.5	2.7
1207	75060	3205410	2.1	0.3	2.3	2.5
1208	75060	3205420	1.4	-0.5	1.6	2.1
1209	75060	3205430	1.3	-0.7	1	1.4
1210	75060	3205440	1	-1.3	0.5	0.8
1211	75070	3205210	20.6	18.7	20.3	20
1212	75070	3205220	19.4	18.5	19.1	20.3
1213	75070	3205230	17.8	17.5	17	17
1214	75070	3205240	16	15	15.4	15
1215	75070	3205250	14.5	13.2	14	13
1216	75070	3205260	12.6	11.6	12.7	11.6
1217	75070	3205270	11.7	10.2	11.6	10.4
1218	75070	3205280	11	8.6	10.3	9
1219	75070	3205290	10	7	8.8	7.7
1220	75070	3205300	8.7	6	7.5	6.6
1221	75070	3205310	7.5	5.4	6.3	6.3
1222	75070	3205320	6	4.8	5.5	5.7

Point	Y	X	16-Mar	16-Oct	17-Apr	17-Jul
1223	75070	3205330	4.8	4.3	4.8	5.3
1224	75070	3205340	4.4	3.7	4.9	4.7
1225	75070	3205350	4.2	3.4	4.5	4.3
1226	75070	3205360	3.8	3	4.3	3.8
1227	75070	3205370	3.6	2.6	3.9	3.6
1228	75070	3205380	3.3	2.3	3.6	3.3
1229	75070	3205390	2.7	1.4	3.2	2.7
1230	75070	3205400	2.3	0.6	2.5	2.6
1231	75070	3205410	1.6	-0.1	1.8	2.3
1232	75070	3205420	1.3	-0.7	1.3	1.6
1233	75070	3205430	0.8	-1	0.7	1.1
1234	75070	3205440	-0.6	-1.4	0.8	0.6
1235	75080	3205200	19	19.2	19.3	19.5
1236	75080	3205210	18.7	19	19.5	19
1237	75080	3205220	17.8	18.7	18.3	18
1238	75080	3205230	16.5	16.5	16.4	16.3
1239	75080	3205240	15.2	14	15	14.3
1240	75080	3205250	13.7	14.5	13.5	12.3
1241	75080	3205260	11.9	11	12.5	10.7
1242	75080	3205270	11.3	9.5	11.1	9.6
1243	75080	3205280	10.6	8	9.7	8.4
1244	75080	3205290	9.7	6.4	8.4	7.3
1245	75080	3205300	8.6	5.7	7	6.4
1246	75080	3205310	7.4	5.3	5.7	5.7
1247	75080	3205320	6	4.6	5.3	5.4
1248	75080	3205330	4.7	4	4.7	4.9
1249	75080	3205340	3.9	3.6	4.7	4.5
1250	75080	3205350	2.9	3.3	4.4	4
1251	75080	3205360	3.6	2.7	4	3.7
1252	75080	3205370	3.4	2.5	3.7	3.4
1253	75080	3205380	3	1.1	3.5	3
1254	75080	3205390	2.5	1	2.9	2.6
1255	75080	3205400	1.8	0.3	2.3	2.3
1256	75080	3205410	1.3	-0.5	1.4	1.9
1257	75080	3205420	0.7	-0.7	1	1.3
1258	75080	3205430	0.4	-1.3	0.5	0.8
1259	75090	3205190	18.5	18	19.2	19.3
1260	75090	3205200	18.5	18.1	19.3	19
1261	75090	3205210	17.5	17.9	18.5	18.5
1262	75090	3205220	16.3	17.5	17.5	17.3
1263	75090	3205230	15.7	15	15.6	15.4
1264	75090	3205240	14.7	13.3	14.3	13.4
1265	75090	3205250	13	11.7	13.2	11.4
1266	75090	3205260	11.8	10.3	11.9	10.1

Point	Y	X	16-Mar	16-Oct	17-Apr	17-Jul
1267	75090	3205270	10.7	8.7	10.5	9
1268	75090	3205280	10.1	7.3	9.3	7.8
1269	75090	3205290	9.6	6.3	8	6.8
1270	75090	3205300	9.3	5.7	7.5	6.2
1271	75090	3205310	8.4	4	5.3	5.6
1272	75090	3205320	7.3	4.4	5	5.3
1273	75090	3205330	5.9	3.7	4.6	4.7
1274	75090	3205340	4.2	3.4	4.2	4.3
1275	75090	3205350	3.6	3	3.7	3.7
1276	75090	3205360	3.5	2.6	3.6	3.5
1277	75090	3205370	2.7	2.1	3.3	3.3
1278	75090	3205380	2.5	1.3	2.6	2.7
1279	75090	3205390	2.1	0.5	2.1	2.5
1280	75090	3205400	1.4	-0.3	1.6	2.1
1281	75090	3205410	0.7	-0.7	1.3	1.6
1282	75090	3205420	0.3	-1.1	0.8	1.3
1283	75100	3205190	20	17.3	19.6	19
1284	75100	3205200	18.8	16.8	18.8	18.5
1285	75100	3205210	17.2	16.7	18.6	17.8
1286	75100	3205220	15.6	16	17.5	16.5
1287	75100	3205230	14.4	14	16.5	14.5
1288	75100	3205240	13.7	12.5	15	12.5
1289	75100	3205250	11.3	11	13.7	10.7
1290	75100	3205260	10.8	9.5	12.5	9.5
1291	75100	3205270	10.4	8	9.7	8.5
1292	75100	3205280	9.5	6.4	8.4	7.4
1293	75100	3205290	8.8	6	7.1	6.6
1294	75100	3205300	8	5.4	5.9	5.8
1295	75100	3205310	7	4.7	5.2	5.4
1296	75100	3205320	5.7	4.1	4.8	4.8
1297	75100	3205330	4.4	3.5	4.4	4.5
1298	75100	3205340	3.7	3.2	3.8	4
1299	75100	3205350	3.6	2.8	3.6	3.6
1300	75100	3205360	3.3	2.5	3.5	3.3
1301	75100	3205370	2.7	1.6	2.8	2.9
1302	75100	3205380	2.2	0.8	2.3	2.6
1303	75100	3205390	1.6	0.2	1.8	2.3
1304	75100	3205400	1	-0.5	1.4	1.7
1305	75100	3205410	0.5	-0.8	1	1.4
1306	75100	3205420	0.3	-1.5	0.5	0.8
1307	75110	3205210	17.4	15.5	17	18.4
1308	75110	3205220	15.5	14.6	15.7	15.6
1309	75110	3205230	14.5	13.3	14.5	13.6
1310	75110	3205240	13	11.7	13	11.6

Point	Y	X	16-Mar	16-Oct	17-Apr	17-Jul
1311	75110	3205250	11.6	10.3	11.6	10.2
1312	75110	3205260	10.3	8.7	10.3	9
1313	75110	3205270	9.7	7.3	8.8	7.8
1314	75110	3205280	9	6.4	7.5	7
1315	75110	3205290	8.3	5.7	6.3	6.3
1316	75110	3205300	7.5	5.1	5.5	5.6
1317	75110	3205310	6.6	4.5	4.8	5.3
1318	75110	3205320	5.7	3.7	4.6	4.6
1319	75110	3205330	4.3	3.3	4.1	4.3
1320	75110	3205340	2.7	3.2	3.7	3.7
1321	75110	3205350	3.4	2.5	3.6	3.4
1322	75110	3205360	3.2	2.3	3.1	3.1
1323	75110	3205370	2.5	1.3	2.6	2.7
1324	75110	3205380	1.8	0.5	2	2.4
1325	75110	3205390	1.3	-0.3	1.6	2
1326	75110	3205400	0.6	-0.6	1.3	1.6
1327	75110	3205410	0.6	-1	0.7	1.3
1328	75120	3205220	15.6	14	15.3	14.7
1329	75120	3205230	14.4	11.5	13.6	12.7
1330	75120	3205240	11.7	10	12.3	11
1331	75120	3205250	10.9	9.5	9.7	9.6
1332	75120	3205260	9.7	8	8.5	8.5
1333	75120	3205270	9.2	6.9	8	7.4
1334	75120	3205280	8.4	6	6.7	6.7
1335	75120	3205290	7.7	5.4	5.9	6
1336	75120	3205300	6.8	4.7	5.2	5.3
1337	75120	3205310	6.1	4.3	4.7	4.9
1338	75120	3205320	5.3	3.5	4.3	4.4
1339	75120	3205330	4.1	3.1	3.8	4
1340	75120	3205340	3.6	2.6	3.6	3.6
1341	75120	3205350	3.3	2.5	3.3	3.3
1342	75120	3205360	3	1.6	2.9	2.8
1343	75120	3205370	2.3	0.9	2.3	2.6
1344	75120	3205380	1.7	0.1	1.7	2.3
1345	75120	3205390	1.2	-0.5	1.3	1.7
1346	75120	3205400	-0.7	-1	0.9	1.4
1347	75130	3205240	12	10	11.5	10.3
1348	75130	3205250	10.3	8.7	10	9
1349	75130	3205260	9.3	7.5	8.5	8
1350	75130	3205270	8.5	6.5	7.3	7.3
1351	75130	3205280	7.7	5.6	6.3	6.4
1352	75130	3205290	7	5	5.6	5.6
1353	75130	3205300	6.3	4.5	4.9	5.1
1354	75130	3205310	5.5	3.8	4.4	4.6

Point	Y	X	16-Mar	16-Oct	17-Apr	17-Jul
1355	75130	3205320	4.7	3.3	4	4.2
1356	75130	3205330	4	2.8	3.7	3.7
1357	75130	3205340	3.4	2.6	3.4	3.4
1358	75130	3205350	3.3	2.2	3.2	3.1
1359	75130	3205360	2.7	1.4	2.6	2.7
1360	75130	3205370	2	0.5	2	2.4
1361	75130	3205380	1.5	-0.3	1.6	2
1362	75130	3205390	0.5	-0.8	1.1	1.6
1363	75130	3205400	0.7	-1.4	0.6	1.3
1364	75140	3205250	9.5	8.3	9.3	8.5
1365	75140	3205260	8.1	7.2	7.9	7.6
1366	75140	3205270	8.8	6.2	6.6	6.8
1367	75140	3205280	7.1	5.4	5.9	6.1
1368	75140	3205290	6.4	4.6	5.3	5.3
1369	75140	3205300	5.6	4.1	4.6	4.7
1370	75140	3205310	4.7	3.5	4.2	4.4
1371	75140	3205320	4	3.1	3.8	3.9
1372	75140	3205330	3.6	2.7	3.6	3.5
1373	75140	3205340	3.5	2.5	3.3	3.3
1374	75140	3205350	3.1	1.7	2.9	2.8
1375	75140	3205360	2.6	0.9	2.3	2.6
1376	75140	3205370	1.7	0	1.8	2.3
1377	75140	3205380	1.2	-0.6	1.4	1.7
1378	75140	3205390	0.7	-1.3	0.9	1.4
1379	75150	3205270	5.4	5.7	6.3	6.5
1380	75150	3205280	6.3	4.9	5.6	5.7
1381	75150	3205290	5.6	4.4	5	5
1382	75150	3205300	4.7	3.9	4.4	4.6
1383	75150	3205310	4.2	3.4	4	4.2
1384	75150	3205320	3.6	3	3.7	3.7
1385	75150	3205330	3.5	2.6	3.4	3.4
1386	75150	3205340	3.3	2.3	3.2	3.1
1387	75150	3205350	3.1	1.3	2.6	2.7
1388	75150	3205360	2.3	0.5	2.3	2.4
1389	75150	3205370	1.6	-0.3	1.6	2
1390	75150	3205380	0.8	-0.7	1.3	1.6
1391	75160	3205280	5.5	4.7	5.3	5.5
1392	75160	3205290	4.8	4.3	4.7	4.7
1393	75160	3205300	4.3	3.7	4.3	4.3
1394	75160	3205310	3.7	3.3	3.7	3.8
1395	75160	3205320	3.6	2.8	3.6	3.5
1396	75160	3205330	3.4	2.6	3.3	3.3
1397	75160	3205340	3.2	1.8	3	2.8
1398	75160	3205350	2.8	0.8	2.5	2.6

Point	Y	X	16-Mar	16-Oct	17-Apr	17-Jul
1399	75160	3205360	2	0	2	2.3
1400	75160	3205370	1.3	-0.6	1.5	1.7
1401	75160	3205380	0.7	-1.1	1	1.4
1402	75170	3205300	4	3.6	4	4.1
1403	75170	3205310	3.7	3.3	3.6	3.7
1404	75170	3205320	3.6	2.7	3.4	3.4
1405	75170	3205330	3.4	2.3	3.2	3.1
1406	75170	3205340	3.3	1.4	2.7	2.7
1407	75170	3205350	2.6	0.5	2.3	2.4
1408	75170	3205360	1.6	-0.3	1.7	2
1409	75170	3205370	0.8	-1	1.3	1.6
1410	75180	3205310	3.7	3	3.5	3.5
1411	75180	3205320	3.4	2.6	3.3	3.3
1412	75180	3205330	3.2	1.9	2.9	2.8
1413	75180	3205340	3.2	0.9	2.6	2.6
1414	75180	3205350	2.1	0	2.2	2.3
1415	75180	3205360	1.3	-0.5	1.5	1.7
1416	75190	3205330	3.3	1.5	2.7	2.7
1417	75190	3205340	2.9	0.5	2.4	2.4
1418	75190	3205350	1.7	-0.3	1.8	2
1419	75190	3205360	0.8	-0.7	1.3	1.5
1420	75200	3205350	1.5	0.3	2.3	2.2
1421	75200	3205360	2.8	-0.5	1.5	1.7
1422	75210	3205350	0.5	-0.6	1.3	1.6

Appendix C:

Accumulative volumes, volumes per contour and

Percentage increase or decrease in Volume

The next four tables are extractions, where the lowest height is -1 m and the highest height is 20 m. Each table contains columns indicating the accumulative 2D surface area, each contour interval's area separately, then the percentage of each single contour for the total 2D area. If all single contour areas are added together, it adds up to approximately 143 000 m. Accumulative volumes, volumes per contour and percentage increase or decrease in volumes are also given.

March 2016

Plane_ Height	Acc Area_2D	Separate Areas in m²	% Area	Acc Volume	Vol/Cont	% of Vol/Cont
20	74.134464	0	0.0	15.943591	15.943591	0.002051288
19	456.0108	381.876336	0.3	270.944687	255.001096	0.032808216
18	1023.027558	567.016758	0.4	1018.526466	747.581779	0.096183212
17	1564.526615	541.499057	0.4	2311.047021	1292.52056	0.166294555
16	2609.228489	1044.701874	0.7	4367.449704	2056.40268	0.264574956
15	3832.150513	1222.922024	0.9	7561.502579	3194.05288	0.410944026
14	5294.671629	1462.521116	1.0	12110.90912	4549.40654	0.585322633
13	6917.509799	1622.83817	1.1	18209.98512	6099.076	0.78470174
12	8561.912068	1644.402269	1.2	25910.73244	7700.74733	0.99077136
11	12026.47513	3464.563057	2.4	36395.5122	10484.7798	1.348962517
10	15376.24368	3349.768558	2.3	50073.03955	13677.5274	1.759738608
9	19389.57692	4013.333239	2.8	67486.1555	17413.116	2.240356142
8	23461.59461	4072.01769	2.9	88920.89329	21434.7378	2.757774461
7	27695.22203	4233.62742	3.0	114531.1629	25610.2696	3.294994705
6	32364.86538	4669.643351	3.3	144528.3443	29997.1814	3.859410906
5	38876.31064	6511.445254	4.6	180005.0685	35476.7242	4.564404054
4	55069.04757	16192.73693	11.4	225711.331	45706.2625	5.880527428
3	92650.29781	37581.25024	26.4	296390.0119	70678.6809	9.093456751
2	109706.2715	17055.97366	12.0	399806.1743	103416.162	13.30543226
1	120682.2005	10975.92903	7.7	514925.0874	115118.913	14.81109784
0	130414.6037	9732.403227	6.8	640799.3438	125874.256	16.19487082
-1	142690.6393	12276.03561	8.6	777247.6715	136448.328	17.55532152
	850736.5208	**142616.5049**		**3608596.837**		**100**

October 2016

Plane_ Height	Acc Area_2D	Separate Areas in m²	% Area	Acc Volume	Vol/Cont	% of Vol/Cont
20	0		0.0	0	0.01	1.45061E-06
19	0	0	0.0	0	0.01	1.45061E-06
18	957.420587	957.420587	0.7	464.199123	464.199123	0.06733727
17	1711.977473	754.556886	0.5	1834.207518	1370.0084	0.198735027
16	2360.920546	648.943073	0.5	3875.15753	2040.95001	0.296062606
15	3071.26648	710.345934	0.5	6585.278413	2710.12088	0.393133318
14	4229.179975	1157.913495	0.8	10238.37086	3653.09245	0.529921881
13	5685.260335	1456.08036	1.0	15142.43217	4904.06131	0.711388893
12	7386.298239	1701.037904	1.2	21679.16768	6536.73551	0.94822653
11	9656.633352	2270.335113	1.6	30178.78686	8499.61919	1.232964742
10	12582.77923	2926.145877	2.1	41247.61724	11068.8304	1.605657535
9	15626.51547	3043.736236	2.1	55373.14777	14125.5305	2.049066048
8	19060.35451	3433.839044	2.4	72676.57155	17303.4238	2.510054978
7	23126.98454	4066.630032	2.9	93741.0108	21064.4392	3.055632297
6	28607.777	5480.792462	3.8	119460.5105	25719.4997	3.73090083
5	36666.32019	8058.543188	5.7	152094.3697	32633.8592	4.733905942
4	50114.24248	13447.92229	9.4	194843.6878	42749.3182	6.201266302
3	74907.45337	24793.21089	17.4	256533.9343	61690.2465	8.948859608
2	97125.28219	22217.82882	15.6	344827.5578	88293.6235	12.80797673
1	107600.694	10475.41178	7.3	447328.389	102500.831	14.86889096
0	119479.7762	11879.08225	8.3	560633.6961	113305.307	16.43620092
-1	137648.0246	18168.24841	12.7	689364.3144	128730.618	18.67381469
	757605.1608	**137648.0246**	**96.5162**		**689364.334**	**100**

April 2017

Plane_ Height	Acc Area_2D	Separate Areas in m²	% area	Acc Volume	Vol/Cont	% of Vol/Cont
20	0		0.0	0	0.01	1.1989E-06
19	519.357403	519.357403	0.4	222.100281	222.100281	0.026627562
18	1293.479987	774.122584	0.5	1145.726119	923.625838	0.110733331
17	1974.545947	681.06596	0.5	2782.048029	1636.32191	0.196178331
16	2856.63548	882.089533	0.6	5195.138875	2413.090846	0.289305015
15	3927.477021	1070.841541	0.8	8576.576414	3381.437539	0.405399921
14	5285.439411	1357.96239	1.0	13177.2347	4600.658288	0.551572071
13	7010.253245	1724.813834	1.2	19310.03382	6132.799114	0.735260151
12	9400.292912	2390.039667	1.7	27413.71711	8103.683297	0.971549091
11	12159.43505	2759.142138	1.9	38238.67778	10824.96067	1.297802532
10	15094.20114	2934.766085	2.1	51809.6272	13570.94942	1.627018615
9	18693.50502	3599.303888	2.5	68725.31747	16915.69027	2.028018977
8	23151.78898	4458.283956	3.1	89677.0421	20951.72463	2.51189839
7	29108.93836	5957.149378	4.2	115735.0461	26058.00399	3.124089278
6	35727.56758	6618.629226	4.6	148165.7401	32430.69398	3.888109902
5	46447.27901	10719.71143	7.5	188735.1548	40569.41468	4.863859621
4	69788.26937	23340.99036	16.4	246095.0492	57359.89445	6.876867134
3	95650.60726	25862.33789	18.1	330499.5385	84404.48929	10.11923861
2	111911.474	16260.86671	11.4	434649.0215	104149.483	12.48646225
1	127068.3878	15156.91387	10.6	554205.3146	119556.2931	14.33358186
0	143019.926	15951.53818	11.2	690515.3274	136310.0128	16.34218222
-1	143652.0564	632.130365	0.4	834099.2001	143583.8727	17.21424393
	903740.9174	**143652.0564**				**99.99999999**

July 2017

Plane_ Height	Acc Area_2D	Separate Areas in m²	% Area	Acc Volume	Vol/Cont	% of Vol/Cont
20	0		0.0	0	0.01	1.22989E-06
19	752.022529	752.022529	0.5	381.208569	381.208569	0.046884459
18	1455.02199	702.999459	0.5	1500.291079	1119.08251	0.137634834
17	1993.52339	538.501397	0.4	3228.092979	1727.8019	0.21250062
16	2666.05892	672.535536	0.5	5533.816671	2305.723692	0.283578641
15	3725.06019	1059.001273	0.7	8705.410747	3171.594076	0.39007117
14	4843.74246	1118.682266	0.8	12975.53672	4270.12597	0.525178504
13	6369.19046	1525.448	1.1	18613.71418	5638.177461	0.693433783
12	8316.59333	1947.40287	1.4	25959.51975	7345.805573	0.90345325
11	10906.2947	2589.701357	1.8	35455.40008	9495.880331	1.167888785
10	14295.4196	3389.124907	2.4	47986.40144	12531.00136	1.541175272
9	18178.3825	3882.962952	2.7	64147.29201	16160.89057	1.9876117
8	22616.1175	4437.735002	3.1	84482.44375	20335.15174	2.500999889
7	28205.9077	5589.790158	3.9	109740.117	25257.67325	3.106415867
6	35147.8457	6941.938013	4.9	141286.4374	31546.32036	3.879850259
5	44534.5801	9386.734367	6.6	180761.0912	39474.65388	4.854948036
4	59555.2825	15020.70238	10.5	232527.8983	51766.807	6.366747603
3	82464.2793	22908.99682	16.1	303637.5446	71109.64634	8.745703987
2	121998.04	39533.76037	27.7	406191.1837	102553.6391	12.61296908
1	133638.919	11640.87947	8.2	534438.2205	128247.0367	15.77297425
0	140143.48	6504.561158	4.6	671870.1401	137431.9196	16.90261377
-1	141887.18	1743.699884	1.2	813080.8632	141210.7231	17.36736501
	883692.942	**141887.1802**				**100**

Appendix D:

Annual average rainfall in Mtunzini area from 1998 to 2018

LEGEND

*** Data is missing/not yet available in the current month --- data unavailable/not requested = average is unreliable due to missing daily values

Monthly Daily Rain (mm) Data for station [0304357 6] - MTUNZINI Measured at 08:00

Year	JAN	FEB	MAR	APR	MAY	JUN	JUL	AUG	SEP	OCT	NOV	DEC
1998	89.4	136.2	83.4	85.2	17.2	0	54.4	14.8	84	138.4	60	123.8
1999	111	311.4	74.6	30	98.2	20.2	89.2	96.8	119.6	213	64.2	137
2000	248.4	89.4	205.2	83.4	126	4.8	0	0.0=	120.4	109.2	426.2	289.6
2001	137.8	158.8	101.6	89	24	4	5.4	8.4	208.8	73.0=	117.4	108
2002	127.8	84.8	0.4	6.2	2.6	61.4	349.2	21.6=	66	39.8	127.2	8.8=
2003	35.0=	43.2	36.0=	57.6	9	104	42.2	18.6	97	0	136.6	41.6
2004	364.8	218	160.6	119.4	26	3.4	150.4	51.4	110.2	50.4	168.6	24.2
2005	105.6	133.4	108.4	13.8	50.4	72.6	2.4	25.8	52.8	141.2	174.6	123.2
2006	83.4	139.2	121.8	181.8	133	178.2	0	185	59.4	220.6	249.8	266.4
2007	122.8	14.4	47.2	306.2	4.4	303	15	64.2	115.6	373	253.4	89.8
2008	146.8	142.4	344.2	160	20	15.2	5	54.6	91	43.8	85.8	122.8
2009	168.6	82.2	40.6	87.6	33.8	27	4.2	122.2	42.8	88.2	115.4	96
2010	84.6	99.4	79.4	62.8	23.4	47	18.2	40.2	29.2	115.6	120.4	98.4
2011	191.8	80.2	60.4	130.4	22.2	33.2	227.2	83.8	62.8	102.4	238.2	122
2012	51	96.6	224.6	39.4	4	29.2	22	9.8	269.8	219	86.8	134.4
2013	286.6	142.6	99.8	35.2	39.4	36.2	45.8	25	84.6	127	144.8	104.6
2014	34	93.8	133.4	50.4	41.6	27.6	14	12.8	13.2	80.8	25.6	68
2015	61.2	118.4	37.6	66.2	6.6	15.8	238	5.4	58.8	29.2	76.4	138.2
2016	47.4	14.2	76.8	69	206	42.8	187.4	50.6	96.4	95.2	96	40
2017	76.4	244.6	77.4	24.8	59.2	5.8	13.4	14	17.4	27.6	16	18.4=
2018	105	133.4	81.4	81.2	230.6							

`

Appendix E:

Wind data

Wind Data courtesy of the South African Weather Bureau for Average Wind Direction (Degrees from North)

Data for station [0304357 6] - MTUNZINI -28.9470 31.7070 41 m

2016 to 2017 at 08:00, 14:00 and 20:00 (Extracted 2017/05/16 14:16)

LEGEND

Wind direction (in degrees clockwise from true north) reported at either 08:00 14:00 or 20:00

0 indicates calm conditions

---- indicates that data is unavailable or was not requested

*** indicates that data is missing or not yet available in the current month

The following wind direction ranges are applicable:

N dir>=348.75 OR dir < 11.25

NNE 11.25 to 33.74

NE 33.75 to 56.24

ENE 56.25 to 78.74

E 78.75 to 101.24

ESE 101.25 to 123.74

SE 123.75 to 146.24

SSE 146.25 to 168.74

S 168.75 to 191.24

SSW 191.25 to 213.74

SW 213.75 to 236.24

WSW 236.25 to 258.74

W 258.75 to 281.24

WNW 281.25 to 303.74

NW 303.75 to 326.24

NNW 326.25 to 348.74

`

Average Wind Direction (Degrees from North)

Data for station [0304357 6] - MTUNZINI -28.9470 31.7070 41 m

2016 08:00 (Extracted 2017/05/16 14:16)

Day	JAN	FEB	MAR	APR	MAY	JUN	JUL	AUG	SEP	OCT	NOV	DEC
1	50	0	50	50	280	0	70	60	60	0	250	0
2	60	50	240	230	260	0	240	270	0	290	250	220
3	60	30	0	310	0	0	280	50	0	280	20	20
4	50	240	0	60	260	250	0	250	0	0	20	260
5	50	240	0	0	0	260	50	0	40	***	10	230
6	50	240	0	240	0	0	80	0	250	***	260	30
7	260	240	40	250	310	0	230	0	90	***	260	220
8	250	240	250	300	190	0	70	250	280	***	20	0
9	260	240	240	0	0	0	250	250	230	***	250	220
10	0	250	260	0	40	0	260	0	280	***	240	230
11	50	80	250	0	90	240	0	0	60	***	250	270
12	60	70	280	60	50	260	90	0	10	***	50	0
13	250	60	50	0	50	50	240	0	250	***	260	50
14	0	30	250	0	0	70	0	270	350	***	240	230
15	240	220	30	60	0	0	0	270	50	***	280	30
16	230	0	20	50	0	270	270	260	80	***	30	220
17	270	240	70	240	270	280	180	80	250	***	210	0
18	0	80	260	240	0	30	0	70	240	***	210	20
19	30	300	250	80	20	0	0	60	250	40	220	40
20	50	220	250	280	260	260	0	260	60	20	240	240
21	50	240	250	80	0	240	0	310	270	40	20	240
22	70	270	260	0	0	0	0	240	260	260	220	240
23	50	50	70	220	90	70	260	270	260	220	40	320
24	30	***	60	270	180	60	250	0	300	50	40	210
25	240	40	40	60	250	40	210	0	250	210	230	240
26	220	30	30	230	250	0	70	230	50	220	230	50
27	40	***	50	60	0	0	250	40	0	30	20	30
28	240	340	260	260	0	260	0	60	0	50	40	300
29	250	50	0	0	0	50	0	0	0	260	230	230
30	40	***	50	260	0	0	240	0	0	220	20	240
31	40	***	260	***	0	***	250	60	***	70	***	30

`

Average Wind Direction (Degrees from North)

Data for station [0304357 6] - MTUNZINI -28.9470 31.7070 41 m

2017 08:00 (Extracted 2017/05/16 14:16)

Day	JAN	FEB	MAR	APR	MAY	JUN	JUL	AUG	SEP	OCT	NOV	DEC
1	30	0	40	250	40	---	---	---	---	---	---	---
2	30	30	240	0	0	---	---	---	---	---	---	---
3	220	210	50	40	0	---	---	---	---	---	---	---
4	230	10	260	20	***	---	---	---	---	---	---	---
5	0	240	0	0	40	---	---	---	---	---	---	---
6	250	240	230	220	0	---	---	---	---	---	---	---
7	240	60	270	0	280	---	---	---	---	---	---	---
8	210	50	30	0	0	---	---	---	---	---	---	---
9	40	220	230	0	30	---	---	---	---	---	---	---
10	220	240	200	50	0	---	---	---	---	---	---	---
11	230	30	260	280	60	---	---	---	---	---	---	---
12	20	20	260	80	210	---	---	---	---	---	---	---
13	230	240	280	0	240	---	---	---	---	---	---	---
14	240	260	70	230	240	---	---	---	---	---	---	---
15	0	250	40	230	230	---	---	---	---	---	---	---
16	210	0	220	240	***	---	---	---	---	---	---	---
17	190	0	30	0	***	---	---	---	---	---	---	---
18	290	50	30	240	***	---	---	---	---	---	---	---
19	20	230	230	240	***	---	---	---	---	---	---	---
20	250	240	240	240	***	---	---	---	---	---	---	---
21	230	240	0	240	***	---	---	---	---	---	---	---
22	20	220	60	240	***	---	---	---	---	---	---	---
23	30	240	60	0	***	---	---	---	---	---	---	---
24	20	260	0	230	***	---	---	---	---	---	---	---
25	230	70	230	0	***	---	---	---	---	---	---	---
26	230	230	290	0	***	---	---	---	---	---	---	---
27	50	280	40	40	***	---	---	---	---	---	---	---
28	30	10	0	0	***	---	---	---	---	---	---	---
29	240	***	250	0	***	---	---	---	---	---	---	---
30	50	***	50	0	***	---	---	---	---	---	---	---
31	90	***	40	***	***	---	---	---	---	---	---	---

`

Average Wind Direction (Degrees from North)

Data for station [0304357 6] - MTUNZINI -28.9470 31.7070 41 m

2016 14:00 (Extracted 2017/05/16 14:16)

Day	JAN	FEB	MAR	APR	MAY	JUN	JUL	AUG	SEP	OCT	NOV	DEC
15	190	190	50	40	130	70	40	120	50	***	70	30
16	180	220	100	40	140	220	220	120	90	***	30	180
24	10	***	110	40	120	40	260	100	80	80	40	200
19	100	110	210	40	40	90	60	40	190	20	100	30
13	130	100	80	50	200	20	130	50	240	***	200	210
4	90	220	130	50	190	230	50	200	60	0	190	200
14	110	40	230	50	160	80	60	220	80	***	200	100
1	110	110	60	70	110	60	40	190	40	90	120	130
10	100	160	70	70	50	90	160	120	220	***	180	210
29	170	***	70	70	60	30	140	50	100	190	180	190
11	80	120	220	70	30	230	70	60	50	***	140	140
27	50	210	200	80	90	190	200	40	0	100	70	40
25	210	100	40	110	240	40	290	50	190	160	180	110
22	90	150	190	110	80	280	140	220	220	80	200	190
9	110	190	260	120	40	50	210	180	220	***	160	190
28	160	80	210	130	120	220	150	50	300	90	40	190
3	110	110	110	140	50	40	110	80	120	290	30	40
12	90	120	130	140	50	230	50	50	30	***	30	30
18	110	80	120	150	70	40	60	50	250	60	180	60
8	210	190	230	150	80	80	70	200	50	***	200	10
21	100	170	240	160	50	240	210	110	130	60	40	110
20	110	220	190	180	240	210	70	290	70	30	120	180
2	120	90	200	190	190	130	230	120	130	290	70	120
6	210	180	120	210	110	120	230	140	190	***	210	30
17	120	260	180	210	190	110	250	70	240	***	180	100
26	270	50	40	220	190	50	60	160	110	110	120	50
23	100	40	50	220	50	70	200	210	190	210	60	20
5	60	200	110	220	130	230	40	40	50	***	190	180
7	210	200	60	240	190	100	250	120	220	***	80	200
30	110	***	60	240	50	50	190	60	0	220	120	100
31	100	***	190	***	70	***	120	50	***	150	***	80

`

Average Wind Direction (Degrees from North)

Data for station [0304357 6] - MTUNZINI -28.9470 31.7070 41 m

2017 14:00 (Extracted 2017/05/16 14:16)

Day	JAN	FEB	MAR	APR	MAY	JUN	JUL	AUG	SEP	OCT	NOV	DEC
1	90	70	190	180	50	---	---	---	---	---	---	---
2	70	210	110	30	70	---	---	---	---	---	---	---
3	220	130	110	220	60	---	---	---	---	---	---	---
4	190	30	130	40	***	---	---	---	---	---	---	---
5	60	200	150	40	50	---	---	---	---	---	---	---
6	200	190	130	230	110	---	---	---	---	---	---	---
7	240	90	130	160	200	---	---	---	---	---	---	---
8	160	190	80	100	100	---	---	---	---	---	---	---
9	40	140	190	70	20	---	---	---	---	---	---	---
10	190	120	180	70	50	---	---	---	---	---	---	---
11	90	80	120	190	40	---	---	---	---	---	---	---
12	60	150	200	20	230	---	---	---	---	---	---	---
13	210	110	110	50	240	---	---	---	---	---	---	---
14	140	200	20	220	210	---	---	---	---	---	---	---
15	70	200	40	190	210	---	---	---	---	---	---	---
16	200	90	160	170	***	---	---	---	---	---	---	---
17	160	20	40	180	***	---	---	---	---	---	---	---
18	110	10	40	190	***	---	---	---	---	---	---	---
19	100	230	200	190	***	---	---	---	---	---	---	---
20	160	230	130	190	***	---	---	---	---	---	---	---
21	190	240	60	190	***	---	---	---	---	---	---	---
22	40	180	50	120	***	---	---	---	---	---	---	---
23	20	170	50	150	***	---	---	---	---	---	---	---
24	90	30	210	210	***	---	---	---	---	---	---	---
25	210	100	190	100	***	---	---	---	---	---	---	---
26	150	230	100	40	***	---	---	---	---	---	---	---
27	40	110	50	30	***	---	---	---	---	---	---	---
28	190	30	190	100	***	---	---	---	---	---	---	---
29	110	***	170	110	***	---	---	---	---	---	---	---
30	30	***	40	80	***	---	---	---	---	---	---	---
31	110	***	40	***	***	---	---	---	---	---	---	---

`

Average Wind Direction (Degrees from North)

Data for station [0304357 6] - MTUNZINI -28.9470 31.7070 41 m

2016 20:00 (Extracted 2017/05/16 14:16)

Day	JAN	FEB	MAR	APR	MAY	JUN	JUL	AUG	SEP	OCT	NOV	DEC
1	90	60	70	40	0	0	250	260	270	0	220	230
2	100	60	0	250	0	280	260	50	270	290	60	0
3	70	130	80	0	220	70	0	210	290	0	30	40
4	70	250	0	60	250	270	50	280	60	0	210	230
5	70	240	60	240	0	300	60	60	110	***	250	240
6	240	240	60	220	240	70	220	0	250	***	190	30
7	240	240	70	270	240	0	0	0	240	***	70	240
8	260	240	250	0	0	70	260	220	240	***	220	50
9	80	230	290	0	80	0	270	320	230	***	210	230
10	90	0	60	70	90	0	0	70	330	***	190	190
11	80	110	250	60	50	260	80	80	50	***	70	0
12	80	90	80	270	60	310	80	110	220	***	220	40
13	0	70	230	70	70	40	70	90	250	***	260	230
14	170	50	280	60	0	80	60	250	80	***	250	50
15	230	250	80	50	0	80	80	0	70	***	40	60
16	130	250	70	80	0	230	250	80	240	***	40	200
17	0	0	260	260	0	100	290	60	210	***	230	70
18	70	50	70	0	60	90	80	60	260	40	250	30
19	80	100	270	80	80	60	90	220	0	50	90	50
20	80	240	260	0	0	240	70	280	70	60	80	210
21	70	***	240	260	60	270	260	80	250	200	40	50
22	80	120	0	90	80	0	260	200	210	40	130	220
23	70	***	60	200	110	80	230	0	280	260	40	80
24	230	50	270	70	280	70	260	270	220	220	230	200
25	220	60	60	60	260	80	310	90	20	190	130	60
26	0	***	50	280	0	90	60	0	100	60	80	50
27	80	270	240	80	70	330	0	70	0	60	40	30
28	230	80	200	0	0	270	330	90	0	60	220	210
29	0	70	70	90	70	80	290	60	90	240	220	200
30	60	***	50	250	50	50	250	60	0	300	180	70
31	80	***	0	***	60	***	0	50	***	240	***	60

`

Average Wind Direction (Degrees from North)

Data for station [0304357 6] - MTUNZINI -28.9470 31.7070 41 m

2017 20:00 (Extracted 2017/05/16 14:16)

Day	JAN	FEB	MAR	APR	MAY	JUN	JUL	AUG	SEP	OCT	NOV	DEC
1	60	70	230	280	70	---	---	---	---	---	---	---
2	40	190	70	70	60	---	---	---	---	---	---	---
3	220	60	230	250	70	---	---	---	---	---	---	---
4	140	30	270	40	***	---	---	---	---	---	---	---
5	50	240	200	40	60	---	---	---	---	---	---	---
6	220	260	0	240	0	---	---	---	---	---	---	---
7	240	60	0	0	220	---	---	---	---	---	---	---
8	110	220	60	0	30	---	---	---	---	---	---	---
9	70	160	190	40	40	---	---	---	---	---	---	---
10	210	90	250	50	40	---	---	---	---	---	---	---
11	50	70	0	0	130	---	---	---	---	---	---	---
12	220	210	240	40	230	---	---	---	---	---	---	---
13	220	90	60	300	240	---	---	---	---	---	---	---
14	0	0	50	230	240	---	---	---	---	---	---	---
15	40	0	220	200	230	---	---	---	---	---	---	---
16	190	0	0	300	***	---	---	---	---	---	---	---
17	190	50	40	200	***	---	---	---	---	---	---	---
18	40	40	210	270	***	---	---	---	---	---	---	---
19	190	230	240	250	***	---	---	---	---	---	---	---
20	210	240	0	250	***	---	---	---	---	---	---	---
21	0	200	60	250	***	---	---	---	---	---	---	---
22	60	160	40	0	***	---	---	---	---	---	---	---
23	40	230	40	170	***	---	---	---	---	---	---	---
24	250	70	240	250	***	---	---	---	---	---	---	---
25	280	210	180	0	***	---	---	---	---	---	---	---
26	0	220	50	60	***	---	---	---	---	---	---	---
27	60	60	70	60	***	---	---	---	---	---	---	---
28	200	40	250	60	***	---	---	---	---	---	---	---
29	80	***	0	0	***	---	---	---	---	---	---	---
30	60	***	40	0	***	---	---	---	---	---	---	---
31	60	***	60	***	***	---	---	---	---	---	---	---

`

LEGEND

Wind speed (in m/s) reported at either 08:00 14:00 or 20:00
0.0 indicates calm conditions
---- indicates that data is unavailable or was not requested
*** indicates that data is missing or not yet available in the current month
= indicates that the average for the month is unreliable due to missing daily values
1 m/s = 1.944 knots = 3.6 km/h

Average Wind Speed (m/s)

Data for station [0304357 6] - MTUNZINI -28.9470 31.7070 41 m

2016 08:00 (Extracted 2017/05/16 14:16)

Day	JAN	FEB	MAR	APR	MAY	JUN	JUL	AUG	SEP	OCT	NOV	DEC
1	3.5	0	4.1	5	2.6	0	2.2	1.5	3.4	0	1.8	0
2	2.5	3.4	4.8	4.2	1.2	0	7.3	1.3	0	1.6	1.5	3.3
3	1.6	2.8	0	1.5	0	0	1.7	4	0	1.9	4.5	3.7
4	3.1	6.5	0	2.4	2.1	4.3	0	1.8	0	0	3.5	3
5	5.8	5.7	0	0	0	2	4.4	0	3.5	***	2.3	4.4
6	6.8	4.3	0	6.1	0	0	3.4	0	5	***	1.8	3.4
7	1.1	3.1	4.6	5.2	1.8	0	4.2	0	1.9	***	2.2	3.6
8	4.8	5.1	3.6	1.3	2.2	0	2.4	5.5	1.1	***	2.4	4.4
9	1.7	4.9	3.1	0	0	0	2.2	3	5.8	***	3.2	5
10	0	3	1.2	0	4.4	0	1.3	0	1.5	***	4.1	3.4
11	2	1.2	3.2	0	2.3	6.6	0	0	2.3	***	2	2
12	2.1	2.7	2	1.7	1.8	3.5	1.1	0	4.8	***	2.9	0
13	1.4	2.5	3.3	0	2.9	2.6	1.8	0	5.9	***	2.5	1.5
14	0	4.5	4.9	0	0	2.3	0	3.1	1.6	***	3.6	2.4
15	3	2	1.2	3.5	0	0	0	1.6	4.2	***	1.2	1.4
16	2.9	0	1.4	3.8	0	1.1	1.2	1.9	4.1	***	5	4.7
17	1.5	3.9	1.6	3.4	1.3	1.2	2.7	1.2	3.5	***	2.8	0
18	0	1.7	1.2	2.5	0	3.1	0	2.3	7.5	***	6.8	3
19	3.4	1.7	4.1	1.6	2.9	0	0	2.2	2.8	5.2	1.5	4.6
20	3.9	2	2.7	1.9	5.1	2.5	0	1.2	1.9	1.9	2.5	4.3
21	3.6	4.8	2.5	2.4	0	2.8	0	1.2	1.5	2.4	3.7	1.7
22	3.1	2.1	3.4	0	0	0	0	5.2	2	1.9	6.8	2.6
23	2.5	3.5	2.4	6.4	1.3	1.8	2.8	3.9	2.6	5.8	1.6	1.3
24	5	***	3	1.2	1.3	2.1	4.5	0	1.7	2.1	1.6	5.8
25	4	4.9	2.4	2	3.5	3	3.4	0	3.8	5.3	5.1	3.9
26	4.8	4.4	6.5	6.8	2.3	0	1.3	3.4	4.1	1.1	2.6	2.9
27	2.8	***	3.7	1.9	0	0	1.5	3.7	0	3.1	2.2	3.1
28	5.2	5.5	1.4	2.5	0	3.1	0	2.6	0	1.1	4.6	1.2
29	3.5	11.3	0	0	0	2.3	0	0	0	3.9	5.8	6
30	3.3	***	3.2	4.8	0	0	1.3	0	0	5.1	1.7	2.3
31	4.4	***	2.4	***	0	***	2.2	2.1	***	2.4	***	3
Avg	**3**	**3.6=**	**2.5**	**2.4**	**1.3**	**1.5**	**1.7**	**1.7**	**2.5**	**2.6=**	**3.1**	**3**

`

Average Wind Speed (m/s)

Data for station [0304357 6] - MTUNZINI -28.9470 31.7070 41 m

2017 08:00 (Extracted 2017/05/16 14:16)

Day	JAN	FEB	MAR	APR	MAY	JUN	JUL	AUG	SEP	OCT	NOV	DEC
1	3.2	0	3.2	2.9	1.3	---	---	---	---	---	---	---
2	3.7	2.2	1.5	0	0	---	---	---	---	---	---	---
3	3.6	3.1	2.1	3.8	0	---	---	---	---	---	---	---
4	5.4	2.5	1.7	2.3	***	---	---	---	---	---	---	---
5	0	1.5	0	0	1.7	---	---	---	---	---	---	---
6	1.9	3.9	3.3	7.6	0	---	---	---	---	---	---	---
7	3.6	1.3	1.4	0	1.8	---	---	---	---	---	---	---
8	3.5	1.7	1.7	0	0	---	---	---	---	---	---	---
9	1.8	2.3	5	0	2.7	---	---	---	---	---	---	---
10	4.5	2.2	5.7	2.1	0	---	---	---	---	---	---	---
11	1.2	3.2	1.9	1.6	2	---	---	---	---	---	---	---
12	2.9	3	2.5	1.5	6.5	---	---	---	---	---	---	---
13	4.4	2.6	1.5	0	5.5	---	---	---	---	---	---	---
14	2.8	1.9	1.2	3.7	8.9	---	---	---	---	---	---	---
15	0	1.7	1.5	3.9	5.1	---	---	---	---	---	---	---
16	7.9	0	2.3	2	***	---	---	---	---	---	---	---
17	5.5	0	1.8	0	***	---	---	---	---	---	---	---
18	2.1	2.5	3.9	1.3	***	---	---	---	---	---	---	---
19	3.6	5.5	5	1.1	***	---	---	---	---	---	---	---
20	1.9	5.4	2.3	2.3	***	---	---	---	---	---	---	---
21	3.9	3.8	0	3.3	***	---	---	---	---	---	---	---
22	2.9	3.8	1.3	1.3	***	---	---	---	---	---	---	---
23	4	3.5	2.2	0	***	---	---	---	---	---	---	---
24	1.5	1.3	0	3.3	***	---	---	---	---	---	---	---
25	6.1	1.8	3.8	0	***	---	---	---	---	---	---	---
26	3.3	4.7	1.7	0	***	---	---	---	---	---	---	---
27	2.4	1.6	2.6	1.9	***	---	---	---	---	---	---	---
28	2.6	1.7	0	0	***	---	---	---	---	---	---	---
29	1.2	***	1.6	0	***	---	---	---	---	---	---	---
30	2.3	***	2.2	0	***	---	---	---	---	---	---	---
31	1.4	***	2.6	***	***	---	---	---	---	---	---	---
Avg	3.1	2.5	2.2	1.5	2.5=							

`

Average Wind Speed (m/s)

Data for station [0304357 6] - MTUNZINI -28.9470 31.7070 41 m

2016 14:00 (Extracted 2017/05/16 14:16)

Day	JAN	FEB	MAR	APR	MAY	JUN	JUL	AUG	SEP	OCT	NOV	DEC
1	6.2	8.5	4.3	3.2	3	3.1	1.9	5.6	5.2	1.4	1.9	2.4
2	4	6.8	4.7	3.1	3.6	3.5	6.5	4.5	4.3	1.5	4.4	3.8
3	7.6	6.3	7.5	2.2	2.7	3.1	2.3	3.1	5.6	1.3	8.8	6.2
4	6.3	8.6	5.3	5.6	5.2	6.1	4.1	6.7	4.9	0	4.5	9.9
5	5	7.6	8.1	6.2	4.3	3.2	5	2.4	5	***	4.3	3.9
6	7.1	5.3	6.1	6.1	3.8	3.2	8.4	2.9	4.5	***	5	5.8
7	5	5.8	4.9	5.6	4.1	1.9	4	4.2	4.6	***	4.1	5.7
8	3.7	7.8	6.7	3.4	3.2	2.7	1.9	7.5	5.6	***	7	4
9	4.1	6	3.3	5.2	3.7	3.3	6.9	4.5	5.8	***	3.3	5.3
10	3.8	4.2	1.7	2.5	4.7	2.3	2.6	4.7	3	***	3	2.8
11	5.5	4.6	7.2	4	3.1	6.5	3.7	3.4	5.3	***	2.6	1.5
12	3.7	6.4	3.8	3.3	3	3.5	2.6	3	5.3	***	5.2	4.8
13	4.5	8.2	3.4	2.9	3.5	4.7	3.5	4.4	4.7	***	3	7
14	5.3	5.7	3.6	3.6	3.2	2.7	3.1	4.4	3.9	***	5.8	4.4
15	5.5	4	4.8	4.3	3.4	3.1	2.5	4.6	5.5	***	3.4	4
16	1.7	4.5	6.2	3.4	2.3	7	7.9	3.2	4.9	***	5.6	6.2
17	3.9	1.8	4.6	5.2	3.1	2.9	3.7	3.9	3.3	***	4.6	7.7
18	5.8	3.9	4.1	3.1	4.5	3.2	2.7	4.6	6.2	4.2	6	6.5
19	5.9	6.4	5.9	3.7	3.8	3.1	3.1	1.8	1.9	3.8	6.7	5.7
20	6.9	6.7	3.2	5.3	5.4	3.6	3.1	1.6	2.7	6.5	3.8	5.3
21	7.5	3.3	6.1	4	3.9	3.4	5.2	2.9	2.7	3.4	4.1	5
22	6	3.5	3.3	6.8	2.7	1.2	2.7	8.1	4.6	4.3	5.4	5.7
23	5.9	5.7	5	6.5	3.6	3.4	6.3	3.7	1.9	5.1	5.8	4.3
24	3	***	3.5	3.2	1.4	4.4	3.6	2.3	4.2	6.1	2.7	6.1
25	5.3	4	5.3	3.3	4.1	3.4	3.2	4.5	4.6	4.5	4.7	2.8
26	1.7	5.2	6.1	6.1	3.4	2.9	3	3.5	1.2	3.8	2.4	4.1
27	6.2	10.9	2.8	3.8	2.2	2	5.1	4.9	0	5	6.1	5.5
28	3.9	12.9	6.8	3.9	2.3	6.1	3	4.3	1.2	4.9	4.9	5.2
29	4.1	***	3.8	3.5	2.9	2.9	2.9	3.1	2.9	6.2	4.4	6
30	6.7	***	3.9	7.5	4.4	4.4	5.3	4.3	0	3.7	3.8	5.2
31	8	***	5.6	***	4.2	***	2	6.3	***	2.2	***	8
Avg	5.2	6.1=	4.9	4.3	3.5	3.6	3.9	4.2	3.9	3.8=	4.6	5.2

`

Average Wind Speed (m/s)

Data for station [0304357 6] - MTUNZINI -28.9470 31.7070 41 m

2017 14:00 (Extracted 2017/05/16 14:16)

Day	JAN	FEB	MAR	APR	MAY	JUN	JUL	AUG	SEP	OCT	NOV	DEC
1	6.1	5.4	4.4	3.6	4.4	---	---	---	---	---	---	---
2	6.5	5.2	3.8	4.8	4.4	---	---	---	---	---	---	---
3	9.1	3.1	3	5.9	3	---	---	---	---	---	---	---
4	4.3	5.6	2.8	3.9	***	---	---	---	---	---	---	---
5	4.8	8.5	3.6	3.2	2.2	---	---	---	---	---	---	---
6	6.8	2.6	3.2	4.3	4.3	---	---	---	---	---	---	---
7	4	5.1	3.2	1.9	5.6	---	---	---	---	---	---	---
8	4.4	5.5	4.6	5.3	2.9	---	---	---	---	---	---	---
9	3.8	4	5	3.9	4.1	---	---	---	---	---	---	---
10	6.5	3	5.8	5.1	2.8	---	---	---	---	---	---	---
11	7.5	5.9	3.6	3.1	3.4	---	---	---	---	---	---	---
12	4.4	4.8	5.8	3	5.9	---	---	---	---	---	---	---
13	4.6	4.4	4.3	2.1	6.8	---	---	---	---	---	---	---
14	3.1	3.1	2.6	5.4	10.4	---	---	---	---	---	---	---
15	4.8	2.9	2.1	5.9	5.1	---	---	---	---	---	---	---
16	8.4	1.1	3.2	4.7	***	---	---	---	---	---	---	---
17	5.8	3.8	4.1	5.4	***	---	---	---	---	---	---	---
18	4.1	4.6	3.7	5.7	***	---	---	---	---	---	---	---
19	6.7	5.4	6	6.1	***	---	---	---	---	---	---	---
20	4.9	5.5	3.2	5.7	***	---	---	---	---	---	---	---
21	2.4	5.6	4.8	6	***	---	---	---	---	---	---	---
22	5.5	3.3	3.4	3.1	***	---	---	---	---	---	---	---
23	3.9	4.1	4.2	3.6	***	---	---	---	---	---	---	---
24	4.4	2.8	7	2.8	***	---	---	---	---	---	---	---
25	6.7	2.7	2.9	3	***	---	---	---	---	---	---	---
26	3.9	4.5	4	3.5	***	---	---	---	---	---	---	---
27	3.8	2.8	2.8	3.8	***	---	---	---	---	---	---	---
28	4.8	4.7	3.8	5.4	***	---	---	---	---	---	---	---
29	4.4	***	2.8	3.5	***	---	---	---	---	---	---	---
30	3.4	***	4.6	4.6	***	---	---	---	---	---	---	---
31	4.4	***	4.2	***	***	---	---	---	---	---	---	---
Avg	5.1	4.3	4	4.3	4.7=							

`

Average Wind Speed (m/s)

Data for station [0304357 6] - MTUNZINI -28.9470 31.7070 41 m

2016 20:00 (Extracted 2017/05/16 14:16)

Day	JAN	FEB	MAR	APR	MAY	JUN	JUL	AUG	SEP	OCT	NOV	DEC
1	1.6	3.5	3.3	3.8	0	0	2.5	3	1.8	0	1.4	1.4
2	1.8	4	0	2.1	0	1.2	2.6	3.2	1.2	1.7	2.9	0
3	2.4	2.2	2.3	0	4.8	2.6	0	7.4	1.7	0	5.5	6.7
4	3.7	4.4	0	4	2.2	3	5.1	1.4	2.7	0	5	8
5	3.9	3.4	3.6	4	0	1.6	3.8	2.7	3.5	***	2.9	1.9
6	3.2	2	3.5	5.1	1.5	1.7	7.3	0	1.5	***	3.8	6.2
7	4.6	3.4	2.9	3.2	2.3	0	0	0	5	***	1.9	5.6
8	2.1	3.7	3.8	0	0	2.6	2	6.2	2.2	***	4.9	3.5
9	2.3	2.7	1.8	0	2	0	1.7	1.3	4.1	***	6.1	4.3
10	1.8	0	1.2	2.8	2.9	0	0	1.5	1.2	***	1.6	1.8
11	3.5	2.1	2.6	2.2	4	2.9	1.6	3.6	4.3	***	2	0
12	2.5	1.9	2.1	2.7	1.9	1.3	1.9	3.9	1.4	***	4.9	4.4
13	0	4	7.1	2.4	2.3	3.3	1.3	4.8	2.3	***	2.2	3.7
14	1.2	5.4	1.6	2.5	0	2.4	1.7	2.3	3.3	***	3.7	2.8
15	4.5	6.5	3.4	3.4	0	1.7	2.1	0	4.4	***	3	2.5
16	1.8	4.1	3.3	3.4	0	4.1	3.8	3	5.8	***	4.1	2.6
17	0	0	2.9	1.4	0	1.7	1.2	3.8	2.9	***	5.8	3.3
18	3	6.5	2.6	0	4	2.7	1.7	3.5	4	2.7	2	5.3
19	4.2	3.7	2.2	2.5	3.3	2.2	2.8	1.4	0	3.1	3.3	3.3
20	3.2	4.9	2.4	0	0	2.1	2.1	1.5	3	4.6	3	2.7
21	3.5	***	3.8	1.7	3	1.7	2.4	2	2.6	2.5	2.1	2.7
22	3.7	1.3	0	2.4	2.8	0	2.5	4.9	2.5	3.3	2.4	3.8
23	4.4	***	3.6	3.4	2.1	1.8	1.4	0	1.5	1.7	3.3	4.6
24	5.3	4.7	1.7	2.5	1.5	2.5	2.3	1.1	1.1	7.3	5.5	5.9
25	3.3	3	4.1	2.8	2.1	2.9	1.3	3.2	1.3	1.9	1.9	1.3
26	0	***	5.2	1.5	0	2.7	2.6	0	1.5	1.7	1.7	4
27	3.8	5.8	3.4	2.4	2.4	1.3	0	3	0	2.6	3.7	5
28	3.4	7.9	1.8	0	0	1.6	1.1	4.2	0	3.2	6	3.6
29	0	3.3	3	2	1.6	2.5	1.6	2.9	1.3	4	2	2.9
30	4	***	2.9	4.2	2.4	6.9	2.1	3.4	0	1.7	1.5	1.8
31	2.8	***	0	***	2.4	***	0	4	***	3	***	4.2
Avg	2.8	3.6=	2.6	2.3	1.7	2	2	2.7	2.3	2.5=	3.3	3.5

`

Average Wind Speed (m/s)

Data for station [0304357 6] - MTUNZINI -28.9470 31.7070 41 m

2017 20:00 (Extracted 2017/05/16 14:16)

Day	JAN	FEB	MAR	APR	MAY	JUN	JUL	AUG	SEP	OCT	NOV	DEC
1	3.9	3.9	3.3	1.2	2.2	---	---	---	---	---	---	---
2	3.7	4.4	1.2	3	2.1	---	---	---	---	---	---	---
3	7.7	1.7	3.6	1.9	2.2	---	---	---	---	---	---	---
4	2.1	4.7	1.2	3.5	***	---	---	---	---	---	---	---
5	3	5.5	4.3	2.7	2.8	---	---	---	---	---	---	---
6	5.9	1.3	0	4.6	0	---	---	---	---	---	---	---
7	2.9	1.6	0	0	2.3	---	---	---	---	---	---	---
8	1.2	5	2.4	0	1.9	---	---	---	---	---	---	---
9	2.7	1.4	6.3	2.1	4.1	---	---	---	---	---	---	---
10	1.7	1.9	3.1	2.8	3.6	---	---	---	---	---	---	---
11	2.7	3.2	0	0	1.9	---	---	---	---	---	---	---
12	5.6	4.3	1.8	2.6	6.7	---	---	---	---	---	---	---
13	4.2	3.2	1.6	1.3	6.9	---	---	---	---	---	---	---
14	0	0	2.7	6.1	9.5	---	---	---	---	---	---	---
15	3.4	0	5.1	4.9	6	---	---	---	---	---	---	---
16	6.9	0	0	1.2	***	---	---	---	---	---	---	---
17	2.3	2.2	4.9	4.6	***	---	---	---	---	---	---	---
18	1.6	4.7	5.7	2	***	---	---	---	---	---	---	---
19	2	5.1	2.2	2.1	***	---	---	---	---	---	---	---
20	3.8	3.7	0	2.4	***	---	---	---	---	---	---	---
21	0	6	1.7	2.7	***	---	---	---	---	---	---	---
22	3.8	3.9	2.8	0	***	---	---	---	---	---	---	---
23	4.8	1.3	3.1	2.1	***	---	---	---	---	---	---	---
24	2.6	1.9	5.3	1.3	***	---	---	---	---	---	---	---
25	1.7	4.7	2.8	0	***	---	---	---	---	---	---	---
26	0	2.7	1.2	2.4	***	---	---	---	---	---	---	---
27	2.4	1.8	2.1	2.3	***	---	---	---	---	---	---	---
28	2.9	3.8	2.7	1.3	***	---	---	---	---	---	---	---
29	1.3	***	0	0	***	---	---	---	---	---	---	---
30	2.9	***	3.8	0	***	---	---	---	---	---	---	---
31	2.5	***	2.8	***	***	---	---	---	---	---	---	---
Avg	3	3	2.5	2	3.7=							